FEDERAL UNIVERSITY OF CEARÁ
TECHNOLOGY CENTER
HYDRAULIC AND ENVIRONMENTAL ENGINEERING DEPARTMENT
CIVIL ENGINEERING POSTGRADUATE PROGRAM
(ENVIRONMENTAL SANITATION)

THOBIAS PEREIRA SILVA

ADM1 MODELING AND APPLICATION FOR ANAEROBIC CONVERSION OF FRUIT AND VEGETABLE WASTE

FORTALEZA– CE
2026

THOBIAS PEREIRA SILVA

ADM1 MODELING AND APPLICATION FOR ANAEROBIC CONVERSION OF FRUIT AND VEGETABLE WASTE

A thesis submitted to the Graduate Program in Civil Engineering (Water Resources), Department of Hydraulic and Environmental Engineering, Federal University of Ceará, in partial fulfillment of the requirements for the degree of Doctor of Philosophy in Civil Engineering (Water Resources). Area of concentration: Environmental Sanitation.

Advisor: André Bezerra dos Santos, PhD
Co-advisor: Renato Carrhá Leitão, PhD

FORTALEZA – CE

2026

CATALOGAÇÃO

THOBIAS PEREIRA SILVA

ADM1 MODELING AND APPLICATION FOR ANAEROBIC CONVERSION OF FRUIT AND VEGETABLE WASTE

A thesis submitted to the Graduate Program in Civil Engineering (Water Resources), Department of Hydraulic and Environmental Engineering, Federal University of Ceará, in partial fulfillment of the requirements for the degree of Doctor of Philosophy in Civil Engineering (Water Resources). Area of concentration: Environmental Sanitation.

Approved on: 01/01/2026.

EXAMINATION BOARD

André Bezerra dos Santos, PhD (Advisor)
Federal University of Ceará (UFC)

Renato Carrhá Leitão, PhD (Co-Advisor)
Empresa Brasileira de Pesquisa Agrícola (EMBRAPA)

Prof. Dr. Tito Gehring
Ruhr-Universität Bochum, Alemanha

Prof. Dr. Theo Syrto Octavio de Souza
Universidade de São Paulo (USP)

Prof. Dr. Marcelo Zaiat
Universidade de São Paulo (USP)

Prof. Dr. Ricardo Steinmetz
Empresa Brasileira de Pesquisa Agrícola (EMBRAPA)

To God.

To my parents.

ACKNOWLEDGEMENTS

To God, the author and finisher of all things, for the grace, strength, and guidance granted throughout this entire journey.

To my parents, Ana Cristina da Silva and Fernando Pereira, for their unconditional love, unwavering support, and steadfast confidence in my path.

To the Federal University of Ceará (UFC), the Department of Hydraulic and Environmental Engineering (DEHA), the Brazilian Agricultural Research Corporation (Embrapa), and the Biomass Technology Laboratory (LTB), for their indispensable institutional support and for the valuable technical and academic contributions that enriched this work.

To the Cearense Foundation for Scientific and Technological Development Support (FUNCAP, Rede Verdes), for the essential financial support, without which this research would not have been possible.

To my advisors, Dr. André Bezerra dos Santos and Dr. Renato Carrhá Leitão, as well as Dr. Tito Augusto Gehring, for their guidance, encouragement, and the valuable knowledge, experience, and insights that were fundamental to the development of this research.

To my colleagues at the Brazilian Agricultural Research Corporation (Embrapa), especially Chagas, Priscilla, Camila, Daniel, Ulisses, Maíra, Carmélia, and Nícolas, for their essential support in the acquisition and generation of the experimental data used in this research, as well as for their technical assistance and collaboration throughout the experimental phase.

I also extend my sincere gratitude to all collaborators who, directly or indirectly, contributed to the execution of this study.

*“**27** But God chose the foolish things of the world to shame the wise; God chose the weak things of the world to shame the strong. **28** God chose the lowly things of this world and the despised things—and the things that are not—to nullify the things that are, **29** so that no one may boast before him.”*

1 Corinthians 1:27-29

ABSTRACT

Although the Anaerobic Digestion Model No. 1 (ADM1) is widely used to simulate anaerobic digestion (AD) processes, its application to fruit and vegetable waste (FVW) remains limited when substrate characteristics, reactor configuration, and alternative metabolic routes are considered. In this context, this doctoral research aimed to evaluate, calibrate, and structurally extend ADM1 for representing different anaerobic conversion pathways of FVW through an integrated experimental and computational approach. The substrate consisted of collected FVW subjected to pretreatment, generating two fractions: a solid fraction (S-FVW) and a liquid fraction (L-FVW). The latter was applied in the experimental and modeling stages of wet anaerobic digestion (W-AD) and dark fermentation (DF). The thesis was developed in three complementary stages. First, a bibliometric analysis focused on ADM1 applications in dry anaerobic digestion (D-AD) identified a clear predominance of studies dedicated to W-AD, revealing that high-solids systems still remain comparatively underexplored and often require specific kinetic adaptations, particularly in hydrolysis and disintegration processes. Second, ADM1 was applied, adjusted, and calibrated for W-AD of L-FVW in Upflow Anaerobic Sludge Blanket (UASB) reactors. The results demonstrated that adequate representation of this substrate under UASB operational conditions requires substrate-dependent adjustment of hydrolysis, disintegration, and microbial uptake parameters, leading to high predictive accuracy for biogas production and intermediate process dynamics, with coefficients of determination reaching 0.99. Third, for DF of L-FVW in an Anaerobic Structured-Bed Reactor (AnSTBR) with attached biomass, the standard ADM1 structure proved insufficient to represent metabolic pathways associated with hydrogen production under acidogenic conditions. To address this limitation, additional pathways related to lactate formation and consumption were incorporated into the model structure, together with kinetic adjustments adapted to reactor operation and substrate characteristics. The modified model significantly improved predictive performance for hydrogen yield, gas composition, volatile fatty acids (VFA), and biogas production, with coefficients of determination above 0.90. The main original contribution of this thesis lies in demonstrating that ADM1 can be progressively adapted beyond its conventional formulation, from parameter recalibration to structural modification, in order to represent distinct anaerobic valorization routes of FVW within a unified mechanistic framework. These findings expand the applicability of ADM1 to emerging waste-to-energy systems and provide a scientific basis for future virtual biorefinery strategies for organic waste valorization.

Keywords: Anaerobic digestion; ADM1; fruit and vegetable waste; bioenergy.

RESUMO

Embora o *Anaerobic digestion model No. 1* (ADM1) seja amplamente utilizado para simular processos de digestão anaeróbia (DA), sua aplicação a resíduos de frutas e hortaliças (RFH) ainda permanece limitada quando se consideram características do substrato, configuração do reator e rotas metabólicas alternativas. Nesse contexto, esta pesquisa de doutorado teve como objetivo avaliar, calibrar e estender estruturalmente o ADM1 para representar diferentes rotas de conversão anaeróbia de RFH por meio de uma abordagem integrada experimental e computacional. O substrato consistiu em resíduos de frutas e hortaliças coletados e submetidos a pré-tratamento, gerando duas frações: uma fração sólida (RFH-S) e uma fração líquida (RFH-L). Esta última foi aplicada nas etapas experimentais e de modelagem da DA úmida e da fermentação escura (FE). A tese foi desenvolvida em três etapas complementares. Primeiramente, uma análise bibliométrica focada em aplicações do ADM1 na digestão anaeróbia seca (DA-S) identificou uma predominância clara de estudos dedicados à digestão anaeróbia úmida (DA-U), revelando que sistemas com alto teor de sólidos ainda permanecem comparativamente pouco explorados e frequentemente requerem adaptações cinéticas específicas, particularmente nos processos de hidrólise e desintegração. Em seguida, o ADM1 foi aplicado, ajustado e calibrado para DA-U de RFH-L em reatores Anaeróbios de Fluxo Ascendente (UASB). Os resultados demonstraram que a representação adequada desse substrato sob condições operacionais de reatores UASB requer ajuste dependente do substrato para parâmetros de hidrólise, desintegração e captação microbiana, resultando em elevada precisão preditiva para produção de biogás e dinâmica de intermediários do processo, com coeficientes de determinação atingindo 0,99. Por fim, para a FE de RFH-L em reator anaeróbio de leito fixo estruturado (AnSTBR) com biomassa aderida, a estrutura padrão do ADM1 mostrou-se insuficiente para representar as rotas metabólicas associadas à produção de hidrogênio sob condições acidogênicas. Para superar essa limitação, rotas adicionais relacionadas à formação e ao consumo de lactato foram incorporadas à estrutura do modelo, juntamente com ajustes cinéticos adaptados à operação do reator e às características do substrato. O modelo modificado melhorou significativamente o desempenho preditivo para rendimento de hidrogênio, composição gasosa, ácidos graxos voláteis (AGV) e produção de biogás, com coeficientes de determinação superiores a 0,90. A principal contribuição original desta tese consiste em demonstrar que o ADM1 pode ser progressivamente adaptado além de sua formulação convencional, desde a recalibração de parâmetros até a modificação estrutural,

a fim de representar distintas rotas de valorização anaeróbia de RFH dentro de uma estrutura mecanística unificada. Esses resultados ampliam a aplicabilidade do ADM1 a sistemas emergentes de conversão de resíduos em energia e fornecem base científica para futuras estratégias de biorrefinarias virtuais voltadas à valorização energética de resíduos orgânicos.

Palavras-chave: ADM1; Bioenergia; Digestão Anaeróbia; Resíduos de Frutas e Vegetais.

LIST OF FIGURES

Figure 1.1 – Structural Decomposition of the Mass Balance Equation into Matrices 41

Figure 3.1 – Schematic representation of the proposed system highlighting the modeled components. 50

Figure 4.1 – Sensitivity indices (SI) of k_{dec}, k_{dis}, $k_{hyd,ch}$, $k_{hyd,li}$, $k_{hyd,pr}$, $k_{s,aa}$, $k_{s,ac}$, $k_{s,c4}$, $k_{s,fa}$, $k_{s,h2}$, $k_{s,pro}$, $k_{s,su}$, $k_{m,aa}$, $k_{m,ac}$, $k_{m,c4}$, $k_{m,fa}$, $k_{m,h2}$, $k_{m,pro}$, $k_{m,su}$, based on absolute-relative sensitivity function analysis. 72

Figure 4.2 – Comparison of Biogas and Methane Production: Simulations with Reference Standards, Optimized Variables, and Experimental Production. 75

Figure 4.3 – Presents the comparison between experimental and optimized methane and biogas production across the operational phases of the reactor, together with the corresponding variations in OLR applied during reactor operation. 77

Figure 4.4 – Comparison between volatile fatty acids (VFA) concentrations in the digestate obtained experimentally and by the optimized model, and comparison of the effluent pH measured experimentally and predicted by the model. 80

Figure 4.5 – Impact of varying combinations of kinetic parameter (k_{dis}, $k_{hyd,ch}$, $k_{s,ac}$, $k_{m,ac}$, $k_{s,fa}$ and k_{dis}) on biogas production. 82

Figure 5.1 – Metabolic pathways of lactate formation and degradation and their role in hydrogen production during dark fermentation 95

Figure 5.2 – Comparison between experimental data (*Experimental*) and ADM1 simulations before (*Reference Standard*) and after model calibration (*Optimized*): (a) total biogas production and H_2 production rate (*Reference Standard*) (b) total biogas production and H_2 production rate (*Experimental* and *Optimized*); (c) biogas composition (H_2 and CO_2); (d) acetate, propionate, butyrate, and lactate profiles. 110

Figure 5.3 – The Dynamic Behavior of Short-Chain Fatty Acids and Lactate in Dark Fermentation of Liquid Fruit and Vegetable Waste (L-FVW): (a) Lactate, (b) Acetate, (c) Butyrate, and (d) Propionate. 116

Figure 5.4 – Comparison between optimized model simulations and experimental measurements of key organic acids (HLac, HAc, HPro, HBu) during dark fermentation of L-FVW (phase 2). 121

Figure 6.1 – Network of keywords in publications indexed in the Web of Science, with a gradient of colors representing the period of publication (Blue → Yellow indicates Old → Recent). For interpretation of the colors, see the web version of this article. 147
Figure 6.2 – Reaction Pathways Described in the ADM1 Model. 152
Figure 11.1 – Schematic representation of the proposed system highlighting the modeled components. 202
Figure 12.1 – Inhibition factors. 203
Figure 14.1 – Temporal evolution of the frequency of terms associated with anaerobic digestion, modeling, and organic residues in publications indexed in Web of Science..... 209

LIST OF TABLES

Table 3.1 – Work program 51
Table 4.1 – Projected Operating Conditions. 58
Table 4.2 – Substrate characteristics and gas production results 66
Table 4.3 – Distribution of influent COD after disintegration according to factors *f* in L-FVW 69
Table 4.4 – ThOD of different fractions. 70
Table 4.5 – Reference standard and optimized values of the most sensitive parameters 74
Table 5.1 – Main characteristics of liquid fruit and vegetable waste. 90
Table 5.2 – Degradation reactions of sugar, lactic acid, acetic acid, and hydrogen with stoichiometric coefficients for different pathways. 94
Table 5.3 – Stoichiometric representation (Peterson matrix) of the glucose degradation process in the modified ADM1, including alternative pathways for lactate and ethanol integrated into the model. 97
Table 5.4 – Parameter ranges considered in the sensitivity analysis 101
Table 5.5 – Results of AnSTBR operation during operational phases. 103
Table 5.6 – Modified stoichiometric kinetic parameters. 113
Table 5.7 – Estimated coefficients for sugars and lactate degradation obtained from the ADM1 simulation on experimental results. 114
Table 6.1 – Characterization of Substrates: FVW, FW, and OFMSW 130
Table 6.2 – Representative characterization of transformer input. 131
Table 6.3 – Keywords Searched and Corresponding Number of Publications. 138
Table 6.4 – 12 Publications Associated with ADM1, D-AD, and FW (including FVW, OFMSW, and related substrates. 143
Table 6.5 – Top 10 Most Productive Countries in AD (1947–2023) and Top 10 Most Productive Institutions (2011–2023) 145
Table 6.6 – Modification of the Petersen matrix in the original ADM1 157
Table 10.1 – Biochemical rate coefficients ($v_{i,j}$) and kinetic rate equations (ρ_j) for soluble components (i = 1–12; j = 1–19). 200
Table 10.2 – Biochemical rate coefficients ($v_{i,j}$) and kinetic rate equations (ρ_j) for soluble components (i = 13–24; j = 1–19) 201
Table 13.1 – Stoichiometric parameters in ADM1 204

Table 13.2 – Physiochemical and biochemical kinetic parameters in ADM1 205
Table 13.3 – Acid and gas parameters in ADM1 206
Table 14.1 – Biochemical rate coefficients ($v_{i,j}$) and kinetic rate equations (ρ_j) for soluble components (i = 1–14; j = 1–23). Bold letters indicate additional processes or components added to the ADM1 in this work. 207
Table 14.2 – Biochemical rate coefficients ($v_{i,j}$) and kinetic rate equations (ρ_j) for soluble components (i = 15–28; j = 1–23). Bold letters indicate additional processes or components added to the ADM1 in this work. 208

LIST OF ABBREVIATIONS

ABR	Anaerobic baffled reactors
AcoD	Anaerobic Co-Digestion
AD	Anaerobic Digestion
ADM1	Anaerobic Digestion Model No. 1
ADR	Advective-Diffusive
AE	Algebraic Equation
AM2	Anaerobic Model Nº. 2
AM2HN	Two-Stage Anaerobic Digestion Mode
AnSTBR	Anaerobic Structured-Bed Reactor
AOCS	American Oil Chemists' Society
ASBR	Anaerobic Sequencing Batch Reactor
ASM1	Activated Sludge Model Nº. 1
ASM2	Activated Sludge Model Nº. 2
ASM3	Activated Sludge Model Nº. 3
BMP	Biochemical Methane Potential
CFD	Computational Fluid Dynamics
CIT	Total Inorganic Carbon
COD	Chemical Oxygen Demand
COD_p	Particulate Chemical Oxygen Demand
CONAB	Companhia Nacional de Abastecimento
CrC	Crystalline Cellulose
CSTR	Continuous Stirred Tank Reactor
D-AD	Dry Anaerobic Digestion
DIET	Direct Interspecies Electron Transfer
DIET	Direct Interspecies Electron Transfer
DM	Dairy Manure
DRANCO	Dry Anaerobic Composting
FAO	Food and Agriculture Organization
FS	Fixed Solids
FVW	Fruit and Vegetable Waste
FW	Food Waste

FW-A	Food Waste Animal
FW-V	Food Waste Vegetable
GDP	Gross Domestic Product
GEE	Greenhouse Gas Emissions
GW	Green Waste
HASL	Hybrid Anaerobic Solid-Liquid
HG-AD	High Solid Anaerobic Digestion
HRT	Hydraulic Retention Time
IC	Inorganic Carbon
IHT	Interspecies Hydrogen Transfer
IWA	International Water Association
LCFAs	Long-Chain Fatty Acids
L-FVW	Liquid Fruit and Vegetable Waste
MAE	Mean Absolute Error
MCP	Multiple Country Publications
MRW	Mixed Rice Waste
MSHS	Multi-Stage High Solids Process
MSLS	Multi-Stage Low Solids Process
MSW	Municipal Solid Waste
N_{org}	Total Organic Nitrogen
NSE	Nash-Sutcliffe Efficiency
ODEs	Ordinary Differential Equations
OFMSW	Organic Fraction of Municipal Solid Waste
OLR	Organic Loading Rate
RMSE	Mean Square Error
RS	Rice Straw
RW	Rice Waste
SAO	Syntrophic Acetate Oxidation
S_{cat}	Total Alkalinity
SCP	Single Country Publications
SD-AD	Semi-Dry Anaerobic Digestion
S-FVW	Solid Fruit and Vegetable Waste
SMS	Spent Mushroom Substrate

SRT	Solids Retention Time
SSB	Solid-State Stratified Bed
SSHS	Single Stage High Solids Process
SSLS	Single Stage Low Solids Process
TAN	Total Ammonia Nitrogen
thCOD	Theoretical Oxygen Demand
TIC	Total Inorganic Carbon
TOC	Total Organic Carbon
TP-orthoP	Organic Phosphorus
TS	Total Solids
UASB	Upflow Anaerobic Sludge Blanket
VCR	Vegetable Crop Residues
VFA	Volatile Fatty Acids
VOA	Volatile organic acids
VS	Volatile Solids
VW	Vegetable Waste
W-AD	Wet Anaerobic Digestion
WS	Web of Science Core Collection

LIST OF ACRONYMS

%	Percentage
$[S^*]_{(l)}$	Molar concentration of the specific gas in the aqueous bulk of the reactor at thermodynamic equilibrium [L^{-3}]
$[S]_{(gas)}$	Molar concentration of the specific gas in the gaseous phase [L^{-3}]
$[S]_{(l)}$	Molar concentration of the specific gas in the aqueous phase [L^{-3}]
$[S]_g$	Molar concentration of the specific gas in the gaseous phase [L^{-3}]
C	Carbon
C/N	Carbon to nitrogen ratio
C/N/P	Carbon to nitrogen to phosphorous ratio
CH_4	Methane
CO_2	Carbon dioxide
CO_2/HCO_3^-	Carbon dioxide to bicarbonate
COD_s-VFA	Soluble Cod converted to VFA
H2	Hydrogen
HCO_3^-	Bicarbonate
k_{ac}	Uptake of acetate
kg	Kilogram
k_{La}	Global transfer coefficient of the specific gas [T^{-1}]
$k_{m,j}$	Specific substrate degradation rate
k_mX_{ac}	Maximal acetate uptake rate
k_{pro}	Up-take of propionate
$K_{s,j}$	Saturation coefficient
K_{Sac}	Half-saturation constant
k_{sbk}	Disintegration of complex organic matter
k_t	Volumetric liquid/gas mass transfer coefficient
m^3	Cubic meter
N	Nitrogen
NH_3	Ammonia
NH_4^+/NH_3,	Ammonium/ammonia
Q	Influent flowrate [$L^3\ T^{-1}$]
q_{inp}	Inlet flow

q_{out}	Outlet flow
$Q_{out,g}$	Total effluent gas flowrate from the digester [L^3 T^{-1}]
S	Substrate concentration [M L^{-3}]
S_{in}	Substrate concentration in the digester influent [M L^{-3}]
VFA/VFA^-	VFA Dissociation to VFA association
V_{gas}	Volume of the digester headspace [L^3]
V_{liq}	Liquid working volume of the anaerobic digester [L^3]
VS/TS	Volatile solid to total solids ratio
X_{c4}	Butyric and valeric acids degraders
X_{c5}	Valerate degrader
ν_j	Biochemical rate coefficient for process j involving the specific gas [M L^{-3} T^{-1}]
ρ_j	Specific kinetic rate for process j involving the specific gas [L^{-3} T^{-1}]

CONTENTS

ABSTRACT ..... **VIII**
RESUMO ..... **X**
LIST OF FIGURES ..... **XII**
LIST OF TABLES ..... **XIV**
LIST OF ABBREVIATIONS ..... **XVI**
LIST OF ACRONYMS ..... **XIX**
CONTENTS ..... **XXI**

1 GENERAL INTRODUCTION AND STRUCTURE OF THE THESIS **25**
1.1 Introduction to the research topic **25**
1.2 Mathematical modeling of anaerobic processes **33**
1.2.1 Modeling process ***35***
1.2.2 Mass balance ***38***
1.2.3 Stoichiometry ***43***
1.2.4 Kinetics ***45***
1.3 Thesis Structure **46**

2 GENERAL OBJECTIVE AND SPECIFIC OBJECTIVES **49**
2.1 General objectives **49**
2.2 Specific objectives **49**

3 METHODOLOGICAL STRATEGY AND RESEARCH PLAN **50**
3.1 System description and modeling strategy **51**

4 ARTICLE I: ANAEROBIC DIGESTION MODEL NO. 1 APPLIED TO BIOENERGY GENERATION FROM FRUIT AND VEGETABLE WASTE IN UPFLOW ANAEROBIC SLUDGE BLANKET REACTORS **54**
4.1 Introduction **55**
4.2 Material and methods **57**
4.2.1 Experimental set-up ***57***
4.2.2 Experimental program ***58***

4.2.3 Experimental analysis 59
4.3 Model development and simulation 59
4.3.1 Anaerobic Digestion Model No. 1 59
4.3.2 Determination of components and units considered for the model 61
4.3.3 Model implementation 61
4.3.4 Statistics and predictive performance 63
4.3.4.1 Model efficiency coefficients 63
4.3.4.2 Sensitivity analysis and parameter estimation 64
4.4 Results and discussion 65
4.4.1 Characterization of the subtract influent 65
4.4.2 Experimental results and reactor performance 66
4.4.3 Fractionation of fruit and vegetable waste for biodegradation 69
4.4.4 Sensitivity analysis 71
4.4.5 Comparison of simulated results with experimental results 74
4.4.6 Simulation of the model variables after adjustment 78
4.4.7 Evaluation of parameter interaction 80
4.5 Possible future direction 83
4.6 Conclusion 84

5 ARTICLE II: ADVANCING ADM1 FOR HYDROGEN PRODUCTION VIA DARK FERMENTATION OF LIQUID FRUIT AND VEGETABLE WASTE 86
5.1 Introduction 87
5.2 Materials and methods 89
5.2.1 Experimental set-up 89
5.2.2 Experimental design 90
5.2.3 Experimental analysis 91
5.3 Model development and simulation 92
5.3.1 Determination of components and units considered for the model 92
5.3.1.1 Estimation of Kinetic and Stoichiometric Parameters–Model Prediction 92
5.3.1.2 Determination and verification of stoichiometric coefficients of metabolic products from monosaccharide fermentation 94
5.3.2 Statistics and predictive performance 99
5.3.2.1 Statistical assessment of model performance 99

5.3.2.2 Sensitivity assessment and calibration strategy 100
5.3.2.3 Model calibration and validation procedure 102
5.4 Results and discussion 103
5.4.1 Reactors performance 103
5.4.2 Initial model predictions with default parameters 103
5.4.3 Sensitivity analysis 105
5.4.4 Model calibration and parameter estimation 109
5.4.5 Extension of the model with additional metabolic pathways 115
5.4.5.1 Lactate formation route and lactate consumption route 116
5.4.5.2 Ethanol formation route 118
5.4.6 Integrated model performance and parameter interaction across operational phases 119
5.4.7 Suggested improvements for dark fermentation modeling 121
5.5 Possible future direction 122
5.6 Conclusion 123

6 ARTICLE III: BIBLIOMETRIC ANALYSIS OF ANAEROBIC DIGESTION MODEL NO. 1 (ADM1) FOR DRY ANAEROBIC DIGESTION OF FRUIT AND VEGETABLE WASTE, FOOD WASTE, AND ORGANIC FRACTION OF MUNICIPAL SOLID WASTE 125
6.1 Introduction 126
6.2 Anaerobic digestion of FVW 129
6.3 Types of processes, reactors, and technologies 132
6.4 Bibliometric methods 135
6.4.1 Data collection 135
6.4.2 Software for bibliometric analysis and scientific mapping 136
6.4.3 Data analysis 137
6.4.3.1 Publishing trend 139
6.4.3.2 Contributions of countries and institutions 144
6.4.3.3 Research trends and hot spots: keyword analysis 146
6.5 Models for simulating anaerobic digestion processes 147
6.5.1 ADM1 149
6.5.1.1 Modifications in ADM1 155
6.5.1.2 Simplification in ADM1 162

6.6 Possible future direction 163
6.7 Conclusions 165

7 FUTURE RESEARCH DIRECTIONS 166
8 GENERAL CONCLUSION 168
9 LIST OF REFERENCE 171
10 APPENDIX A: GENERAL INTRODUCTION AND STRUCTURE OF THE THESIS 200
11 APPENDIX B: METHODS AND TOOLS 202
12 APPENDIX C: SUPPLEMENTARY MATERIAL – ARTICLE I 203
13 APPENDIX D: SUPPLEMENTARY MATERIAL – ARTICLE II 207
14 APPENDIX E: SUPPLEMENTARY MATERIAL – ARTICLE III 209
15 INDEX 210

1 GENERAL INTRODUCTION AND STRUCTURE OF THE THESIS

1.1 Introduction to the research topic

Food waste has become one of the most pressing environmental and socio-economic challenges worldwide. Rapid population growth, urbanization, and changes in consumption patterns have significantly increased the generation of municipal solid waste worldwide, particularly its organic fraction (FAO, 2021, 2023; UNEP, 2024). Organic waste represents a substantial proportion of global waste streams and is largely composed of biodegradable materials originating from food production and consumption systems. Globally, approximately 13% of food produced is lost along the supply chain before reaching retail stages, while an additional 19% is wasted at the retail and consumer levels (FAO, 2023; UNEP, 2024). These losses occur at different stages, including harvesting, post-harvest handling, transportation, processing, distribution, and commercialization, often as a result of strict quality standards and logistical inefficiencies. As a consequence, large quantities of edible and inedible biomass are discarded before reaching the final consumer. Furthermore, food loss and waste are responsible for approximately 8–10% of global greenhouse gas emissions, highlighting the environmental implications associated with inadequate waste management (IPCC, 2019).

The economic dimension of food production further highlights the relevance of this issue. The global food system represents one of the largest sectors of the world economy, involving extensive production, processing, transportation, commercialization, and distribution chains that generate millions of jobs and contribute significantly to national economies. According to (FAO, 2021, 2023), the economic value of global food loss and waste exceeds hundreds of billions of dollars annually, reflecting inefficiencies across the entire supply chain. In Brazil, the agrifood sector plays a particularly important role in the national economy. According to the Brazilian Institute of Geography and Statistics (IBGE, 2026), the agricultural sector grew by 11.7% in 2025 compared with the previous year, reaching a gross added value of approximately R$ 775.3 billion, corresponding to about 6.1% of the national gross domestic product (GDP). However, large volumes of organic residues are generated throughout this production chain, especially during harvesting, processing, distribution, and retail stages. In particular, wholesale supply centers (CEASAs), which operate as major hubs for the distribution of fruits and vegetables across Brazilian cities, handle thousands of tons of produce daily and consequently generate substantial quantities of organic residues (Companhia

Nacional de Abastecimento) (CONAB, 2023), The continuous growth of food production and consumption has therefore been accompanied by a parallel increase in the generation of organic waste (BRASIL, 2026a, 2026b). From a circular economy perspective, these residues represent not only an environmental challenge but also a significant opportunity for resource recovery. Their valorization through bioenergy and bioproduct generation could create new revenue streams, support local job creation, and strengthen sustainable waste management strategies within urban food supply chains.

The fruit and vegetable sector is particularly affected by these losses due to high perishability and strict aesthetic requirements for market acceptance (SHEN et al., 2013). Consequently, significant volumes of fruit and vegetable waste (FVW) are generated worldwide (SILVA JÚNIOR et al., 2022). When improperly managed, these residues are commonly disposed of in landfills, leading to the release of greenhouse gas emissions and contributing to environmental degradation (LIU et al., 2012).

Interest has grown in alternatives that enable the valorization of FVW by converting it into inputs for energy production and higher-value-added products (SILVA et al., 2024). In this context, anaerobic digestion (AD) has emerged as one of the most promising technologies (SHI et al., 2017). Widely recognized in wastewater treatment and increasingly applied to the valorization of solid organic waste, this biological process offers several advantages, including operational flexibility, the ability to process a wide range of organic substrates, and the generation of valuable products such as methane, hydrogen, and organic acids (CHERNICHARO, 2007a; JENKINS et al., 2008). Additionally, AD requires relatively low land area, produces less sludge compared to aerobic treatment processes, and can be implemented under diverse operational configurations (VALENCIA; ZHANG; CHANG, 2022; ZAMRI et al., 2021). These characteristics make the technology particularly suitable for regions with warm climates, such as Brazil, where ambient temperatures favor biological conversion processes and support its application across different production scales. Understanding the current relevance of AD in waste valorization requires examining its technological development over time (CHERNICHARO, 2007a; CHONG et al., 2012; VON SPERLING; CHERNICHARO, 2005).

The use of AD as a technological process for the treatment and valorization of organic waste has evolved significantly over the past decades. Early applications of AD date back to the late nineteenth and early twentieth centuries, when the process was primarily associated with sewage treatment and the stabilization of organic sludge (BUSWELL; SOLLO,

1948). During this period, the technology was mainly developed within the sanitation sector, focusing on organic matter removal and sludge management. From the 1970s onward, the global energy crisis stimulated renewed interest in AD as a source of renewable energy, promoting the development of biogas recovery systems and expanding the application of AD to agricultural residues, animal manure, and food waste. Subsequent advances in microbiology, process engineering, and environmental sciences enabled the implementation of more efficient reactor configurations and process control strategies (WAN et al., 2013).

More recently, research has increasingly focused on the concept of anaerobic biorefineries, emphasizing the integrated production of multiple biofuels and bioproducts, including methane, hydrogen, and organic acids (CARECCI et al., 2024; CREMONEZ et al., 2021; DE BUCK; POLANSKA; VAN IMPE, 2020). Within this context, AD has evolved from a conventional waste treatment technology into a key platform for circular bioeconomy strategies and sustainable biofuel production (EMEBU; PECHA; JANACOVA, 2022). The increasing technological complexity of anaerobic systems, combined with the diversity of substrates and operational configurations, has created the need for tools capable of describing, predicting, and optimizing process performance. In this context, mathematical modeling has emerged as an essential approach for interpreting the complex biochemical interactions occurring during AD and for supporting reactor design, control, and scale-up.

A major milestone in the scientific understanding of AD occurred in 2002 with the development of the Anaerobic Digestion Model No. 1 (ADM1) (BATSTONE et al., 2002). Prior to its formulation, several modeling approaches had been proposed to describe AD processes, including empirical correlations and simplified kinetic models based on first-order reactions or Monod-type expressions. Although these models provided useful insights into specific aspects of the process, they generally offered limited representation of the complex biochemical pathways and microbial interactions involved in AD.

The ADM1 was developed by the International Water Association (IWA) Task Group on Mathematical Modelling of AD Processes with the objective of providing a standardized and comprehensive framework for describing anaerobic systems (BATSTONE et al., 2002). The model introduced a structured and mechanistic representation of the main biochemical stages of digestion, incorporating multiple microbial groups, intermediate compounds, and physicochemical processes occurring in the system (FRUNZO et al., 2019). In addition to its comprehensive structure, ADM1 was designed to be flexible and modular, allowing adaptations, extensions, and parameter adjustments for different substrates, reactor

configurations, and operational conditions. Since its introduction, ADM1 has become a reference framework for the simulation, analysis, and optimization of anaerobic systems, playing a central role in the understanding, design, and scale-up of biological processes used for organic waste valorization.

Although ADM1 represents a comprehensive framework for describing AD processes, it was originally developed and calibrated primarily for sewage sludge digestion in continuous stirred tank reactors (CSTRs) (BATSTONE et al., 2015). Consequently, its direct application to other substrates, reactor configurations, and operational conditions may require adjustments. Organic wastes such as FVW present physicochemical and biodegradation characteristics that differ substantially from sewage sludge, including higher fractions of readily biodegradable carbohydrates, faster hydrolysis rates, and greater susceptibility to rapid acidification. In addition, variations in reactor design, such as high-solids systems, batch configurations, or multi-stage processes, introduce hydrodynamic and operational differences that are not fully represented in the original ADM1 structure. For these reasons, several studies have proposed modifications, parameter recalibrations, and extensions of the model in order to better capture the specific dynamics of different substrates and reactor systems, thereby improving its predictive capability and applicability to a broader range of anaerobic technologies (GALI et al., 2009; GE et al., 2023).

FVW represents a highly reactive and compositionally dynamic substrate, characterized by elevated moisture content, high fractions of readily biodegradable carbohydrates, and pronounced seasonal variability (DE MENEZES et al., 2024). These features promote rapid hydrolysis and acidogenesis, often leading to fast accumulation of volatile fatty acids (VFA) and potential process instability. As a result, modeling the AD of FVW requires careful consideration of substrate-specific kinetics and metabolic interactions that may not be fully represented in models originally calibrated for sewage sludge.

The AD process can be classified according to operational and structural criteria. One of the most commonly used parameters is the substrate solids content. Based on total solids (TS), AD can be classified as wet digestion (W-AD), operating with TS below 10%; semi-dry digestion (SD-AD), with TS between 10 and 15%; and dry digestion (D-AD), in which TS exceeds 15% (AJAY et al., 2011; ARELLI et al., 2018; BOLLON et al., 2011; ELSAMADONY; TAWFIK; SUZUKI, 2015; GARCIA-BERNET et al., 2011; KOTHARI et al., 2014; SALAMAT et al., 2022; WANG et al., 2023). This distinction directly affects material handling, mixing strategies, reactor configuration, and the overall performance of the

process. Another classification approach considers the organization of metabolic stages into single-phase systems, in which the entire digestion occurs within a single reactor, or two-phase systems, in which the initial stages are separated from the methanogenic stages, thereby promoting greater stability and control. AD can also be integrated into biorefinery platforms for the combined production of biofuels, biofertilizers, and chemical compounds, thereby expanding its role within circular production chains.

AD is a complex biological process that can be segregated into five fundamental stages: disintegration, hydrolysis, acidogenesis, acetogenesis, and methanogenesis (CHERNICHARO, 2007a, 2007b; CHERNICHARO et al., 2015). Disintegration corresponds to the initial stage, in which particulate organic matter is fragmented into smaller particles through physical, chemical, and enzymatic actions, increasing the substrate surface area and facilitating subsequent degradation (GUERRERO et al., 2019; MIHI et al., 2024; VAVILIN et al., 2008; WELLINGER; MURPHY; BAXTER, 2013). This is followed by hydrolysis, a stage considered limiting for most solid wastes, in which polymers such as carbohydrates, proteins, and lipids are converted into soluble molecules, including simple sugars, amino acids, and fatty acids (BATSTONE; TAIT; STARRENBURG, 2009; VAVILIN et al., 2008).

The third stage is acidogenesis, in which the hydrolyzed products are metabolized by acidogenic bacteria, resulting in the formation of volatile organic acids, alcohols, hydrogen, carbon dioxide, and other intermediates. This stage accounts for a large share of the production of compounds that determine the medium's acidity and directly influence process stability (LIN et al., 2021a; XU et al., 2014b). Subsequently, acetogenesis takes place, a phase in which these more complex organic intermediates are mainly converted into acetate, hydrogen, and carbon dioxide by acetogenic microorganisms. This conversion is essential to enable progression to the final stage, since only a limited number of specific compounds can be utilized by methanogenic microorganisms (BONK et al., 2019; CHO et al., 2013; DEMIREL; SCHERER, 2008).

At the final stage, it is necessary to understand the biochemical pathways that enable biogas formation. Methanogenesis comprises two main metabolic pathways: the hydrogenotrophic and acetoclastic pathways. In the hydrogenotrophic pathway, methanogenic archaea use hydrogen as an electron donor to reduce carbon dioxide, producing methane and water. This pathway is typical of conditions with significant hydrogen availability and plays an essential role in maintaining the redox balance of the system, since the efficient removal of hydrogen allows the other stages of digestion to proceed properly (GUERRERO et al., 2019; MIHI et al., 2024; VAVILIN et al., 2008; WELLINGER; MURPHY; BAXTER, 2013).

In the acetoclastic pathway, methanogenic microorganisms directly convert acetate into methane and carbon dioxide. This route is particularly important because a large fraction of the organic carbon degraded during AD is ultimately transformed into acetate during the preceding metabolic stages. In many anaerobic systems, acetoclastic methanogenesis represents the dominant pathway for methane formation. However, its efficiency depends on stable environmental conditions, particularly neutral pH and low concentrations of inhibitory compounds such as free ammonia and VFA (CHERNICHARO, 2017; ROMERO-GÜIZA et al., 2016).

Process stability can also be affected by inhibitory compounds generated during digestion. Among these, ammonia plays a particularly important role. The equilibrium between ammonium (NH_4^+) and free ammonia (NH_3) depends strongly on pH and temperature, and elevated concentrations of free ammonia may inhibit methanogenic microorganisms, leading to reduced methane production and process instability (NI, 1999). Therefore, understanding ammonia dynamics is essential for both process control and accurate modeling of anaerobic systems (KOCH et al., 2010, 2011; LÜBKEN et al., 2007; WEINRICH et al., 2021).

The acetoclastic and hydrogenotrophic pathways coexist and interact in a complementary manner. The predominance of one route over the other depends on factors such as substrate composition, temperature, intermediate accumulation, and microbial community structure (SILVA et al., 2022, 2023). Process stability therefore requires an appropriate balance between these pathways, since excessive accumulation of hydrogen or acetate may compromise the overall performance of AD. Based on these biochemical foundations, it becomes necessary to understand how the process can be technically implemented. AD exhibits considerable technological versatility and can be applied across different reactor configurations, each suited to the substrate characteristics and process objectives. For wastes with low solids content, continuous stirred systems, upflow reactors, and hybrid units combining suspended and attached biomass are commonly employed. For materials with higher solids concentrations, D-AD technologies stand out due to their lower water demand and greater volumetric compactness, and are widely applied to substrates such as FVW and the organic fraction of municipal solid waste (CHERNICHARO, 2007a).

AD can be designed as single-phase or two-phase systems and can also operate in continuous, semicontinuous, or batch modes. Recent studies have demonstrated the successful application of a wide range of configurations, such as Upflow Anaerobic Sludge Blanket (UASB), CSTR, Anaerobic Sequencing Batch Reactor (ASBR), anaerobic baffled reactors

(ABR), Anaerobic Structured-Bed Reactor (AnSTBR), tubular reactors, solid–liquid hybrid systems, percolating beds, and stratified beds. For D-AD, well-established technologies such as DRANCO, Valorga, Kompogas, and Bekon stand out, being characterized by high tolerance to solids and good conversion efficiencies (DA SILVA JÚNIOR et al., 2025; ESPOSITO et al., 2011a; FUESS; ZAIAT; DO NASCIMENTO, 2019; JUNG et al., 2013; LIMA; MARTINS, 2014; SHEFALI; THEMELIS, 2002). The selection of an appropriate reactor configuration depends on several operational and environmental factors, including substrate characteristics, organic loading rate (OLR), solids content, temperature regime, and the available installation area. Additional aspects such as the desired bioconversion pathway, local climatic conditions, and the biochemical profile of the waste also influence reactor design and operational strategy. This broad availability of systems demonstrates that AD constitutes a flexible technological platform, capable of addressing both conventional treatment processes and advanced strategies for the valorization of complex organic wastes (CHERNICHARO, 2017).

Despite its strengths, the application of ADM1 to UASB reactors presents additional challenges. The granular biomass, vertical plug-flow behavior, and partial solids retention characteristic of UASB systems generate spatial gradients in substrate and intermediate concentrations that are not fully captured by the standard ADM1 framework (DEL NERY et al., 2018; REN et al., 2009). This can lead to discrepancies between predicted and observed VFA accumulation, methane production, and inhibition dynamics, particularly under high OLRs or fluctuating feeding regimes. Such reactor-specific phenomena highlight the need for careful calibration and adaptation of ADM1 parameters when modeling UASB systems (CHEN et al., 2015; POKORNA-KRAYZELOVA et al., 2017).

The diversity of metabolic pathways, the complexity of microbial consortia, and the variety of technological configurations make the AD process highly dynamic (BATSTONE et al., 2015; CHERNICHARO, 2007a), which requires tools capable of describing, predicting, and optimizing its behavior. In this context, mathematical modeling emerges as a fundamental tool for understanding the operation of anaerobic systems, predicting their dynamic behavior, and supporting the optimization of bioenergy production from complex substrates such as FVW (BOCHER et al., 2008; LIN et al., 2021b). The development and calibration of robust models therefore represent an important step toward improving the efficiency, stability, and scalability of anaerobic technologies applied to organic waste valorization.

Historically, AD was first consolidated as a wastewater treatment technology. With the advancement of circular economy concepts and the increasing generation of solid organic

waste, the focus progressively shifted toward the valorization of high-solids substrates such as FVW (MEENA et al., 2020). Parallel to this evolution, mathematical modeling advanced from simplified kinetic expressions to structured mechanistic frameworks such as ADM1, enabling deeper understanding and predictive control of increasingly complex systems.

Despite the considerable advances in AD technologies and modeling frameworks, important challenges remain when treating highly biodegradable substrates such as FVW. This substrate is characterized by rapid degradation of readily available carbohydrates, high moisture content, and significant compositional variability, which can promote rapid acidification and compromise process stability. Moreover, FVW can be processed under different operational strategies, ranging from diluted liquid systems to high-solids digestion processes, each presenting distinct mass transfer conditions and microbial dynamics.

In addition, this substrate may be directed toward different biochemical conversion pathways, including methane production through conventional AD or hydrogen generation via dark fermentation (DF). These operational and metabolic variations introduce significant complexity to process prediction and highlight limitations in the direct application of existing modeling frameworks without proper calibration and adaptation. Therefore, further research integrating experimental data with mechanistic modeling approaches is required to improve the understanding, simulation, and predictive capacity of anaerobic systems treating highly reactive organic substrates.

In conclusion, the scope of this research addresses the critical need to optimize the valorization of FVW through anaerobic digestion, moving beyond conventional waste disposal toward a circular bioeconomy. While AD presents a robust technological platform for bioenergy production, its application to highly reactive substrates like FVW poses significant stability challenges that current standardized models, such as the original ADM1, do not fully capture. Therefore, this study is justified by the necessity of adapting and calibrating mechanistic frameworks to better describe the complex biochemical dynamics and inhibitory risks associated with these residues. By integrating experimental observations with refined modeling strategies, this work seeks to provide a reliable tool for predicting process performance, ultimately supporting the scalability and efficiency of anaerobic biorefineries in the context of the Brazilian agrifood sector.

1.2 Mathematical modeling of anaerobic processes

According to the theoretical foundations established by Aris (1979), Bassanezi (2002), and Davis, Lin, and Segel (1976), a mathematical model consists of a set of equations constructed to represent a specific entity, commonly referred to as the prototype. This prototype may correspond to a physical, biological, chemical, or conceptual system, whose behavior is governed by well-defined mechanisms and interactions. Mathematical modeling thus emerges as an intermediary between theory and observation, translating conceptual assumptions into formal expressions capable of describing, interpreting, and predicting the behavior of real systems. Although the notion of a model appears in both empirical sciences and mathematics, its meaning varies across disciplinary contexts. In all cases, however, models rely on an underlying non-linguistic entity whose properties must be consistent with the principles imposed by the supporting theory.

Within this framework, it is essential to distinguish between the prototype, the theoretical assumptions, and the mathematical model itself. The prototype represents the real system of interest, such as an anaerobic reactor or a microbial consortium. The theoretical assumptions define the conceptual structure that governs the interpretation of the system, including hypotheses regarding kinetics, transport phenomena, and biological interactions. The mathematical model is a formal representation of these assumptions, expressed as equations, variables, and parameters that approximate the behavior of the prototype. This distinction clarifies the separation between the tangible system, the abstract theoretical basis, and the mathematical structure used to analyze system dynamics.

From a methodological standpoint, one of the most widely adopted approaches for constructing mathematical models is the application of fundamental laws of nature, formulated from experimental observations and repeatedly validated within scientific practice. In this approach, the behavior of a system is described by balance equations, or equations of motion, that express the conservation of mass, energy, or charge and relate fluxes, reaction rates, and source terms to the system's state variables. These equations may be formulated within different mathematical frameworks, such as Newtonian, Lagrangian, or Eulerian descriptions, depending on the nature of the processes involved and the level of abstraction required.

An alternative and equally general approach to model construction is based on variational principles, which rely on global statements about system behavior. In this formulation, the governing equations arise from the extremization of a scalar functional, such

as the action, and naturally reveal the system's structural properties, including symmetries and conservation laws in space and time. Although variational formulations are more commonly associated with physical systems, their conceptual relevance lies in providing a unified perspective on the origin and internal consistency of the governing equations.

In situations where the fundamental laws are not explicitly known, or where the complexity of the system precludes a direct formulation from first principles, model development may also rely on analogies with previously investigated phenomena. In this case, formal similarities between distinct systems are exploited, allowing similar mathematical structures to describe processes that are physically different but dynamically comparable. Regardless of the approach adopted, the modeling process ultimately leads to a system of differential equations that describes the temporal evolution of the relevant variables and forms the basis for theoretical analysis, numerical simulation, and practical applications in design and operation (DAVIS; LIN; SEGEL, 1976; SAMARSKII; MIKHAILOV, 2002).

In the context of AD, mathematical models inherently simplify reality by neglecting certain details while retaining the dominant mechanisms that control system behavior. The prototype embodies the set of valid propositions that the model seeks to satisfy, and the model's predictive and descriptive capabilities increase as additional process features are incorporated. These features include external factors such as temperature, substrate composition, and operational mode, as well as internal factors such as microbial population dynamics, metabolic pathways, inhibition phenomena, and gas–liquid mass transfer. However, the optimal level of model complexity depends strongly on its intended purpose, as excessive detail may compromise parameter identifiability, calibration robustness, or interpretability.

Anaerobic reactors can therefore be modeled at different levels of abstraction, depending on the assumptions adopted and the equations selected to represent the process. At the simplest level, a batch reactor may be described by a basic mass balance capturing substrate consumption over time. This formulation can be progressively extended to include microbial growth kinetics, temperature dependence, pH dynamics, gas production, and transport processes, leading to increasingly comprehensive and mechanistic descriptions. Such a hierarchical construction illustrates how mathematical modeling provides a flexible framework in which conceptual understanding, experimental data, and theoretical principles converge, enabling a systematic analysis of anaerobic processes across multiple scales.

Finally, it is important to distinguish between the stages of modeling and simulation. Mathematical modeling refers to the formulation of an abstract representation of a

system based on theoretical assumptions and mathematical relationships. In contrast, simulation corresponds to the numerical implementation and solution of the resulting equations. Together, these stages allow the extraction of essential features of anaerobic processes, support empirical validation, and provide a rational basis for interpretation, optimization, and control (ARIS, 1979; BASSANEZI, 2002).

Building on these conceptual and methodological foundations, the development of mathematical models for anaerobic processes involves a systematic sequence of steps that translate theoretical assumptions into operational equations capable of describing reactor behavior. This modeling process requires the definition of system boundaries, identification of relevant state variables, formulation of conservation equations, and the selection of appropriate kinetic and transport expressions to represent the dominant mechanisms of the process (ARIS, 1979; BASSANEZI, 2002; BATSTONE et al., 2015; DAVIS; LIN; SEGEL, 1976). In AD systems, these steps become particularly important due to the complexity of the microbial consortia, the diversity of biochemical pathways, and the strong interactions between biological reactions and physicochemical phenomena. Consequently, different modeling strategies have been proposed to represent anaerobic processes with varying degrees of detail and mechanistic interpretation. The main characteristics of these approaches and their application to AD systems are discussed in the following section.

1.2.1 Modeling process

A mathematical model for AD must be capable of predicting system behavior under different operational conditions and supporting performance improvement through process optimization. The use of models is fundamental for understanding the internal dynamics of anaerobic systems, since they allow the evaluation of complex interactions among substrates, intermediates, microbial groups, and environmental variables. Several authors highlight that modeling plays a central role in interpreting process behavior, guiding experimental planning, and supporting reactor design and control strategies (KEGL et al., 2025; LAUWERS et al., 2013; XU; LI; WANG, 2015).

Given the diversity of modeling approaches, selecting an appropriate model depends on several factors, including the specificity of the problem being analyzed, the level of knowledge about the system, the availability of experimental data, and the intended application. In general, models can be classified according to their level of complexity as empirical,

deterministic, or stochastic. They can also be categorized according to the degree of mechanistic knowledge incorporated into their structure, leading to the well-established classifications of black-box, grey-box, and white-box models. Black-box models rely exclusively on input–output relationships and do not explicitly represent the underlying physical or biochemical processes. Grey-box models combine mechanistic understanding with adjustable parameters that possess physical meaning but require calibration. White-box models are formulated from first principles and aim to explicitly represent the biochemical and physicochemical mechanisms governing the system (BRITO-ESPINO et al., 2020; HU et al., 2018; LAUWERS et al., 2013; REGMI et al., 2019).

In the context of AD, different modeling strategies have been proposed to represent the degradation of organic matter and the formation of biogas. According to Kelg et al. (2025), these models can broadly be grouped into mechanistic, kinetic, and phenomenological approaches. Kinetic models typically describe microbial growth and substrate consumption using simplified mathematical expressions, such as first-order kinetics, logistic growth models, or Gompertz-type functions. These formulations are frequently used to describe single-stage or multistage degradation processes and to represent microbial growth patterns under controlled experimental conditions (GOMPERTZ, 1825; VOGELS et al., 1975).

Phenomenological models, in contrast, are generally based on statistical relationships between input and output variables. These approaches include linear and nonlinear regression models as well as more advanced machine learning techniques, such as Random Forests, Support Vector Machines, and Artificial Neural Networks. Such methods are particularly useful for prediction when large datasets are available, although they often lack direct interpretability in terms of the underlying biochemical mechanisms (BREIMAN, 2001; CORTES; VAPNIK, 1995; MCCULLOCH; PITTS, 1943).

Mechanistic models represent a different class of approaches, as they explicitly incorporate the biochemical and physicochemical transformations occurring within the system. These models allow the simulation of substrate consumption, formation of intermediate compounds, microbial growth dynamics, and inhibition phenomena. Mechanistic frameworks in AD modeling include elementary digestion models, such as the ADM1 and BioModel, as well as more advanced formulations that incorporate mass transfer phenomena or spatial heterogeneity through diffusion models and computational fluid dynamics (CFD) approaches (DANCKWERTS, 1951; HUA; WU; KUMAR, 2005; UMMAH, 2002; VERSTEEG; MALALASEKERA, 1999).

Among these approaches, the ADM1 is considered one of the most comprehensive mechanistic models for describing the AD process (BATSTONE et al., 2002, 2015). The model was originally formulated to represent the biochemical and physicochemical processes occurring in CSTR, providing a structured framework for describing substrate degradation, microbial activity, and biogas production. BioModel, proposed earlier, also represents a mechanistic formulation based on mass balances, initially developed to describe the digestion of manure and later extended to more complex substrates (ANGELIDAKI; ELLEGAARD; AHRING, 1993, 1999).

ADM1 stands out among AD models due to its structured representation of biochemical pathways, its compatibility with mass conservation principles, and its flexibility for structural modification. The model is organized using a matrix-based structure that describes the stoichiometric relationships between microbial processes and chemical components, allowing the systematic incorporation of new metabolic pathways or process conditions. These characteristics have made ADM1 a widely adopted framework for the analysis, simulation, and optimization of AD systems.

Despite its widespread use, important challenges remain regarding the application of ADM1 to complex substrates such as FVW. Most studies have focused on conventional low-solids AD systems, while the behavior of highly biodegradable substrates with rapid hydrolysis rates and variable composition remains less explored. In addition, inconsistencies exist in the literature regarding structural model modifications, hydrolysis kinetics adjustments, and parameter calibration strategies, particularly under high-solids or strongly acidogenic conditions.

Before presenting the mathematical formulation of AD models, it is necessary to establish the fundamental physical principles that describe the transformations occurring within the reactor. These transformations are mathematically represented through mass balances, which constitute the fundamental framework for describing the temporal evolution of chemical species within the system. In anaerobic reactors, the application of mass conservation enables the quantitative description of biochemical reactions, physicochemical processes, and transport phenomena that govern substrate degradation and product formation. Therefore, mass balance equations provide the link between the conceptual representation of the process and its mathematical formulation, forming the basis for the dynamic models used in AD simulation.

1.2.2 Mass balance

A reactor is a system designed to carry out chemical, biochemical, and/or physicochemical reactions under controlled conditions of temperature, pH, pressure, and medium composition. Its operation is based on the interaction between a substrate, whether solid or liquid waste, and a consortium of microorganisms (sludge), to promote the degradation, conversion, or production of specific compounds. Several types of reactors can be employed for this purpose, but all follow fundamental operating principles (WANG; ZHONG, 2007).

Regardless of the configuration adopted, the behavior of any reactor is governed by the principle of mass conservation, which states that mass cannot be created or destroyed, but only transformed. This means that the total mass of the system remains constant, although its components may be converted into different forms, phases, or states of aggregation (FAGHRI; ZHANG, 2006; HASELI, 2020). The mass balance, therefore, constitutes a mathematical tool that describes these transformations, in accordance with the Laws of Thermodynamics, particularly the First Law, related to energy conservation, and the Second Law, related to entropy (GIRARDI NETO; SILVA; PINHEIRO, 2017; SMITH et al., 2019) as expressed in Eq. [1.1]. Although AD models are typically formulated through mass balances, the transformations occurring within the reactor must be consistent with the fundamental laws of thermodynamics.

$$\Delta U = Q - W \qquad [1.1]$$

Where ΔU represents the variation of internal energy of the system (J), Q is the heat transferred to the system (J), and W is the work performed by the system on its surroundings (J). This equation represents the First Law of Thermodynamics and expresses the principle of energy conservation in closed systems, indicating that any variation in internal energy results from the balance between heat transfer and mechanical work. Although AD models are primarily formulated through mass balances, the biochemical reactions occurring in the reactor are intrinsically associated with energy transformations and thermodynamic constraints that govern microbial metabolism and reaction feasibility.

For open systems such as biochemical reactors, the energy balance must also account for mass flows entering and leaving the control volume, as shown in Eq. [1.2]. These flows transport enthalpy, kinetic energy, and potential energy across the system boundaries.

$$\frac{dE_{vc}}{dt} = \dot{Q} - \dot{W} + \sum \dot{m}_{in}\left(h_{in} + \frac{v_{in}^2}{2} + gz_{in}\right) - \sum \dot{m}_{out}\left(h_{out} + \frac{v_{out}^2}{2} + gz_{out}\right) \quad [1.2]$$

Where E_{vc} is the total energy stored in the system (J), t is time (s), $\dot{Q}$ represents the rate of heat transfer to the system (W), and $\dot{W}$ is the rate of work performed by the system (W). The terms $\dot{m}_{in}$ and $\dot{m}_{out}$ denote the mass flow rates entering and leaving the control volume (kg s^{-1}), respectively. The parameter h represents the specific enthalpy of the stream (J kg^{-1}), v is the flow velocity (m s^{-1}), g is the gravitational acceleration (9.81 m s^{-2}), and z corresponds to the elevation relative to a reference level (m). This formulation accounts for the transport of energy associated with mass flows across the system boundaries.

Mass conservation is the fundamental principle underlying the formulation of mechanistic models applied to AD systems (MORAN et al., 2019). In control-volume approaches, mass flows act as the primary vectors for the transport of physical and chemical properties across system boundaries. In open systems such as anaerobic reactors, the inlet and outlet mass flow rates govern the convective transport of substrates, products, and intermediate compounds, thereby directly influencing the dynamic behavior of the process. In this context, variations in the influent composition or OLR modify the mass balances of key components and consequently affect reaction pathways and microbial activity within the reactor.

In the context of process modeling, the conservation of entropy in open systems can be expressed through the entropy balance equation, which accounts for entropy transport across system boundaries and its internal generation due to irreversible processes, as shown in Eq. [1.3].

$$\frac{dS_{vc}}{dt} = \sum \frac{\dot{Q}_k}{T_k} + \sum \dot{m}_{in} s_{in} - \sum \dot{m}_{out}\, s_{out} + \dot{S}_{gen} \quad [1.3]$$

Where S_{vc} represents the entropy within the control volume (J K^{-1}), t is time (s), $\dot{Q}_k$ denotes the heat transfer rate associated with boundary k (W), and T_k is the absolute temperature at boundary k (K). The terms $\dot{m}_{in}$ and $\dot{m}_{out}$ correspond to the mass flow rates entering and leaving the system (kg s^{-1}), while s_{in} and s_{out} represent the specific entropy of the inlet and outlet streams (J kg^{-1} K^{-1}). The term $\dot{S}_{gen}$ represents the rate of entropy generation due to irreversible processes occurring within the system.

In addition to describing material transport, mass flows also play an important role from a thermodynamic perspective. In the formulation of the First and Second Laws of Thermodynamics for open systems, mass flow rates appear multiplying intensive properties such as enthalpy, entropy, and internal energy. This mathematical structure demonstrates that matter acts as the physical carrier through which energy and entropy are transported between the system and its surroundings. In practical terms, the convective transport of matter simultaneously carries thermodynamic properties, coupling mass balances with energy and entropy balances.

In anaerobic reactors, fluctuations in influent composition or organic loading rate may therefore influence not only the distribution of chemical species but also the overall thermodynamic state of the system. Variations in substrate loading, for example, can affect the internal energy balance and microbial stability if operational conditions such as temperature are not adequately controlled. Furthermore, the Second Law of Thermodynamics imposes an additional constraint through the entropy balance, ensuring that the biochemical transformations occurring within the reactor follow physically admissible directions. In AD systems, entropy generation is associated with irreversible processes such as microbial metabolism, mixing, and reaction kinetics, which must be implicitly respected in the formulation of mechanistic models such as the ADM1.

In mathematical modeling of reactors, the mass balance serves as the basis for formulating the equations that describe the system's internal dynamics. In mechanistic models such as ADM1, these relationships are expressed through systems of ordinary differential equations (ODEs) (as expressed in Eq. [1.4] and [1.5]) coupled with algebraic equations, allowing the simultaneous representation of biochemical, physicochemical, and transfer processes (BATSTONE et al., 2002, 2015). In general form, these equations describe the temporal variation of component concentrations within the reactor and synthesize the combined effects of hydraulic transport, biochemical reactions, and physicochemical interactions between phases.

$$\frac{dx}{dt} = D(x_{in} - x) + K \cdot r(x) \qquad [1.4]$$

Where x represents the concentration of a state variable in the reactor (kg m^{-3} or mol m^{-3}), x_{in} is the concentration of the same component in the influent stream (kg m^{-3} or mol m^{-3}), and t denotes time (d or s). The parameter D is the dilution rate (d^{-1}), defined as the ratio

between the influent flow rate and the reactor volume ($D = Q/V$), where Q is the volumetric influent flow rate ($m^3\ d^{-1}$) and V is the reactor volume (m^3). The term K represents the stoichiometric matrix relating reactions to system components (dimensionless), and $r(x)$ is the vector of reaction rates describing the biochemical transformations occurring in the reactor (kg $m^{-3}\ d^{-1}$ or mol $m^{-3}\ d^{-1}$).

Figure 1.1 – Structural Decomposition of the Mass Balance Equation into Matrices

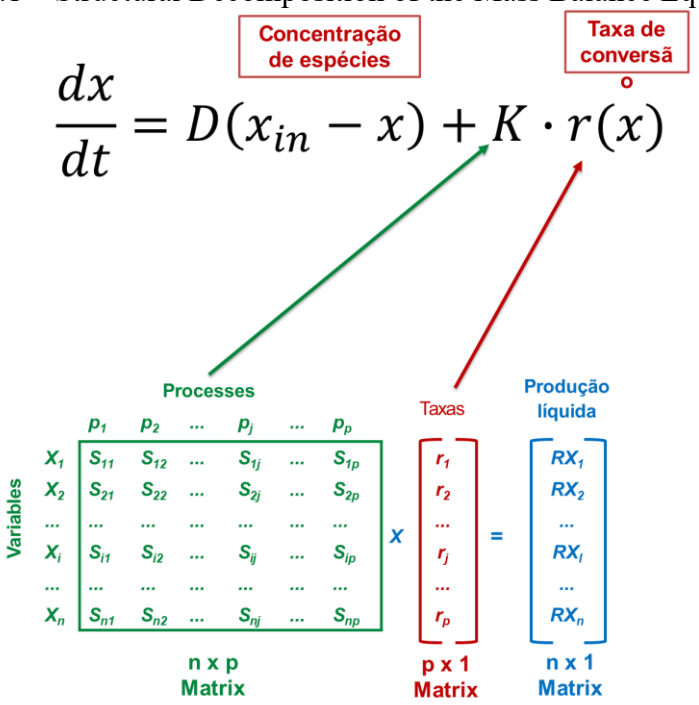

In dynamic models, the evolution of each state variable is typically represented by ODEs (LI; LEE; KIM, 2021). A general formulation is shown in Eq. [1.5], where the temporal variation of the state variable depends on inflow–outflow transport processes and reaction kinetics. The reaction term represents the biological transformations occurring within the system and is formulated as the product of reaction rates and stoichiometric coefficients. In structured models such as ADM1, these relationships are organized through the stoichiometric matrix, commonly referred to as the Petersen stoichiometric matrix. Each column of this matrix corresponds to a biochemical process, while each row represents a component involved in the system. This structure ensures that all reactions satisfy the requirements of elemental mass conservation and chemical oxygen demand (COD) balance, allowing complex biochemical pathways to be represented in a mathematically consistent manner.

$$\frac{dx}{dt} = f(x, u, t, \theta) \quad [1.5]$$

Where x is the vector of state variables representing the concentrations of the system components (kg m^{-3} or mol m^{-3}), u is the vector of input variables such as influent composition and operational conditions, t denotes time, and θ represents the vector of model parameters, including kinetic and stoichiometric coefficients. The function f describes the nonlinear relationships that govern the biochemical reactions, transport processes, and physicochemical interactions occurring within the system.

Finally, the mass balance formulation must also account for interphase transfer processes, particularly the exchange of methane, carbon dioxide, and hydrogen between the liquid and gas phases. These transfers are governed by physicochemical equilibrium relationships, such as Henry's law, which relate the dissolved concentration of a gas to its partial pressure in the gas phase. The representation of these processes is essential for linking biochemical reactions occurring in the liquid phase with biogas production and release, as well as for describing the equilibrium of inorganic carbon species that directly influence pH stability within anaerobic reactors.

In ADM1, these equations can be grouped into three main categories (BATSTONE et al., 2002, 2015). The first category corresponds to biochemical processes, where ODEs describe microbial growth and substrate degradation, including the formation of intermediate metabolites such as VFA, alcohols, and hydrogen, as well as final products such as carbon dioxide and methane. The second category corresponds to component mass balances, in which each compound in the model is tracked through its production, consumption, inflow, and outflow terms. The third category represents interphase mass transfer processes, particularly the exchange of carbon dioxide, hydrogen, and methane between the liquid and gas phases, which links biochemical reactions occurring in the liquid phase with biogas generation.

A general representation of this formulation in ADM1 can be illustrated through the mass balance for inorganic carbon (IC), presented in Eq. [1.6]:

$$\frac{dS_{liq,IC}}{dt} = \frac{q_{in}S_{in,IC}}{V_{liq}} - \frac{q_{out}S_{liq,IC}}{V_{liq}} + \sum_{j=1}^{19} \rho_j \nu_{10,j} - \rho_{T,CO2} \quad [1.6]$$

where V_{liq} is the liquid reactor volume (m^3), q_{in} and q_{out} are the influent and effluent flow rates ($m^3\ d^{-1}$), respectively, and q/V_{liq} represents the hydraulic retention time (HRT, d). $S_{in,IC}$ and $S_{liq,IC}$ denote the influent and liquid-phase inorganic carbon concentrations (kmolC m^{-3}), ρ_j is the rate of biochemical process j, $\nu_{IC,j}$ is the corresponding stoichiometric coefficient for inorganic carbon, and ρ_{T,CO_2} represents the gas-liquid transfer rate of carbon dioxide.

This balance is based on the fact that the difference between the total inorganic carbon (TIC) concentration and its dissolved species, such as SCO_2 and $SHCO_3^-$, must be zero when the system is adequately represented. Differences between inflow and outflow concentrations reflect biochemical conversions occurring within the reactor. The summation term corresponds to the reactions listed in the model's stoichiometric matrix, representing the contribution of each process j to the formation or consumption of IC.

In this specific case, the equation refers to column 10 of the ADM1 matrix (as show in Appendix A, Table 10.1 and Table 10.2, and Appendix D, Table 12.1, Table 12.2, Table 12.3), which represents SIC (kmol C m^{-3}) in the biochemical processes j, including the consumption of sugars, amino acids, propionate, acetate, and hydrogen. An analogous formulation is applied to the remaining model components, allowing the systematic and quantitative description of reactor behavior under different operating conditions.

1.2.3 Stoichiometry

Stoichiometry is one of the fundamental pillars of mathematical modeling of anaerobic processes, as it establishes the quantitative relationships between consumed substrates and formed products during biochemical and physicochemical reactions (KIM; CUI, 2017; KRICH et al., 2005; RUGGERI; TOMMASI; SANFILIPPO, 2015). While mass balances define the mathematical structure of the model, stoichiometry determines how the transformation of matter occurs within the system. In mechanistic models such as the ADM1 stoichiometry specifies how each component participates in metabolic pathways throughout the AD process, enabling a consistent representation of the conversion of complex organic matter into soluble intermediates, microbial biomass, and biogas (BATSTONE et al., 2002, 2015).

Stoichiometry is not limited to describing classical chemical reactions but also encompasses complex biological processes involving multiple microbial populations and diverse metabolic pathways. These transformations follow the functional organization of the microbial community, including hydrolytic, acidogenic, acetogenic, and methanogenic groups,

each responsible for the conversion of specific substrates (ANGELIDAKI et al., 2009; RITTMANN; MCCARTY, 2001). Consequently, the proper definition of stoichiometric relationships is essential to ensure that the model correctly represents the redistribution of carbon, hydrogen, oxygen, nitrogen, and sulfur throughout the process, in accordance with elemental conservation principles (BATSTONE et al., 2015; KRICH et al., 2005).

Stoichiometry in AD extends beyond the description of classical chemical reactions and incorporates complex biological processes involving multiple microbial populations and interconnected metabolic pathways. These transformations follow the functional organization of the microbial community, including hydrolytic, acidogenic, acetogenic, and methanogenic groups, each responsible for the conversion of specific substrates into intermediate or final products (ANGELIDAKI et al., 2009; RITTMANN; MCCARTY, 2001). Consequently, the correct definition of stoichiometric relationships is essential to ensure that the redistribution of carbon, hydrogen, oxygen, nitrogen, and sulfur throughout the process complies with the principles of elemental conservation. In ADM1, these relationships are commonly expressed on a COD basis, which represents the electron equivalents associated with organic matter transformations and allows consistent tracking of oxidation–reduction processes within the system (BATSTONE et al., 2015; KRICH et al., 2005).

In models such as ADM1, these relationships are systematically represented through the Petersen stoichiometric matrix, a structured framework widely used in biological process modeling. Each row of the matrix corresponds to a system component (e.g., carbohydrates, proteins, amino acids, VFA, biomass, and gaseous species), while each column represents a specific biochemical process. The matrix coefficients indicate the consumption or production of each component, providing a structured framework that ensuring closure of mass, COD, and elemental balances for all modeled reactions (BATSTONE et al., 2015; HENZE et al., 2000)

The use of a stoichiometric matrix also allows the incorporation of key process-related information, including alkalinity generation, electron transfer, gas formation, biomass synthesis, and macromolecule degradation (RITTMANN; MCCARTY, 2001; RITTMANN; HOLUBAR, 2014). Furthermore, it enables the explicit inclusion of microbial yield coefficients, carbon partitioning among metabolic products, and electron distribution among competing metabolic pathways, which are essential to preserve biochemical consistency and predictive reliability in AD models (SMOLDERS et al., 1994).

Overall, stoichiometry provides the structural backbone of AD models, ensuring that the differential equations derived from mass balances are physically and biochemically coherent (ARIS, 1979). Without a consistent stoichiometric framework, the predictive capability of AD models would be compromised, thereby compromising the predictive capability of simulations. For this reason, the construction and verification of the stoichiometric matrix represent critical steps in the development and application of mathematical models to AD (BOGAERTS; WOUWER, 2023; PALANICHAMY; PALANI, 2014a).

1.2.4 Kinetics

A comprehensive mathematical model, such as ADM1, describes the biochemical, chemical, and physicochemical processes from particle disintegration to the formation of methane and carbon dioxide, resulting from the conversion of intermediate products generated during substrate degradation. These phenomena evolve through sequential stages, including disintegration, hydrolysis, acidogenesis, acetogenesis, and methanogenesis, which may involve both reversible and irreversible transformations.

ADM1 incorporates kinetic expressions to represent the reaction rates associated with each of these stages. The disintegration and hydrolysis of carbohydrates, lipids, and proteins are generally described using first-order kinetics (ECKENFELDER, 1966), as expressed in Eq. [1.7], where S denotes the substrate concentration and k is the kinetic constant. This formulation assumes that the reaction rate is directly proportional to the available substrate concentration, a particularly suitable assumption for lumped representations of particulate organic matter. Biomass decay is also described using first-order kinetics, with dead biomass treated as particulate material within the system (Eq. [1.7]).

$$\frac{dS}{dt} = -kS \qquad [1.7]$$

In contrast, pH-related inhibition effects are represented in ADM1 by empirical functions, while inhibition by dissolved hydrogen and free ammonia is modeled using non-competitive inhibition terms. The remaining regulatory mechanisms associated with substrate uptake and microbial growth are described using Monod-type kinetics (MONOD, 1949), as shown in Eq. [1.8]. In this formulation, K_s represents the half-saturation constant, the substrate concentration at which the microbial growth rate is half its maximum (μ_{max}). The Monod

expression accounts for substrate saturation effects, providing a more realistic representation of biological systems in which increasing substrate concentrations do not lead to unlimited increases in reaction rates.

$$\mu = \mu_{max} \frac{S}{K_s + S} \quad [1.8]$$

The hydrolysis step may be described using different kinetic approaches, including first-order, second-order, and the Contois surface-limited model (CONTOIS, 1959). The selection of the most appropriate formulation depends on the substrate's characteristics and the dynamics governing the initial stages of digestion. In many cases, first-order kinetics are insufficient to capture the complexity of the hydrolysis process, particularly when surface limitations dominate or when distinct substrate fractions exhibit markedly different degradation rates.

Ramirez et al. (2009) compared the standard ADM1 formulation based on first-order hydrolysis with a modified version employing the Contois model, demonstrating that changes in the hydrolysis kinetics significantly affect overall process performance. Similarly, Myint, Nirmalakhandan, and Speece (2007) showed that hydrolysable fractions such as cellulose and hemicellulose exhibit distinct degradation rates due to surface-related limitations, reinforcing the need to adapt kinetic formulations to the specific nature of the substrate under investigation.

1.3 Thesis Structure

The present thesis addresses the research gaps identified in the previous sections through a structured approach that integrates bibliometric analysis, experimental validation, and mathematical modeling. The study evaluates the applicability of the ADM1 to FVW, including its calibration for W-AD systems and its structural extension to hydrogen-oriented acidogenic processes. In addition, the current state of ADM1 applications in D-AD systems is critically assessed through a bibliometric review.

The thesis consists of eight chapters, four of which are written in the format of scientific articles intended for submission to peer-reviewed journals. All chapters follow a sequential organization consistent with the central theme of the study, which focuses on the

application, calibration, and adaptation of ADM1 across different AD configurations, including wet anaerobic systems and acidogenic processes for biogas and hydrogen production.

Chapter 1 presents the theoretical background of AD and the principles guiding the mathematical modeling of these processes. Essential aspects such as mass balance, stoichiometry, and kinetics are discussed, together with fundamental concepts related to the mathematical representation of biological systems. This chapter establishes the theoretical framework necessary for understanding the modeling approaches applied in the subsequent chapters.

Chapter 2 outlines the general and specific objectives of the thesis, defining the scientific goals that guide the development of the experimental studies, simulations, and comparative analyses.

Chapter 3 compiles the methodological procedures employed throughout the thesis, including experimental design, analytical methods, and modeling procedures.

Chapter 4 contains the second article, entitled "Anaerobic Digestion Model No. 1 Applied to Bioenergy Generation from Fruit and Vegetable Waste in Up-flow Anaerobic Sludge Blanket Reactors." This chapter describes the practical application of the model in UASB reactors, focusing on model calibration, sensitivity analysis, predictive performance, and the model's suitability for the evaluated experimental conditions. This article was published in Bioresource Technology in 2025.

Chapter 5 presents the third article, which focuses on the mathematical modeling of hydrogen production under acidogenic conditions. This chapter discusses the adaptation of ADM1 to represent metabolic pathways associated with dark fermentation, including hydrogen generation kinetics and related inhibition effects. This article is currently prepared for submission to the journal International Journal of Hydrogen Energy.

Chapter 6 corresponds to the first article, entitled "Bibliometric Analysis of Anaerobic Digestion Model No. 1 for Dry Anaerobic Digestion of Fruit and Vegetable Waste, Food Waste, and Organic Fraction of Municipal Solid Waste." This chapter presents a comprehensive bibliometric review of ADM1 applications in dry digestion systems, highlighting research trends, methodological gaps, and the main adaptations reported in the literature. This article was published in the Journal of Environmental Chemical Engineering in 2024.

Chapters 7 and 8 present the general conclusions of the thesis and recommendations for future research.

The articles included in this thesis follow the classical structure adopted in scientific publications, consisting of the sections Introduction, Methodology, Results and Discussion, Final Considerations, and References. Figures, tables, and graphs are numbered consecutively throughout the thesis in order to avoid duplication and maintain structural consistency.

2 GENERAL OBJECTIVE AND SPECIFIC OBJECTIVES

2.1 General objectives

To analyze, calibrate, modify, and extend the ADM1 by integrating experimental data with numerical simulations to improve its representation of L-FVW conversion under single-stage W-AD and DF conditions, while performing a bibliometric and critical assessment of its reported applicability, structural adaptations, and limitations for D-AD of FVW.

2.2 Specific objectives

- To implement and calibrate ADM1 for the W-AD of liquid FVW in UASB reactors, assessing its predictive performance for methane production and intermediate dynamics.
- To evaluate the capability of the standard ADM1 to represent dark fermentation processes, identifying systematic deviations between model predictions and experimental observations.
- To extend the ADM1 structure by incorporating additional metabolic pathways associated with hydrogen production based on experimentally observed VFA profiles.
- To assess the robustness and predictive performance of the modified ADM1 in representing hydrogen production, gas composition, and acidogenic pathway distribution.
- To identify the kinetic and stoichiometric parameters exerting the greatest influence on hydrogen production and metabolic competition through sensitivity analysis.
- To conduct a bibliometric and systematic analysis of ADM1 applications D-AD of FVW identifying research trends and scientific evolution in the field.
- To critically evaluate the structural modifications, kinetic adaptations, and operational assumptions reported for ADM1 in high-solids systems, highlighting methodological limitations and modeling challenges.

3 METHODOLOGICAL STRATEGY AND RESEARCH PLAN

This research was conducted at the Biomass Technology Laboratory of Embrapa Agroindústria Tropical (Fortaleza, Brazil), in collaboration with CEASA–Maracanaú and the Federal University of Ceará (UFC). The study is part of a research framework dedicated to FVW valorization through AD, hydrogen production, and integrated bioenergy systems.

The experimental investigations are associated with a patented technological platform entitled "System for Pre-treatment of Fermentable Organic Waste Followed by Anaerobic Reactors for Hydrogen and/or Methane Production" (Process No. BR 10 2025 022817 3), as show in Figure 3.1. Within this framework, mathematical modeling constitutes an essential and structuring component, supporting reactor design, operational parameter definition, performance prediction, and system optimization. The modeling and simulation developments presented in this thesis are therefore directly integrated into the conceptual and technological structure of the patented system.

Figure 3.1 – Schematic representation of the proposed system highlighting the modeled components.

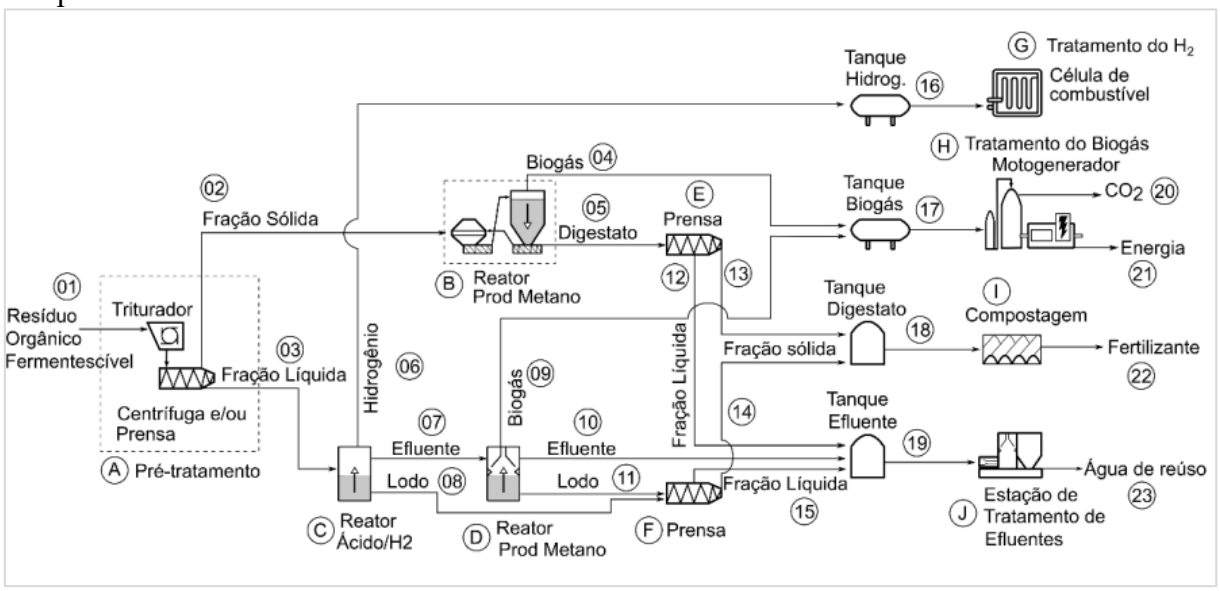

Note: Description of the system in Appendix A.

Initially, the methods and tools required for the detailed execution of the work were defined to support the selection of the most appropriate approaches (Table 3.1).

Table 3.1 – Work program

A.	Practical Application of ADM1 to W-AD of FVW
	B1. Experimental characterization of FVW under W-AD conditions
	• Determination of physicochemical properties (TS, VS, COD fractions, biodegradability).
	B2. Implementation and calibration of ADM1 for liquid-phase digestion of FVW
	• Parameter fitting (hydrolysis constants, kinetic factors, yields).
	• Sensitivity and uncertainty analysis.
	• Evaluation of model accuracy against experimental methane and biogas profiles.
	B3. Identification of substrate- and phase-specific gaps in the unmodified ADM1
	• Diagnosis of model limitations when applied to FVW digestion at low solids.
B.	Extension and Modification of ADM1 for DF of FVW
	C1. Inclusion of metabolic pathways for hydrogen-producing DF
	• Integration of lactate, ethanol, acetate, and butyrate formation routes.
	• Adjustment of stoichiometric matrices and inhibition functions.
	C2. Calibration of the modified ADM1 for hydrogen production
	• Parameter estimation tailored to thermally pretreated inoculum and inhibited methanogenesis.
	• Joint fitting of hydrogen, biogas volume, and VFA accumulation.
	C3. Validation of the modified model's ability to represent pathway shifts
	• Analysis under conditions of pH stress, substrate overload, and inoculum inhibition.
C.	Literature-Based Foundations and Assessment of ADM1 for D-AD
	A1. Comprehensive review of ADM1 applications in D-AD systems
	• Survey of studies employing ADM1 under high-solid conditions.
	• Identification of common modifications, assumptions, and model limitations.
	A2. Critical evaluation of ADM1 performance for high-solids, low-moisture environments
	• Assessment of hydrolysis constraints, mass-transfer limitations, inhibition patterns, and model suitability.
	• Identification of methodological and conceptual gaps that motivate later model refinements.
	• Literature-Based Foundations and Assessment of ADM1 for D-AD

3.1 System description and modeling strategy

The present research models an FVW treatment system structured as an integrated biorefinery as show in Figure 3.1, focusing on the simultaneous conversion of organic matter into methane (CH_4) and hydrogen (H_2) via AD pathways. Given the complexity of the system and the diversity of biochemical processes involved, a modular modeling strategy was adopted, in which each operational unit (core) was initially modeled independently. This approach allows for a robust, controlled description of the dominant phenomena at each stage, while enabling subsequent coupling of the submodels to provide a comprehensive representation of the overall system.

It is important to emphasize that although the biorefinery configuration is described in full, the mathematical modeling developed in this research primarily focuses on the core AD units responsible for biofuel production. Auxiliary and downstream processes are included at a conceptual level or through mass and energy balances, as the full dynamic integration of all system components represents a subsequent level of complexity beyond the main scope of this

thesis. Therefore, detailed dynamic modeling is restricted to the liquid-phase anaerobic units responsible for hydrogen and methane production under wet operational conditions.

The proposed system begins with a physical pretreatment step, in which FVW is subjected to centrifugation and/or pressing, yielding two fractions: a liquid fraction and a solid fraction. This separation aims to optimize the performance of subsequent processes by adjusting the substrate's physicochemical characteristics to the different AD configurations.

The liquid fraction is directed to a two-stage AD system. In the first reactor (c), dark fermentation (DF) occurs, converting soluble carbohydrates into hydrogen, volatile organic acids, and intermediate metabolites. This stage is modeled based on a modified ADM1, incorporating specific metabolic pathways for H_2 production and explicit inhibition of methanogenesis. In the second reactor (d), the organic acids generated are converted into methane through acetoclastic and hydrogenotrophic methanogenesis. This stage is described using a kinetic model compatible with the classical ADM1 framework.

In parallel, the solid fraction of the substrate is directed to a D-AD reactor (b), operated at high total solids content, with the primary objective of maximizing methane production. Although this unit composes the patented biorefinery configuration, it is not dynamically modeled within the scope of this thesis. Instead, its representation is addressed through a bibliometric and critical assessment of ADM1 applications in high-solids systems, focusing on reported structural adaptations, hydrolysis limitations, and kinetic modifications described in the literature.

The sludge generated throughout the process undergoes a solid–liquid separation step. The liquid fraction is sent to a wastewater treatment unit (j), while the solid fraction, corresponding to the digestate, is directed to composting (i), with potential application as a biofertilizer. Although these stages are not described using detailed kinetic models, their mass and energy flows are incorporated into the overall system balance to ensure consistency at the biorefinery scale.

The methane-rich biogas may undergo purification processes and be used for thermal energy generation (h), electricity production, or as a vehicle fuel. The hydrogen produced (g) is directed to treatment, purification, and storage for energy applications, such as use in fuel cells. Within the modeling framework, gas production rates and compositions are explicitly accounted for, enabling evaluation of the system's energetic performance.

The proposed configuration offers the following main advantages: (i) high energy efficiency associated with the integrated production of CH_4 and H_2; (ii) operational flexibility

resulting from the modular configuration and its adaptability to substrate characteristics; and (iii) environmental sustainability promoted by the valorization of organic waste, reduction of greenhouse gas emissions, and generation of high-value-added products. Additionally, the adopted modeling strategy provides a scalable framework that allows future integration of all process units without compromising the rigor of the core process models.

The full version of this paper is published in Bioresource Technology (2025) under the name “Anaerobic Digestion Model No. 1 applied to bioenergy generation from fruit and vegetable waste in Upflow Anaerobic Sludge Blanket reactors”. DOI: https://doi.org/ 10.1016/j.biortech.2025.132644

4 ARTICLE I: ANAEROBIC DIGESTION MODEL NO. 1 APPLIED TO BIOENERGY GENERATION FROM FRUIT AND VEGETABLE WASTE IN UPFLOW ANAEROBIC SLUDGE BLANKET REACTORS

ABSTRACT:

This study applied the Anaerobic Digestion Model No. 1 (ADM1) to fruit and vegetable waste (FVW) anaerobic digestion, adjusting substrate-dependent parameters and system configuration in AQUASIM 2.0. Key model parameters were determined, including fractions of carbohydrates, lipids, proteins, and inert particles. Sensitivity analysis identified the decay rate of biomass (k_{dec}), the disintegration rate constant (k_{dis}), the hydrolysis rate constant for carbohydrates ($k_{hyd,ch}$), the half-saturation constant for acetate ($k_{s,ac}$), maximum uptake rates for acetate ($k_{m,ac}$), long-chain fatty acids ($k_{m,fa}$), and sugars ($k_{m,su}$) as the most influential parameters on biogas production. These were estimated using experimental data to refine the model, achieving an R^2 of 0.99 and root mean square error of 0.34. Inhibition indices confirmed acetate’s influence, and free ammonia was observed to interfere with acetate absorption, affecting biogas production. The adjusted ADM1 effectively represented biogas and methane production, demonstrating its applicability to FVW anaerobic digestion systems. The results emphasize the need to adjust ADM1 for different substrates and demonstrate its potential as a valuable tool for identifying potential system failures.

Keywords: ADM1; Biogas technology; Mathematical modeling; Parameter estimation.

4.1 Introduction

Anaerobic digestion (AD) is a multi-stage, multi-phase biochemical process involving a complex diversity of microorganisms, with its stability and efficiency depending on factors such as substrate composition, reactor type, and environmental and operational conditions (ZHAO et al., 2019a). AD has gained importance due to its potential to convert organic waste into bioenergy, primarily methane (BUŁKOWSKA et al., 2018). Additionally, AD offers environmental benefits by reducing organic waste volume and greenhouse gas emissions, aligning with circular economy principles, and enhancing sustainable waste management practices (HILKIAH IGONI et al., 2008; LI et al., 2018a). However, achieving efficient and sustainable operation of biogas plants has become increasingly challenging due to the variability in substrates and the necessity for mathematical models that ensure stability, financial viability, and optimal performance. Therefore, system modeling is essential for optimizing, controlling, and designing AD plants (HANGOS; CAMERON, 2001; RASMUSON et al., 2014).

Various AD models are used to predict crucial parameters such as methane production potential, maximum production rate, and the lag phase period. These models include first-order models, the Gompertz model, BioModel, and General Integrated Solid Waste Co-Digestion (GISCOD) (ZHAO et al., 2019a), as well as the Exponential, Fitzhugh, Cone, Transfer, and the modified Gompertz models (LI et al., 2018b).

The development of Anaerobic Digestion Model No. 1 (ADM1) by the International Water Association (IWA) Working Group (BATSTONE et al., 2015) represented a significant advancement in AD modeling. Initially, ADM1 was applied to simulate methane production during the anaerobic digestion of sewage sludge (BUŁKOWSKA et al., 2018). Since then, it has been tested on various substrates (ESPOSITO et al., 2011a; LI, 2022). On the other hand, ADM1 may not be feasible in all cases due to requirements such as detailed substrate characterization and calibration with numerous parameters, including particulate concentrations, carbohydrates, lipids, proteins, and volatile fatty acids (VFAs) (ASTALS et al., 2013; RAZAVIARANI; BUCHANAN, 2015), which can limit its applications (ASTALS et al., 2013). ADM1 requires 24 substrate-specific parameters, encompassing particulate, soluble, and ionic fractions, and an additional 15 carbon fractions, 4 nitrogen fractions, and several variables to characterize substrate composition, inhibition conditions, and other operational aspects.

The most common method for the proper final disposal of fruit and vegetable waste is landfilling (LIU et al., 2012). However, this approach entails significant logistical costs related to collection and transportation, in addition to contributing to greenhouse gas emissions. Another alternative is incineration, which is costly due to high moisture content of this kind of waste that imposes high energy demands for combustion (SHEN et al., 2013). A more economically and environmentally promising alternative is AD, which not only reduces the volume of waste but also generates renewable energy in the form of biogas (methane) and, potentially, hydrogen. Furthermore, this process enables the recovery of water for reuse and nutrients through the digestate, which can be utilized as a high-quality organic amendment.

AD has emerged as the most promising method for the treatment and valorization of FVW, primarily due to its high biodegradability and potential for bioenergy recovery. In recent years, AD has become one of the most widely implemented technologies for the valorization of the organic fraction of waste (ZAYEN et al., 2025). From both economic and environmental perspectives, AD not only significantly reduces waste volume, but also generates renewable energy in the form of biogas (methane) and, potentially, hydrogen. Additionally, this process enables the recovery of water for reuse and nutrients through the digestate, which can be used as a high-quality organic amendment. However, despite its advantages, the process of AD of FVW requires careful management, as this waste degrades rapidly, promoting acidification, the accumulation of VFAs, and a reduction in pH, all of which can inhibit methanogenesis (BOUALLAGUI et al., 2009; SILVA, 2024). Additionally, the excessive generation of ammonia can also hinder methane production (JI et al., 2017).

The use of FVW for energy production via AD requires careful consideration of the organic loading rate (OLR) limitations that may affect the reactor. Jiang et al. (2012) point out that reducing the OLR and rigorous pH monitoring are necessary to guarantee the system's stability. These measures are essential because FVW contains a high carbohydrate content that is rapidly degraded and hydrolyzed, forming VFAs. The accumulation of these acidic compounds can ultimately acidify the reactor, compromising its performance (MATA-ALVAREZ; MACÉ; LLABRÉS, 2000). Co-digestion is often suggested as an effective strategy to mitigate these challenges. This process improves the system's alkalinity and increases its stability, allowing for more efficient and sustainable operation of the anaerobic reactor (SHEN et al., 2013). Calibrating the ADM1 to predict and analyze these behaviors is essential, especially to understand the processes of substrate disintegration and hydrolysis and the formation of inhibitory products to optimize the results.

Calibrating ADM1 to predict and analyze these behaviors is essential, especially to understand substrate disintegration, hydrolysis, and the formation of inhibitory products. Despite the relevance of this approach, the literature still lacks studies that apply ADM1 specifically to FVW with a comprehensive parameter calibration process. Most existing studies either apply the model generically or focus solely on kinetic analyses, without detailed substrate-specific adaptations.

Therefore, this study aimed to address this gap by calibrating the ADM1 model specifically for the AD of the liquid phase of FVW. A detailed physicochemical characterization of the substrate was carried out, and experimental data under varying operating conditions - particularly different OLRs - were used to adjust and validate the model. The results contribute to enhancing ADM1's applicability to FVW, offering a more accurate predictive tool for this specific and underrepresented substrate in the modeling literature.

4.2 Material and methods

4.2.1 Experimental set-up

An experiment was conducted using a 12.6 L Upflow Anaerobic Sludge Blanket (UASB) reactor, operated under mesophilic conditions at 30±1 °C, at the facilities of the Embrapa Tropical Agroindustry in Fortaleza, Ceará, Brazil. The reactor was inoculated with mixed anaerobic sludge composed of 1 kg of sludge obtained from the wastewater treatment plant of the Heineken brewery and 6 kg of anaerobic sludge collected from a municipal wastewater treatment plant treating urban sewage, resulting in an inoculum with 4.0% total solids (TS, w/w, wet basis) and 68.4% volatile solids (VS, expressed as percentage of total solids).

The reactor was operated for 272 days, fed with pre-treated FVW, which was diluted at increasing concentrations. The raw FVW had Chemical Oxygen Demand (COD) of 115.9 g L^{-1}. The FVW pre-treatment comprised of grinding and centrifuging, resulting in a liquid fraction that was collected and stored at 4°C to prevent biodegradation before being used to feed the reactor. Silva Júnior et al. (2022) provide detailed characteristics of this raw and liquid substrate.

4.2.2 Experimental program

The reactor was operated under varying conditions, including pH levels from 4.5 to 7.7, a hydraulic retention time (HRT) between 1.0 and 4.1 days, and an OLR ranging from 1.5 to 13.0 kg m^{-3} d^{-1} (Table 4.1). This setup aimed to minimize water consumption and assess AD's potential under higher substrate concentration conditions. The raw and diluted substrates used to feed the reactors were analyzed, revealing minimal concentrations of acetic, propionic, and butyric acids. These values informed the calculations for defining input variables, including the concentrations of the particulate and soluble fractions across the 24 ADM1 components.

The experimental data used to adapt and validate the ADM1 model in this study were obtained from a broader research project investigating the AD of FVW in one- and two-stage reactor configuration. Specifically, the data used in the present work were derived from one of the UASB reactors tested in that study, providing a robust experimental basis for model calibration and validation. Aliquots of the reactor effluent were collected five days per week for analysis of COD, TS, VS, pH, VFAs, and biogas composition. Mass balances for soluble, particulate, and gaseous components were solved dynamically within the ADM1 framework to ensure consistency between substrate degradation, biomass growth, and methane production.

Table 4.1 – Projected Operating Conditions.

Parameter	Unit	Experimental phases					
		P1	**P2**	**P3**	**P4**	**P5**	**P6**
Feed flow	L d^{-1}	3.1	7.3	10.5	8.4	10.0	11.5
Total COD	gO_2 L^{-1}	6.0	7.5	9.5	11.0	13.0	15.0
OLR	kg $m^{-3}d^{-1}$	1.5	3.5	5.0	7.5	10.0	13.0

Note: The dilution factor ranged from 0.05 to 0.11 and refers to the dilution of the raw FVW used to prepare the reactor influent in order to achieve the target COD concentration defined for each operational phase. COD – Chemical Oxygen Demand; OLR – Organic Loading Rate.

The feed was prepared by diluting the raw FVW based on its COD concentration. Throughout the operational phases, the influent COD was progressively increased by reducing the dilution of the raw substrate. In addition, the influent flow rate was gradually increased, which, combined with the higher COD concentration, resulted in a progressive increase in the OLR applied to the reactor. Detailed physicochemical characteristics of the raw and liquid substrates are reported by da Silva Júnior et al. (2025).

4.2.3 Experimental analysis

The following analyses were carried out: COD (total), TS, VS, pH, and carbohydrate concentration were determined by (APHA, 2022). TA and VFA were determined using the Kapp titrimetric method (BUCHAUER; INNSBRUCK, 1998). Lipids were quantified following the American Oil Chemists' Society Am 5-04 method (AMERICAN OIL CHEMISTS' SOCIETY (AOCS), 2004), using a high-pressure, high-temperature extraction system on the Ankom XT-15 equipment (ANKOM, 2009). Protein content was determined by the Dumas combustion method with the NDA 701 Nitrogen/Protein Analyzer (VELP SCIENTIFICA, 2019), using EDTA as the reference standard in accordance with AOAC method 992.23. Mass loss assessed moisture content through desiccation in an oven set at 105 °C (AOAC (ASSOCIATION OF OFFICIAL ANALYTICAL CHEMISTS), 2016).

Total Organic Carbon (TOC) was analyzed using a Shimadzu SSM 5000ª Total Organic Carbon Analyzer, which utilizes catalytic combustion at 900 °C. Carbon in the sample is oxidized to carbon dioxide (CO_2), which is detected by a non-dispersive infrared detector (NDIR). This equipment allows for the measurement of total carbon (TC), inorganic carbon (IC), and TOC in both solid and aqueous samples. IC is determined by acidifying and oxidizing the sample at 200 °C, while TOC is calculated by subtracting IC from TC (TOC = TC - IC). Samples, up to 1 g each, are placed in labeled vials by the user and are removed post-analysis for reuse or proper disposal. The quantification of CH_4, CO_2, and H_2 in the biogas was determined by gas chromatography with ionization detection by dielectric barrier discharge (GC BID-2010 Plus, Shimadzu Corporation, Japan), equipped with a GS-GASPRO column (60 m×0.32 mm) (Agilent Technologies Inc., USA). Helium gas was used as the carrier gas (White Martins LTDA, Brazil) at a flow rate of 2 mL min^{-1}, with a run time of 9 min. The oven, injector, and detector temperatures were 50 °C, 100 °C, and 250 °C, respectively.

4.3 Model development and simulation

4.3.1 Anaerobic Digestion Model No. 1

The ADM1 model, developed by (BATSTONE et al., 2015) and published in 2002, was applied to describe the AD processes in these experiments. This complex model incorporates 19 biochemical conversion processes and 24 dynamic state variables based on the

Petersen matrix. Simulations were conducted using AQUASIM 2.0 software (Reichert, 1998), with additional support from Matlab-Simulink.

AD involves multiple processes, each represented by a set of equations that describe their behavior during fermentation. The hydrolysis and disintegration of the substrate include extracellular solubilization steps, which are modeled using first-order kinetics, as described in Eq. [4.1]. In contrast, acidogenesis, acetogenesis, and methanogenesis processes are extracellular biochemical reactions that follow Monod-type kinetics, driven by substrate availability, as outlined in Eq. [4.2].

$$\rho = K_{dis,hyd} * X_{dis,hyd} \quad [4.1]$$

$$\rho = K_m * \frac{S}{K_s + S} * X * I \quad [4.2]$$

Where ρ represents the rate of disintegration or hydrolysis of the substrate, categorized as carbohydrates, lipids, and proteins (kgCOD m^{-3} d^{-1}); $X_{dis,hyd}$ represents the substrate concentration (kgCOD m^{-3} d^{-1}); $k_{dis,hyd}$ is the kinetic parameter for disintegration or hydrolysis (d^{-1}), k_m denotes the maximum rate constant for substrate uptake ($kgCOD_{sub}$ $kgCOD_{bio}^{-1}$ d^{-1}); X is the biomass concentration ($kgCOD_{bio}$ m^{-3}); S represents the substrate concentration ($kgCOD_{sub}$ m^{-3}); k_s is the half-saturation constant (kgCOD m^{-3}); and I represents the inhibition factor.

The model was implemented following the standard steps for mathematical modeling studies. Initially, essential experimental data were gathered and organized, emphasizing substrate characterization, which enabled the calculation of the 24 components for both the substrate/waste and the inoculum/sludge, along with other relevant variables. This data represents the feed (input) and the initial reactor condition, specifically the inoculum (sludge). Subsequently, parameters and variables-including stoichiometric, kinetic, and physicochemical values-were verified or determined. Processes such as disintegration, hydrolysis, absorption, and the decay rate of components within the Petersen matrix, as outlined by (BATSTONE et al., 2015), were accounted for, along with any inhibitory effects caused by the accumulation of components due to absorption inhibition.

The model underwent an initial evaluation to verify its accuracy in predicting results, using data extensively referenced in the literature. This step ensured that the

configuration was consistent with expected outcomes. Following this, the input parameters for the substrate and dependent variables were adjusted to correspond with the experimentally determined substrate properties. Lastly, a simulation was performed to represent the system operating under conditions where the reactor was fed with FVW.

4.3.2 Determination of components and units considered for the model

The substrate characterization was performed experimentally to align with the state variables required by ADM1. Measured values included carbohydrates, crude proteins, lipids, butyric, propionic, and acetic acids, as well as TS, VS, and pH. The following steps were undertaken to optimize the modeling: (i) selecting the model components; (ii) determining and calculating the input variables identified in the experiments; (iii) adjusting the initial substrate concentrations; (iv) validating the data, checking the code, and comparing with literature data; and (v) running scenarios. The model was calibrated to laboratory-scale experimental data at approximately 10% TS using a trial-and-error approach (ABBASSI-GUENDOUZ et al., 2012).

The primary control factors associated with the reactor include the biochemical processes for methane conversion and formation, the reactor type and configuration, the mixing mode, and the operating temperature. Operating parameters can impact various performance variables, such as waste-to-methane conversion efficiency, pH, COD, temperature, alkalinity, and nitrogen levels. For ammonia removal, key factors include temperature, pressure, and waste characteristics (HANGOS; CAMERON, 2001). The model also sought to verify carbohydrate, lipid, protein, and inert fraction values and parameters associated with component disintegration and hydrolysis.

4.3.3 Model implementation

As mentioned previously, ADM1 was implemented using the software AQUASIM 2.0 (REICHERT, 1998). The model structure available in the software is primarily formulated for continuous stirred tank reactors (CSTR). However, the experimental system used in this study was an UASB reactor, selected due to its capacity to operate under high OLR.

To represent the real UASB reactor within a modeling framework originally developed for CSTR systems, the reactor was implemented in AQUASIM as an equivalent completely mixed reactor. In this representation, the hydrodynamic behavior of the UASB was

approximated by assuming complete mixing, while the characteristic biomass retention of the sludge blanket was represented by maintaining a high solids retention time (SRT) relative to the hydraulic retention time. This approach allows the ADM1 formulation to reproduce the main process dynamics of UASB systems without modifying the original structure of the model. It should be noted that no external sludge recirculation was applied in the experimental reactor. Instead, biomass retention was implicitly represented through the presence of the sludge bed typical of UASB systems, which promotes the accumulation of active biomass and enables operation at relatively short hydraulic retention times while maintaining long solids retention times.

Compared with other anaerobic processes, the UASB reactor allows operation with short HRT and extended SRT, enabling the treatment of substantial wastewater volumes within compact reactor volumes (DUTTA; DAVIES; IKUMI, 2018). Model calibration was performed exclusively on variables that could be adjusted or experimentally supported, particularly those associated with the composition of FVW. All other parameters were maintained at the default values established in the ADM1 framework (BATSTONE et al., 2015). The mass balances for soluble compounds, particulate components, and gas transfer are represented by Eqs. [4.3], [4.4] and [4.5], respectively (BATSTONE et al., 2015):

$$\frac{dS_i}{dt} = \frac{q_{in}S_{in,i}}{V_{liq}} - \frac{q_{out}S_{out,i}}{V_{liq}} + \sum_{j=1,19} \rho_j \vartheta_{i,j} \quad [4.3]$$

$$\frac{dX_i}{dt} = \frac{q_{in}X_{in,i}}{V_{liq}} - \frac{q_{out}X_{out,i}}{V_{liq}} + \sum_{j=1,19} \rho_j \vartheta_{i,j} \quad [4.4]$$

$$\frac{dS_{gas,i}}{dt} = \frac{q_{gas}S_{gas,i}}{V_{liq}} + \rho_{T,i}\frac{V_{liq}}{V_{gas}} \quad [4.5]$$

Where S_i and X_i represent the concentrations of a soluble component and particulate/active biomass, respectively (kgCOD m^{-3}); q_{in} and q_{out} denote the influent and effluent flow rates to and from the reactor, respectively. V_{liq} is the working volume of the reactor (m^3); $\sum_{j=1,19} \rho_j \vartheta_{i,j}$ represents the sum of the products between the specific kinetic rates for process j and their respective stoichiometric coefficients.

Initial conditions refer to the reactor state at the beginning of the simulation, where the fluid's concentration and/or properties inside the reactor must be specified. In this context,

the sludge at the start is expressed in mg L^{-1}. These initial conditions determine how the reactor initiates its operation. Depending on the scenario, the reactor may already be partially filled or contain residual biomass, COD, or other components that impact the simulation outcomes.

Input refers to the continuous flow of material entering the simulation compartment, which includes the product of the flow rate and the component concentration. Its primary function is to define how the reactor will be fed. The values related to the initial conditions of the sludge are crucial, encompassing biomass components such as: X_{su}, X_{aa}, X_{fa}, X_{c4}, X_{pro}, X_{ac}, and X_{h2}; substrate components like: S_{su}, S_{aa}, S_{fa}, S_{va}, S_{bu}, S_{pro}, S_{ac}, and S_{h2}; inert components including X_I *and* S_I; and gases and inorganics such as S_{CH4}, S_{CO2}, S_{IC}, and S_{NH4}. In the case of the input compartment, the feeding concentration is already predefined, making it unnecessary to calculate the "input" within the reactor compartment.

4.3.4 Statistics and predictive performance

4.3.4.1 Model efficiency coefficients

The model predictions were compared with experimental data from the reactor, as described in Section 5.2.2. Statistical analyses were performed using Past, OriginPro, and Microsoft Excel. The evaluation included linear regression, root mean square error (RMSE), mean absolute error (MAE) (VILMS PEDERSEN et al., 2020), and the Nash-Sutcliffe efficiency (NSE) coefficient (NASH; SUTCLIFFE, 1970).

The RMSE quantifies the deviation between measured and predicted values and is calculated as (Eq. [4.6]):

$$RMSE = \sqrt{\frac{\sum_{t=1}^{n}(y_{m,t} - y_{c,t})^2}{n}} \quad [4.6]$$

And Nash-Sutcliffe coefficient of efficiency (KOCH et al., 2010; LIU et al., 2017) is given by (Eq. [4.7[4.7]):

$$E = 1 - \frac{\sum_t (y_{m,t} - y_{c,t})^2}{\sum_t (y_{m,t} - \bar{y}_m)^2} \quad [4.7]$$

Where $y_{m,t}$ and $y_{c,t}$ denote the experimental and model-predicted values of the state variable at time *t*, respectively; $\bar{y}_m$ is the average of the measured data; and *n* is the total number of observations. Model performance was assessed for key process variables, including methane (CH_4) production, total biogas generation, and selected volatile fatty acids (VFAs), according to the calibration objective.

The Nash–Sutcliffe efficiency coefficient (E) varies from $-\infty$ to 1, where E = 1 represents perfect agreement between simulated and measured values, E = 0 indicates that the model performs no better than the mean of the observations, and E < 0 suggests poor predictive capability.

4.3.4.2 Sensitivity analysis and parameter estimation

An essential phase in process modeling, particularly when applying a model, is investigating parameters to assess their impact on the results quality. This step ensures that the estimated values are accurate, contributing to the optimization of the model while minimizing its complexity.

In this context, a sensitivity analysis was conducted following the guidelines provided in the AQUASIM 2.0 (REICHERT, 1998) manual to identify which ADM1 parameters exhibit the highest sensitivity during biogas and methane production. The analysis focused on methane yield across the different phases. The parameters examined included the microbial decay rate constant (k_{dec}), the disintegration constant (k_{dis}), and the hydrolysis constants for carbohydrates, lipids, and proteins ($k_{hyd,ch}$, $k_{hyd,li}$, and $k_{hyd,pr}$, respectively). Additionally, the half-saturation constants ($k_{s,aa}$, $k_{s,ac}$, $k_{s,c4}$, $k_{s,fa}$, $k_{s,h2}$, $k_{s,pro}$, and $k_{s,su}$) and the maximum substrate uptake rates ($k_{m,aa}$, $k_{m,ac}$, $k_{m,c4}$, $k_{m,fa}$, $k_{m,h2}$, $k_{m,pro}$, and $k_{m,su}$) were analyzed. The sensitivity index (SI) was calculated using the Eq. [4.8]:

$$SI = \delta_{y,p}^{a,r} = p\frac{\partial y}{\partial p} \qquad [4.8]$$

Where *y* represents the specific target variable, in this case, methane concentration, while *p* denotes the model parameter being analyzed for sensitivity. The SI measures the absolute change in *y* resulting from a 100% change in *p*. A positive value of SI indicates a positive correlation between the parameter *p* and the target variable *y*, whereas a negative value

suggests a negative correlation. The equation used to estimate the parameters is presented below Eq. [4.9]:

$$\chi^2(p) = \sum_{i=1}^{n} \left(\frac{y_{meas,i} - y_i(p)}{\delta_{meas,i}} \right)^2 \quad [4.9]$$

Where χ^2 represents the sum of the squared weighted deviations between the actual measured values and the model estimates, with parameter estimation concluding when this value is minimized. In this equation, $y_{meas,i}$ denotes the *i-th* experimental measurement value, y_i (p) is the estimated value of the model variable corresponding to the *i-th* measurement, $\delta_{meas,i}$ represents the standard deviation, $p = (p_1, \ldots pm)$ are the model parameters, and n is the number of data points.

The parameters were estimated based on the sensitivity analysis results, where higher-sensitivity parameters exhibited lower standard deviations. Sensitive parameters were estimated by minimizing the sum of the squared weighted deviations between experimentally measured values and model predictions. The estimation process corresponds to model calibration, aiming to maximize the agreement between simulated and observed values. The target variable chosen to estimate the parameters was the biogas yield.

4.4 Results and discussion

4.4.1 Characterization of the subtract influent

ADM1 relies on COD fractions, which must be inferred from the physicochemical characterization of the substrate (KOCH et al., 2010). In this study, the FVW was characterized based on its COD, TS, VS, and nutritional composition. The liquid fraction of the FVW was obtained by crushing and centrifuging a mixture of various fruits, legumes, and vegetables, with oranges accounting for 42% of the mixture-the most prevalent waste identified in the study area (SILVA JÚNIOR et al., 2022).

The liquid substrate obtained from processing contained 116 $gO_2\ L^{-1}$ of COD, 4% TOC, 9% TS, 93% VS, 45.7 g L^{-1} of carbohydrates, 8% TS of lipids, and 13% TS of crude protein. The raw liquid substrate also exhibited high concentrations of organic acids, including 162 mg L^{-1} of acetic acid, 232 mg L^{-1} of propionic acid, and 192 mg L^{-1} of isobutyric acid.

These compounds are key intermediates in the AD process, as they directly influence microbial activity and the subsequent conversion of substrates into biogas. The presence of these acids suggests that fermentation had already begun, reflecting the ongoing biochemical transformations occurring within the substrate.

Table 4.2 – Substrate characteristics and gas production results

Parameter	Unit	Experimental phases					
		P1	P2	P3	P4	P5	P6
Time	d	15	50	56	131	34	22.0
Feed flow	L d^{-1}	3.1	7.3	10.5	8.4	10.0	11.5
Total COD[a]	gO_2 L^{-1}	5.6±0.1	6.6±0.6	7.1±0.5	9.7±0.4	11.6±0.6	13.2±0.8
OLR	kg $m^{-3}d^{-1}$	1.5	3.5	5.0	7.5	10.0	13.0
TOC[b]	%	0.22	0.24	0.26	0.34	0.40	0.45
TS[b]	%	0.37	0.37	0.37	0.49	0.62	1.29
VS[b]	%TS	86	86	86	75	70	77
Influent pH[a]	-	4.5±0.1	6.1±1.0	6.7±0.5	7.3±0.7	8.7±0.5	7.7±0.9
Carbohydrates[c]	%ST	36	24	40	52	54	67
Lipids[c]	%ST	10	11	12	12	12	6
Crud proteins[c]	%ST	16	18	19	20	19	10
Effluent pH[a]	-	8.2±0.2	8.6±0.2	8.4±0.1	8.3±0.3	8.0±0.2	8.2±0.2
COD rem eff[a]	%	90±3	95±2	96±2	93±3	79±16	64±6
Biogas[a]	NL d^{-1}	9.9±0.6	18.6±2.9	23.1±1.8	30.2±2.2	39.5±2.0	51.2±1.9
Methane	NL d^{-1}	6.3±0.5	11.1±1.1	13.2±1.3	18.0±2.0	23.2±2.5	26.7±0.9
Methane[a]	%	65±2	61±7	57±6	60±9	58±8	52±2
Methane yield	NL_{CH4} $m^{-3}d^{-1}$	500±40	880±90	1,050±100	1,430±160	1,840±200	2,120±70
Methane yield	NL_{CH4} $kgCOD_{rem}^{-1}$	268±6	242±29	237±27	203±26	207±39	260±23
Methane yield	NL_{CH4} $kgCOD_{inf}^{-1}$	250±8	229±24	228±26	189±27	156±15	165±4
Methane yield	NL_{CH4} $kgSV_{inf}^{-1}$	99±7	173±17	205±20	280±32	360±39	416±13
Conversion rates	%	72±4	66±11	64±12	53±13	46±8	46±5

Note 1: The dilution factor ranged from 0.05 to 0.11. WW – wet weight; COD – Carbon Oxygen Demand; OLR – Organic Load Rate; TS – Total Solids and VS – Volatile Solids; TOC – Total Organic Carbon.
Note 2: a – The analyses were performed daily, coinciding with each feeding of the reactor, which occurred once per day, seven days a week; b – The substrate was analyzed before and after dilution for each operational phase; c – Analyses were carried out before diluting the substrate, and the values for each phase were obtained by diluting the raw substrate.

The reactor feed was prepared using varying COD concentrations, achieved by diluting the primary substrate. Table 4.2 presents the physicochemical characteristics of the FVW at different concentrations, corresponding to the previously established reactor operating conditions. In contrast to the findings reported in some studies, the FVW analyzed in this work did not exhibit significant or detectable levels of cellulose, hemicellulose, or lignin (KOCH et al., 2010; SHI et al., 2014; ZHAO et al., 2009).

4.4.2 Experimental results and reactor performance

Operating data from the UASB reactor, collected over six phases, enabled a comprehensive assessment of the system's efficiency in biogas production and organic matter conversion. The analysis focused on key operational parameters, including biogas and methane

flow rates, methane content, methane yield relative to COD removal, influent COD, influent volatile solids, and reactor volume. A summary of the main results from the experimental operation is presented in Table 4.2.

During UASB reactor operation, volumetric methane production increased from 9.9 NL CH_4 d^{-1} to 51.2 NL CH_4 d^{-1}, driven by the rise in applied organic loading. This increase reflects the greater availability of substrate, which supports the growth of anaerobic biomass and enhances the conversion of intermediates into methane. However, it remains uncertain to what extent further increases in organic load will continue to yield productive gains without compromising overall reactor performance.

Although the methane concentration in the biogas decreased, the overall methane yield was not compromised. The increase in OLR, associated with higher substrate input and flow rate, intensified the reactor's internal processes, leading to greater production of intermediates that serve as precursors to methanogenesis. This intensification stimulated bubble formation, which influenced internal hydrodynamics and likely contributed to both methane production and accumulation. These interactions were supported by statistical analyses: application of Kendall's tau coefficient between OLR and volumetric methane production yielded a value of 0.578, indicating a positive correlation between the variables. Moreover, the *p-value*<0.001, well below the 0.05 threshold, confirms that the correlation is statistically significant.

The efficiency of organic matter conversion into methane, represented by the conversion rate, decreased as the organic load increased. This trend was evident across the different operational phases, with the corresponding conversion rates presented in Table 4.2. This decline is likely related to the limitations imposed by the hydrolysis and disintegration rates, which can restrict organic matter degradation due to the complex characteristics of FVW. (KOCH et al., 2010) and (LI et al., 2021) highlight this complexity, suggesting that adjustments to the hydrolysis (k_{hyd}) and disintegration (k_{dis}) rate constants are essential during model calibration for this type of substrate. These variables directly influence the time required to degrade the more recalcitrant components of FVW, which may explain the observed reduction in conversion efficiency over the course of reactor operation.

As the organic load applied to the reactor increased during the operational phases, the availability of particulate material for disintegration also rose, directly influencing organic matter conversion. In the ADM1, this increase in load leads to greater formation of soluble compounds through the disintegration and hydrolysis of particulate matter (X_c fraction), which

subsequently feed the downstream stages of AD. In particular, acidogenesis, which is responsible for converting sugars and amino acids into volatile fatty acids (VFAs), becomes more intense. However, when the OLR exceeds the capacity of methanogenic archaea (represented in the model by the acetoclastic and hydrogenotrophic populations) to consume these VFAs, the intermediates begin to accumulate, primarily acetic, propionic, and butyric acids.

This accumulation lowers the system's pH, a condition represented in ADM1 by acid-base equilibrium equations, which directly influence the growth rates of specific microbial groups sensitive to pH. The resulting inhibition of methanogenic archaea, which are particularly vulnerable to acidic environments, compromises the final stage of AD. This reduces the conversion of VFAs into methane and promotes increased CO_2 production. Jiang, Heaven and Banks (2012) observed this behavior, linking high organic loading rates to elevated CO_2 concentrations in biogas, reflecting both VFA accumulation and system acidification. Nevertheless, during the phases with the highest organic load, the highest volumetric methane yield was recorded, reaching 2.1 NL CH_4 L^{-1}. This suggests that the system retained part of its methanogenic activity, although signs of potential instability were also evident.

The high yields observed during the first phase can be attributed to the lower mass of COD removed, which resulted in a higher specific methane yield, both per unit of COD removed and per unit of influent. As the operation progressed and higher organic loads were applied, a decrease in COD removal efficiency was observed, along with a reduction in the conversion rate of organic matter into methane. This behavior aligns with predictions from the ADM1 model, which indicates that increasing substrate input places additional demand on the hydrolysis and acidogenesis steps, leading to more intense production of VFAs.

However, if the rate at which VFAs are converted by methanogenic archaea (i.e., during the acetogenesis and methanogenesis stages in the model) does not keep pace with their formation, intermediates begin to accumulate, potentially leading to acidification of the medium. This condition directly affects the growth rate of methanogenic microorganisms and reduces the efficiency of organic matter conversion into methane, meaning that a smaller fraction of the removed load is actually transformed into useful (recovered) biogas. Nevertheless, as the total amount of substrate increases with higher loading rates, the system continues to produce greater absolute volumes of methane. This increased volumetric production in the later phases, even with lower conversion efficiency, can be attributed to the higher input of organic matter, part of which remains undegraded. This effect is reflected in the

observed removal percentages: in the final phases, only 79% and 64% of the applied COD was removed, respectively, highlighting the increasing kinetic limitations of the initial steps of the process.

4.4.3 Fractionation of fruit and vegetable waste for biodegradation

ADM1 requires input data derived from the operational performance of the digestion system. In this study, most model parameters were based on original default values. However, variables and constants related to substrate characterization were determined through calculation, following the methodology proposed by (CHEN et al., 2016). The values defining the reactor feed and initial conditions were obtained from controlled laboratory experiments and subsequent calculations to determine the variables for the model, as show in Table 4.3.

Table 4.3 – Distribution of influent COD after disintegration according to factors *f* in L-FVW

Parameter	Description	Unit	L-FVW
f_{ch_xc}	Carbohydrates from X_c	-	0.490
f_{pr_xc}	Proteins from X_c	-	0.135
f_{li_xc}	Lipids from X_c	-	0.084
f_{si_xc}	Solubre from X_c	-	0.284
f_{xi_xc}	Inerts from X_c	-	0.007

The variable X_c represents the initial concentration of the granular FVW substrate, calculated and converted to kgCOD m^{-3}. X_c is divided into specific particulate fractions of proteins (X_{pr}), lipids (X_{li}), carbohydrates (X_{ch}), and inerts (X_i), based on fixed stoichiometric expressions (*f*-factors) (CHEN et al., 2016). The X_i fraction also includes the concentration of specific microorganisms in the system (KOCH et al., 2010; LI et al., 2021; ZHAO et al., 2019a).

The theoretical oxygen demand (thCOD) of these components was calculated to estimate the amount of oxygen required for the complete oxidation of the organic compounds present in the FVW (Table 4.4). This calculation is essential for accurately defining the substrate composition and ensuring a proper biochemical balance within the reactor. The organic load applied to the reactor was determined according to the experimental design parameters defined for each operating condition. These settings allow for precise adjustments in reactor performance, facilitating the control of organic degradation and optimizing both biogas production and organic matter removal.

The equation proposed by Koch et al. (2010) was used to calculate the X_c value for each operational phase. This equation considers the TS content, substrate concentration, and

the variables described previously. The unit specifications required for the calculation are detailed by (ANGELIDAKI; SANDERS, 2004) (see supplementary material).

Table 4.4 – ThOD of different fractions.

Fraction	Elementary formula	Molar mass	ThOD		
		g mol^{-1}	kg_{O2} $kgTS^{-1}$	kg_{O2} m^{-3}	kgTS kg_{O2}^{-1}
Protein (*Pr*)	$C_5H_7O_2N$	113	1.4	1.4	0.7
Carbohydrates (*Ca*)	$(C_6H_{10}O_5)_n$	162	1.2	1.2	0.8
Lipid (*Li*)	$C_{57}H_{104}O_6$	884	2.9	2.9	0.4
Particulate inerts (X_i)	$CH_{1.4}O_{0.4024}N_{0.1429}$	21.8	1.5	1.5	0.7
Soluble inerts (S_i)	$CH_{1.946}O_{0.6754}N_{0.1429}$	26.8	1.3	1.3	0.8

Note: ThOD - Theoretical Oxygen Demand.

Some of the model's input parameters, including stoichiometric coefficients such as $f_{ch,xc}$, $f_{li,xc}$, $f_{pr,xc}$ e $f_{xi,xc}$, were adjusted. To determine these values, the method proposed by Koch et al. (2010) was applied and subsequently refined by (ZHAO et al., 2019a). The equations used for calculating these fractions are based on COD values.

The equations define the fractions in which CH, PR, LI, and I represent carbohydrates, proteins, lipids, and inert compounds, respectively. The values of X_{ch}, X_{li}, and X_{pr}, derived from the degradation of X_c, were calculated using the set of equations proposed by (LÜBKEN et al., 2007) . The model was then implemented with these initial modifications - specifically, the updated fraction values (*f*) and the composition of the *X* inputs while all other fractions retained the default ADM1 parameters.

The calculated values for the fractions varied across different operational phases due to the dilution applied in each experimental stage. Since FS and VS depend on substrate composition and TS concentration, dilution had a direct impact on the *f* fraction. As dilution decreased, SV was proportionally reduced, while FS increased, leading to a rise in the f fraction. Similar variations in fraction calculations across different reactor operating phases have also been reported by (NABATEREGA; NAZYAB; ESKICIOGLU, 2023) and (LI, 2022).

Li et al. (2021) and Zhao et al. (2019a) reported that, to simplify model initialization, equal initial concentrations may be assumed for the seven microbial groups: X_{su}, X_{aa}, X_{fa}, X_{c4}, X_{pro}, X_{ac}, and X_h. In this approach, the inert fraction associated with TS was used as an indirect reference to estimate initial biomass-related values, applying the conversion factor. kgTS kgO_2^{-1}. This procedure does not imply that inert material represents active microbial biomass, but rather provides an operational criterion for initializing microbial concentrations when direct microbial quantification is not available for the system.

4.4.4 Sensitivity analysis

The sensitivity analysis results are shown in Figure 4.1. The results of the sensitivity analysis indicate that the highest values were observed for k_{dec}, k_{dis}, and $k_{hyd,ch}$, followed by $k_{s,ac}$, $k_{s,fa}$, and $k_{s,su}$, and finally, $k_{m,ac}$. The highest SI were found for k_{dec}, k_{dis}, and $k_{hyd,ch}$. The parameter k_{dec} represents the decay rate of microorganisms, modeled as a first-order process, reflecting mechanisms such as cell death, lysis, and endogenous respiration. In the SI, k_{dec} values ranged from –0.15 to 0.62, indicating a significant influence, particularly during the early stages of reactor operation. This impact arises from the fact that, at the beginning of the process, the microbial community is still adapting, and part of the inoculated biomass does not encounter favorable conditions for maintaining metabolic activity, leading to cell death. Introducing the decay rate at this stage directly affects biogas production by reducing the active fraction of biomass responsible for biochemical reactions, especially acidogenesis and methanogenesis. As the process progresses and more stable environmental conditions are established (e.g., pH, temperature, and substrate availability), microbial community stabilization is observed. At this point, the influence of k_{dec} gradually diminishes, as the system reaches a balance between growth and decay, which is characteristic of the stationary phase of AD.

The parameter k_{dis} represents the decomposition rate of particulate matter, which constitutes the initial and often rate-limiting stage of AD. This process governs the release of soluble compounds (such as sugars, amino acids, and volatile fatty acids), which serve as substrates for the subsequent stages of acidogenesis, acetogenesis, and methanogenesis. At the beginning of reactor operation, k_{dis} exerts a significant influence, as evidenced by the value of 0.51 observed in scenario SI. This value reflects the limitation imposed by the availability of soluble organic matter, since a large portion of the initial substrate (FVW) was in particulate form, requiring time to undergo hydrolysis. As digestion progresses, this particulate fraction is gradually degraded, reducing the influence of k_{dis} on biogas production, as indicated by its drop to –0.23. This decrease suggests that, after the initial adaptation and hydrolysis period, the system reaches a condition in which soluble substrates are continuously available, and process control shifts to downstream stages.

Similar to k_{dis}, the parameter $k_{hyd,ch}$ exhibited a peak of 0.3 at the beginning of the operation, followed by a decline to –0.3 and stabilization by the fifth day. This behavior suggests that both stages, the decomposition of particulate matter and the hydrolysis of carbohydrates — act as limiting steps in methane production during the initial phases of

digestion. The limitation arises because the release of soluble substrates is essential to sustain the subsequent stages of the anaerobic process. The decreasing influence of these parameters over time reflects the system's transition out of the adaptation phase. These results highlight the importance of fine-tuning kinetic parameters, as default values may not adequately represent actual operating conditions.

Figure 4.1 – Sensitivity indices (SI) of k_{dec}, k_{dis}, $k_{hyd,ch}$, $k_{hyd,li}$, $k_{hyd,pr}$, $k_{s,aa}$, $k_{s,ac}$, $k_{s,c4}$, $k_{s,fa}$, $k_{s,h2}$, $k_{s,pro}$, $k_{s,su}$, $k_{m,aa}$, $k_{m,ac}$, $k_{m,c4}$, $k_{m,fa}$, $k_{m,h2}$, $k_{m,pro}$, $k_{m,su}$, based on absolute-relative sensitivity function analysis.

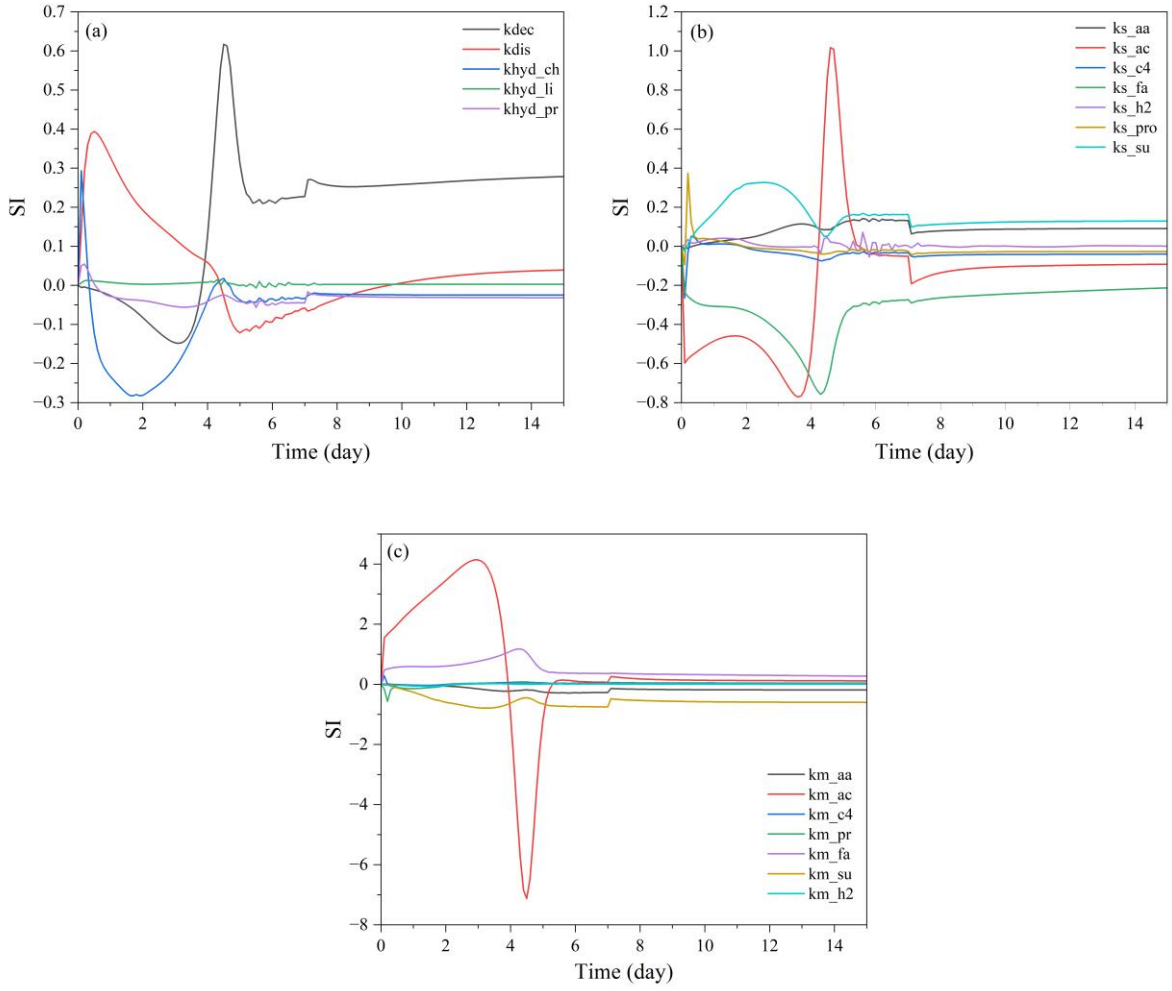

Chen et al. (2016), who investigated the AD of *Hydrilla verticillate,* reported similar behaviors for the evaluated constants. (ZHAO et al., 2019a) and (LI et al., 2021) observed analogous patterns in their study of food waste (FW) and vegetable crops, respectively. These findings underscore the importance of disintegration and carbohydrate

hydrolysis constants in methane production and highlight that precise calibration of these parameters is essential for optimizing biogas yields across a range of substrates.

Substrate composition directly influences the sensitivity of hydrolysis-related kinetic parameters, determining which fractions exert the greatest impact on methane production. In plant-based substrates, such as FVW and FW, the higher content of structural carbohydrates makes $k_{hyd,ch}$ a predominant factor, as the release of fermentable sugars depends on the efficiency of this step. In contrast, for other types of substrates, methane production may be more sensitive to different fractions — such as proteins or lipids — thereby influencing other kinetic parameters. These observations are consistent with the findings of Bułkowska et al. (2018) and Razaviarani and Buchana (2015), who emphasized how specific material characteristics affect the dynamics of the AD process.

Half-saturation constants ($k_{s,process}$) are critical for microbial growth, as they define the substrate concentration at which the microbial uptake rate is reduced to half of its maximum value (LIU; XU; WEI, 2024). Among these $k_{s,ac}$ and $k_{s,fa}$ exhibited the highest variations in the SI, with negative values, indicating that their default estimates may constrain biogas production during the AD of FVW. This occurs because these constants regulate the affinity of methanogenic and *β-oxidizing* populations for acetic acid and long-chain fatty acids, respectively. Inadequate values can lead to an overestimation of inhibition due to low substrate availability, thereby underestimating actual microbial activity. Consequently, the need to adjust these parameters becomes evident to ensure that the model more accurately represents the system dynamics when processing substrates rich in complex organic matter, such as FVW.

In practice, this indicates that biogas production from acetic acid depends directly on substrate availability. Since the initial $k_{s,ac}$ value follows the ADM1 standard, it may not adequately represent the characteristics of FVW. High values of $k_{s,ac}$ reduce microbial affinity for acetic acid, limiting its conversion into methane. Similarly, elevated $k_{s,fa}$ values can lead to the accumulation of fatty acid intermediates, potentially causing process inhibition and reduced efficiency. These outcomes highlight the limitations of using standard ADM1 values for complex plant-based substrates like FVW, emphasizing the need for parameter adjustments to avoid over- or underestimation of biogas production. Furthermore, lower half-saturation constants suggest higher microbial affinity for substrates, which enhances biomass growth and process performance. The influence of $k_{s,su}$ – associated with sugar uptake — was also evident, which aligns with the fact that the primary methane production route in FVW digestion is based

on carbohydrate conversion. Therefore, $k_{s,su}$ becomes a critical parameter in the AD of such feedstocks.

Based on the sensitivity analysis results, the parameters k_{dec}, k_{dis}, $k_{hyd,ch}$, $k_{s,ac}$, $k_{s,fa}$, $k_{s,su}$, and $k_{m,ac}$ were selected for estimation in AQUASIM 2.0 (REICHERT, 1998) to minimize the weighted sum of squared deviations between experimental data and model predictions. The optimization process initially employed the *simplex* algorithm Nelder and Mead (1965) to promote convergence, followed by the *secant* algorithm (RALSTON; JENNRICH, 1978), both implemented within the AQUASIM 2.0 software (REICHERT, 1998).

Parameter values were determined through iterative runs of each algorithm. Initial estimates were based on the standard model defaults, with predefined minimum and maximum bounds, as well as standard deviations. The standard deviations were set according to the percentage variability observed in the experimental data, aiding curve fitting and ensuring coherence between the simulated and measured results, thereby reflecting the reliability of the experimental dataset. The selected sensitive parameters were calibrated against biogas production data to ensure close agreement between the simulated and experimental curves. Table 4.5 presents the reference standard values used in the simulations alongside the corresponding optimized values.

Table 4.5 – Reference standard and optimized values of the most sensitive parameters

Parameter	Unit	Ref. Standard	Optimized value
k_{dec}	d^{-1}	0.02	0.019
k_{dis}	d^{-1}	0.5	0.492
$k_{hyd,ch}$	d^{-1}	10	5.845
$k_{s,ac}$	kgCOD m^{-3}	0.15	0.010
$k_{s,fa}$	kgCOD m^{-3}	0.40	0.218
$k_{s,su}$	kgCOD m^{-3}	0.50	0.010
$k_{m,ac}$	kgCOD $kgCOD^{-1}d^{-1}$	8	2.644

4.4.5 Comparison of simulated results with experimental results

After optimization to ADM1, the simulated results were evaluated against the experimental data from the UASB reactor operation, using performance metrics such as RMSE, NSE, and R^2. A low RMSE value indicates strong model performance, while NSE and R^2 provide additional insights. The NSE assesses the model's predictive capability, particularly for time-series data, whereas R^2 quantifies the proportion of variance in the observed data explained by the model, serving as a measure of the fit quality. Figure 4.2a illustrates biogas and methane production during the initial operational phase used for model calibration, comparing simulations performed with ADM1 reference parameters and optimized values derived from

operational data, as summarized in Table 4.5. For methane production, a slight deviation from the model prediction was observed during the initial days, likely due to early-stage dynamics, but this discrepancy diminished as the system stabilized. After parameter optimization, the model's performance improved notably, with RMSE values increasing from 0.80 to 0.99 and R^2 values rising from 0.79 to 0.95 for both biogas and methane production.

Figure 4.2 – Comparison of Biogas and Methane Production: Simulations with Reference Standards, Optimized Variables, and Experimental Production.

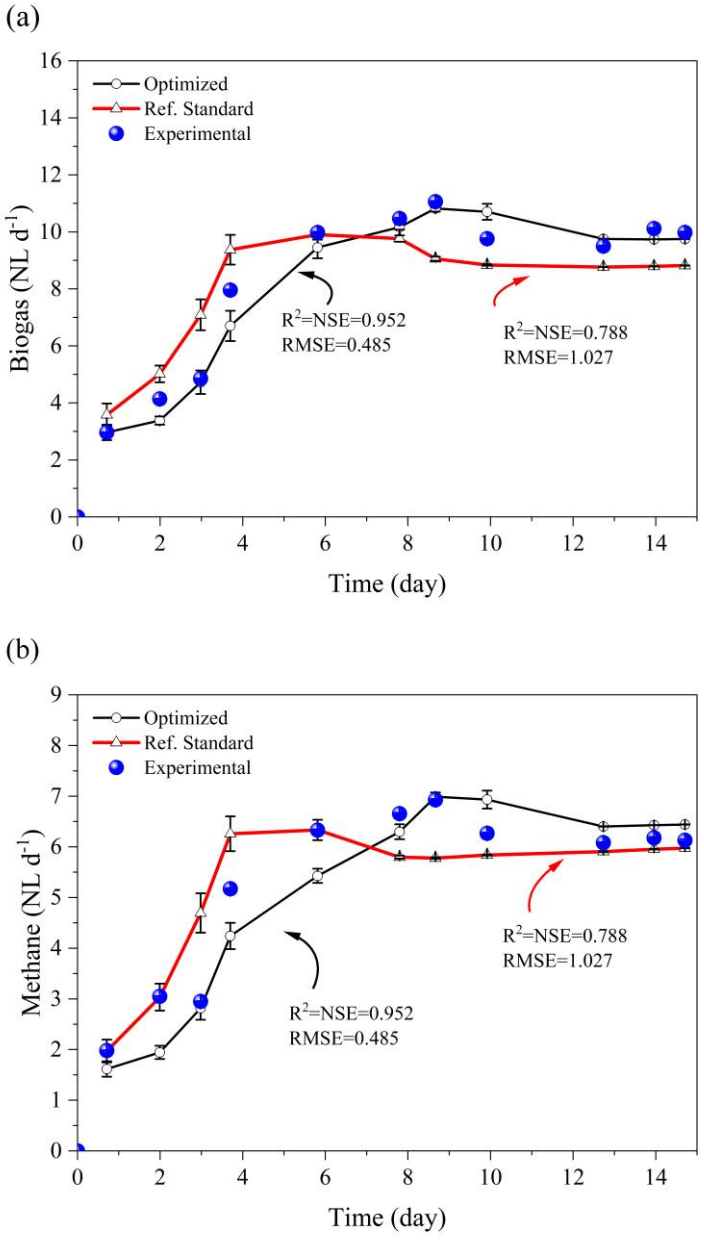

Regarding RMSE, experimental biogas production ranged from 0 to 11.1 NL d^{-1}. An RMSE of 0.34 represents approximately 3% of the maximum observed value, indicating a low average deviation relative to the data scale. In comparison, methane production (Figure

4.2b) ranged from 0 to 6.9 NL d^{-1}, with a higher RMSE of 0.49% around 7% of the maximum. Although this percentage is comparatively greater than that of biogas, it still reflects a satisfactory fit, especially when considering the overall performance metrics used in model evaluation. This underscores the necessity of adjusting the model to accurately reflect the actual conditions of a given reactor. Several authors have emphasized this need by considering specific substrate characteristics. For example, Zhao et al. (2019a), Li et al. (2021), Chen et al. (2016) and Tartakovsky et al. (2008) have adjusted or modified ADM1 variables to better account for operating conditions and substrate-specific properties.

The parameter adjustments made during the initial phase were subsequently applied to later operational stages to assess the model's robustness under varying operational conditions. Figure 4.3 presents the comparison between experimental and optimized methane and biogas production across the different operational phases of the reactor, together with the corresponding OLR variations. Experimental methane and biogas production profiles closely followed the trends predicted by the optimized model. Although the experimental values showed greater variability — mainly due to fluctuations in substrate concentration and other operational parameters — the model yielded more consistent and linear trends, accurately following the overall behavior. Across all operational phases, the comparison between experimental and simulated data resulted in an R^2 value of 0.76, aligning with the findings reported by Chen et al. (2016) and confirming the model's applicability under real-world conditions.

As described in Section 4.4.3, substrate-specific values were calculated to adjust key variables, including the fractions of carbohydrates, lipids, proteins, and other components. The initial adjustments focused on sensitive parameters, which were assumed to remain constant across all phases, as they are inherently dependent on substrate composition. Once calibrated, these adjusted values were applied to subsequent operational phases characterized by changes in feeding conditions — specifically, variations in substrate concentration. The predictive performance obtained under these later operational conditions is presented in Figure 4.3, which compares experimental and optimized methane and biogas production across the different reactor phases.

Figure 4.3 presents the comparison between experimental and optimized methane and biogas production across the operational phases of the reactor, together with the corresponding OLR variations applied during operation. For methane production, the optimized model achieved an R^2 and NSE of 0.84, with an RMSE of 2.87. For biogas production, model

performance was higher, with R^2 and NSE values of 0.92 and an RMSE of 5.8. Although the RMSE for biogas was numerically higher, this reflects the broader absolute range of biogas production values, while the higher R2 and NSE indicate stronger predictive performance for this variable.

Figure 4.3 – Presents the comparison between experimental and optimized methane and biogas production across the operational phases of the reactor, together with the corresponding variations in OLR applied during reactor operation.

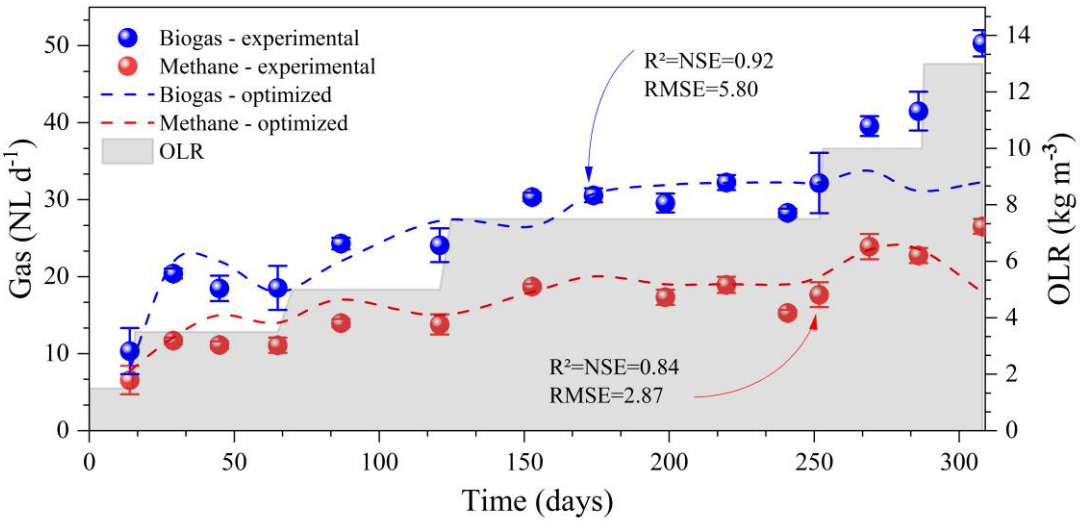

During reactor operation, the OLR was gradually increased by raising the concentration of FVW in the feed. Although an increase in biogas production — particularly in methane content — was expected under these conditions, a decrease in methane concentration was observed (data not shown). Moreover, the application of the optimized parameter values (Table 4.5) to scenarios with higher organic loads did not result in a significant improvement in biogas output. As previously discussed, the elevated substrate concentration may have induced inhibitory effects, potentially related to increased ammonium levels, which are known to impair acetate uptake by methanogenic archaea. However, additional targeted analyses are necessary to verify this hypothesis and better characterize the extent of such inhibition under elevated loading conditions.

The determination of free ammonia, together with acetate monitoring and methane production profiles, is essential for assessing potential process inhibitions. In addition, microbial community analysis offers valuable insights by identifying the presence of acetoclastic methanogens (*Methanosaeta* and *Methanosarcina*) and hydrogenotrophs (*Methanobacterium*). In the event of inhibition, a decline in acetoclastic archaea and an increase

in hydrogenotrophic populations are typically observed, primarily as a result of elevated ammonia concentration (KAYHANIAN, 1999).

Overall, the model demonstrated satisfactory agreement with the actual behavior of the UASB reactor during the AD of FVW throughout the study period, particularly under moderate loading conditions, where the calibrated parameters remained representative of reactor performance. Similar patterns were reported by (ZHAO et al., 2019a), who observed that, in the later stages of operation, fluctuations in biogas production became more pronounced with increasing organic load. Although their model achieved an R^2 of 0.98, its predictive accuracy declined after 90 days due to compromised linearity. In contrast, the reactor assessed in this study exhibited significant deviations only after 250 days of operation, suggesting a more extended period of stability before such effects became evident.

4.4.6 Simulation of the model variables after adjustment

ADM1 enables the identification of consumption and production patterns for specific components. In the initial analyses, acetic and propionic acids exhibited the highest concentrations, reaching 358 g L^{-1} and 65 g L^{-1}, respectively. On the other hand, the concentration of butyric acid, although relevant for the system's feed calculations, was negligible. The acetate generation rate was the most significant contributor to biogas production, as predicted by (SARKER et al., 2019) and (WANG et al., 2023). Furthermore, the substrate was critical in supporting microbial growth and maintenance. The period of elevated acetate production coincided with the highest instability in biogas generation. Once acetate generation and consumption stability was achieved, biogas production became more linear, as shown in Figure 4.2a.

In the ADM1 model, inhibition factors are derived from equations that describe biological and physicochemical processes. When the inhibition factor approaches 1, it indicates negligible inhibition, allowing the process to occur normally. Conversely, when the inhibition factor falls below 1, it reduces the associated reaction rate, potentially leading to the accumulation of the inhibited component. This accumulation arises because the component is not degraded efficiently due to inhibition, adversely affecting process stability and biogas production.

In this context, the simulation revealed that digestion of FVW is susceptible to inhibition of acetate consumption by ammonia. However, as the operation progresses, this

inhibition decreases, approaching a value close to 1. When acetate conversion is inhibited either by free ammonia or another toxic compound, an imbalance occurs between acetate production and consumption (SIEGRIST et al., 2002). The simulation also highlighted both the potential inhibition of acetate consumption and the increase in its concentration throughout the simulation during the first few days (Appendix C – Figure 12.1).

The substrate (FVW) is primarily composed of oranges, as reported by (SILVA JÚNIOR et al., 2022), which is reflected in its initial low pH (Table 4.2). However, during the first few days of operation, the pH rose to values close to 8. As acetate began to accumulate, a sharp decline in pH was observed, reaching as low as 4.5. This behavior highlighted the necessity of a pH control compartment, which played a critical role in maintaining the reactor's pH near neutrality (~7). Stabilizing the pH helped mitigate inhibitory effects associated with acidification, thereby enhancing the system's operational stability.

The behavior of VFAs and pH are presented in Figure 4.4a and 4.4b, respectively. pH is a controllable variable in real systems, and as shown in Figure 4.4b, the experimental pH values remained relatively stable, hovering around 8, as indicated in Table 4.2. This stability is attributed to the intentional control of pH to keep it above 7, a range considered optimal for AD. Such control was significant due to the nature of the substrate used (FVW), which is readily biodegradable and therefore prone to the accumulation of organic acids during hydrolysis and acidogenesis, potentially leading to acidification of the medium.

Figure 4.4a illustrates significant fluctuations in VFA concentrations throughout the reactor's operation, with peaks observed in all phases. The most pronounced fluctuation occurred in the first phase, reaching 718 mg L^{-1}, suggesting an initial adaptation period of the microbial community to the substrate. Similarly, the model simulation predicted elevated VFA concentrations during the early phases, ranging from 624 to 868 mg L^{-1}. This alignment between simulated and experimental results indicates that the model effectively captured the dynamics of acid production and accumulation, particularly during periods when the system was more susceptible to acidification.

The statistical comparison of the data showed that the model's representation of pH was satisfactory, with an R^2 of 0.99 and an RMSE of 0.58. Since pH is a variable with internal control in the model, the simulated values tend to closely match the experimental data. In contrast, the representation of VFAs showed greater variability, which aligns with the dynamic and multifactorial nature of real systems, particularly at laboratory scale. Variations in substrate composition, retention time, storage conditions, and operational handling naturally lead to

fluctuations in VFA production, which the model attempts to capture within the limits of its formulation. Therefore, the variation observed between the experimental and simulated data reasonably reflects the complexity of the process and remains consistent with expectations for this type of system, as indicated by an R^2 of 0.74.

Figure 4.4 – Comparison between volatile fatty acids (VFA) concentrations in the digestate obtained experimentally and by the optimized model, and comparison of the effluent pH measured experimentally and predicted by the model.

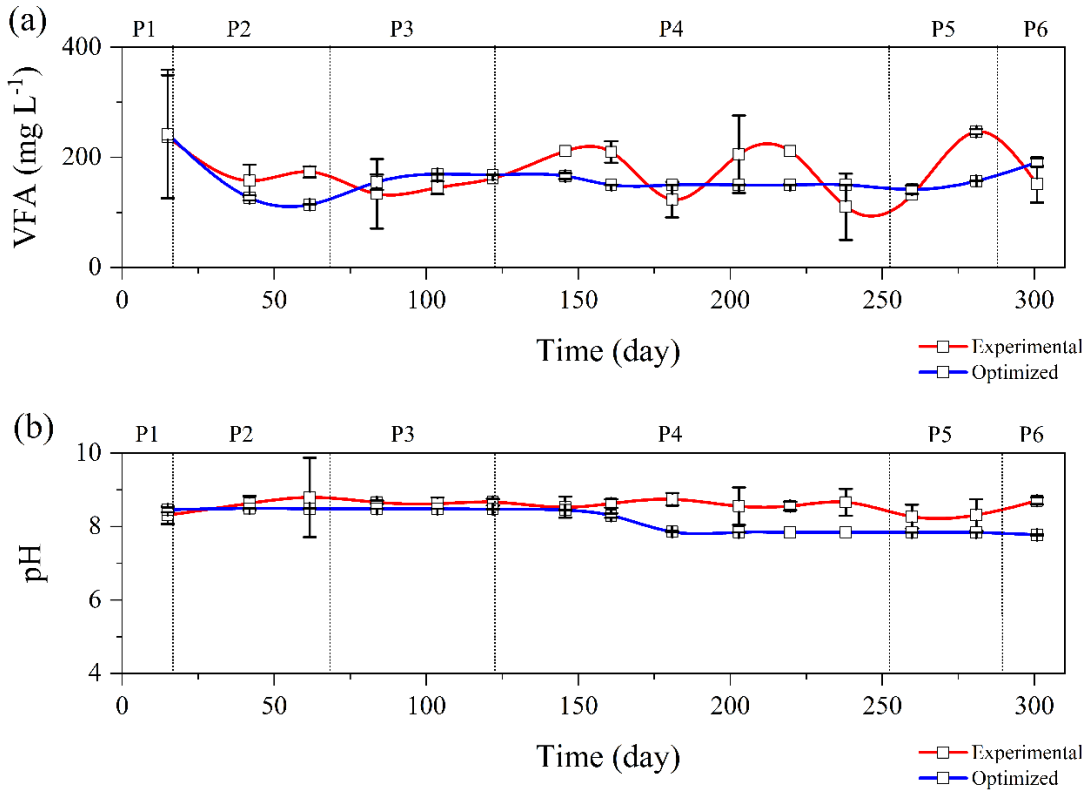

4.4.7 Evaluation of parameter interaction

The ADM1 framework comprises a complex set of parameters interconnected through a series of chain reactions, encompassing both reversible and irreversible conversion processes. These parameters exhibit substantial interdependence, as emphasized by (KOCH et al., 2010) and (LI et al., 2021), highlighting the inherent challenges in accurately calibrating and validating the model to capture the dynamic behavior of the system.

A pairwise interaction analysis was conducted to investigate the interactions among the sensitive kinetic parameters of ADM1. Initially, the limits for each parameter were defined,

and an algorithm was executed in GNU Octave 9.3.0 to generate 60 random values for each parameter within the specified bounds, resulting in a matrix of 3,600 possible parameter combinations. These values, along with the AQUASIM 2.0 model file (REICHERT, 1998) containing the implemented data and system configuration, were externally linked to AQUASIM 2.0. The model was then executed for each parameter combination, producing a file that recorded all parameter sets along with the corresponding fit variable.

The resulting parameter combinations were evaluated based on biogas and methane production, allowing for the identification of parameter boundaries specific to the substrate under study. Dimensionless parameter values were determined by calculating the ratio between each parameter value and its corresponding calibrated value, with an allowed variation of up to ±80% from the calibrated baseline.

The degree of fit is assessed by calculating $\log(\chi^2)$, R^2, and the Nash-Sutcliffe efficiency coefficient. Figure 4.5a, b and c illustrate the interactions between the evaluated parameters and their impact on the model's fit, as represented by $\log(\chi^2)$. Figure 4.5a shows that k_{dis} parameter had a limited impact compared to $k_{hyd,ch}$. Lower values of $k_{hyd,ch}$ were associated with higher $\log(\chi^2)$ values, indicating a poorer fit under these conditions. In contrast, variations in k_{dis} produced minimal changes in biogas output, suggesting that this parameter has a negligible effect on the model's performance. These findings contrast with those of (LI et al., 2021), who reported that lower k_{dis} values significantly influenced biogas production. This discrepancy may be attributed to differences in substrate composition, operating conditions, or the parameter calibration strategies employed in each study.

As shown in the base projection of the graph, the most favorable $\log(\chi^2)$ values were obtained when $k_{hyd,ch}$ exceeded 4. In contrast, k_{dis} values had minimal impact on the model outcomes. Nguyen (2014) suggested increasing the original k_{dis} value from 0.5 to 5.0, which proved effective under the conditions analyzed in that study. However, in the present work, such adjustments did not yield significant improvements, highlighting the importance of context-specific calibration. Figure 4.5b illustrates the interaction between the half-saturation constant for acetate ($k_{s,ac}$) and the maximum acetate uptake rate ($k_{m,ac}$). The results indicate that lower $k_{m,ac}$ values negatively affected biogas production, while $k_{s,ac}$ had a comparatively limited influence. Nevertheless, $k_{m,ac}$ values above 2.5 and $k_{s,ac}$ values below 0.6 led to better model performance, with optimal conditions observed around $k_{m,ac} \approx 3$ and $k_{s,ac} < 0.2$, which corresponded to the lowest $\log(\chi^2)$ values.

Figure 4.5 – Impact of varying combinations of kinetic parameter (k_{dis}, $k_{hyd,ch}$, $k_{s,ac}$, $k_{m,ac}$, $k_{s,fa}$ and k_{dis}) on biogas production.

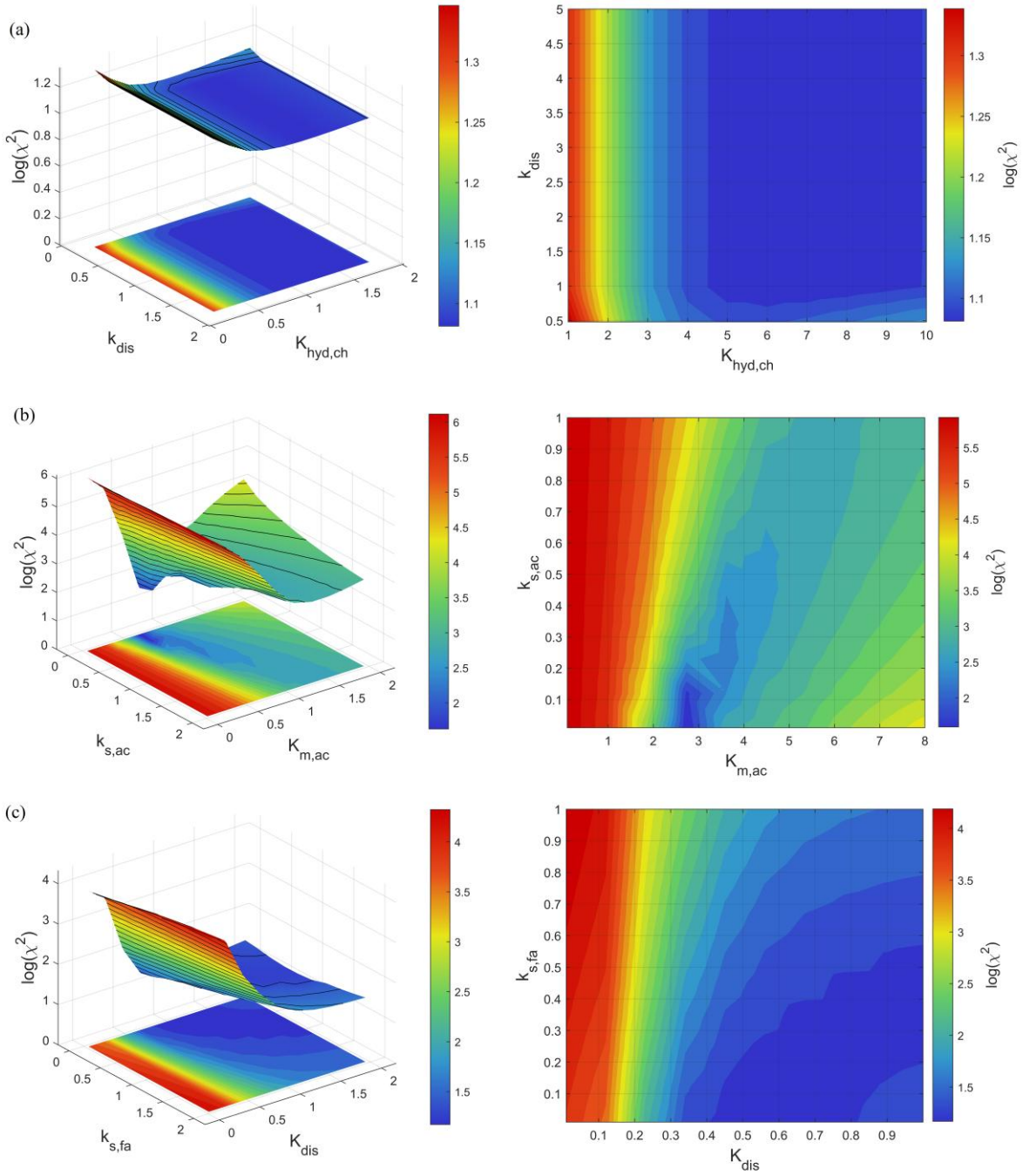

This behavior suggests that calibrating $k_{m,ac}$ is more critical for accurately predicting biogas production than adjusting $k_{s,ac}$, highlighting the model's greater sensitivity to the maximum acetate uptake rate relative to its availability (Figure 4.5b). For this analysis, wider parameter bounds were applied to explore a broader range of potential values. A similar approach was employed by Koch et al. (2010) who used the Nash-Sutcliffe efficiency coefficient along the z-axis to evaluate the interaction between $k_{s,pro}$ and $k_{m,pro}$. Their results

indicated that the parameter space boundaries of $k_{s,pro}$ exerted a greater These findings underscore the importance of considering parameter variability during calibration and the sensitivity of $k_{s,pro}$ under specific conditions.

Figure 4.5c presents the interaction between the long-chain fatty acid (LCFA) half-saturation constant ($k_{s,fa}$) and the disintegration rate constant (k_{dis}). The most favorable $k_{s,fa}$ values for minimizing $\log(\chi^2)$ were below 0.6, while k_{dis} values ranged between 0.4 and 0.8. Notably, k_{dis} exhibited a more pronounced influence on model performance in this context compared to its interaction with $k_{hyd,ch}$, suggesting that its effect is condition-dependent.

4.5 Possible future direction

The FVW utilized in this study undergoes a pre-treatment process that separates it into two fractions: a liquid fraction (TS of 9%) and a semi-solid fraction (TS of 14%). This pre-treatment is applied to maximize the recovery of the liquid fraction while obtaining a semi-solid substrate with the lowest possible moisture content.

This study focuses on the liquid fraction, implementing a phased approach to adapt both the reactor and biomass to the FVW. The process begins with higher dilution, followed by a gradual increase in FVW concentration. This strategy is designed to eliminate dilution-related costs, lower potential operating expenses, and minimize the required reactor size for the AD process.

Future studies will focus on evaluating the application of alternative pre-treatment methods to enhance performance, including physicochemical, thermal, and enzymatic approaches, which are currently under investigation. Additionally, another promising research direction involves the use of direct interspecies electron transfer (DIET) or bioelectrochemical processes to improve AD performance. These strategies offer significant advantages, particularly in optimizing electron transfer between microbial species, potentially increasing process efficiency.

During the simulations, the inhibitory potential of free ammonia was identified. Experimental studies and assessments are essential to clarify the factors contributing to ammonia accumulation in the system, considering parameter variations under different operating conditions. Additionally, other aspects are being studied and evaluated for their application in the AD of FVW. One such approach is two-stage digestion, which includes a pre-

hydrolysis phase to promote acid generation and accelerate methane production while also mitigating potential failures caused by inhibitory compounds formed in earlier stages.

There is also an interest in evaluating the feasibility of strategies such as effluent recirculation to dilute the substrate and co-digestion with carbon-rich materials to balance the C/N ratio, given the system's susceptibility to nitrogen-related inhibition. Additionally, the use of municipal and industrial effluents is being considered, as they can provide essential nutrients absent in FVW, thereby enhancing the efficiency of AD.

Given these factors, FVW can be integrated into biorefineries, enabling the full utilization of both its liquid and solid fractions. This approach allows for the exploration of its potential across various technologies and promising by-products, maximizing bioenergy recovery and the use of digestates in the agricultural industry.

In addition to their environmental benefits, biorefineries offer significant economic potential by enabling the recovery and commercialization of multiple products within an integrated system. Bioenergy generation can ensure the facility's energy self-sufficiency, reducing electricity-related operating costs. Furthermore, the sale of carbon credits from greenhouse gas (GHG) emission mitigation can serve as an additional revenue stream.

The valorization of digestates in the agricultural industry, whether as biofertilizers or soil conditioners, further enhances the economic viability of the process. Integrating AD with complementary technologies, such as co-digestion and effluent recirculation, optimizes system performance and expands the range of commercial applications. As a result, biorefineries not only become financially self-sustaining over time but can also generate profit from multiple revenue streams, establishing themselves as a sustainable and economically attractive model for organic waste utilization.

4.6 Conclusion

This study aimed to apply and adapt the original ADM1 model to the FVW substrate, with a particular focus on calibrating key kinetic parameters specific to this feedstock especially those most sensitive to biogas production. The primary inhibition factors and their relationships with the model's most influential constants were also evaluated. The parameters identified as most sensitive to biogas production were k_{dec}, k_{dis}, $k_{hyd,ch}$, $k_{s,ac}$, $k_{m,ac}$, $k_{m,fa}$, and $k_{m,su}$. For these parameters, representative values for the FVW substrate were estimated at 0.02, 0.49, 5.85, 0.01, 0.22, 0.01, and 2.64, respectively. With appropriate adjustments, the ADM1 model

showed strong predictive accuracy for the AD of the liquid fraction of FVW, with simulated biogas production closely aligning with experimental result.

A modified version is under preparation for submission.

5 ARTICLE II: ADVANCING ADM1 FOR HYDROGEN PRODUCTION VIA DARK FERMENTATION OF LIQUID FRUIT AND VEGETABLE WASTE

ABSTRACT:

This study adapts the Anaerobic Digestion Model No. 1 (ADM1) to represent dark fermentation of liquid fruit and vegetable waste (L-FVW), a heterogeneous substrate in which lactate formation is experimentally observed. The objective is to incorporate lactate production and consumption into the model structure and evaluate its ability to reproduce the main metabolic patterns measured in an Anaerobic Structured Bed reactor. The modified model includes specific kinetic and yield parameters for lactate pathways and is calibrated using experimental data from five operational phases. The adapted ADM1 reproduces biogas production (R^2 = 0.926), hydrogen yield (R^2 = 0.965), gas composition (H_2: R^2 = 0.938; CO_2: R^2 = 0.901), and the dynamics of volatile fatty acids, including lactate accumulation and conversion. The results show that integrating lactate routes significantly improves predictive accuracy and that carbohydrate hydrolysis and sugar uptake control most metabolic fluxes. The study concludes that the modified ADM1 effectively supports the optimization of hydrogen-oriented fermentation.

Keywords: AnSTBR; dark fermentation; fruit and vegetable waste; lactate pathways; modified ADM1.

5.1 Introduction

Several tools have been developed with the aim of optimizing processes and identifying failures before or during the implementation of full-scale projects. In this context, the model proposed by the International Water Association (IWA), the Anaerobic Digestion Model No. 1 (ADM1) (BATSTONE et al., 2002), stands out. ADM1 was originally developed to describe the anaerobic digestion of sewage sludge in Continuous Stirred Tank Reactors (CSTRs), enabling the prediction of biogas production. In addition, ADM1 allows the identification of inhibitory compounds and operational limitations that affect the performance of anaerobic digestion (AD) systems (WASZKIELIS; BIALOBRZEWSKI; BULKOWSKAK, 2022).

Due to its modular and flexible structure, ADM1 can be adapted to different applications and experimental configurations, including modifications that exclude the methanogenic stage, thereby enabling the simulation of biological hydrogen production (BLUMENSAAT; KELLER, 2005; PENUMATHSA et al., 2008). Some of these adaptations involve the inclusion of metabolic products not considered in the original model, such as lactic acid, a byproduct of acidogenesis that does not play a relevant role in conventional methanogenic systems but may have a significant impact on hydrogen-oriented processes (ECONOMOU et al., 2024).

The need for such adaptations becomes particularly evident when ADM1 is applied to the dark fermentation (DF) of complex substrates, such as agro-food residues. Unlike synthetic substrates or pure sugars, these residues exhibit high compositional heterogeneity, which directly influences dominant metabolic pathways, the formation of intermediate products, and overall process stability. Thus, the physicochemical characteristics of the substrate not only govern the performance of the biological system but also impose adjustments to the structure and parameters of the adopted mathematical model.

In this context, fruit and vegetable waste (FVW) emerges as a substrate of considerable interest at both national and international levels, driven by the increase in food demand associated with population growth. Concurrently, a significant rise in food waste has been observed along the food supply chain, intensified by factors such as aesthetic standards for commercialization, high perishability, regulatory requirements, and limitations related to transportation, storage, treatment, and marketing processes. As a result, FVW frequently loses

its suitability for human consumption and is predominantly disposed of in sanitary landfills (LIU et al., 2012).

Despite this scenario, FVW presents substantial potential for application in AD processes due to its favorable physicochemical characteristics, including the high availability of readily biodegradable carbohydrates and the presence of organic acids. However, raw FVW exhibits operational limitations associated with its high total solids (TS) content, typically around 15%, which prevents its direct application in biological hydrogen production processes. Therefore, a physical pretreatment is required, involving grinding, centrifugation, and sieving steps, with the aim of separating the substrate into two fractions with distinct characteristics: a liquid fruit and vegetable waste (L-FVW), with a reduced TS content (approximately 9%), and a solid fruit and vegetable waste (S-FVW), with a higher TS concentration, around 14% (DE MENEZES et al., 2024). In the present study, hydrogen production was carried out exclusively using the L-FVW, while the S-FVW was directed to dry anaerobic digestion (D-AD) for methane production in a dry methanization reactor, as investigated in an independent study (SILVA et al., 2024)

Recent studies have reported relevant concentrations of lactic acid during the fermentation process of L-FVW waste widely generated by the food sector (DE MENEZES et al., 2024), The presence of this metabolite reinforces the need for its inclusion in mathematical models aimed at hydrogen production, as its formation can significantly influence the electron balance and the distribution of metabolic products. The incorporation of these components into the modeling framework requires the definition of new kinetic and stoichiometric parameters (WASZKIELIS; BIALOBRZEWSKI; BULKOWSKAK, 2022), particularly considering that the composition of L-FVW, determined by the proportions of its fractions, directly affects the behavior of the AD process.

In addition to limitations related to substrate composition, biological hydrogen production is subject to thermodynamic constraints, resulting in relatively low yields, typically ranging from 2 to 4 mol of H_2 per mol of glucose consumed, compared to the theoretical maximum of 12 mol of H_2 per mol of glucose (SAADY, 2013). Furthermore, hydrogen production systems operate within narrow pH ranges, requiring strict control of this variable as well as adequate nutrient availability, which leads to higher operational costs and the need for specialized labor. The high sensitivity to operational fluctuations makes these systems prone to instability, particularly due to rapid pH drops caused by volatile fatty acid accumulation, shifts in metabolic pathways that reduce hydrogen yields (e.g., lactate or ethanol fermentation),

inhibition by dissolved hydrogen, and competition with other microbial groups such as methanogens and homoacetogens (HALLENBECK; BENEMANN, 2002; SHOW et al., 2012). Moreover, the presence of complex substrates rich in lignocellulosic compounds, proteins, and lipids hinders degradation and reduces the efficiency of biochemical conversion (NABATEREGA et al., 2021; ZHOU et al., 2018).

Within this context, the objective of this study was to investigate and evaluate the applicability of ADM1 to hydrogen production from the dark fermentation of the L-FVW. Kinetic parameters associated with sugar consumption, as well as yield coefficients for the formation of acetic, propionic, and butyric acids, were estimated using experimental data obtained from continuous hydrogen production assays conducted under different organic loading rates (OLR). Although previous studies have addressed the mathematical modeling of dark fermentation, the application of ADM1 to continuous systems using L-FVW has not yet been reported in the literature. Additionally, the model structure was modified to include lactate and ethanol as metabolites derived from the degradation of L-FVW, aiming to provide a more realistic description of the hydrogen production process, based on previously published data (DE MENEZES et al., 2024; MENEZES et al., 2024; SILVA JÚNIOR et al., 2022).

5.2 Materials and methods

5.2.1 Experimental set-up

The experiments were conducted in an anaerobic structured-bed reactor (AnSTBR) made of glass, with a total volume of 8 L and a working volume of 4 L. The reactor had an internal diameter of 10 cm and was operated under mesophilic conditions at 30 ± 1 °C. The system contained a fixed structured bed filled with Biomídia used as support media for biomass immobilization, allowing microbial growth in adhered form. The Biomídia units were attached to a set of iron rods in order to maintain bed stability and prevent movement caused by bed expansion under the applied upflow velocity. Continuous feeding was performed using the L-FVW at a flow rate of 0.5 L h^{-1}. Liquid recirculation was applied to enhance mixing and mass transfer, resulting in an upflow (superficial) velocity of 1 m h^{-1}.

The reactor was initially inoculated with anaerobic brewery sludge at 10% (v/v) of the working volume. Prior to inoculation, the sludge was thermally pretreated to inhibit methanogenic archaea. The thermal pretreatment consisted of heating the sludge to 90 °C for 10 min, followed by rapid cooling in an ice bath for an additional 10 min until ambient temperature (25 °C) was reached, under constant agitation (DE MENEZES et al., 2024). Before continuous operation, the system was subjected to a 4-day adaptation period under batch conditions. After this start-up phase, the reactor was switched to continuous operation.

5.2.2 Experimental design

The reactor was operated for a total period of 180 days and fed with L-FVW diluted to progressively increasing organic concentrations. The raw L-FVW, obtained after substrate pretreatment, exhibited a chemical oxygen demand (COD) of 116 g L^{-1}, total solids (TS) of 9%, and total volatile solids (TVS) corresponding to 94% of TS (DE MENEZES et al., 2024; SILVA JÚNIOR et al., 2022). Substrate pretreatment consisted of mechanical grinding followed by centrifugation, resulting in the separation of a liquid fraction (L-FVW), which was collected and stored at 4 °C to prevent biodegradation prior to its use as reactor feed. The raw L-FVW was subsequently diluted to achieve the desired organic loading rates applied during reactor operation. The detailed physicochemical characterization of both the raw substrate and its liquid fraction is reported by Silva Júnior et al. (2022), and a summary of these properties is presented in Table 5.1.

Table 5.1 – Main characteristics of liquid fruit and vegetable waste.

Component	Unit	L-FVW	Explanations
Total Solids (TS)	%	11.0.	from analysis
Volatile Solids (SV)	%	10.3	from analysis
Fixed Solids (FS)	%	0.7	=TS-VS (calculated)
VS/TS	%	92.7	=VS/TS (calculated)
Density of wet food waste	kg m^{-3}	1,000	assumed
Moisture	%	90.6	from analysis
Total Carbon (TC)	TC% DB	35.7	from analysis
Total Nitrogen (TN)	TN% DB	1.5	calculated
C/N	%	23.8	=TC/TN
Lipids (X_{li})	mg L^{-1}	0.80	from analysis
Row proteins (X_{pr})	mg L^{-1}	1.25	from analysis
Carbohydrates (X_{ch})	mg L^{-1}	45.65	from analysis
Total COD	kg COD kg VS^{-1} (WB)	0.12	from analysis
VS COD	kg COD kg VS^{-1} (DB)	1.33	from analysis
Organic acids			
Acetic acid	mg L^{-1}	162	from analysis
Propionic acid	mg L^{-1}	232	from analysis
Isobutyric acid	mg L^{-1}	192	from analysis

Data: Adapted from de Menezes et al. (2024).
Note: COD_t estimated 270 g kg^{-1} WW, TC is 47.6% TS; WB – Wet basis; DB – Dry basis.

For each operational phase, the liquid substrate was diluted to achieve influent COD concentrations of 10, 12, 15, 18, and 20 g L^{-1}, respectively. A constant hydraulic retention time (HRT) of 6 h was maintained throughout all phases. Based on the applied influent concentrations and hydraulic conditions, the corresponding OLR were 40, 48, 60, 72, and 80 kg COD m^{-3} d^{-1}.

The reactor pH was continuously monitored and adjusted, when necessary, by the addition of 15 M NaOH to ensure that the effluent pH was maintained at approximately 4.5. This operational strategy was adopted to suppress methanogenic archaea and favor hydrogen-producing fermentative pathways. The experimental data obtained under these conditions were subsequently used for calibration and validation of the ADM1 model, adapted in this study to represent the dark fermentation of L-FVW within a two-stage anaerobic reactor framework.

5.2.3 Experimental analysis

COD (5220 D. Closed Reflux, Colorimetric Method), total solids (TS) (2540 B. Total Solids Dried at 103–105°C), volatile solids (VS) (2540 E. Fixed and Volatile Solids Ignited at 550°C), and nitrogen total Kjeldahl (4500-Norg B. Macro-Kjeldahl Method) were analyzed according to the Standard Methods for Examination of Water and Wastewater (APHA, 2022). The total carbohydrate content was determined using Dubois's colorimetric method with sucrose as the reference sugar (DUBOIS et al., 1956). Volatile fatty acids (VFA) and alcohols were determined in high-performance liquid chromatography using a Shimadzu chromatograph with a refractive index detector (RID – M20A) and an Aminex HPX-87 column (Bio-Rad, 300×7.9 mm). The mobile phase was a 5 mM sulfuric acid solution, run in isocratic mode at 0.6 mL/min, with an injection volume of 20 µL and an oven temperature of 65°C for 35 min. The volumetric biogas production was determined using a Ritter automatic meter connected to the reactor headspace. The biogas composition was evaluated by gas chromatography (GC-2010, Shimadzu) using methane, hydrogen, carbon dioxide, and nitrogen as reference gases for the calibration curve (PARANHOS; SILVA, 2018). The equipment used a thermal conductivity detector, with temperatures of the injector, detector, and column set to 30, 200, and 230°C, respectively. Argon was applied as a carrier gas.

Lipids were quantified according to the American Oil Chemists' Society Am 5-04 method (AMERICAN OIL CHEMISTS' SOCIETY (AOCS), 2004), using a high-pressure, high-temperature extraction system on the Ankom XT-15 (ANKOM, 2009). Protein content was determined by the Dumas combustion method with the NDA 701 Nitrogen/Protein

Analyzer (VELP SCIENTIFICA, 2019), using EDTA as the reference standard in accordance with AOAC method 992.23. Mass loss was assessed to determine moisture content by desiccation in an oven set at 105 °C (AOAC (ASSOCIATION OF OFFICIAL ANALYTICAL CHEMISTS), 2016).

Total Organic Carbon (TOC) was analyzed using a Shimadzu SSM-5000 TOC Analyzer, which employs catalytic combustion at 900 °C. Carbon in the sample is oxidized to carbon dioxide (CO_2), which is detected by a non-dispersive infrared detector (NDIR). This equipment allows for the measurement of total carbon (TC), inorganic carbon (IC), and TOC in both solid and aqueous samples. IC is determined by acidifying and oxidizing the sample at 200 °C, while TOC is calculated by subtracting IC from TC (TOC = TC - IC). The user places up to 1 g of samples in labeled vials and removes them post-analysis for reuse or proper disposal.

5.3 Model development and simulation

5.3.1 Determination of components and units considered for the model

The primary control factors associated with the reactor include the biochemical processes for hydrogen conversion and formation, the reactor type and configuration, the mixing mode, and the operating temperature. Operating parameters can affect various performance variables, including waste-to-hydrogen conversion efficiency, pH, COD, temperature, alkalinity, and nitrogen levels. For ammonia removal, key factors include temperature, pressure, and waste characteristics (HANGOS; CAMERON, 2001). The model also sought to verify carbohydrate, lipid, protein, and inert fraction values and parameters associated with component disintegration and hydrolysis.

5.3.1.1 Estimation of Kinetic and Stoichiometric Parameters–Model Prediction

The proposed and implemented modifications are based on the anaerobic processing of L-FVW under favorable conditions for hydrogen production. Initially, the AnSTBR reactor was operated with increasing OLR, from 40 to 80 g COD m^{-3} d^{-1}. During L-FVW fermentation, VFAs (acetic, butyric, propionic, and isobutyric acids) were identified, along with lactic acid.

Considering the observed stoichiometric behavior, specific metabolic pathways were investigated, including the decarboxylation and reduction of lactic acid, a precursor of butyric, propionic, and acetic acids (Eq. [5.1]). Ethanol was also considered due to its relevance as a co-product, frequently co-formed with lactate in certain fermentative routes (ANTONOPOULOU et al., 2012a; MO et al., 2023), with both compounds described by Monod-type kinetics.

The inclusion of lactate and ethanol also required the incorporation of specific acid–base equilibrium equations for these compounds. In addition, first-order dynamic equations were introduced to represent the decay of lactate-degrading microbial populations (X_{lac}) and Lactobacillus ($X_{lac,su}$).

To ensure compatibility with the original ADM1 equations and variables, pH inhibition effects and microbial growth limitations due to inorganic nitrogen availability were also considered (Eq. [5.1], [5.2], and [5.3]). In this context, the term $I_{IN,lim}$ represents microbial limitation associated with inorganic nitrogen availability and does not explicitly account for inhibitory effects caused by free ammonia accumulation. The explicit incorporation of ammonia inhibition was not adopted in the present model structure because the available analytical dataset did not support robust estimation of additional inhibition parameters, although its inclusion may be considered in future studies focused on nitrogen dynamics during L-FVW fermentation.

Lactate uptake rate:

$$\rho_{21} = k_{m,lac} \frac{S_{lac}}{K_{s,lac} + S_{lac}} . X_{lac} . I_{pH} . I_{IN,lim} \quad [5.1]$$

Sugar uptake rate

$$\rho_{5} = k_{m,su} \frac{S_{su}}{K_{s,su} + S_{su}} . X_{su} . I_{pH} . I_{IN,lim} \quad [5.2]$$

Sugar uptake rate by lactobacillous

$$\rho_{22} = k_{m,lac,su} \frac{S_{su}}{K_{s,lac,su} + S_{su}} . X_{lac,su} . I_{pH} . I_{IN,lim} \quad [5.3]$$

Where $k_{m,ac}$, $k_{m,su}$ and $k_{m,lac,su}$ are the maximum specific uptake rates according to Monod kinetics (kg COD kg COD^{-1} d^{-1}); $k_{s,lac}$, $k_{s,su}$ and $k_{s,lac,su}$ are half-saturation constants (kg

COD m^{-3}); S_{lac} and S_{su} are the concentrations of lactate and sugars, respectively; and X_{lac} and $X_{lac,su}$ are the concentrations of lactate- and ethanol-degrading microorganisms, respectively (kg COD m^{-3}).

5.3.1.2 Determination and verification of stoichiometric coefficients of metabolic products from monosaccharide fermentation

In the model framework, lactate was considered as an intermediate metabolite and ethanol as a potential fermentation product (Figure 5.1), both derived from glucose ($C_6H_{12}O_6$) conversion pathways reported in the literature (COSTELLO; GREENFIELD; LEE, 1991a, 1991b; REN; WANG; HUANG, 1997; SKIADAS; GAVALA; LYBERATOS, 2000). These compounds are not included in the original ADM1 structure due to their limited relevance in conventional AD systems. The formation of lactate and ethanol was represented through stoichiometric reactions corresponding to homofermentative [$n_{1,su}$], heterofermentative [$n_{2,su}$], and bifidogenic (Bifidus pathway) [$n_{3,su}$] routes, as described by Dareioti, Vavouraki and Kornaros (2014) and Economou et al. (2024). The associated reactions and stoichiometric coefficients are summarized in Table 5.2.

Table 5.2 – Degradation reactions of sugar, lactic acid, acetic acid, and hydrogen with stoichiometric coefficients for different pathways.

Reactions of degradation in ADM1		**Fractions**
Sugar	$C_6H_{12}O_6+2H_2O \rightarrow 2CH_3COOH+2CO_2+4H_2$	$n_{1,su}$
	$3C_6H_{12}O_6 \rightarrow 4CH_3CH_2COOH+2CH_3COOH+2CO_2+2H_2O$	$n_{2,su}$
	$C_6H_{12}O_6 \rightarrow CH_3CH_2CH_2COOH+2CO_2+2H_2$	$n_{3,su}$
Sugar	$C_6H_{12}O_6 \rightarrow 2CH_3CH(OH)COOH$	$n_{1,su}$
	$C_6H_{12}O_6 \rightarrow CH_3CH(OH)COOH + CH_3CH_2OH + CO_2$	$n_{2,su}$
	$2C_6H_{12}O_6 \rightarrow 3CH_3COOH + 2CH_3CH(OH)COOH$	$n_{3,su}$
Lactate	$3CH_3CH(OH)COOH \rightarrow 2CH_3CH_2COOH + CH_3COOH + CO_2 + H_20$	$n_{1,lac}$
	$2CH_3CH(OH)COOH \rightarrow CH_3CH_2CH_2COOH + 2CO_2 + 2H_2$	$n_{2,lac}$
Acetic	$3CH_3COOH + H_2 \rightarrow CH_3CH_2CH_2COOH + 2H_2O$	$n_{1,bu,su,ac}$=1
Hydrogen	$4H_2 + 2CO_2 \rightarrow CH_3COOH + 2H_20$	$n_{1,ac,h2}$=1
Products of degradation		**Stoichiometric Coefficients** kg COD kg COD^{-1}
Sugars uptake	Acetic acid (CH_3COOH)	$f_{ac,su}=0.67n_{1,su}+0.22n_{2,su}$
	Propionic acid (CH_3CH_2COOH)	$f_{pro,su}=0.78n_{2,su}$
	Butyric acid ($CH_3CH_2CH_2COOH$)	$f_{bu,su}=0.83n_{3,su}$
	Hydrogen (H_2)	$f_{h2,su}=0.33n_{1,su}+0.17n_{3,su}$
Sugars uptake	Lactate ($CH_3CH(OH)COOH$)	$f_{lac,su}=0.5(1+n_{1,su})$
	Acetic acid (CH_3COOH)	$f_{ac,su}=0.5(n_{3,su})$
	Ethanol (CH_3CH_2OH)	$f_{eth,su}=0.5n_{2,su}$
Lactate uptake	Acetic acid (CH_3COOH)	$f_{ac,lac}=0.22n_{1,lac}$
	Propionic acid (CH_3CH_2COOH)	$f_{pro,lac}=0.78n_{1,lac}$
	Butyric acid ($CH_3CH_2CH_2COOH$)	$f_{bu,lac}=0.83(1-n_{1,lac})$
	Hydrogen (H_2)	$f_{h2,lac}=0.17(1-n_{1,lac})$
Acetic and H_2 uptake	Butyric acid ($CH_3CH_2CH_2COOH$)	$f_{bu,su,ac}=1.25n_{1,bu,su,ac}$
Hydrogen uptake	Acetic acid (CH_3COOH)	$f_{ac,h2}=n_{1,ac,h2}$

Note: The values of $n_{i,j}$ depend on the substrate type and the operating system, as they are calculated based on the concentrations of acids and other components derived from substrate degradation. Therefore, no fixed intervals can be defined for these fractions, since they are determined by system-specific operational conditions and may vary between substrates and even within the same substrate under different operating conditions.

Each equation corresponds to the stoichiometric fractions $n_{1,su}$, $n_{2,su}$, and $n_{3,su}$. In the original ADM1 framework, the sum of these fractions is constrained to unity. In the modified approach adopted in this study, the stoichiometric coefficients for lactate, acetate, and ethanol were defined as functions of the fractions associated with each fermentation pathway. Following the recommendations for adapting ADM1 to alternative sugar uptake routes (ECONOMOU et al., 2024), $n_{3,su}$ was treated as independent of $n_{1,su}$ and $n_{2,su}$, allowing greater flexibility in representing alternative monosaccharide fermentation pathways. The production of the remaining fermentation products (acetic, propionic, and butyric acids, as well as hydrogen) was then calculated based on the defined pathway fractions, ensuring overall mass balance consistency (ANTONOPOULOU et al., 2012a, 2012b).

Figure 5.1 – Metabolic pathways of lactate formation and degradation and their role in hydrogen production during dark fermentation

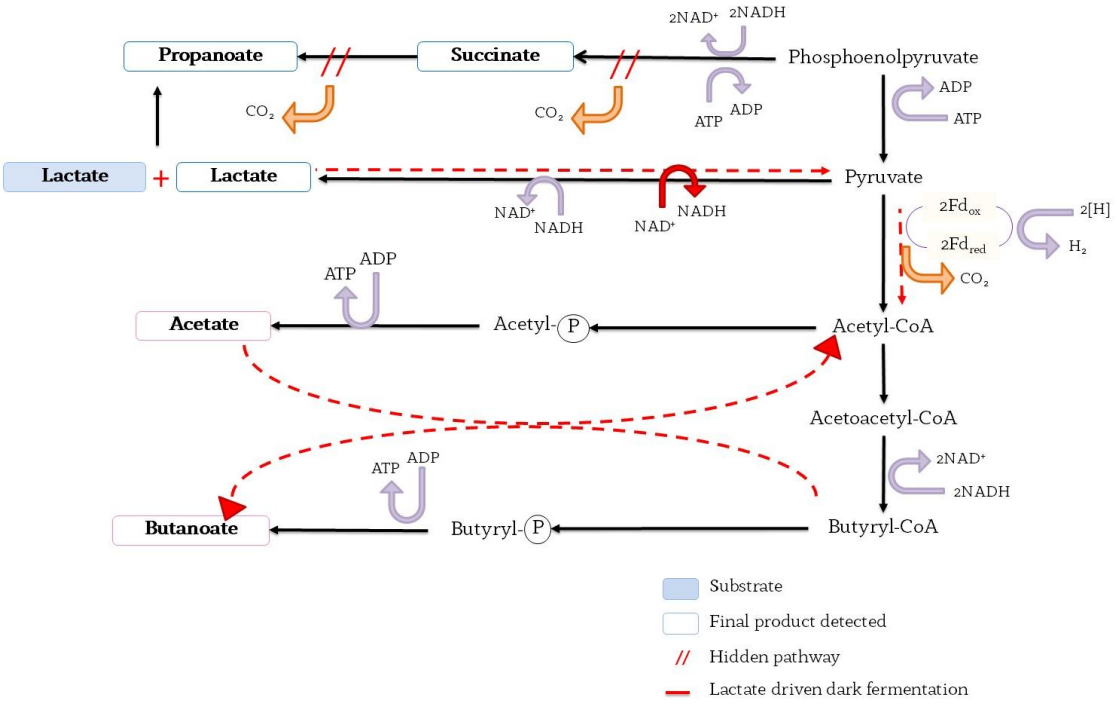

Data: adapted from de Menezes et al. (2023).

The first pathway ($n_{1,lac}$) corresponds to the acrylate pathway, which converts lactate into propionate, acetate, and carbon dioxide. The second pathway ($n_{2,lac}$) was introduced in this study to represent a reductive butyric route, in which lactate is converted into butyrate,

carbon dioxide, and hydrogen. In this case, the sum of $n_{1,lac}$ and $n_{2,lac}$ equals 1, ensuring a balanced distribution among the potential lactate degradation pathways. Table 5.2 summarizes the stoichiometric coefficients used in the modified ADM1; the original values are reported in Batstone et al. (2002).

The thermal pretreatment applied to the sludge specifically aimed to inactivate heat-sensitive microbial groups, particularly acetoclastic (X_{ac}) and hydrogenotrophic (X_{h2}) methanogenic archaea, through enzyme denaturation and disruption of cell membranes. As a direct consequence, the metabolic pathways associated with the conversion of acetate to methane (ρ_{11}) and hydrogen to methane (ρ_{12}) were functionally interrupted. In the modeling context, this implies that the corresponding stoichiometric reactions ($n_{1,ac}$ and $n_{1,ac,h2}$), as well as their respective kinetic expressions, were deactivated in the model, since there is no significant production or consumption of these intermediates in the evaluated system.

The thermal pretreatment applied to the sludge specifically aimed to inactivate heat-sensitive microbial groups, particularly acetoclastic (X_{ac}) and hydrogenotrophic (X_{h2}) methanogenic archaea, by enzyme denaturation and cell membrane disruption. In the model, these microbial populations were set to zero, effectively deactivating the corresponding metabolic pathways for acetate and hydrogen conversion to methane (ρ_{11} and ρ_{12}). As a result, the stoichiometric reactions ($n_{1,ac}$ and $n_{1,ac,h2}$) and their kinetic expressions were not active in the simulations. Since X_{ac} and X_{h2} were inactivated in the model, the corresponding decay rates ($k_{dec,Xac}$ and $k_{dec,Xh2}$) were not considered in the simulations.

The modifications required to represent the specific reactor operating conditions in the model are summarized in the modified Petersen matrix shown in Table 5.3, while the complete description of all modeled processes and components is provided in Appendix D (Table 13.1 and Table 13.2).

Table 5.3 – Stoichiometric representation (Peterson matrix) of the glucose degradation process in the modified ADM1, including alternative pathways for lactate and ethanol integrated into the model.

j	**Component → *i*** **Process ↓**	**5** S_{bu}	**6** S_{pro}	**7** S_{ac}	**8** S_{h2}	**13** S_{eth}	**14** S_{lac}	**15** X_c	**27** X_{lac}	**28** $X_{lac,su}$	**Rate (ρj,kg COD($m^3 \cdot d)^{-1}$)**
5.2	Uptake of Sugar	$(1-Y_{su})\cdot f_{bu,su}$	$(1-Y_{su})\cdot f_{pro,su}$	$(1-Y_{su})\cdot f_{ac,su}$	$(1-Y_{su})\cdot f_{h2,su}$	$(1-Y_{su})\cdot f_{eth,su}$					$k_{m,su} \cdot \frac{S_{su}}{k_s + S_{su}} \cdot X_{su} \cdot I_1$
20	Decay of X_{lac}							1	−1		$k_{dec,Xla} \cdot X_{lac}$
21	Uptake of lactate	$(1-Y_{lac})\cdot f_{bu,lac}$	$(1-Y_{lac})\cdot f_{pro,lac}$	$(1-Y_{lac})\cdot f_{ac,lac}$	$(1-Y_{lac})\cdot f_{h2,lac}$		−1		Y_{lac}		$k_{m,lac} \cdot \frac{S_{lac}}{k_{s,lac} + S_{lac}} \cdot X_{lac} \cdot I_1$
22	Sugars uptake rate by Lactobacillus						$(1-Y_{su})\cdot f_{lac,su}$			$Y_{lac,su}$	$k_{m,lac,su} \cdot \frac{S_{su}}{k_{s,lac,su} + S_{su}} \cdot X_{lac,su} \cdot I_1$
23	Decay of Lactobacillus							1		−1	$k_{dec,Xla,su} \cdot X_{lac,su}$
		Total Butyrate (kg COD m^{-3})	Total Propionate (kg COD m^{-3})	Total Acetate (kg COD m^{-3})	Hydrogen gas (kg COD m^{-3})	Total Ethanol (kg COD m^{-3})	Total Lactate (kg COD m^{-3})	Composites (kg COD m^{-3})	Lactate Degraders (kg COD m^{-3})	Lactobacillus (kg COD m^{-3})	Inhibition factors $I1=I_{pH1}\cdot I_{IN,lim}$ $I2=I_{pH1}\cdot I_{h2}\cdot I_{IN,lim}$ $I3=I_{pH1}\cdot I_{NH3}\cdot I_{IN,lim}$

Data: Adapted from Batstone et al. (2002), Economou et al. (2024) and Antonopoulou et al. (2012a, 2012b).

For reference, an alternative approach could represent methanogen inhibition through operational or kinetic constraints, retaining the pathway $n_{1,ac,h2}$, hydrogen uptake, and biomass decay equations as in standard ADM1 (ANTONOPOULOU et al., 2012a; ECONOMOU et al., 2024). This alternative is mentioned for informational purposes only and was not implemented in the present study, since the thermal inactivation of X_{ac} and X_{h2} was sufficient to suppress methanogenesis under the experimental conditions.

However, for informational purposes, if methanogenesis inhibition had not been achieved through thermal pretreatment of the inoculum, it would have been necessary to model this inhibition directly by specifying specific operational conditions. In this case, the metabolic pathway represented by $n_{1,ac,h2}$, which describes hydrogen consumption by homoacetogenic bacteria, should be retained in the model (Eq. [5.4]). The hydrogen converted into acetate would be quantified by the stoichiometric fraction $f_{ac,h2} = n_{1,ac,h2}$ (Table 5.2) (ANTONOPOULOU et al., 2012b). Additionally, the kinetic rate equation for hydrogen uptake based on Monod kinetics (ANTONOPOULOU et al., 2012a), as well as a first-order decay equation for hydrogen-degrading microorganisms (X_{h2}) (ECONOMOU et al., 2024), should also be included, as follows:

$$\rho_{12} = k_{m,ac,h2} \frac{S_{h2}}{K_{s,ac,h2} + S_{h2}} . X_{h2} . I_{pH} . I_{IN,lim} \; (Hydrogen\ uptake\ rate) \qquad [5.4]$$

Where $k_{m,ac,h2}$ is the maximum specific Monod uptake rate (kg COD kg COD^{-1} d^{-1}), $k_{s,ac,h2}$ is the half-saturation constant (kg COD m^{-3}), S_{h2} is the hydrogen concentration (kg COD m^{-3}), and X_{h2} is the concentration of hydrogen-degrading microorganisms (kg COD m^{-3}).

In conventional ADM1, the sum of the sugar uptake fractions $n_{1,su}$ (acetate), $n_{2,su}$ (acetate and propionate), and $n_{3,su}$ (butyrate) is constrained to unity, as these pathways represent the only considered fates of sugars in the model. When additional fermentation products or intermediates are explicitly included, such as lactate and ethanol, the mass balance closure is achieved over an expanded set of pathways, and the sum of $n_{1,su}$, $n_{2,su}$, and $n_{3,su}$ is no longer required to equal 1, provided that overall COD conservation is maintained.

In the ADM1 modified for dark fermentation, stoichiometric coefficients are calculated for lactate, acetate, and ethanol, products of sugar degradation. During lactate degradation, products such as propionate (main) and acetate (secondary) are formed via the acrylate or succinate pathways, depending on the microorganism involved [$n_{1,lac}$]. In addition, butyrate is

produced as the main product, with hydrogen and carbon dioxide as by-products, through either the classical pathway or the acetyl-CoA pathway [$n_{2,lac}$]. Reverse reactions also occur, such as the conversion of acetate and/or hydrogen into butyrate (reductive fermentation via acetyl-CoA, known as reverse butyrogenesis, *Clostridium kluyveri* and other *Clostridia*) [$n_{1,bu,as,ac}$=1], and the conversion of hydrogen into acetate (homoacetogenesis, via the Wood–Ljungdahl pathway – *Acetobacterium woodii*, *Clostridium aceticum*) [$n_{1,ac,h2}$=1] (DIEKERT; WOHLFARTH, 1994; THAUER; JUNGERMANN; DECKER, 1977). These modifications are not applied in the present study, since the thermal inactivation of Xac and Xh2 was sufficient to suppress methanogenesis.

5.3.2 Statistics and predictive performance

5.3.2.1 Statistical assessment of model performance

The adequacy of the modified model to reproduce reactor behavior was examined through quantitative comparison between simulated outputs and experimental observations. This evaluation focused on the main process variables used during calibration, including hydrogen (H_2) production, total biogas generation, and selected VFAs.

Model performance was characterized using complementary statistical indicators in order to capture both absolute deviation and relative predictive skill. The root mean square error (RMSE) and mean absolute error (MAE) (VILMS PEDERSEN et al., 2020) were employed to quantify the magnitude of discrepancies between predicted and measured values, whereas the Nash–Sutcliffe efficiency (NSE) coefficient was used to assess the model's ability to reproduce the observed temporal dynamics relative to the mean of the dataset (NASH; SUTCLIFFE, 1970).

For a given state variable, let $y_{m,t}$ denote the experimental value and $y_{c,t}$ the corresponding simulated value at time *t*. The mean of measured observations is represented by $\bar{y}_m$, and *n* corresponds to the total number of data points. The RMSE was calculated according to Eq. [5.5]:

$$RMSE = \sqrt{\frac{\sum_{t=1}^{n}(y_{m,t} - y_{c,t})^2}{n}} \quad [5.5]$$

The NSE coefficient was determined as follows (KOCH et al., 2010; LIU et al., 2017) (Eq. [5.6[4.7]):

$$E = 1 - \frac{\sum_t (y_{m,t} - y_{c,t})^2}{\sum_t (y_{m,t} - \bar{y}_m)^2} \quad [5.6]$$

The NSE coefficient theoretically ranges from $-\infty$ to 1. Values approaching unity indicate strong agreement between simulated and experimental data, whereas values near zero suggest that the model provides predictive capability comparable to the average of the measured observations. Negative values indicate that the model fails to adequately represent system behavior. All statistical calculations were performed using Past, OriginPro, and Microsoft Excel.

5.3.2.2 Sensitivity assessment and calibration strategy

Parameter evaluation represents a fundamental step in process modeling, particularly when complex kinetic structures are involved. Assessing the influence of model parameters on predicted outputs allows the identification of those exerting greater control over system behavior, supporting reliable parameter estimation while avoiding unnecessary model overparameterization.

In this study, a local sensitivity analysis was performed according to the procedure implemented in AQUASIM 2.0 (REICHERT, 1998), aiming to determine the relative influence of selected ADM1 parameters on biogas and hydrogen production. The response variable adopted for the sensitivity calculations was hydrogen yield throughout the different operational phases.

The evaluated kinetic parameters comprised the microbial decay rate constant (k_{dec}), the disintegration constant (k_{dis}), and the hydrolysis rate constants associated with carbohydrates, lipids, and proteins ($k_{hyd,ch}$, $k_{hyd,li}$, and $k_{hyd,pr}$, respectively). Moreover, the half-saturation coefficients ($k_{s,aa}$, $k_{s,ac}$, $k_{s,c4}$, $k_{s,fa}$, $k_{s,h2}$, $k_{s,pro}$ and $k_{s,su}$) and the maximum substrate uptake rates ($k_{m,aa}$, $k_{m,ac}$, $k_{m,c4}$, $k_{m,fa}$, $k_{m,h2}$, $k_{m,pro}$ and $k_{m,su}$) were included in the analysis. The baseline values and variation ranges adopted for the evaluated parameters are summarized in Table 5.4.

Additional parameters introduced to describe lactate-related metabolic pathways were also considered. These included the half-saturation constants $k_{s,lac}$ and $k_{s,lac,su}$, together with the corresponding maximum uptake rates $k_{m,lac}$ and $k_{m,lac,su}$. The decay coefficients associated with lactate-degrading biomass (X_{lac}) and lactobacilli populations, represented by $k_{dec,xlac}$ and $k_{dec,xlac,su}$, were fixed at 0.02 d^{-1}, consistent with the standard decay rates adopted in the original ADM1 structure. Since these parameters were not independently modified, they were not subjected to sensitivity evaluation.

Table 5.4 – Parameter ranges considered in the sensitivity analysis

	Stoichiometric and kinetic coefficient	Range	Unit
k_{dec}	Biomass decay	0 – 0.05	day^{-1}
k_{dis}	Disintegration rate of composites	0 – 5	day^{-1}
$k_{hyd,ch}$	Hydrolysis rate of carbohydrates	0 – 10	day^{-1}
$k_{hyd,li}$	Hydrolysis rate of lipids	0 – 10	day^{-1}
$k_{hyd,pr}$	Hydrolysis rate of proteins	0 – 10	day^{-1}
$k_{m,aa}$	Maximum uptake rate of amino acids	0 – 80	day^{-1}
$k_{m,ac}$	Maximum uptake rate of acetate	0 – 10	day^{-1}
$k_{m,c4}$	Biomass decay of valerate and butyrate	0 – 50	day^{-1}
$k_{m,fa}$	Biomass decay of LCFA	0 – 100	day^{-1}
$k_{m,h2}$	Biomass decay of hydrogen	0 – 50	day^{-1}
$k_{m,lac}$	Maximum uptake rate of lactate*	0 – 10	day^{-1}
$k_{m,lac,su}$	Maximum uptake rate of monosaccharides for lactate fermentation**	0 – 50	day^{-1}
$k_{m,pro}$	Maximum uptake rate of propionate	0 – 20	day^{-1}
$k_{m,su}$	Maximum uptake rate of sugar	0 – 50	day^{-1}
$k_{s,aa}$	Half-saturation coefficient of amino acids	0 – 1	kg COD m^{-3}
$k_{s,ac}$	Half-saturation coefficient of acetate	0 – 1	kg COD m^{-3}
$k_{s,c4}$	Half-saturation coefficient of valerate and butyrate	0 – 1	kg COD m^{-3}
$k_{s,fa}$	Half-saturation coefficient of LCFA	0 – 1	kg COD m^{-3}
$k_{s,h2}$	Half-saturation coefficient of hydrogen	0 – 1	kg COD m^{-3}
$k_{s,lac}$	Half-saturation coefficient of lactate	0 – 1	kg COD m^{-3}
$k_{s,lac,su}$	Half-saturation coefficient of monosaccharide fermentation to lactate	0 – 15	kg COD m^{-3}
$k_{s,pro}$	Half-saturation concentration of propionate	0 – 1	kg COD m^{-3}
$k_{s,su}$	Half-saturation coefficient of sugar	0 – 1	kg COD m^{-3}
Y_{aa}	Yield uptake amino acids	0 – 1	kg COD kg COD^{-1}
Y_{ac}	Yield uptake acetate sugars	0 – 1	kg COD kg COD^{-1}
Y_{c4}	Yield uptake butyrate and valerate	0 – 1	kg COD kg COD^{-1}
Y_{fa}	Yield uptake LCFA	0 – 1	kg COD kg COD^{-1}
Y_{h2}	Yield uptake hydrogen	0 – 1	kg COD kg COD^{-1}
Y_{lac}	Yield uptake lactate	0 – 1	kg COD kg COD^{-1}
$Y_{lac,su}$	Yield uptake monosaccharides by *Lactobacillus*	0 – 1	kg COD kg COD^{-1}
Y_{pro}	Yield uptake propionate	0 – 1	kg COD kg COD^{-1}
Y_{su}	Yield uptake sugars	0 – 1	kg COD kg COD^{-1}

The analysis further incorporated the yield coefficients of the substrate-utilizing microbial groups, namely Y_{su}, Y_{aa}, Y_{fa}, Y_{c4}, Y_{pro}, Y_{ac}, and Y_{h2}, as well as the additional yield parameters Y_{lac} and $Y_{lac,su}$ associated with lactate pathways. These coefficients directly affect substrate-to-biomass conversion efficiency and may significantly impact hydrogen generation, sludge production, and COD partitioning.

The sensitivity index (SI) was determined according to Eq. [5.7]:

$$SI = \delta_{y,p}^{a,r} = p\frac{\partial y}{\partial p} \quad [5.7]$$

Where y corresponds to the selected response variable (hydrogen concentration) and p represents the parameter under evaluation. The SI quantifies the absolute variation in y resulting from a proportional (100%) change in p. Positive SI values indicate that increases in the parameter produce increases in the response variable, whereas negative values denote an inverse relationship. Parameter estimation was conducted through minimization of the weighted least-squares objective function defined in Eq. [5.8]:

$$\chi^2(p) = \sum_{i=1}^{n}\left(\frac{y_{meas,i} - y_i(p)}{\delta_{meas,i}}\right)^2 \quad [5.8]$$

In this formulation, χ^2 represents the sum of squared weighted deviations between experimental measurements and simulated values. The term $y_{meas,i}$ denotes the *i-th* observed data point, $y_i(p)$ corresponds to the model prediction associated with the same observation, $\delta_{meas,i}$ is the standard deviation of the measurement, $p = (p_1, \ldots pm)$ represents the vector of model parameters, and n is the total number of observations. Parameter estimation was considered complete when χ^2 reached a minimum.

Parameters exhibiting higher sensitivity were prioritized during calibration, as they exert greater influence on model outputs and typically present reduced estimation uncertainty. The calibration procedure therefore consisted of minimizing the weighted deviation between measured and simulated values in order to improve predictive agreement. The response variable adopted for parameter estimation was the biogas yield.

5.3.2.3 Model calibration and validation procedure

Model calibration was performed exclusively using experimental data from Phase 1, which corresponded to a period of stable operation in terms of organic loading rate and organic acid composition. The calibrated parameter set was subsequently applied, without further adjustment, to Phases 2–5 for cross-phase validation under varying operational

conditions. Model performance was evaluated by comparing simulated and experimental profiles of biogas production (H_2 and CO_2) and soluble metabolites (acetate, butyrate, propionate, and lactate), using the coefficient of determination (R^2) and root mean square error (RMSE) as goodness-of-fit metrics.

5.4 Results and discussion

5.4.1 Reactors performance

Throughout the five operational phases, the reactors performance was systematically evaluated based on COD removal, carbohydrate conversion, hydrogen production rate, VFA generation, the hydrogen fraction in the biogas, and the reactor's controlled pH conditions (Table 5.5).

Table 5.5 – Results of AnSTBR operation during operational phases.

Parameter	Unit	Experimental phases				
		P1	P2	P3	P4	P5
Phase duration	d	52	49	14	16	17
theoretical COD	g L^{-1}	10	12	15	18	20
OLR	kg COD $m^{-3}d^{-1}$	40	48	60	72	80
L-FVW input						
COD total	g L^{-1}	9.27±0.51	11.26±1.62	14.49±1.06	17.86±0.76	18.53±0.79
OLR	kg COD $m^{-3}d^{-1}$	37.06±2.02	45.02±6.49	57.95±4.24	71.43±3.05	74.13±6.42
TS	%	0.95±0.02	1.14±0.07	1.42±0.06	1.71±0.05	1.90±0.12
VS	%TS	0.89±0.19	1.07±0.15	1.33±0.10	1.60±0.07	1.78±0.15
Lipids	mg L^{-1}	69	83	104	124	138
Crud proteins	mg L^{-1}	104	124	155	186	207
Carbohydrates	mg L^{-1}	4,702±953	4,824±829	5,837±1083	7,828±549	7,828±459
Acetic acid	g L^{-1}	13.98	16.78	20.97	25.16	27.96
Propionic acid	g L^{-1}	20.02	24.02	30.03	36.04	40.04
Butyric acid	g L^{-1}	16.57	19.88	24.85	29.82	33.14
pH	-	11.00	11.00	11.00	11.00	11.00
L-FVW output						
pH	-	5.18±0.58	5.01±0.34	4.63±0.15	4.83±0.11	4.54±0.36
COD removed	%	16±6	13±7	14±7	13±5	15±5
Carbohydrate conversion	%	89±6	92±2	91±2	90±1	91±1
Hydrogen	%	32±6	28±2	30±3	29±3	25±5
Yield	L_{H2} $L^{-1}d^{-1}$	0.51±0.13	0.61±0.25	2.20±0.52	1.68±0.52	1.25±0.25
VFA effluent	mg L^{-1}	2,424±218	2,581±298	3,407±117	3,655±310	4,044±345

Note: COD – Carbon Oxygen Demand; OLR – Organic Load Rate; TS – Total Solids and VS – Volatile Solids; TOC – Total Organic Carbon; VFA – Volatile Fatty Acids.

5.4.2 Initial model predictions with default parameters

Initially, the model was executed using the experimental input data together with the default parameter set proposed by Batstone et al. (2002), without any prior adjustment, to

predict biogas production and composition, as well as the concentrations of volatile fatty acids (S_{ac}, S_{pro}, S_{bu} and S_{lac}). As expected, the model predictions showed poor agreement with the experimental results, with a systematic tendency to overestimate biogas production, hydrogen yield, and acidogenic metabolite accumulation, a behavior also reported in previous ADM1 applications to dark fermentation systems (ALEXANDROPOULOU; ANTONOPOULOU; LYBERATOS, 2016).

A closer inspection of the initial simulations indicates that this overestimation arises from the combined effect of several interacting kinetic and stoichiometric factors rather than from inhibitory phenomena. In particular, the default ADM1 parameterization assumes ideal hydrolysis and substrate availability, typically associated with suspended-growth systems, which does not fully represent the mass-transfer limitations and metabolic constraints of reactors operated with adhered biomass. Under these assumptions, the relatively high default value of the carbohydrate hydrolysis constant ($k_{hyd,ch}$) promoted an excessive and rapid release of soluble sugars, generating an unrealistically high acidogenic flux. This sustained oversupply of fermentable substrates propagated through the downstream pathways, resulting in inflated predictions of volatile fatty acid accumulation and hydrogen production.

Given the strong coupling between hydrolysis kinetics, substrate uptake rates, biomass yields, and metabolic pathway distribution in hydrogenogenic systems, these deviations cannot be attributed to a single parameter. This motivated the application of a sensitivity analysis to identify the parameters exerting the greatest influence on model outputs, providing a structured basis for subsequent parameter calibration.

Inhibition processes were explicitly incorporated into the model formulation. While the ADM1 framework already includes pH-dependent inhibition functions for several metabolic steps, it does not originally account for pH inhibition associated with lactate-related pathways under hydrogenogenic conditions. Given the relevance of lactate as a key intermediate in dark fermentation systems, an additional pH-dependent inhibition function for lactate degradation was incorporated into the model as a structural modification (CHEN et al., 2016; VAVILIN; RYTOV; LOKSHINA, 1996).

The inhibition parameters were not directly adopted from the default ADM1 configuration, which was originally developed for methanogenic reactors operating near neutral pH and low hydrogen partial pressure. Instead, all inhibition functions were recalibrated to reflect the operational window of hydrogenogenic dark fermentation, based on experimentally relevant pH ranges and metabolic thresholds reported in the literature (DAREIOTI;

VAVOURAKI; KORNAROS, 2014; ECONOMOU et al., 2024; GUPTA et al., 2024; MOKHTARANI; ZANGANEH; MOGHTADERI, 2025).

Following the ADM1 formalism, inhibition was implemented through pH-dependent functions that constrain microbial uptake rates using lower and upper pH limits. These limits define the onset and the full expression of microbial activity, acting as regulatory boundaries rather than kinetic fitting parameters. In the present study, these limits were redefined to represent hydrogenogenic conditions instead of conventional methanogenic operation.

Specifically, the lower and upper pH limits for hydrogen uptake and production processes were set between 5.0 and 6.0. Acetate-related inhibition was constrained to a pH range of 6.0–7.0. An additional inhibition function was introduced for lactate degradation, with pH limits defined between 5.0 and 6.2, to represent the experimentally observed sensitivity of lactate-oxidizing pathways to acidic conditions. Sugar consumption toward lactate formation was restricted to a pH range of 4.8–5.8. These bounds were used to calculate the corresponding inhibition functions, ensuring a gradual reduction of microbial activity outside the optimal pH window.

By redefining and extending the pH inhibition structure of the ADM1, the model captures pH-driven metabolic regulation more realistically, suppressing undesired pathways such as methanogenesis while preserving hydrogenogenic activity. As these inhibition functions establish physiological feasibility limits rather than controlling dynamic parameter fitting, their influence was considered intrinsic to the system behavior and was therefore not subjected to a dedicated sensitivity analysis.

5.4.3 Sensitivity analysis

Before the parametric adjustments required for model calibration, a sensitivity analysis was conducted to identify the parameters with the greatest influence on hydrogen production during the operation of the anaerobic reactor fed with L-FVW (BOUTOUTE et al., 2021). This step is essential for focusing calibration efforts on the most relevant parameters, thereby reducing the problem's dimensionality and optimizing the fitting process. The analysis revealed that certain kinetic and stoichiometric parameters have a significant impact on hydrogen production dynamics, allowing them to be grouped by function within the model (CHEN et al., 2016).

Among the parameters identified as most influential, those governing substrate availability, metabolic competition, and redox balance showed the strongest effect on hydrogen production in dark-fermentation reactors fed with L-FVW (VAVILIN et al., 2008). Hydrolysis is one of the rate-limiting steps in the AD of L-FVW, due to the high content of particulate carbohydrates characteristic of this substrate. The $k_{hyd,ch}$ showed high sensitivity in the analysis, indicating that small variations in its value significantly affect the availability of soluble substrates, particularly monosaccharides (S_{su}), which fuel the subsequent fermentation pathways. The adopted reference value (10 d^{-1}) did not adequately reflect the actual fermentation dynamics, suggesting that adjustments to this parameter are critical for model calibration (CHEN et al., 2016).

The other hydrolysis parameters had a lower impact but still play a relevant role in the availability of intermediates. The parameter $k_{hyd,pr}$ required more precise adjustments, since its variation exerted a greater influence on hydrogen production, reflecting its contribution to the generation of soluble amino acids (S_{aa}), which are subsequently metabolized in the acidogenic steps. In contrast, the value of $k_{hyd,li}$ was relatively low compared to the others, which is consistent with the smaller proportion of the lipid fraction in L-FVW and the lower relevance of this component to the dominant fermentative pathway (NABATEREGA; NAZYAB; ESKICIOGLU, 2023). Taken together, these results highlight that the outcome of the hydrolysis stage is not limited to substrate solubilization but also determines the metabolic fluxes that drive subsequent fermentation processes.

The main parameters associated with substrate uptake showed high sensitivity because hydrolysis coefficients (k_{hyd}) constrain the supply of soluble intermediates to subsequent pathways. In this context, the maximum uptake rates (k_m) in the modified ADM1, namely $k_{m,aa}$, $k_{m,su}$, $k_{m,lac}$, and $k_{m,lac,su}$, exerted a strong influence on hydrogen production and substrate degradation. Each of these parameters governs critical biochemical steps: $k_{m,aa}$ regulates the conversion of amino acids into VFAs and H_2; $k_{m,su}$ controls the utilization of sugars, the primary source of reducing equivalents for hydrogenogenic pathways; while $k_{m,lac}$ and $k_{m,lac,su}$ modulate the metabolism of lactate, a key intermediate that redistributes carbon and electrons among competing fermentation routes (BLANCO; OLIVEIRA; ZAIAT, 2019). Together, their variation alters the balance of metabolic fluxes, thereby impacting both the efficiency of substrate conversion and the overall hydrogen yield.

The parameter $k_{m,aa}$ denotes the maximum uptake rate of amino acids by acidogenic/proteolytic populations. Although L-FVW contains a lower protein fraction

compared to carbohydrates, amino acids derived from the nitrogenous fraction can be converted into organic acids and ammonia (YUAN et al., 2014). This pathway contributes only marginally to H_2 production, but it strongly influences medium alkalinity, buffering the pH and indirectly modulating hydrogenase activity. Moreover, some amino acids directly produce H_2 via oxidative deamination, while others generate reducing co-products that compete with H_2 formation.

The parameter $k_{m,lac,su}$ represents the maximum uptake rate of monosaccharides directed toward lactic fermentation, predominantly by homofermentative microorganisms such as *Lactobacillus* spp. This pathway acts as a competitive metabolic route to hydrogen production, as lactate formation occurs without H_2 release and consumes reducing equivalents (NADH) that hydrogenases could otherwise use for H_2 formation. High $k_{m,lac,su}$ values intensify the diversion of carbon and electron fluxes toward the lactic pathway, reducing the overall efficiency of substrate-to-hydrogen conversion. Conversely, lower values limit this competition, favoring acetogenic and butyric pathways, which are directly associated with H_2 generation (ANTONOPOULOU et al., 2012a).

The parameter $k_{m,lac}$ is associated with the maximum uptake rate of lactate by lactate-oxidizing microorganisms that convert lactate into acetate with concomitant H_2 production under thermodynamically favorable conditions, such as low hydrogen partial pressure. This pathway can recover part of the H_2 potential lost to lactic fermentation and helps to remove accumulated lactate, thus avoiding inhibition due to excessive acidification (SAGAR et al., 2018). High $k_{m,lac}$ values enhance this regenerative conversion, improving process stability and increasing precursor availability for H_2 production, whereas lower values lead to lactate accumulation and reduced system efficiency.

Thus, $k_{m,lac,su}$ and $k_{m,lac}$ exert direct but opposite effects on hydrogen production: the former regulates the intensity of metabolic competition for primary substrates. At the same time, the latter controls the capacity to recover hydrogen from intermediate products. The balance between these parameters is crucial for maximizing selectivity and operational stability in hydrogenogenic reactors fed with L-FVW.

Overall, the high sensitivity of these parameters indicates that hydrogen production in hydrogenogenic reactors operating with L-FVW is strongly dependent on the competition between the acetogenic/butyric and lactic pathways, the kinetics of primary and secondary substrate conversion, and conditions that modulate the microbial redox balance. Therefore, the fine-tuning of $k_{m,su}$, $k_{m,lac,su}$, $k_{m,lac}$, and $k_{m,aa}$ is essential not only for maximizing H_2 production

but also for maintaining operational stability and selectivity of fermentative routes (NABATEREGA; NAZYAB; ESKICIOGLU, 2023; SILVA et al., 2025).

The half-saturation constants (k_s) influence hydrogen production by modulating the microbial affinity for substrates, an effect less pronounced than that of the k_m, yet still relevant under substrate-limiting conditions (ARNALDOS et al., 2015). Low $k_{s,su}$ values indicate high affinity of acidogenic microorganisms for sugars, sustaining high conversion rates and favoring H_2-producing pathways even when substrate availability is low. Conversely, $k_{s,lac,su}$ governs the competition for sugars between *Lactobacillus*: low values favor lactate formation (a non-H_2-producing route), whereas higher values reduce this competition under limiting conditions. The $k_{s,lac}$ parameter determines the efficiency of lactate-oxidizing microorganisms in converting lactate into acetate and H_2, with low values being desirable to enhance this recovery. Finally, $k_{s,aa}$, although less relevant for L-FVW due to its low protein content, contributes to pH stability and the formation of intermediates. Therefore, the k_s parameters act as fine-tuning variables for metabolic selectivity and reactor performance under varying substrate conditions (ZHAO et al., 2019b).

The sensitivity analysis of the simulated hydrogenogenic reactor showed that the microbial yield coefficients Y_{aa}, Y_{su}, Y_{lac}, and $Y_{lac,su}$ significantly influence hydrogen production, as explained by the model's biochemical and structural mechanisms (WEINRICH et al., 2019). These parameters determine the fraction of consumed substrate converted to biomass, directly affecting the carbon balance and the pool of reducing equivalents available for H_2 production. High Y_{su} and Y_{aa} values increase the incorporation of sugars and amino acids into acidogenic biomass, thereby reducing the electron flux toward the H_2-producing acetogenic and butyric pathways (FORTELA et al., 2019). Similarly, Y_{lac} and $Y_{lac,su}$ modulate the efficiency of lactate and sugar conversion into lactic microorganism biomass, intensifying competition for substrates and diverting reducing equivalents away from hydrogenogenesis (ECONOMOU et al., 2024). In contrast, lower values of these coefficients promote the channeling of substrate toward fermentative catabolism, increasing NADH availability for hydrogenases and, consequently, H_2 yield. Therefore, in the modified ADM1, yield coefficients function as control points governing the partition between microbial growth and the generation of metabolic products and are key determinants for optimizing both process selectivity and efficiency.

Based on the sensitivity analysis results, the parameters k_{dis}, $k_{hyd,ch}$, $k_{m,aa}$, $k_{m,su}$, $k_{s,aa}$, $k_{m,su}$, Y_{aa} and Y_{su}, as well as the parameters corresponding to the new fermentation pathways, $k_{m,lac}$, $k_{m,lac,su}$, $k_{s,lac}$, $k_{s,lac,su}$, Y_{lac} and $Y_{lac,su}$, were selected for estimation in AQUASIM 2.0

(REICHERT, 1998) aiming to minimize the weighted sum of squared deviations between experimental data and model predictions. The optimization process initially employed the simplex algorithm (NELDER; MEAD, 1965) to promote convergence, followed by the secant algorithm (RALSTON; JENNRICH, 1978), both implemented in AQUASIM 2.0 (REICHERT, 1998).

5.4.4 Model calibration and parameter estimation

Calibration was carried out progressively, beginning with the inputs of VFAs (acetate, propionate, and butyrate) and lactate to align the initial conditions with the experiment. Subsequently, the parameters k_{dis} and $k_{hyd,ch}$, which are critical for substrate release and adjustment of total biogas production, were refined. The kinetic parameters (k_m and k_s) for sugars, amino acids, and lactate were then adjusted to reproduce the VFA profiles. Microbial yields (Y_{su}, Y_{aa}, Y_{lac} and $Y_{lac,su}$) were calibrated to balance acid formation and H_2 production. At the same time, the partitioning fractions ($n_{i,j}$) were tuned to reconcile the relative predominance of metabolic pathways with the experimental data. Finally, the gas–liquid mass transfer coefficient (k_{La}) was adjusted to refine the gas composition, resulting in good agreement between the simulated curves for total biogas, H_2, CO_2, and VFAs and the experimental profiles.

Figure 5.2 compares laboratory data (*Experimental*) with ADM1 simulations obtained using the original parameter set (*Reference Standard*) and after model calibration (*Optimized*). Figure 5.2a presents the total biogas production rate and the hydrogen (H_2) production rate simulated with the Reference Standard parameters. In this case, both variables are clearly overestimated in comparison with the Experimental data shown in Figure 5.2b, a behavior also reported by (ANTONOPOULOU et al., 2012a).

Figure 5.2b shows the comparison between Experimental data and the Optimized simulation for total biogas and H_2 production, indicating that parameter calibration significantly reduced the deviation observed with the Reference Standard model. The initial overestimation arises from the assumption of ideal solubilization and conversion conditions in the default ADM1 framework, which leads to higher effective substrate availability than that experimentally observed for heterogeneous residues such as L-FVW (BONG et al., 2018; MASEBINU et al., 2018; SILVA JÚNIOR et al., 2022). The resulting overprediction of soluble sugars accelerates acidogenic reactions and artificially directs the electron flux toward hydrogen production.

The implications of this behavior are further evidenced in the biogas composition shown in Figure 5.2c, which compares the Experimental data with the Reference Standard and Optimized simulations. The Reference Standard model predicts an H_2/CO_2 ratio exceeding unity, whereas both the Experimental and Optimized curves exhibit coupled H_2 and CO_2 production. Such a decoupling predicted by the Reference Standard simulation is inconsistent with the stoichiometric and redox constraints of fermentative pathways, which require simultaneous CO_2 formation to maintain electron balance, thereby rendering this scenario thermodynamically unfeasible (VAVILIN et al., 2008).

Figure 5.2 – Comparison between experimental data (*Experimental*) and ADM1 simulations before (*Reference Standard*) and after model calibration (*Optimized*): (a) total biogas production and H_2 production rate (*Reference Standard*) (b) total biogas production and H_2 production rate (*Experimental* and *Optimized*); (c) biogas composition (H_2 and CO_2); (d) acetate, propionate, butyrate, and lactate profiles.

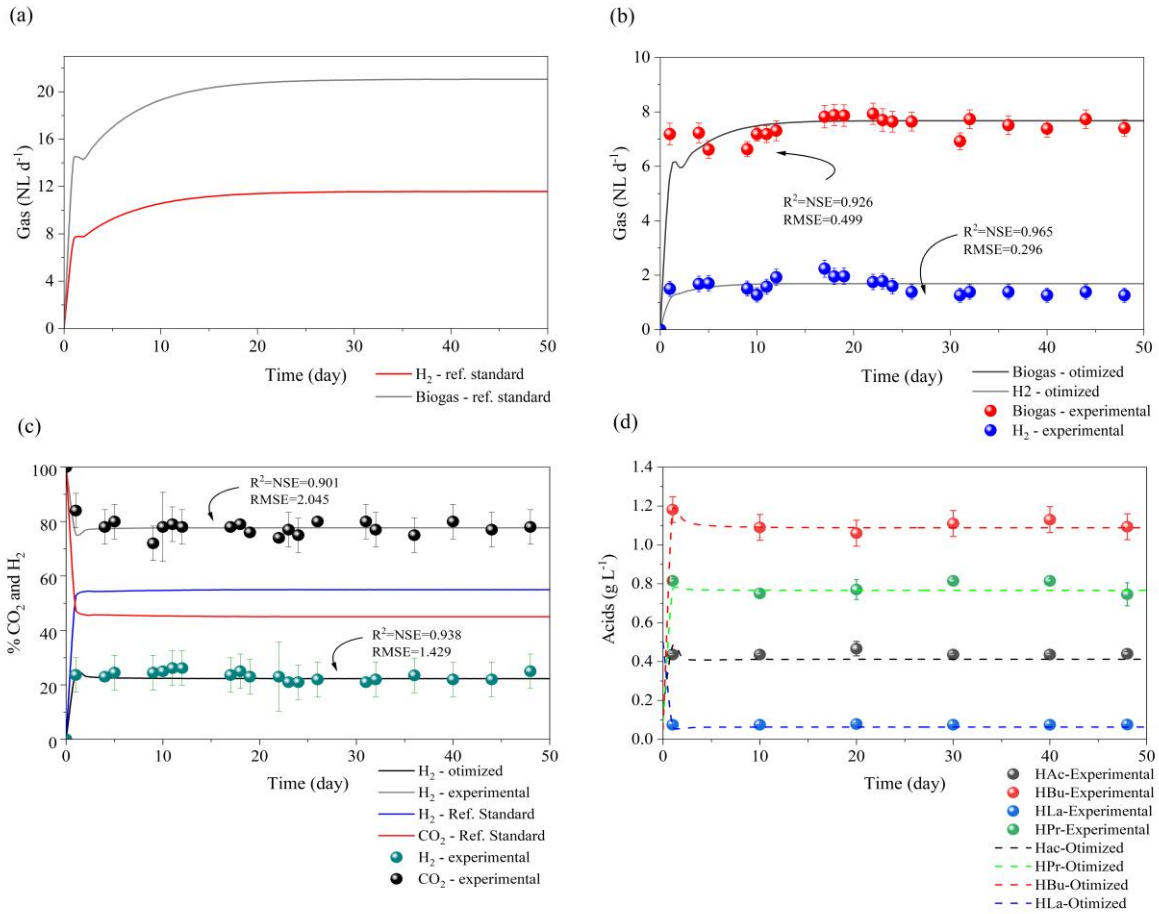

A similar inconsistency is observed in the VFA profiles (Figure 5.2d). Experimentally, butyrate was the dominant accumulated acid, whereas the Reference Standard simulation predicted acetate as the main product. This outcome reflects an artificial

prioritization of acetogenic pathways, which theoretically maximize hydrogen production (4 mol H_2 per mol glucose via the acetate route) but rarely dominate in real fermentative systems due to the concurrent operation of the butyrate pathway, which yields lower hydrogen production (2 mol H_2 per mol glucose) (SAADY, 2013)**.** Therefore, the overestimation of acetate and H_2 highlights the need for adjusting hydrolysis constants, kinetic parameters, and pathway partitioning fractions to realistically represent the metabolic balance of the reactor and the experimentally observed product distribution.

Among the hydrolysis coefficients, originally fixed at 10 d^{-1} in the conventional ADM1 framework (BATSTONE et al., 2002), the carbohydrate hydrolysis constant ($k_{hyd,ch}$) was adjusted to 0.628 d^{-1}. In this context, it is important to consider the role of the disintegration constant (k_{dis}), which governs the conversion of particulate organic matter into soluble substrates prior to hydrolysis and may influence the apparent hydrolysis rates estimated during model calibration, particularly when dealing with heterogeneous substrates such as FVW.

Although this value is markedly lower than the default ADM1 assumption, it should not be interpreted as a limitation of the intrinsic hydrolysis capacity of the substrate. Batch methane potential (BMP) tests performed with the liquid fraction of L-FVW did not indicate hydrolytic constraints, supporting the interpretation that carbohydrates were readily convertible under favorable batch conditions, which assess ultimate biodegradability rather than process kinetics (ANGELIDAKI et al., 2009).

In the context of continuous dark fermentation, however, hydrolysis in ADM1 represents a lumped kinetic step that controls the effective rate at which fermentable monosaccharides become available to the acidogenic microbial community (BATSTONE et al., 2002; KOCH et al., 2011). Thus, the reduced $k_{hyd,ch}$ obtained during calibration reflects an effective hydrolysis rate, accounting for the regulated and temporally distributed release of soluble sugars rather than their ultimate conversion potential (HASSAM et al., 2015; RAJAGOPAL; MASSÉ; SINGH, 2013). Mechanistically, this behavior can be explained by the heterogeneous nature of L-FVW, composed of different fruits and vegetables that, although rich in readily assimilable carbohydrates such as glucose, fructose, and sucrose, also contain structural fractions including starch and dietary fiber. These fractions influence mass transfer, enzymatic accessibility, and intracellular uptake dynamics, leading to a decoupling between overall carbohydrate conversion (>90%) and the observed rates of acidogenic product accumulation (AXELSSON et al., 2012).

Consequently, carbohydrates were efficiently converted but not predominantly directed toward the accumulation of classical volatile fatty acids, indicating that the acidogenic flux was kinetically constrained and redistributed toward alternative metabolic sinks, such as biomass synthesis, maintenance metabolism, or soluble products not quantified in this study. This decoupling between substrate conversion and metabolite accumulation is consistent with previous ADM1-based studies, where reduced apparent hydrolysis constants were required to reproduce dynamic behavior in systems fed with complex or heterogeneous substrates (KOCH et al., 2010; RAJAGOPAL; MASSÉ; SINGH, 2013).

For proteins and lipids, which were present at lower concentrations in the substrate, the hydrolysis coefficients exhibited lower sensitivity during calibration, requiring only minor adjustments to 7.745 d^{-1} and 9.951 d^{-1}, respectively. In contrast, the carbohydrate fraction exhibited higher sensitivity during calibration, which may reflect the heterogeneous composition of carbohydrates in fruit and vegetable waste. This fraction can include readily degradable sugars and starch, as well as more structurally complex components such as pectin, cellulose, and hemicellulose, which may exhibit different hydrolysis kinetics. In principle, representing the particulate carbohydrate pool (X_{ch}) as multiple fractions with distinct degradation rates could improve the description of hydrolysis dynamics. However, such an approach requires detailed compositional characterization of the substrate, including the quantification of structural carbohydrate fractions. Since only total carbohydrate content was available for the L-FVW used in this study, the conventional ADM1 representation with a single carbohydrate fraction was maintained, and the calibrated hydrolysis coefficient was interpreted as an effective parameter representing the aggregated behavior of the carbohydrate pool.

Since carbohydrates primarily release soluble sugars (S_{su}) and proteins release amino acids (S_{aa}), the kinetic parameters governing substrate uptake and conversion (k_s, k_m, and Y) also showed high sensitivity (SILVA et al., 2024). The half-saturation constants (k_s) regulate microbial affinity for soluble substrates, the maximum specific uptake rates (k_m) define the upper limit of conversion into biomass and soluble products, and the yield coefficients (Y) determine the partitioning of substrate carbon between cell growth and the formation of reducing metabolites. Therefore, the calibration of $k_{s,aa}$, $k_{s,su}$, $k_{m,aa}$, $k_{m,su}$, Y_{aa}, and Y_{su} was essential to reconcile the effective substrate availability, modulated by hydrolysis kinetics, with the experimentally observed consumption profiles and the limited accumulation of acidogenic products. The final calibrated parameters are summarized in Table 5.6.

The cellular yield values were defined based on the balance between substrate consumption and product formation. Initially, the yield associated with Y_{lac} was set equal to that of Y_{su} to provide an unbiased starting condition (ALEXANDROPOULOU; ANTONOPOULOU; LYBERATOS, 2016). As shown in Table 5.6, during calibration, the Y_{su} value was set to 0.191 kmol C kg COD^{-1}, using the integrated curves for biogas and VFA production as references, since this parameter controls the fraction of substrate converted into biomass versus gaseous/soluble products. The value of Y_{lac}, in turn, was adjusted to 0.136 kmol C kg COD^{-1}, based on the residual lactate concentration and its influence on hydrogen production volume throughout the operation, reflecting a metabolic flux shift from the lactic pathway toward the hydrogen-producing pathway.

Table 5.6 – Modified stoichiometric kinetic parameters.

	Stoichiometric and kinetic coefficient	Default	Optimized	Unit
$f_{si,xc}$	Soluble inert from composites	0.1	0.064[(a)]	kg COD kg COD^{-1}
$f_{xi,xc}$	Particulate inert from composites	0.25	0.302[(a)]	kg COD kg COD^{-1}
$f_{ch,xc}$	Carbohydrates from composites	0.2	0.529[(a)]	kg COD kg COD^{-1}
$f_{pr,xc}$	Proteins from composites	0.2	0.117[(a)]	kg COD kg COD^{-1}
$f_{li,xc}$	Lipids from composites	0.25	0.078[(a)]	kg COD kg COD^{-1}
C_{xc}	Carbon content of carbohydrates	0.0313	0.0327[(a)]	kmole C kg COD^{-1}
N_{xc}	Nitrogen content of composites	varies	0.001466[(a)]	kmole C kg COD^{-1}
N_I	Nitrogen content of inert	varies	0.000714[(b)]	kmole C kg COD^{-1}
N_{bac}	Nitrogen content of biomass	0.00625	0.005[(b)]	kmole C kg COD^{-1}
Y_{aa}	Yield uptake amino acids	0.08	0.074[(c)]	kg COD kg COD^{-1}
Y_{lac}	Yield uptake lactate	0.1	0.136[(c)]	kg COD kg COD^{-1}
$Y_{lac,su}$	Yield uptake monosaccharides by *Lactobacillus*	0.03	0.036[(c)]	kg COD kg COD^{-1}
Y_{su}	Yield uptake sugars	0.1	0.191[(c)]	kg COD kg COD^{-1}
k_{dis}	Disintegration rate of composites	5	1.300[(c)]	day^{-1}
$k_{hyd,ch}$	Hydrolysis rate of carbohydrates	10	0.628[(c)]	day^{-1}
$k_{hyd,pr}$	Hydrolysis rate of proteins	10	7.745[(d)]	day^{-1}
$k_{hyd,li}$	Hydrolysis rate of lipids	10	9.951[(d)]	day^{-1}
$k_{m,aa}$	Maximum uptake rate of amino acids	50	52.569[(c)]	day^{-1}
$k_{m,lac}$	Maximum uptake rate of lactate[*]	2.281	3.279[(c)]	day^{-1}
$k_{m,lac,su}$	Maximum uptake rate of monosaccharides for lactate fermentation[**]	37.82	39.740[(c)]	day^{-1}
$k_{m,su}$	Maximum uptake rate of sugar degraders	30	23.643[(c)]	day^{-1}
$k_{s,aa}$	Half-saturation coefficient of amino acids	0.3	0.308[(c)]	kg COD m^{-3}
$k_{s,lac}$	Half-saturation coefficient of lactate[*]	0.5	0.388[(c)]	kg COD m^{-3}
$k_{s,lac,su}$	Half-saturation coefficient of monosaccharide fermentation to lactate[***]	13.182	4.831[(c)]	kg COD m^{-3}
$k_{s,su}$	Half-saturation coefficient of Sugar	0.5	0.798[(c)]	kg COD m^{-3}

Note1: (a) based on L-FVW ultimate analysis; (b) (Wett; Eladawy; Ogurek, 2006); (c) calibrated from best curve fitting method; (d) fine-tuning.
Note2: *by acetogenic biomass; **by lactate-producing; ***by lactate-producing biomass.

After defining the yields, it became evident that these adjustments alone were insufficient to adequately reproduce the experimental profiles, requiring the consideration of additional kinetic parameters related to growth and conversion rates. Moreover, the $k_{m,su}$ was defined as 24.643 d^{-1}, a value consistent with the rapid carbohydrate assimilation observed experimentally (Table 5.6). However, to achieve simultaneous agreement between the curves

of total biogas, gas composition, and VFA dynamics, it was necessary to adjust both kinetic and saturation parameters that modulate conversion rates: $k_{m,aa}$, $k_{s,su}$, $k_{s,aa}$, $k_{s,lac}$, $k_{s,lac,su}$, $k_{m,lac}$, and $k_{m,lac,su}$. Each of these parameters directly influences the balance between VFA production and accumulation, the conversion rates of sugars and lactate, and consequently, the release profiles of hydrogen (NABATEREGA; NAZYAB; ESKICIOGLU, 2023).

However, kinetic adjustments alone were insufficient to reproduce the experimental profiles accurately. To properly describe the model's metabolic pathways, three conversion routes were considered. The first, conventional route directs monosaccharides toward the formation of acetate, propionate, butyrate, and hydrogen, defined by the fractions $n_{1,su}$, $n_{2,su}$, and $n_{3,su}$. The second route, secondary in nature, describes the conversion of a fraction of sugars into lactate, acetate, and ethanol, thereby diverting flux toward microorganisms such as Lactobacillus. The third route involves the consumption of lactate ($n_{1,la}$ and $n_{2,la}$), producing acetate, butyrate, and hydrogen, thereby capturing the metabolism of lactic intermediates (Table 5.7).

Table 5.7 – Estimated coefficients for sugars and lactate degradation obtained from the ADM1 simulation on experimental results.

Parameter	**Experimental phases**					**Experimental mean**	**Reported range (min–max)**[**]	**ADM1**[***]	**Optimized value**
OLR (kg COD $m^{-3}d^{-1}$)	44	48	60	72	80				
$n_{1,su}$	0.197	0.211	0.265	0.170	0.201	0.209	0.149-0.335	0.495	0.101
$n_{2,su}$	0.326	0.034	0.021	0.015	0.000	0.079	0.006-0.031	0.345	0.102
$n_{3,su}$	0.477	0.755	0.715	0.814	0.799	0.712	0.724-0.783	0.160	0.797
Acetate, $f_{ac,su}$*	0.204	0.149	0.182	0.118	0.135	0.157	0.227-0.105	0.410	0.090
Propionate, $f_{pro,su}$*	0.254	0.026	0.016	0.012	0.000	0.062	0.005-0.024	0.270	0.080
Butyrate, $f_{bu,su}$*	0.396	0.627	0.593	0.676	0.663	0.591	0.650-0.601	0.130	0.661
Hydrogen, $f_{h2,su}$*	0.146	0.198	0.209	0.195	0.202	0.190	0.173-0.235	0.190	0.169
$n_{1,su}$	0.124	0.396	0.100	0.229	0.081	0.186	0.605	-	0.384
$n_{2,su}$	0.150	0.151	0.149	0.154	0.144	0.150	0.150	-	0.104
$n_{3,su}$	0.727	0.453	0.751	0.617	0.775	0.664	0.245	-	0.511
Lactate, $f_{lac,su}$*	0.562	0.698	0.550	0.614	0.540	0.593	0.803	-	0.692
Acetate, $f_{ac,su}$*	0.363	0.226	0.375	0.309	0.388	0.332	0.111-0.206	-	0.256
Ethanol, $f_{eth,su}$*	0.075	0.075	0.074	0.077	0.072	0.075	0.031-0.082	-	0.052
$n_{1,la}$	0.523	0.245	0.285	0.186	0.201	0.288	0.200	-	0.842
$n_{2,la}$	0.477	0.755	0.715	0.814	0.799	0.712	0.800	-	0.158
Acetate, $f_{ac,lac}$*	0.115	0.054	0.063	0.041	0.044	0.063	0.044	-	0.185
Propionate, $f_{pro,lac}$*	0.408	0.191	0.222	0.145	0.157	0.225	0.156	-	0.657
Butyrate, $f_{bu,lac}$*	0.396	0.627	0.593	0.676	0.663	0.591	0.664	-	0.131
Hydrogen, $f_{h2,lac}$*	0.081	0.128	0.122	0.138	0.136	0.121	0.136	-	0.027

Note: *Yields, kg COD kg COD^{-1};
Data: **(ANTONOPOULOU et al., 2012a; ECONOMOU et al., 2024); ***(BATSTONE et al., 2002).

The adjustment of the fractions of these pathways, together with a refinement of the yield associated with sugar assimilation by lactic acid bacteria ($Y_{lac,su}$, from 0.030 to 0.036 kmol C kg COD^{-1}), was essential to reconcile the experimental curves of acids and hydrogen with the model predictions. Although this change was small, it improved the description of the carbon

partitioning mediated by *Lactobacillus*, ensuring a more realistic representation of lactate accumulation and its subsequent conversion into hydrogen-producing intermediates.

The results of these adjustments are summarized in Table 5.6 and Table 5.7, which present the estimated values describing the fermentative processes. For lactate consumption, the Monod $k_{m,lac}$ was defined as 3.279 d^{-1}. For the sugar assimilation pathway via *Lactobacillus*, the adjusted parameters resulted in $k_{m,lac,su}$ = 39.740 d^{-1}, $k_{s,lac,su}$ = 4.831 kg COD m^{-3}, and $Y_{lac,su}$ = 0.036 kmol C kg COD^{-1}. Both the yield and the saturation constant were higher than those reported in the literature (ALEXANDROPOULOU; ANTONOPOULOU; LYBERATOS, 2016, 2018, 2022; ECONOMOU et al., 2024), suggesting a microbiota with greater fermentative activity and a greater affinity for lactic pathways under the heterogeneous conditions imposed by the L-FVW substrate. The deviation observed for $k_{m,lac,su}$, on the other hand, may be explained by differences in the predominant microbial consortia and by the adaptive responses of the populations to the experimental environment, favoring accelerated lactate turnover.

Comparison of simulations with data from a reactor operated with real substrate under different conditions confirmed that the modifications introduced into the model ensured good agreement, reflecting an adequate balance between metabolic pathways and by-product formation. The biogas (R^2 = 0.926; RMSE = 0.499) and hydrogen (R^2 = 0.965; RMSE = 0.296) curves exhibited satisfactory fits, demonstrating the robustness of the implemented adjustments. The composition of the biogas also closely followed the experimental profiles, with H_2 content (R^2 = 0.965) being primarily governed by the calibrated $k_{hyd,ch}$ and by the stoichiometric coefficients that defined the partitioning of carbon among the acidogenic and lactic pathways. These results reinforce the critical role of the interplay between hydrolysis kinetics and pathway distribution in accurately reproducing both gas composition and VFA dynamics.

5.4.5 Extension of the model with additional metabolic pathways

The standard ADM1 does not explicitly consider certain fermentative routes relevant to carbohydrate-rich, heterogeneous substrates such as L-FVW. To improve model accuracy, lactate and ethanol pathways were incorporated.

5.4.5.1 Lactate formation route and lactate consumption route

In the experiments conducted with L-FVW, in addition to the classical products of dark fermentation (Table 5.2), butyrate (S_{bu}), propionate (S_{pro}), acetate (S_{ac}), hydrogen (S_{h2}), and biomass lactate (S_{lac}) was also detected, a metabolite commonly reported in systems operated under high organic loading rates (SASIKALA et al., 1993). The concentration of S_{lac} exhibited marked variations throughout the experimental phases: starting at 77 g L^{-1} in the first phase, reaching 260 g L^{-1} in the fourth phase, and subsequently decreasing to 37 g L^{-1} in the final stage. This behavior suggests that lactate is not merely an accumulation by-product but also actively participates in subsequent metabolism, functioning as a dynamic intermediate between different fermentative pathways.

Figure 5.3 – The Dynamic Behavior of Short-Chain Fatty Acids and Lactate in Dark Fermentation of Liquid Fruit and Vegetable Waste (L-FVW): (a) Lactate, (b) Acetate, (c) Butyrate, and (d) Propionate.

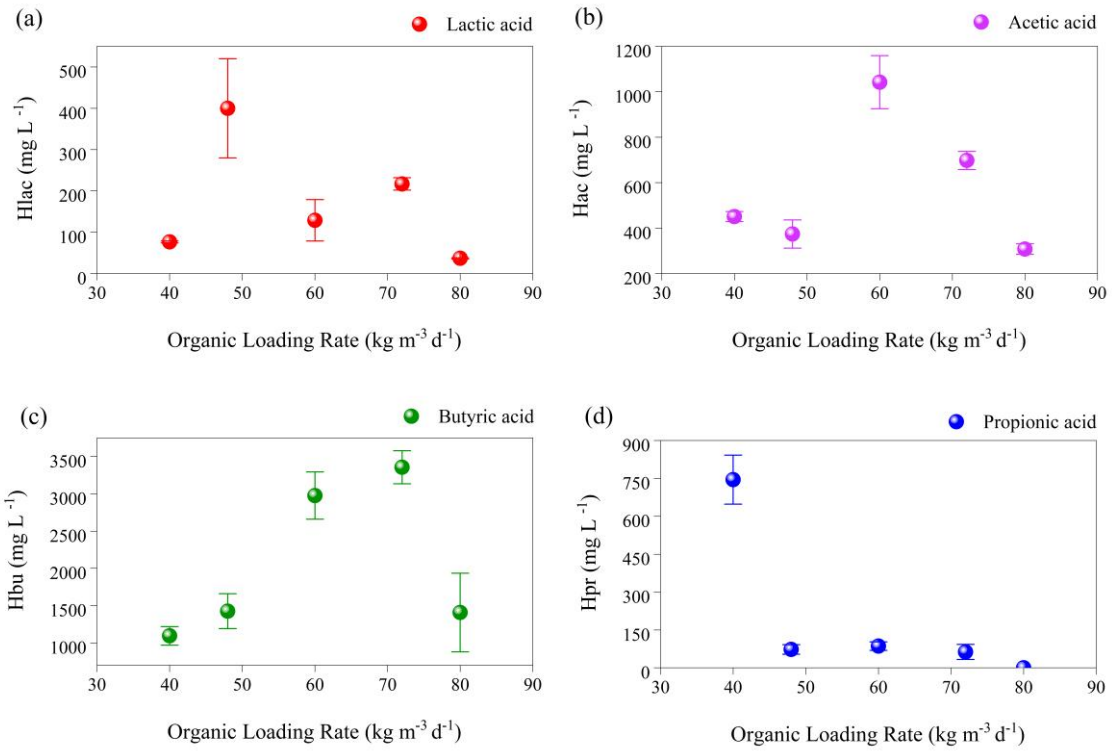

In conventional ADM1, the conversion of monosaccharides is predominantly described by the formation of acetate, propionate, butyrate, and hydrogen (BATSTONE et al.,

2002), whose stoichiometric fractions were adjusted to reflect the experimental balance: $f_{ac,su}$ = 0.090, $f_{bu,su}$ = 0.661, $f_{pro,su}$ = 0.080, and $f_{h2,su}$ = 0.169 (TUGTAS; YESIL; CALLI, 2025). These values indicate that the main electron sink during glycolysis was directed toward butyrate formation, with secondary contributions from acetate and hydrogen. However, the experimental detection of lactate required the incorporation of an alternative pathway, in which part of the monosaccharides is diverted toward lactate, ethanol, and acetate formation. For this pathway, the adjusted coefficients were $f_{lac,su}$ = 0.692, $f_{ac,su}$ = 0.256, and $f_{eth,su}$ = 0.511, reflecting the metabolic competition among different pyruvate fates under increased redox pressure. In this context, glucose reduction to lactate represents a strategy to maintain intracellular redox balance, while parallel fluxes toward ethanol and acetate prevent excessive accumulation of reduced metabolites.

The experimental profile showed that although lactate accumulated during specific phases, its final concentration decreased over time, which may indicate either partial consumption or a reduction in its net production rate. To represent this dynamic behavior, lactate degradation pathways were incorporated into the model, enabling its conversion into other intermediates and hydrogen. The estimated coefficients were $f_{ac,lac}$ = 0.185, $f_{pro,lac}$ = 0.657, $f_{bu,lac}$ = 0.131, and $f_{h2,lac}$ = 0.027. Nevertheless, no significant accumulation of propionate, butyrate, or other volatile fatty acids was observed during phases 4 and 5, despite high carbohydrate conversion rates (90–91 %) and negligible COD removal (13-15%). This indicates that substrate hydrolysis was not a limiting step and suggests that the converted carbohydrates were not effectively directed toward classical acidogenic end products. Instead, the results point to limitations in effective acidification and metabolite accumulation, likely associated with metabolic diversion toward biomass synthesis, maintenance metabolism, or the formation of soluble compounds not quantified in this study.

Therefore, the explicit inclusion of lactate formation and consumption pathways was essential to reproduce the experimentally observed dynamics, allowing the model to capture lactate as a key intermediate linking reductive and oxidative routes. Rather than indicating strong downstream acidogenic fluxes, lactate dynamics in the later phases reflect constraints on acid accumulation and the redistribution of carbon and electrons within the acidogenic network during the dark fermentation of L-FVW.

5.4.5.2 Ethanol formation route

In the experiments with L-FVW, in addition to the main products typically associated with dark fermentation (acetate, butyrate, propionate, and hydrogen), the presence of ethanol (S_{eth}) can also be identified (CHANDRA et al., 2018), linked to the concomitant formation of lactate via the heterofermentative pathway (DIEKERT; WOHLFARTH, 1994). In this pathway, glucose is metabolized by microorganisms that do not follow the classical Embden–Meyerhof–Parnas (EMP) route, but instead the pentose phosphate (or 6-phosphogluconate) pathway. As a result, 1 mol of glucose is converted into 1 mol of lactate, 1 mol of ethanol, and 1 mol of CO_2 (SEOL et al., 2014, 2016; THAUER; JUNGERMANN; DECKER, 1977). This route is typically associated with heterofermentative microorganisms, such as *Leuconostoc mesenteroides*, *Lactobacillus brevis*, *Weissella confusa*, and other lactic acid bacteria (GUPTA et al., 2024; SUNDARA SEKAR; SEOL; PARK, 2017; THAUER; JUNGERMANN; DECKER, 1977). From a redox-cofactor perspective, part of the NADH is reoxidized through ethanol formation, making this pathway energetically less efficient but favorable for maintaining redox balance under strictly anaerobic conditions.

This metabolite is frequently observed in systems operating under high organic loading rates or under redox-imbalanced conditions, when the capacity to dissipate reducing equivalents through the hydrogenotrophic pathway becomes limited (TUGTAS; YESIL; CALLI, 2025). Under such circumstances, part of the pyruvate, rather than being directed toward acetate or butyrate formation, is reduced to ethanol, serving as an alternative route for reoxidizing the NADH generated during glycolysis (DIEKERT; WOHLFARTH, 1994; THAUER; JUNGERMANN; DECKER, 1977).

In the conventional ADM1, this pathway is not explicitly represented, since the model was originally structured for substrates in which ethanol production is negligible. However, for L-FVW, incorporating this route was necessary to capture both the mass and electron balances better. Accordingly, specific stoichiometric coefficients for the conversion of monosaccharides into ethanol ($f_{eth,su}$) were introduced, adjusted based on the experimental data, and the resulting mass balance.

From a metabolic standpoint, the pathway leading to ethanol formation is closely linked to lactate production, since both serve as alternative mechanisms for reoxidizing NADH, albeit with distinct effects on the system (SAADY, 2013; THAUER; JUNGERMANN; DECKER, 1977; XIA et al., 2016). While the conversion of pyruvate to lactate tends to promote

subsequent propionate-producing routes, ethanol formation represents a more stable sink for carbon and electrons, thereby reducing hydrogen yield by redirecting reducing equivalents that would otherwise be channeled into H_2 production (KALYUZHNYI, 1997; SEOL et al., 2014, 2016). Incorporating this pathway into the model improves the carbon balance. It provides a more realistic description of how reducing equivalents are redistributed under metabolic stress, underscoring the competitive role of ethanol in dark fermentation.

5.4.6 Integrated model performance and parameter interaction across operational phases

The model calibration performed under the stable operating conditions of Phase 1 resulted in a parameter set capable of consistently representing the reactor dynamics across all subsequent experimental phases. When applied without further adjustment to Phases 2–5, which involved systematic changes in organic loading rate and organic acid composition, the model maintained its predictive performance, demonstrating strong robustness and transferability of the calibrated parameters.

This robustness was particularly evident in Phase 2, which exhibited the highest lactate concentrations observed during the experimental campaign. Despite the marked shift in the metabolic regime, the modified ADM1 retained its ability to reproduce the system behavior, indicating that the incorporation of lactate-related kinetic and stoichiometric pathways effectively captured the metabolic transitions associated with increased organic loading. The consistent representation of system dynamics across phases confirms that the calibrated model structure adequately reflects the underlying biochemical processes governing dark fermentation under variable operational conditions.

The integrated simulation showed that the parameters obtained during the initial calibration adequately represented the system's dynamic behavior throughout the experimental phases, including variations in OLR and organic acid profiles. The model satisfactorily reproduced the H_2, CO_2, VFA, and lactate production curves, maintaining mass and electron balances consistent with the experimental data.

Prediction of the total biogas flow rate, composed predominantly of CO_2 and H_2, showed consistent performance, with an R^2 of 0.864 and an RMSE of 0.934. When the H_2 flow rate was evaluated individually, even more satisfactory fits were observed (R^2 = 0.868; RMSE = 0.201), indicating that the fermentative pathways implemented to represent hydrogen production adequately captured the experimental behavior. In Phase 2, operated under a high

organic loading (OLR of 48 kg COD m^{-3} d^{-1}), a reduction in the H_2 fraction to 28 ± 2% was observed. This phenomenon is consistent with the system's biochemistry: under higher loading, excess reducing equivalents generated during substrate degradation are diverted from hydrogen production toward alternative fermentation pathways, particularly the synthesis of reduced organic acids that act as electron sinks (MUELLER et al., 2025; SAHA et al., 2023; SONG et al., 2024). Consequently, hydrogen production decreases as metabolic activity redirects electrons toward the formation of acids such as acetate, propionate, and butyrate instead of the gaseous H_2-releasing pathway (KAPDAN; KARGI, 2006; SILVA-MARTÍNEZ et al., 2025), which is evidenced by the increase in acid production shown in Figure 5.3. The model adequately reproduced this shift in metabolic flux distribution, with an R^2 of 0.911 and an RMSE of 1.840 for H_2 flow rate. For CO_2, the main component of biogas and a key variable for closing the mass and conversion balances, the model exhibited similarly robust performance (R^2 of 0.903 and RMSE of 1.840), demonstrating its ability to capture the metabolic redistribution and redox balance of the system in response to the increased OLR.

Regarding the prediction of organic acids (S_{lac}, S_{ac}, S_{bu}, and S_{pro}), Figure 5.4 presents the simulated curves alongside the experimental data. The model achieved an excellent fit for all compounds, with R^2 and RMSE values of 0.962 and 0.026 for acetate, 0.959 and 0.099 for butyrate, 0.904 and 0.051 for lactate, and 0.919 and 0.008 for propionate. These results indicate that the model successfully captured transitions between the predominant metabolic pathways, including lactate oxidation and its conversion to acetate, propionate, and butyrate (ANTONOPOULOU et al., 2012a; ECONOMOU et al., 2024). This mechanistic consistency reinforces the conclusion that the kinetic and stoichiometric modifications incorporated into ADM1 were decisive in describing the dynamics of the dark fermentation process of L-FVW under different operational regimes.

The integrated analysis revealed strong interdependence between hydrolysis and acidogenesis parameters, particularly in their responses to changes in organic loading and substrate composition. High sensitivity was observed for parameters associated with carbohydrate conversion and electron-equivalent redistribution, reflecting metabolic competition among lactate, ethanol, and hydrogen pathways under distinct redox conditions. Overall, the modified model demonstrated robustness and internal metabolic coherence across the evaluated operational phases, indicating it can be reliably applied across different scenarios. However, additional calibration may be necessary to accurately represent processes such as acid inhibition, pH-dependent metabolic shifts, and transient accumulation of intermediates.

Figure 5.4 – Comparison between optimized model simulations and experimental measurements of key organic acids (HLac, HAc, HPro, HBu) during dark fermentation of L-FVW (phase 2).

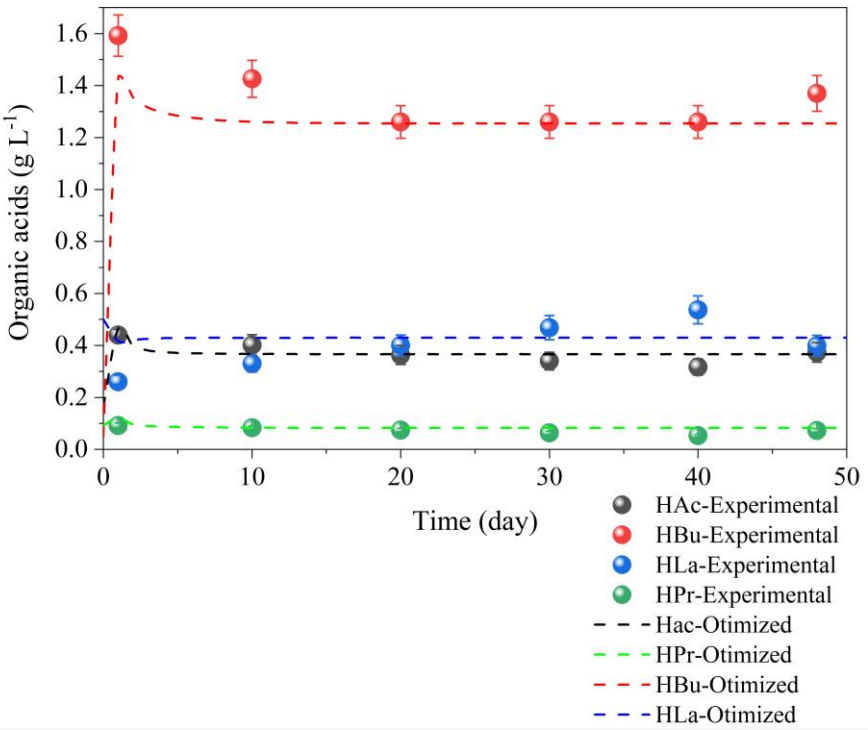

5.4.7 Suggested improvements for dark fermentation modeling

The original ADM1, as well as adaptations designed to represent metabolic pathways associated with hydrogen generation, yield by-products relevant to dark fermentation. However, the model, in its conventional form, does not account for certain pathways observed during L-FVW digestion, as these pathways are of limited importance to the methanogenic phases of traditional anaerobic systems.

Models focused on L-FVW fermentation for acid recovery and H_2 production remain scarce, mainly because of the intrinsic complexity of ADM1 and the large number of parameters required to describe experimental behavior accurately. Therefore, implementing more precise modifications demands careful consideration of inhibitory factors related to the system's operational conditions, such as pH, the concentration of specific acids (particularly acetate), and ammonia formation. These variables directly influence the process stability and kinetics, thereby justifying the adjustments made to render the model more robust and representative.

Beyond these biochemical changes, the inclusion of hydrodynamic aspects that reproduce the actual reactor behavior is also recommended, since ADM1, in its basic configuration, assumes ideal conditions of complete mixing. Controlling both the feed pH and the internal system pH is essential to ensure process stability and to prevent fluctuations that could induce metabolic inhibition or sudden acidification. The same principle applies to the regulation of hydrogen partial pressure, a critical variable that maintains equilibrium among fermentative pathways and ensures overall process efficiency.

When incorporating new metabolic routes, it is necessary to consider the risk of overlap between pathways, which may lead to overestimating H_2 production. This issue is particularly relevant during the primary degradation of sugars, which can occur through multiple competing routes. Therefore, the use of balance equations across pathways is recommended, prioritizing the dominant route based on microbial composition and the characteristics of the inoculum sludge. The inclusion of specific routes, such as the lactate pathway, is likewise essential whenever significant lactate production is observed experimentally. In such cases, specific inhibitory mechanisms should be incorporated to reflect better the observed metabolic interactions.

In summary, the modifications proposed to the ADM1 structure represent a significant step toward a more realistic description of the phenomena governing dark fermentation of organic residues. The incorporation of specific metabolic routes, calibration based on experimental data, and consideration of typical inhibitory effects for this type of substrate have collectively enhanced the model's predictive capacity and reduced discrepancies between simulated and observed results. Although challenges remain in the kinetic characterization and thermodynamic description of competing pathways, the adjustments made provide a solid foundation for continued model refinement and future integration into hybrid approaches for process optimization and control. Thus, the adjusted model not only aligns more closely with experimental reality but also establishes itself as a promising tool for designing strategies to intensify processes and valorize products in biorefineries dedicated to sustainable hydrogen and methane production.

5.5 Possible future direction

The main future development of this research involves implementing an integrated system comprising multiple reactors, representing a waste-based biorefinery aimed at

generating sustainable biofuels, such as hydrogen and methane, through both wet and dry processes. The current strategy of modeling each stage separately aims to calibrate and validate models based on the specific principles and dynamics of each process. Once this step is consolidated, the integration of the different stages will enable comprehensive assessments of energy, economic, and environmental performance.

In addition, microbiological aspects will be further explored to strengthen the understanding of key stoichiometric pathways identified in this work. Special attention will also be given to valorizing fermentation effluents, particularly their potential use in electrolysis systems for additional hydrogen recovery, thereby broadening the energy yield and closing material cycles within the biorefinery concept.

5.6 Conclusion

This study demonstrated that ADM1, when properly modified and calibrated, can accurately model the metabolic processes underlying dark fermentation of L-FVW. Experimentally, the system exhibited high carbohydrate conversion, a consistent predominance of the butyric pathway, and stable hydrogen production, reaching a maximum yield of 2.20 L_{H2} $L^{-1}d^{-1}$. However, the original ADM1 was unable to reproduce these results, overestimating substrate solubilization, the acetogenic fraction, and the hydrogen production potential.

The explicit inclusion of lactate-related pathways, as well as the adjustment of sensitive kinetic and stoichiometric parameters, particularly $k_{hyd,ch}$, $k_{m,su}$, $k_{m,lac,su}$, $k_{m,lac}$, k_s, and the microbial yield coefficients, were essential to capturing the metabolic competition among lactate, acetate, and butyrate. The calibrated model accurately represented the VFA profiles, biogas composition, and hydrogen production dynamics, confirming the central role of hydrolytic limitation and lactogenic pathways in shaping metabolic selectivity in L-FVW-fed reactors.

Thus, the study provides evidence that structural adaptations to ADM1 and substrate-specific calibrations are indispensable when the model is applied to complex and heterogeneous substrates such as L-FVW, which exhibit variable fractions of soluble sugars, fibers, and lactic compounds. Beyond enhancing the model's predictive capacity, the adjustments identified here have the potential to guide operational and control strategies to increase both efficiency and selectivity toward hydrogen. The resulting model represents a

significant advancement in understanding and optimizing organic waste biorefineries dedicated to the sustainable production of biohydrogen.

The full version of this paper is published in Journal of Environmental Chemical Engineering (2024) under the name “Bibliometric analysis of Anaerobic Digestion Model No. 1 for dry anaerobic digestion of fruit and vegetable waste, food waste, and organic fraction of municipal solid waste”. DOI: https://doi.org/10.1016/j.jece.2024.114664.

6 ARTICLE III: BIBLIOMETRIC ANALYSIS OF ANAEROBIC DIGESTION MODEL NO. 1 (ADM1) FOR DRY ANAEROBIC DIGESTION OF FRUIT AND VEGETABLE WASTE, FOOD WASTE, AND ORGANIC FRACTION OF MUNICIPAL SOLID WASTE

ABSTRACT

The Anaerobic Digestion Model No. 1 (ADM1) is a widely spread platform for simulating methanogenic reactors. It is a structured and complex model considering physicochemical and biochemical processes during wastewater and sewage sludge anaerobic digestion (AD). However, many modifications, simplifications, and adaptions exist for specific wastewaters/sludges, processes, and operational conditions. Given this, a bibliometric analysis was carried out to identify the main applications of ADM1 in the dry anaerobic digestion (D-AD) of fruit and vegetable waste (FVW), food waste (FW), and organic fraction of municipal solid waste (OFMSW). The adaptation necessary in ADM1 includes adjusting and separating the disintegration and hydrolysis rates of the substrate and sludge, which have different characteristics, such as the concentration of solids, which is inversely proportional to the hydrolysis velocity. In addition, adaptations are a function of the adopted reactor and other parameters. Finally, the work identifies the current modeling state-of-the-art using ADM1 and the need for further research to improve the model application in D-AD processes.

Keywords: ADM1; dry anaerobic digestion; renewable energy; organic waste.

6.1 Introduction

Anaerobic digestion (AD) is a promising technology extensively applied in wastewater and solid waste treatment processes (HOLM-NIELSEN; AL SEADI; OLESKOWICZ-POPIEL, 2009; RYUE et al., 2019; YIN; GU; WU, 2020). AD is a biological process grouped into four main phases: hydrolysis, acidogenesis, acetogenesis, and methanogenesis (ATELGE et al., 2020; DJAAFRI et al., 2023). Based on the total solids (TS) content, AD can be classified into wet anaerobic digestion (W-AD), which operates with TS below 10%; semi-dry anaerobic digestion (SD-AD), for TS between 10 and 15%; and dry anaerobic digestion (D-AD), keeping TS above 15% (AJAY et al., 2011; ARELLI et al., 2018; BOLLON et al., 2011; ELSAMADONY; TAWFIK; SUZUKI, 2015; GARCIA-BERNET et al., 2011; KOTHARI et al., 2014; SALAMAT et al., 2022; WANG et al., 2023).

W-AD is widespread and is being applied to treat domestic, agro-industrial, and industrial wastewater, sewage sludge, and others (ROSA et al., 2018; SILVA, 2024; SILVA et al., 2022, 2023; SILVA; OLIVEIRA JÚNIOR; CORDEIRO, 2022, 2023). In recent years, D-AD has garnered significant attention due to its array of advantages over W-AD. These include a higher volumetric methane yield, reduced reactor volumes, lower moisture content in the digestate for easier management, and the ability to withstand higher organic load rates (OLR) with TS concentrations of up to 40% (ARELLI et al., 2018; CHO et al., 2013; WANG et al., 2023). In addition, D-AD is free from stratification problems due to floating fibrous material and tolerates the presence of inert materials such as sand and stones (FORSTER-CARNEIRO et al., 2007). On the other hand, the high-solid content causes technical restrictions such as handling, mixing, or pre-treatment compared to the wet process.

Residue physical condition affects mixture homogeneity, rheological behavior, chemical equilibrium, and mass transfer (BOLLON et al., 2011; OLESZKIEWICZ; POGGI-VARALDO, 1997). Process modeling can help in design evaluation, optimization, scale-up, and system control, considering the biological configuration of the models and the biochemical process adjustments (YAHAYA et al., 2022). It also allows the description of biological phenomena and mass transfer and is a tool for designing processes (BOUTOUTE et al., 2021). It can be used to predict the effect of variables on the system performance and possible failures (FDEZ-GÜELFO et al., 2012; SHI et al., 2014). It can also be used to understand the process's complexity, enabling the search for strategic improvements and process kinetics evaluation (LI et al., 2021; ZHAO et al., 2009).

Numerous mathematical models for AD have been proposed. Gavala et al. (2003) compiled a series of works that developed models for AD. Some models apply inhibition of non-ionized volatile fatty acids (VFA) as the main parameter, as proposed by Graed and Andrews (1973), Hill and Barth (1978), Kleinstreuer and Poweigha (1982), Marsili-Libelli and Nardini (1985), Moletta et al. (1986), Smith et al. (1988) and Markl (2004). Models considering the residue composition were published by Bryers (1985), Gavala et al. (1996), Jeyaseelan (1997), and others. Models using H_2 as the key parameter were developed by Mosey (1983), Pullammanapallil et al. (2014b), Costello et al. (1991a, 1991b), Keller et al. (1993), Romli et al. (1994a, 1994b), Ruzicka (1996a, 1996b), and Batstone et al. (2000). Finally, models using NH_3 as a key parameter were reported by Ni (1999), Kiely et al. (1997), Moletta (1986), Hill (1982), Siegrist et al. (1993), Zehnder (1983), and Vavilin et al. (1996).

The AD group of the International Water Association (IWA) (BATSTONE et al., 2002) developed the Anaerobic Digestion Model No. 1 (ADM1), which was generated from the convergence of several ideas from other models into a single one, aiming to reproduce the main AD mechanisms (LAUWERS et al., 2013; PASTOR-POQUET et al., 2019a). Biochemical mechanisms are represented by the disintegration of organic substrates and their conversion during the AD steps of hydrolysis, acidogenesis, acetogenesis, and methanogenesis, expressed as chemical oxygen demand (COD). The physicochemical mechanisms are represented by liquid-gas transfer (CH_4, CO_2, and H_2), the ion balance of VFA (acetic, propionic, butyric, and valeric), inorganic nitrogen in the form of NH_3 and inorganic carbon as CO_2 (BATSTONE et al., 2002). The ADM1 was initially developed for sewage sludge treatment at mesophilic or thermophilic temperatures. However, it has been implemented under other conditions with different substrates (BATSTONE et al., 2002; FENG et al., 2006; LOHANI et al., 2016).

Although AD has demonstrated great potential for treating waste, further research is still needed to demonstrate the potential of this model for designing, operating, and optimizing substrates such as fruit and vegetable waste (FVW), especially in the D-AD process. To the best of our knowledge, no work has reviewed and analyzed the ADM1 application in the D-AD process for FVW. This biomass includes wholesale markets, supermarkets, and agricultural activities, and is generated from the production, transportation, storage, distribution, and consumption of fruit and vegetables. Food and Agriculture Organization (FAO) (FAO, 2023) estimated that in 2023, around 45% of fruit and vegetables are wasted in the production chain (ABUBACKAR et al., 2019; CHATTERJEE; MAZUMDER, 2020;

DEENA et al., 2022; DEVI et al., 2022; EDWIGES et al., 2018; SAGAR et al., 2018). FVW characteristics, such as moisture and volatile solids (VS) content, make it ideal for stable anaerobic digestion (LI et al., 2021; PAGLIACCIA et al., 2019; SILVA JÚNIOR et al., 2022). However, the waste is composed of simple carbohydrates that cause rapid acidification and potential inhibition of methanogenic activity, and it is affected by the seasonality of its properties, such as: moisture content, VS, pH, alkalinity, VFA, C:N:P and other components (PAGLIACCIA et al., 2019). FVW can also be present in parcels of Food Waste (FW) and Organic Fraction of Municipal Solid Waste (OFMSW) (CHATTERJEE; MAZUMDER, 2020; ELSAMADONY; TAWFIK; SUZUKI, 2015; YU et al., 2012), containing a high solids content (FERNÁNDEZ; PÉREZ; ROMERO, 2008; KOTHARI et al., 2014).

Despite the great potential of anaerobic digestion of FVW, significant gaps remain in the application of the ADM1 model, particularly in the context of D-AD. Understanding and improving the use of ADM1 for treating this waste is crucial to transforming an environmental issue into a valuable source of bioenergy. However, the lack of comprehensive bibliometric reviews that map the applications of the ADM1 model, as well as the gaps and opportunities for optimization, hinders the advancement of research and the full realization of its potential. Due to variations in waste characteristics and processing conditions, the ADM1 model, developed for a specific type of waste under predefined conditions, may not be applicable to other wastes with different compositions or processing systems without the necessary adaptations that take these particularities into account. It is therefore essential to study and evaluate the model's potential application under different conditions and with other types of waste.

These wastes have great potential for application in AD. However, there are still significant gaps in the modeling of the digestion of plant-based or food waste that need to be addressed. This study aims to fill this gap through a bibliometric and systematic analysis of ADM1 applications in anaerobic digestion processes. By mapping scientific production and evaluating the suitability of this model for treating wastes such as FVW, OFMSW, and FW, valuable insights are expected to be provided for improving the performance and efficiency of anaerobic digestion processes. The results of this analysis will offer a solid foundation for future research and optimization in the field of anaerobic digestion of high-concentration solid waste, contributing to the development of more effective and sustainable strategies for treating this type of waste.

The introductory section presents processes (D-AD) and technologies for the digestion of FVW, FW, and OFMSW. In the next part, a bibliometric analysis determines the proportion of research on ADM1 associated with the mentioned wastes. Subsequent sections discuss publications relevant to the field of study and, finally, present future perspectives based on the analysis conducted.

6.2 Anaerobic digestion of FVW

One-third of food produced for human consumption is wasted, of which FVW accounts for 45% (FAO, 2023). However, due to its high VS content and easily hydrolyzable organic components, FVW has great potential for anaerobic digestion or fermentation (ABUBACKAR et al., 2019). The AD of FVW has numerous advantages, from energy production to reduction of greenhouse gas emissions (GEE).

FVW has a TS content ranging from 7.4 to 17.9% (wet basis) and a volatile solids content ranging from 83.4 to 95.3% VS/TS (wet basis) favoring hydrolysis that can cause pH reduction and consequent acidification, inhibiting methane production (SCANO et al., 2014; WARD et al., 2008). The organic content includes fructose and hemicellulose (75%), cellulose (5%), and lignin (1%) (FERRER et al., 2014; JI et al., 2017). Other values are found for hemicellulose (9%) and lignin (5%) (BOUALLAGUI et al., 2005). Chatterjee et al. (2020) reported that these values may be lower, being evaluated less frequently (MAGAMA; CHIYANZU; MULOPO, 2022). Santos et al. (SANTOS et al., 2020) studied the composition of certain fruit residues (orange pomace, passion fruit peel, and cashew pomace), range of values obtained for lignin (1.4-34.5%), hemicellulose (6.6-16.2%), and cellulose (12.7-25.4%) higher than the literature above. Silva Junior et al. (2022) also studied the digestion of FVW with 130 g kg^{-1} of TS, but the concentrations of hemicellulose, cellulose, and lignin in the residue were not reported. These characteristics vary according to the residue collected, depending on the substrate fiber composition relative to the shell seeds and plant source (PAUDEL et al., 2017).

FW has a high content of easily biodegradable organic matter (carbohydrates, lipids, and proteins) and high VS. It comprises fruit and vegetable waste, household waste, and waste from restaurants, breweries, and dairies, among others (XU et al., 2018), and is considered suitable for AD (HAGOS et al., 2017). According to Assis et al. (2022), FW is a component of OFMSW and can represent around 30-60%, which can change from one country

to another (BONG et al., 2018; WONG et al., 2018). It generally has a low C/N ratio, fewer trace elements, and irregular particle distribution (HAGOS et al., 2017; SHRESTHA et al., 2023; ZHANG; LEE; JAHNG, 2011). FW comprises 8.3 to 21% lipids, responsible for higher biogas production than proteins and polysaccharides during fermentation. This shows the bioenergy production potential of FW (HE et al., 2023; KARMEE, 2016; LI et al., 2016, 2002). Lipids are hydrolyzed into glycerol and long-chain fatty acids (LCFAs) (BATSTONE; KELLER, 2003), then broken down into medium-chain fatty acids (MCFAs) and VFAs via β-oxidation, with subsequent conversion into acetate and hydrogen (LI et al., 2002).

OFMSW may involve FW, yard waste, paper, and other organic waste (TYAGI et al., 2018). It will be considered when surveying the models, as it is possible to apply ADM1 for such waste, enabling manipulation (MATHERI et al., 2017). Some substrate characterization data are described in Table 6.1.

Table 6.1 – Characterization of Substrates: FVW, FW, and OFMSW

Substrate	Reference	TS	VS	C:N	pH	Carbohydrate	Protein	Lipids
		%	%	%		%	%	%
FW [i]	1	18.1	17.1	13.2	6.5	11.2	3.3	2.3
FW [i]	2	22.8	20.1	18.5	5.1	36.0	21.0	15.0
FW [i]	3	10.9	10.2	15.2	4.2	5.7	2.3	1.3
FW [i]	4	25.9	25.9	17.5	NR	48.0	15.1	10.6
FW [i]	5	23.9	21.8	16.3	NR	NR	NR	NR
OFMSW	6	26.4-34.8	6.6-29.2	NR	4.3-6.2	45.4-65.6	12.2-23.2	4.4-15.0
OFMSW	7	59.7	38.5	19.0	6.2	0.6	0.7	2.4
OFMSW [i]	8	52-58.5	40.9-43.0	21.0-22.0	6.4-6.5	1.6-0.1	0.7-0.6	3.2-1.4
FVW	9	12.8-13.20	12.2-12.3	14-16	NR	53.8-56.2	1.76-2.74	0.64-0.996
FVW	10	7.4-17.9	6.17-17.1	15.2-18.9	3.7-4.2	NR	10.5-17.8	0.8-5.2

Note 1: TS – Total solids; VS – Volatile solids; C:N – Carbon to nitrogen ratio; NR – Not reported; [i]WT_{ts} – by weight of TS. Note 2: 1 (ZHANG; LEE; JAHNG, 2011); 2 (FISGATIVA; TREMIER; DABERT, 2016); 3 (XIAO et al., 2019); 4 (SHI et al., 2018); 5 (MU et al., 2020); 6 (CAMPUZANO; GONZÁLEZ-MARTÍNEZ, 2016; TYAGI et al., 2018); 7 (BASINAS; RUSÍN; CHAMRÁDOVÁ, 2021b); 8 (BASINAS; RUSÍN; CHAMRÁDOVÁ, 2021a); 9 (SILVA JÚNIOR et al., 2022); 10 (BOUALLAGUI et al., 2004; HAGOS et al., 2017; LABATUT; ANGENENT; SCOTT, 2011; SHEN et al., 2013; XU et al., 2018).
Data: Adapted from Xu et al. (2018) and Shrestha et al. (2023).

One requirement for adequate modeling using ADM1 is the precise substrate characterization to define the components generated in the degradation and absorption process. This allows for the estimation of the values closest to the experimental data and reduces potential errors.

ADM1 focuses on kinetic and stoichiometric processes. While the implementation provided in the original model's documentation ((BATSTONE et al., 2002), Appendix) is tailored for fixed-volume continuous stirred tank reactors (CSTRs), this methodology is versatile. As noted by Batstone et al. (2015), it can be effectively adapted to other reactor technologies.

Among the variables, solids retention time (SRT) and hydraulic retention time (HRT) can be assumed to have the same value. SRT is associated with biomass growth rate (microorganisms) (FERNÁNDEZ; PÉREZ; ROMERO, 2008; LI; CHEN; WU, 2019), and HRT is the average residence time of a given particle in a reactor (ATELGE et al., 2020). It is assumed that the digester heterogeneity and flocculation can be omitted. The liquid phase volume is constant, i.e., inlet flowrate (q_{inp}) = outlet flowrate (q_{out}). The input (substrate) and output (digestate and gases) mass balance is derived from the ADM1 input and output data.

OFMSW, FW, and FVW substrates are highly complex and heterogeneous, so a detailed characterization is necessary for accurate modeling, as several organic fractions trigger anaerobic biodegradability (LÜBKEN et al., 2015a). The representative characteristics of the substrate considered as inputs for the model are shown in Table 6.2. The inputs found in the literature were for OFMSW and FW. No inputs specifically designed for ADM1 were identified. However, they can be determined based on substrate analyses.

Table 6.2 – Representative characterization of transformer input.

Components	Unit	OFMSW	FW	FVW	Explanations
Total Solids (TS)	%WW	15.4	21.00±0.36	13.0±0.2	
Volatile Solids (VS)	%WW	11.8	19	94.1±0.3	
Density of wet food waste	kg m^{-3}	1,000	1,000	1,000	assumed
Particulate COD (COD_p)	g m^{-3}	182,000	264,600	-	=CODt-CODs
COD_s-VFA	g m^{-3}	2,300	2,700	-	
Volatile Fatty Acids (VFA)	g m^{-3}	2,300	2,700	-	1% of CODt
Total Organic Carbon (TOC)	gC m^{-3}	53,300	99,360	39,160±5,817	=TC-TIC
Total Organic Nitrogen (N_{org})	g m^{-3}	6,600	7,243	-	(TS/VS) % TKN
Total Ammonia Nitrogen (TAN)	g m^{-3}	1,300	877	-	=TKN-Norg
Organic Phosphorus (TP-orthoP)	gP m^{-3}	900	1,028	-	(TS/VS) % of TP
Orthophosphate (orthoP)	gP m^{-3}	-	124	-	=TP-TP-orthoP
Total Inorganic Carbon (TIC)	moleHCO_3^- m^{-3}	-	169	-	=(TC-TOC)/12
Total Alkalinity (S_{cat})	equ m^{-3}	25	25	-	Assumed
Fixed Solids (FS)	g m^{-3}	-	23,000	-	=TS-VS

Data: Adapted from Nguyen (2014), Zhang et al. (2012), Capson-Tojo et al. (2021) and Silva Junior (2022).
Note: TC – Total carbon; COD_t estimated 270 g kg^{-1} WW, TC is 47,6% TS.

The substrate can be characterized as biodegradable and non-biodegradable, where non-biodegradable soluble organics correspond to S_I while non-biodegradable particulate organics correspond to X_I in ADM1 (LÜBKEN et al., 2015a). It considers S_I 1.5% of total COD or 4.5% of soluble COD. However, these values can change depending on the substrate (BLUMENSAAT; KELLER, 2005). The X_I is calculated based on the biodegradable COD and methane production ratio, knowing that the influencing parameters (disintegration coefficients or hydrolysis rate) are already defined, and the non-biodegradable COD will be easily obtained by adjusting the model considering the gas flow (LÜBKEN et al., 2015a).

6.3 Types of processes, reactors, and technologies

AD is not a recent technique; it has a historical background in processing various solid and liquid wastes and has been extensively utilized for disposing of urban waste (BOUALLAGUI et al., 2005; JI et al., 2017). The system depends on efficient reactors and operational and control strategies. Numerous technologies are already widely applied in liquid and solid waste treatment, some of them at full scale. Kothari et al. (2014) reported that D-AD employs a variety of reactors at laboratory and commercial levels, which can be classified into the following categories (SHEFALI; THEMELIS, 2002):

- Single stage:

a. Single Stage Low Solids Process (SSLS);

b. Single Stage High Solids Process (SSHS).

- Multi-stage:

a. Multi-Stage Low Solids Process (MSLS);

b. Multi-Stage High Solids Process (MSHS).

- Batch and continuous process.

The reactors can also be categorized according to operating temperature (psychrophilic, mesophilic, thermophilic, and extremophilic), flow (upward, downward, and horizontal), mixing (external or internal), rate (low or high), and with or without support medium (SARKER et al., 2019).

Using these technologies to process high solid wastes such as FVW, OFMSW, and FW depends on the design and reactor adopted. Ji et al. (2017) list the main reactors selected to digest FVW in recent years, including batch reactors (AWADALLA et al., 2023; GONÇALVES NETO et al., 2021; SAHA et al., 2023), continuous single-phase reactors (GONÇALVES NETO et al., 2021; JI et al., 2017), and continuous two-stage reactors (acidogenic and methanogenic stages) (GOMEZ-ROMERO et al., 2014; MAGAMA; CHIYANZU; MULOPO, 2022; SHEN et al., 2013; VYAS et al., 2022). Anaerobic baffled reactor (ABR) (GULHANE et al., 2016), anaerobic sequencing batch reactor (ASBR) (BOUALLAGUI et al., 2009; HABIBA; HASSIB; MOKTAR, 2009), CSTR (BOUALLAGUI et al., 2009; HABIBA; HASSIB; MOKTAR, 2009), hybrid anaerobic solid-liquid (HASL) (HAI-LOU; JING-YUAN; JOO-HWA, 2002; XU et al., 2014b; ZHU et al., 2015), leached bed

reactor (LBR) (CHAKRABORTY; PARTHIBA; SELVAM, 2022), solid-state stratified bed (SSB) (HAI-LOU; JING-YUAN; JOO-HWA, 2002), tubular reactor (BOUALLAGUI et al., 2003, 2004) and upflow anaerobic sludge blanket (UASB) (CAVALCANTE et al., 2023; SANTOS et al., 2020). There are also other systems, such as the dry anaerobic composting (DRANCO) process, Valorga system, Kompogas reactor, and Bekon reactor (single-stage batch process), which have the potential to digest FVW with high solids content (ANGELIDAKI; ELLEGAARD; AHRING, 2003; KOTHARI et al., 2014; KUMAR; SAMADDER, 2020; LI; PARK; ZHU, 2011; MOMAYEZ; KARIMI; TAHERZADEH, 2019; RAPPORT et al., 2012; SHEFALI; THEMELIS, 2002; TIWARY et al., 2015).

The solids content in a reactor affects its processing volume. The low water content in the system results in a low reaction volume, providing smaller reactors. However, the equipment may be more expensive due to the specific pumps and structures. D-AD reactors operate in a high OLR and are naturally robust (KOTHARI et al., 2014). They also offer some benefits, such as a higher volumetric yield of methane (WANG et al., 2020), lower energy requirements, lower digestate production and humidity, easier to handle, and better pre- and post-processing (ABBASSI-GUENDOUZ et al., 2012; ARELLI et al., 2018; WANG et al., 2020, 2023).

According to Vandevivere et al. (2003), dry methanization processes have already proved reliable, and this became widespread in the industry after the 1980s in an attempt to segregate the liquid and solid fractions. However, very dry waste (TS > 50%) needs to be diluted with water. Dry waste is transported using belts, screws, and powerful pumps for high flows and viscosities, which are more expensive than pumps used in wet systems. A single pre-treatment is required to remove particles larger than 40 mm or a process to reduce particle diameter. Four designs have proved effective in full-scale plants: 1) DRANCO process, which has a mixture resulting from recirculation of the digestate extracted from the reactor bottom and mixed with the fresh substrate. This mixture of the fresh and recirculated substrate has a ratio of 1 (substrate) to 6 (recirculated) before injection into the digester; 2) Bekon process, which is a single-stage batch reactor and the system does not require complex pre-treatment and can be considered a flexible and applicable system for treating OFMSW (KUMAR; SAMADDER, 2020; LUO et al., 2021; QIAN et al., 2016); 3) Kompogas process, which has a horizontal flow with internal rotation to homogenize the waste; and 4) Valorga system, which has a circular horizontal flow in a cylindrical reactor, and mixing takes place by injecting biogas at high

pressure into the reactor bottom every 15 minutes through a network of injectors (KUMAR; SAMADDER, 2020; MOMAYEZ; KARIMI; TAHERZADEH, 2019; ZAMRI et al., 2021).

The main limitations of the dry waste digestion process may involve the raw material, TS content, rheological behavior and mass transfer (particle size, TS, reactor temperature, hydrodynamics), ammonia inhibition, VFA accumulation, and microbial community adaptation (PAVLOSTATHIS; GIRALDO-GOMEZ, 1991).

Substrates with a high solids content are structured and, therefore, complex to handle and homogenize (VANDEVIVERE; DE BAERE; VERSTRAETE, 2003). D-AD has biological and technological shortcomings owing to the excessive solids content in the digester (WANG et al., 2023). These limit mass transfer between the microorganism and the substrate and/or metabolites, reducing the microbial nutrients accessibility (increasing resistance to diffusive transport of soluble compounds), resulting in low VS degradation and a consequent reduction in biogas production (ABBASSI-GUENDOUZ et al., 2012; WANG et al., 2023; XU et al., 2014a). Most studies show that contents above 15-20% TS reduce methane production (WANG et al., 2020). High loads also lead to the accumulation of inhibitors such as ammonia and VFA, reducing methane production (WANG et al., 2020, 2023). Water absence in the medium contributes to the high potential for inhibitors of acetogenesis and methanogenesis and generates significant differences in rheological behavior and mass transfer.

Newtonian fluids, such as water, behave viscoelastically. However, as the digested solid waste does not contain much water, it is considered a non-Newtonian fluid, straining performance and making it difficult to homogenize the substrate in the reactors, directly affecting methane production (MOSEY, 1983). Nevertheless, according to Pavlostathis and Giraldo-Gomez (1991), adequate mixing can increase gas production since mixing reduces the kinetic limitation of the reaction (LI et al., 2023; MOMAYEZ; KARIMI; TAHERZADEH, 2019).

Also, due to high loads and TS, the ammonia nitrogen (TAN) level is generally high and can lead to AD inhibition by inhibiting ammonia (KUMAR; SAMADDER, 2020; SHAPOVALOV et al., 2020). High concentrations of TAN and VFA also affect the microbiological activity and susceptibility to inhibition. AD operating conditions such as temperature, pH, C/N ratio, OLR, and inoculation can influence process stability. In this study, some possibilities for modeling D-AD are presented.

6.4 Bibliometric methods

A bibliometric analysis is a systematic study of publications within a specific research field. It allows for the collection of detailed information, such as citation analysis, authors' countries of origin, researcher collaborations, the temporal evolution of publications, and the identification of key journals (CIANO et al., 2019). This data enables the mapping of research development over time, from its origins to the most recent studies, providing a clear view of the main trends and existing gaps. In this way, bibliometric analysis helps identify key topics of greater relevance and opportunities for future research in the field (ZENG; CHINI, 2017).

Through this analysis, it is possible to identify the most cited publications and their influence on other studies, as well as to track the evolution of these citations over time. To conduct effective scientific mapping, it is essential to follow five stages: study design, data collection, data analysis, result visualization, and finally, interpretation of the findings (ARIA; CUCCURULLO, 2017; COBO et al., 2011; ZUPIC; ČATER, 2015).

According to Aria and Cuccurullo (2017), the main objective of the study design is to define the research questions, such as delimiting the knowledge base, selecting topics or research areas, and structuring the data from a specific scientific community. In this study, no time frame was established, covering the entire available period. During the data collection stage, an appropriate database is selected by filtering based on predefined keywords. This phase involves constructing a set of terms that reflect the study area. For data analysis, bibliometric and/or statistical software is used to efficiently explore the information. Data visualization includes the creation of maps, tables, and diagrams that clearly represent the associations between topics. Finally, the results are interpreted by the author based on the findings.

6.4.1 Data collection

The data collection process follows several stages, as suggested by Aria And Cuccurullo (2017). The first step involves gathering data from online scientific databases, such as the Web of Science Core Collection (WS), Scopus, or Science Direct (SD). These platforms differ in their coverage of scientific fields and time periods. Both WS and Scopus are subscription-based databases that provide access to citation indexes, although WS has been

more extensively studied. Both platforms offer data access through web interfaces, enabling analysis without significant restrictions (COBO et al., 2011; ZUPIC; ČATER, 2015).

Previous studies report that approximately 97% of WS publications are also available in Scopus (WALTMAN, 2016), suggesting that WS offers broader coverage. Additionally, publications indexed in WS tend to have a higher citation impact compared to those indexed in Scopus (LÓPEZ-ILLESCAS; DE MOYA-ANEGÓN; MOED, 2008; LÓPEZ-ILLESCAS; DE MOYA ANEGÓN; MOED, 2009). Nonetheless, Waltman (2016) notes that similar results can be achieved using both WS and Scopus, indicating that both platforms are effective for bibliometric analysis, depending on the study's objectives.

For the survey, a set of the most relevant keywords in the research area was selected to analyze the conceptual structure of the scientific field. This set enables the connection of different documents through specific keywords related to the subject studied. From this analysis, it is possible to obtain valuable data, such as the correlation between research and its affiliated institutions. Additionally, keywords referring to the selected research, as well as associated terms that complement the scope of the study, were included.

6.4.2 Software for bibliometric analysis and scientific mapping

Bibliometric analysis and scientific mapping require the use of specialized tools that enable data to be collected, analyzed, and visualized in an efficient and detailed manner. A variety of software is available to perform these tasks, each with specific functionalities that assist in the exploration and interpretation of bibliographic data. These tools make it possible to identify patterns, trends, collaboration networks, and emerging areas within a field of study (ARIA; CUCCURULLO, 2017; COBO et al., 2011; FESTAG; DENZLER; SPRECKELSEN, 2022; WALTMAN, 2016).

Among the main software used for bibliometric analysis and scientific mapping are VOSviewer (VAN ECK; WALTMAN, 2010, 2022), CiteSpace (CHEN, 2006), Bibliometrix (ARIA; CUCCURULLO, 2017), and Gephi (BASTIAN; HEYMANN; JACOMY, 2009). VOSviewer, for example, is widely recognized for its ability to create maps of citation and co-authorship networks, facilitating the identification of research clusters. CiteSpace is used to detect emerging trends and analyze the temporal development of scientific topics. Bibliometrix offers an integrated platform for performing statistical and visual analyses on bibliographic data and is highly flexible for customization. Gephi is a powerful tool for visualizing large data

networks, allowing in-depth analysis of the interactions and connections between different elements of research (HATTA et al., 2023).

VOSviewer was chosen for its ability to create maps of citation and co-authorship networks, facilitating the identification of research clusters and helping to visualize connections between authors. Bibliometrix was selected for its flexibility and capability to perform customized statistical and visual analyses on bibliographic data, providing a more detailed analysis tailored to the study's needs. This software plays a crucial role in conducting bibliometric studies, offering a comprehensive and structured view of the research field, enabling the identification of gaps, trends, and opportunities for collaboration.

6.4.3 Data analysis

The Proknow-C method (Knowledge Development Process - Constructivist), as proposed by Afonso et al. (2012), was used to select the publications related to the topic in question.

Keyword combinations were selected based on their relevance to the central theme of the research, covering the main concepts involved. Four specifications were considered: (i) AD (anaerobic digestion), to identify general studies on the process; (ii) ADM1 OR Anaerobic digestion model No.1, referring to the mathematical model widely used to simulate anaerobic digestion; (iii) dry anaerobic digestion OR high-solid OR solid-state, relevant as it is the specific focus of the study; and (iv) the type of waste, in this case, food waste OR fruit and vegetable waste OR FVW OR OFMSW OR FW, to ensure that the analysis was targeted at the relevant waste (Table 6.3).

The data for the articles were collected from the online database Web of Science Core Collection (WS), and the combination of queries is reported inTable 6.3 Table 6.3. The label TS [Title, Abstract, Keywords, and Keywords Plus] was considered. In other words, the specified keywords should be present in the mentioned items (title, abstract, keywords, and keywords plus), as these are the elements used to categorize the articles in the databases. By focusing on these fields, the search becomes more specific and targeted, ensuring that the results are highly relevant to the core themes of the research.

In the methodology, seven keyword combinations were defined for the Web of Science search, covering the four groups mentioned above: AD, ADM1, D-AD, and waste. Each combination represents a specific topic aimed at determining the number of publications

in their respective areas. The combinations are detailed in Table 6.3. The 1st combination refers to publications dealing with AD in general, encompassing all relevant works. The 2nd combination focuses on publications related to AD that specifically address the ADM1 model. The 3rd combination pertains to research on AD that investigates D-AD processes.

The 4th combination includes publications examining substrates such as FVW, FW, and the OFMSW. The 5th combination covers publications that study D-AD while also addressing the ADM1 model, i.e., those that apply or review the potential of the model in dry processes.

The 6th combination emphasizes the application of the ADM1 model in AD processes involving residues such as FVW, FW, and OFMSW. Finally, the 7th combination pertains to a more specific search within the WS, encompassing all publications addressing the D-AD of substrates such as FVW, FW, and OFMSW, alongside the application of the ADM1 model, thereby portraying the D-AD process, the FVW substrate, and ADM1 modeling.

Table 6.3 – Keywords Searched and Corresponding Number of Publications.

Nº	Keywords - TS	Number of publications	Period
1st	Anaerobic digestion	35,496	1947-2023
2nd	Anaerobic digestion **AND** (ADM1 **OR** Anaerobic Digestion Model No. 1)	492	2002-2023
3rd	Anaerobic digestion **AND** (dry anaerobic digestion **OR** high-solid **OR** solid-state)	4,418	1985-2023
4th	Anaerobic digestion **AND** (food waste **OR** fruit and vegetable waste **OR** FVW **OR** OFMSW **OR** FW)	6,751	1978-2023
5th	Anaerobic digestion **AND** (ADM1 **OR** Anaerobic Digestion Model No. 1) **AND** dry anaerobic digestion **OR** high-solid **OR** solid-state	46	2005-2023
6th	Anaerobic digestion **AND** (ADM1 **OR** Anaerobic Digestion Model No. 1) **AND** (food waste **OR** fruit and vegetable waste **OR** FVW **OR** OFMSW **OR** FW)	57	2009-2023
7th	Anaerobic digestion **AND** (ADM1 **OR** Anaerobic Digestion Model No. 1) **AND (**dry anaerobic digestion **OR** high-solid **OR** solid-state) **AND (**food waste **OR** fruit and vegetable waste **OR** organic fraction of municipal solid waste **OR** FVW **OR** OFMSW **OR** FW)	12	2011-2022

Next, duplicate documents are excluded, along with those whose title and/or abstract does not correspond to the research topic, those that are not fully accessible, and those that do not meet the previously established criteria. After creating the portfolios of bibliographic files, a bibliometric analysis was conducted to highlight the most relevant points. A systematic analysis was then performed, involving a detailed reading of the most specific articles and compiling the obtained data. Finally, gaps in knowledge on the subject were identified, and opportunities for future research were explored (ASSIS; GONÇALVES, 2022; VIEGAS et al., 2016).

The WS portfolios selected according to the keywords were extracted in BibTeX format and imported into the R Studio-Pro software. In the R Studio-Pro software, the data was processed and statistically analyzed using the R bibliometrix package (ARIA; CUCCURULLO, 2017; ASSIS; GONÇALVES, 2022; CIANO et al., 2019; DAIM et al., 2006; FRKOVA et al., 2020; VAN ECK; WALTMAN, 2010; ZENG; CHINI, 2017), processed in R-4.3.1. VOSviewer 1.6.20 (VAN ECK; WALTMAN, 2010, 2022) was used to generate some images and process some data, using the packages collected from the WS. The information was collected on June 20, 2023.

Between 1947 and 2023, 35,496 publications related to AD were identified in the SCI-Expanded network database (Table 6.3). Only 0.13% deal with D-AD modeling and 0.1% with FVW (OFMSW and FW) digestion. When comparing all possible combinations, only 12 publications addressed the application of ADM1 in D-AD processes of FVW (OFMSW and FW). These facts prove the need for further research to apply or adapt ADM1 to D-AD and FVW. Despite the small number of specific studies on ADM1 associated with D-AD of FVW (OFMSW and FW), there are other studies that apply it to different substrates that can help with the adjustments that need to be made in order to adapt to the substrate studied.

6.4.3.1 Publishing trend

The description of the anaerobic digestion of sewage sludge by Buswell (1947) was the first to discuss the chemical and biological reactions for this substrate in 1947. Later, Singleton et al. (1949) reported in 1949 on the possibility of treating industrial waste from Lebanon Woolen Mills. After these works, there was a reduced growth until 1976, when only seven works were reported. However, the apogee of research on AD was in 1991, with 150 publications, increasing considerably in later years. The period between 2019 and 2022 was the one with the highest number of publications on AD: 2,997 (2019), 3,494 (2020), 3,780 (2021), and 3,719 (2022).

With the publication of the ADM1 by Batstone et al (2002), research began applying the model in various situations, as well as conducting revisions to assess operational standards and studies of the substrate (waste). Since then, 492 publications have investigated ADM1, either by applying the model directly or by revising it to define the parameters and adjustments needed for specific processes and residues. In light of this, it is believed that the

number of publications applying ADM1 may be less than 492, as it involves different types of studies, including reviews, calibrations, modifications, and others.

Shortly after the publication of ADM1, several articles were released the following year, marking its practical application and solidification as a reference in anaerobic digestion modeling. The first study to address ADM1 (BATSTONE et al., 2002) was the publication by Batstone, Pind and Angelidaki (2003), which evaluated the validity of a common set of kinetic parameters and biological catalysts to model the degradation of butyrate, n-valerate, and i-valerate in protein-fed anaerobic systems, where these acids are byproducts of amino acid degradation. ADM1 was modified to account for the competitive uptake of i-valerate and applied to a thermophilic manure digester that operated for 180 days. The results showed that while butyrate and n-valerate could be modeled based on β-oxidation, i-valerate exhibited distinct kinetics, requiring adjustments to the model for accurate representation in systems predominantly fed leucine-rich proteins.

Batstone and Keller (2003) subsequently applied ADM1 to two case studies in industrial plants. In the first, the addition of acid to control pH and prevent calcium carbonate ($CaCO_3$) precipitation in a paper mill UASB reactor was evaluated, concluding that this practice was neither economical nor effective. In the second, thermophilic operation was analyzed in a solids digester at a gelatin factory to reduce ammonia inhibition and improve gas production, but the results showed that thermophilic conditions did not achieve these objectives satisfactorily. The study also evaluated the accuracy of the model's predictions.

After conducting three studies, the Egyptian researchers Elmitwalli et al. (2003a, 2003b) applied ADM1 in a system consisting of an anaerobic filter followed by a UASB reactor for the treatment of domestic wastewater in Egypt. Meanwhile, the Russian research team led by Fedorovich, Lens and Kalyuzhnyi (2003) utilized ADM1 in a sulfate reduction process in a UASB reactor.

Since the publication of ADM1 by Batstone et al. (2002), numerous studies have been conducted on the subject. Among the most cited are the works of Hagos et al. (2017),, with 410 citations; Abbassi-Guendouza et al. (2012),, with 269 citations; Mata-Alvarez et al. (2011), with 203 citations; Donoso-Bravo et al. (2011), with 196 citations; Jeppsson et al. (2007), with 184 citations; Curry and Pillay (2012), with 172 citations; Palatsi et al. (2010), with 161 citations; Blumensaat and Keller (2005), with 159 citations; and Van Lier et al. (2015), with 157 citations.

Among the studies on ADM1 is the work of Hagos et al. (2017), who reviewed the co-digestion process and attempted to use ADM1 as a tool for optimizing it, despite its limitations, particularly in relation to disintegration and hydrolysis. To improve efficiency in these stages, it is essential to evaluate the degree of biodegradability, substrate composition, particle size, and the dose of the alkalizing agent, as biogas production is often constrained by these factors. The key points of the publication focus on substrate optimization, highlighting that ADM1 facilitates the selection of combinations that enhance biogas production. Furthermore, the model enables performance prediction, identifying critical conditions that affect anaerobic digestion and emphasizing the synergistic interactions that can be amplified through co-digestion, promoting the interaction between different types of waste.

Abbassi-Guendouz et al. (2012) investigate the impact of TS content on anaerobic digestion, using different TS concentrations in batch reactors and the ADM1 model to describe the experimental data. The study focuses on methane production and analyzes the effects of mass transfer and the hydrolysis stage at high TS contents.

The first studies on the application of ADM1 in D-AD systems appeared in 2005. Since then, as of the date of this study, only 46 studies have been published on the subject (Table 6.3). Among the most cited are Abbassi-Guendouz et al. (2012) and Mata-Alvarez et al. (2011), with 260 and 203 citations, respectively. The study by Mata-Alvarez et al. (2011) conducted an important review of the models applicable to solid waste co-digestion processes, highlighting ADM1 as one of the primary models used in this field, thereby contributing to its consolidation in anaerobic digestion research.

Before the increase in AD studies, research on D-AD had already been initiated. However, manuscripts addressing the application of ADM1 in D-AD are few. Kalfas et al. (2006) published in 2006 the first work on applying ADM1 in D-AD of olive pulp with TS of approximately 30% in a CSTR. Bollon et al. (2011) proposed in 2011 a kinetic model based on ADM1 designed to include various aspects of dry digestion, such as particulate matter and high solids content, specifically for OFMSW. Then Zhou et al. (2012) proposed in 2012 a modified ADM1 comparing different types of substrates in mono- and co-digestion (manure, corn silage, municipal solid waste bio-waste, and sewage treatment plant sludge).

The first studies applying ADM1 to substrates such as FW, FVW, and OFMSW emerged in 2009, with the study by Zaher et al. (2009). This pioneering work conducted a preliminary analysis to adapt ADM1, performing prior studies to determine the model's input parameters. This was essential for adjusting ADM1 to the specific characteristics of the

substrate being studied, with a particular focus on OFMSW. There is a total of 47 publications examining the indicated substrates.

The main objective of this research is to evaluate and identify studies that apply the ADM1 model to the D-AD of FVW and related substrates. Table 6.4 presents the 12 publications identified using the terms ADM1, D-AD, and FW. The model is indicated along with any modifications or adaptations made to the ADM1, followed by the adopted process—whether monodigestion, codigestion, or two-stage digestion—and the substrate, listing all those with characteristics similar to the substrates studied.

The 12 publications resulting from the search were analyzed, and the necessary information was extracted. Based on this, they were organized into a table (Table 6.4) divided into four sections: (i) ADM1 applied without substantial changes, (ii) Modifications to ADM1, (iii) Models developed based on ADM1, and (iv) Reviews of ADM1 under the proposed conditions. As noted, no other study has conducted the survey and analysis presented in this paper.

The publication with the highest number of citations is by Mata-Alvarez et al. (2011), published in 2011. The study provides a comprehensive review of co-digestion system modeling, highlighting its key contributions to enhancing and understanding this process, with a particular focus on the nutritional balance and system stability achieved through the combination of different types of solid waste. The publication emphasizes that the ADM1 model is applicable to modeling various processes, including co-digestion. Additionally, the authors address the limitations and necessary adaptations of the model, expressing concerns about the accuracy of the results obtained in co-digestion systems. The article also discusses the importance of integrating experimental data into modeling and its impact on the development of effective waste management policies.

Bedoić et al. (2019) applied the ADM1 model to simulate the process, identifying specific kinetic parameters for grass degradation. Co-digestion with maize silage and cattle slurry enhanced process stability, preventing acidification. The findings suggest that using waste grass, as modeled by ADM1, provides environmental advantages over maize silage, particularly in terms of ecosystem quality

Table 6.4 – 12 Publications Associated with ADM1, D-AD, and FW (including FVW, OFMSW, and related substrates.

Model	Process	Substrate	Reference	TC	Year
(i) ADM1 applied					
Reaction kinetics	D-AD – two-stage	OFMSW	Yu et al. (2012)	23	2012
Estimate biogas production	AcoD	Waste grass	Bedoić et al. (2019)	61	2019
Investigate the relationship between population dynamics and reactor stability (OLR variation)	D-AD	RW, MRW, and VW	Gilvin et al. (2020)	13	2020
Nutrient recovery and comparison with two empirical models (BMP model and first-order model) to obtain transfer coefficients.	D-AD	OFMSW (FW-V, FW-A and GW)	Urtnowski-Morin et al. (2021)	5	2021
(ii) Modified ADM1					
Evaluate DIET performance in methane production and stability and microbial population dynamics and evaluate DIET contribution in methane production. Main modifications: Ignored: Decay rate ($k_{d,j}$) and the inhibition by ammonia. Incorporated: Extracellular electron mediators. Incorporated variables: Specific substrate degradation rate ($k_{m,j}$) and saturation coefficient ($K_{s,j}$).	D-AD	FW	Li et al. (2022)	6	2022
For complex organic substrates. Main modifications: Includes the parameter k_{sbk} depending on the TS, nature, and composition of the substrate, k_{ac}, and k_{pro}. Evaluates the influence of TS content on substrate disintegration rate and acetate and propionate uptake. Considers the variation of the kinetic constants (k_{sbk}, k_{ac} and k_{pro}).	D-AD and SD-AD	FW and RS	Liotta et al. (2015)	27	2015
Simulates anaerobic digestion of FW – acetate consumption and FAN estimate. Main modifications: Included: Applied SAO with Monod kinetics. Quantification of FAN (Modified Davies Equation - considering pH, temperature, and ionic strength of the medium, introduced to an activity coefficient (f) with correction factor in the equation). FAN inhibition function in methanogenic archaea. Another modification: Decoupled butyrate and valerate uptake and added to a new group of bacteria responsible for valerate uptake (X_{c5}), X_{c4} was responsible for butyrate uptake in ADM1 the X_{c4} consumes butyrate and valerate.	D-AD	FW	Capson-Tojo et al. (2021)	6	2021
(iii) ADM1 based					
Development of a model based on ADM1.	D-AD	OFMSW	Pastor-Poquet et al. (2018)	31	2018
Development of a model based on ADM1.	D-AD	OFMSW	Pastor-Poquet et al. (2019a)	5	2019
Development of a kinetic model based on ADM1.	D-AD	OFMSW	Bollon et al. (2011)	50	2011
(iv) Others					
Review: Application of the ADM1 in the AcoD of OFMSW and MSW.	AcoD	MSW	Mata-Alvarez et al. (2011)	203	2011

Note: D-AD – Dry anaerobic digestion, MSW – Municipal Solid Waste, FW-V – Food waste vegetable, FW-A – Food waste animal, GW – Green waste, RW – Rice waste, MRW – Mixed rice waste, VW – Vegetable waste, RS – Rice straw, DIET – direct interspecies electron transfer, BMP – Biochemical methane potential, FAN – free ammonia nitrogen, SAO – Syntrophic acetate oxidation. Riya et al. (2018) do not directly address ADM1 by applying or reviewing. TC – Total Citation..

Bollon et al. (2011) developed a kinetic model based on ADM1, modified to account for the specific characteristics of dry anaerobic digestion, such as the presence of particulate matter and high solids content. The model was calibrated using experimental data on methane production from acetate under dry mesophilic conditions. The fitted kinetic parameters include the maximum rate of acetate consumption ($k_m X_{ac}$ = 440 mgCOD kg^{-1} d^{-1}) and the half-saturation constant (k_s), which increased significantly in dry digestion, suggesting diffusion limitations due to the 'pasty' nature of the medium.

Pastor-Poquet et al. (2018) developed a modeling tool to simulate the D-AD of OFMSW. The model was adapted to capture the dynamics of TS removal and changes in reactor mass/volume, which are specific to D-AD. It accurately simulated the evolution of TS, reactor mass, ammonia, and volatile fatty acids, providing insights into inhibitory mechanisms such as NH_3 accumulation and acidification, both typical of D-AD

Liotta et al. (2015) modified ADM1 to investigate the effect of TS content on the anaerobic digestion of complex organic materials, such as rice straw and food waste, with TS levels ranging from 4.5% to 23%. The model incorporated a linear function to relate the kinetic constants of disintegration, acetate uptake, and propionate uptake. Biomethanation and volatile fatty acid production tests were used to calibrate the model, which showed good agreement between the numerical and observed data

Yu et al. (2012) developed a model for a two-stage D-AD system focused on OFMSW. The D-AD reactor was divided into two zones: the upper part retained the solid waste, while the lower part contained the liquid. CSTR and advective-diffusive (ADR) models were integrated, with ADM1 used to describe the reaction kinetics. The model accurately predicted pH, VFA, and biogas production based on experimental data. Other studies have also been conducted, including those by Gilvin et al. (2020), Li et al. (2022), Capson-Tojo et al. (2021), Urtnowski-Morin et al. (2021), and Pastor-Poquet et al. (2019a).

6.4.3.2 Contributions of countries and institutions

Of the 492 publications associating AD with ADM1, 11.59%, or 57 papers, were produced by Chinese institutions (Table 6.5). Of these, 37 were exclusive to China, while 20 were in collaboration with other countries. A similar pattern is observed in Germany, which published 49 papers, 40 of which were exclusively from German institutions, and 9 involved external contributions. By refining the search, 12 publications were identified that associate

ADM1 with the D-AD of FVW. Of these, 6 were produced by Chinese institutions, with 4 being exclusively from China and 2 in collaboration with other countries. Italy and the United Kingdom followed, each with five publications. These results also highlight the importance of international collaborations in scientific research.

Of all the publications addressing AD, 1,011 (2.8%) are affiliated with the Chinese Academy of Sciences. However, when dealing with the application of ADM1 in AD, Lund University was responsible for the majority (5.9%); the University of Cassino and Southern Lazio accounted for 33.3% of the publications concerning the application of ADM1 in D-AD of FW. Through this information, most of the publications concerning AD are from Chinese institutions, despite the reduced amount of work that addresses the application of ADM1 in dry processes.

Table 6.5 – Top 10 Most Productive Countries in AD (1947–2023) and Top 10 Most Productive Institutions (2011–2023)

	2nd combination							
Rank	**Most Relevant Countries**						**Most Relevant Affiliations**	
	Country	Articles	SCP	MCP	Freq	MCP Ratio	Affiliation	Articles
1	China	57	37	20	0.116	0.351	Lund University	29
2	Germany	49	40	9	0.100	0.184	Technical University of Denmark	27
3	France	36	25	11	0.073	0.306	University of Queensland	26
4	Spain	36	20	16	0.073	0.444	University of Ghent	23
5	Italy	31	17	14	0.063	0.452	University of Naples Federico II	23
6	Canada	21	16	5	0.043	0.238	Delft University of Technology	20
7	USA	20	14	6	0.041	0.300	University Science and Technol China	20
8	Belgium	17	5	12	0.035	0.706	University of Santiago de Compostela	19
9	Denmark	14	3	11	0.028	0.786	Beijing University of Chemical Technol	16
10	Greece	14	12	2	0.028	0.143	University of Cassino and Southern Lazio	15
	7th combination							
Rank	**Most Relevant Countries**						**Most Relevant Affiliations**	
	Country	Articles	SCP	MCP	Freq	MCP Ratio	Affiliation	Articles
1	China	6	4	2	0.105	0.333	University of Cassino and Southern Lazio	4
2	Italy	5	2	3	0.088	0.600	University of Barcelona	3
3	United Kingdom	5	3	2	0.088	0.400	Marian Engineering College	2
4	Greece	4	4	0	0.070	0.000	Polytech Montreal	2
5	Japan	4	1	3	0.070	0.750	School Environment and Information Science	2
6	Canada	3	3	0	0.053	0.000	Tokyo University of Agriculture and Technology	2
7	India	3	1	2	0.053	0.667	University of Cassino	2
8	Spain	3	3	0	0.053	0.000	University of Lyon	2
9	Australia	2	0	2	0.035	1.000	University of Montpellier	2
10	Colombia	2	0	2	0.035	1.000	University of Naples Federico II	2

Note: SCP – Single Country Publications; MCP – Multiple Country Publications.

6.4.3.3 Research trends and hot spots: keyword analysis

The bibliometric network can be graphically modeled and visualized. The data generated during the search can be incorporated into the Bibliometrix routine using the R language, making it possible to identify interactions between the most recurrent words, as well as the central thematic axis of the research (ARIA; CUCCURULLO, 2017). The data was applied to VOSviewer 1.6.20 (VAN ECK; WALTMAN, 2010, 2022) developed in Java, generating Figure 6.1 showing the network of keywords recurring in the survey, using the Kamada-Kawai layout (KAMADA; KAWAI, 1989). The network was built with 36 vertices, using a minimum recurrence of 20 words. Given that the total number of publications is 492, the choice of a minimum recurrence of 20 is recommended in order to focus on the most relevant publications, reducing the set to the main ones (AGBO et al., 2021; PASSAS, 2024; ULLAH; ASGHAR; GRIFFITHS, 2022; WANG et al., 2022a, 2022b).

Keywords bring together and represent the main points and objectives of research, and can summarize key directions for future studies (WANG et al., 2022c). Hot spots and trends in a research field are reflected in the frequency of specific terms. The analysis of keyword networks in publications indexed in the Web of Science enabled the identification of the main research themes and their interconnections. Figure 6.1 illustrates these correlations, where each node represents a keyword, and the lines indicate connections between them. The size of the nodes and lines reflects the strength of relationships and the frequency of term occurrence. This visualization highlights both central and emerging concepts in the field, providing a clear understanding of research dynamics and collaborations, as well as identifying trends and areas of greatest impact.

Thus, considering the total set of 492 publications related to AD and ADM1, 406 publications include 'ADM1' in their keywords, followed by 'AD' (anaerobic digestion) with 313, 'biogas' with 137, 'co-digestion' with 101, 'modeling' with 94, 'methane' with 82, and 'mathematical model' with 78. This data highlights the growing trend of co-digestion, which is evident not only in the numbers but also visually in Figure 6.1, where the topic stands out as one of the most recent (in yellow).

The recurrence of keywords related to vegetable/food waste is relatively low, as shown in Figure 6.1, where, despite the lower number of publications, the topic appears as more recent. Additionally, its connection to mathematical modeling and ADM1 is limited, suggesting significant potential for research to address these gaps. A similar pattern is observed in relation

to D-AD, as highlighted in Table 6.3, where the scarcity of studies applying ADM1 to D-AD of FVW and related topics is evident, indicating another promising area for investigation and the development of relevant research.

Figure 6.1 – Network of keywords in publications indexed in the Web of Science, with a gradient of colors representing the period of publication (Blue → Yellow indicates Old → Recent). For interpretation of the colors, see the web version of this article.

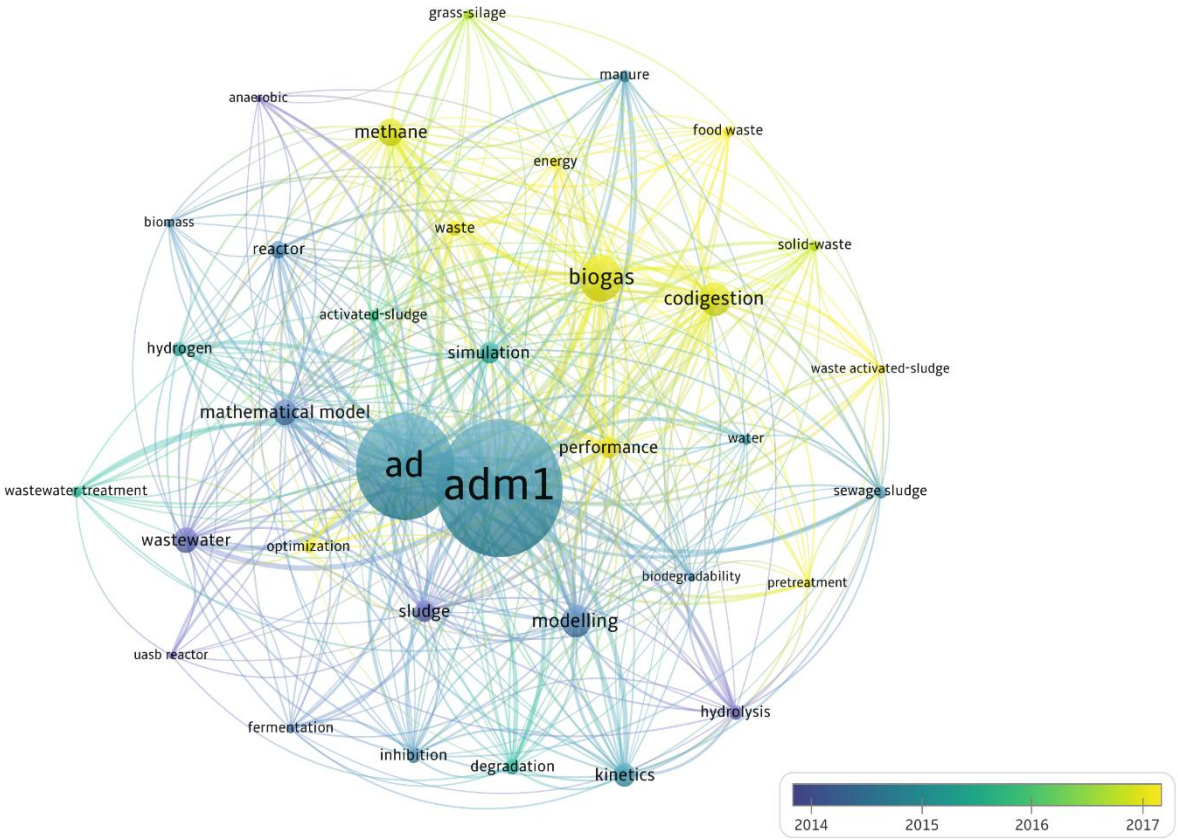

These observations indicate not only under-explored areas but also strategic opportunities to expand knowledge and advance research in these fields. With the growing demand for sustainable and efficient solutions, addressing these gaps could lead to significant advances in the understanding and application of anaerobic digestion, particularly regarding the use of plant-based waste and mathematical modeling using ADM1.

6.5 Models for simulating anaerobic digestion processes

The AD process involves an interplay between the kinetic processes of biochemical and hydrodynamic, both of which are linked to the energy transport of feedstock for biogas

production (LI et al., 2023). Over the past three decades, mathematical modeling has been employed in biological system processes such as AD for prediction, optimization, control, and real-time process monitoring (KHAN et al., 2023). This approach helps in exploring phenomena occurring during various processes in hypothetical scenarios and predict which compounds are produced or consumed, as well as their respective rates (PONTES; PINTO, 2006).

Bioprocess modeling represents the physical, chemical, and biological processes that occur within the reactor (SPYRIDONIDIS et al., 2018), assisting in the selection and optimization of process parameters that influence the recovery of by-products, such as pH, VFA, temperature, alkalinity, and organic loading rate (ABUBACKAR et al., 2019; HAGOS et al., 2017; MANJUSHA; BEEVI, 2016; SPYRIDONIDIS et al., 2018; XU; LI; WANG, 2015). The production of methane and hydrogen involves different types of biomass through biochemical processes, with the combined action of various microorganisms that metabolize organic substrates into gaseous and liquid compounds (KUCHARSKA et al., 2018). Moreover, bioprocess modeling has the potential to reveal the non-linear behavior of the system and quantify the performance of alternative operating configurations (KOTHARI et al., 2014). However, the literature is limited in discussing modeling approaches in the D-AD process of FW, FVW, or OFMSW.

The operation of D-AD is generally carried out empirically, and there is a demand for the development of tools that assist operations in achieving an optimal level of performance (LINDMARK et al., 2012). Typically, experimental studies are time-consuming and require human resources. Mathematical models emerge as tools to enhance the process by better explaining and representing the mechanisms and understanding the effects and interactions of different parameters, operating conditions, variations in input conditions (substrate conditions), and other factors such as perturbations (XU; LI; WANG, 2015).

Brito-Espino et al. (2020) report that the main models applied in AD processes are categorized into three different methodologies: (1) black-box models, which consider only the relationships between input and output variables; (2) gray-box models, which are mechanistic models that have parameters with physical interpretations that can be adjusted; and (3) white-box models, which are the most complex models based on fundamental principles and a deep understanding of the system's physical and chemical processes (ASADI; MCPHEDRAN, 2021; HU et al., 2018; LAUWERS et al., 2013; REGMI et al., 2019; YETILMEZSOY et al., 2021).

White-box dynamic models are mechanically inspired models that aim to accurately describe the dynamic processes occurring during digestion. This requires measurements of the main system components, resulting in a set of variables derived from a combination of different components (LAUWERS et al., 2013).

Since D-AD of OFMSW, FW, and FVW is a complex process, many variables are associated with various equations. Lauwers et al. (2013) reported a wide variety of carbohydrates, proteins and amino acids, fats, LCFA, VFA, alcohols, esters, and aldehydes, that must be defined as important reaction components and pathways.

Given the various existing models disseminated in the literature, this work is focuses on ADM1, which has attracted significant attention from the scientific community involved in anaerobic digestion. This interest stems from its wide applicability and flexibility in restructuring and adapting the model. ADM1 is a structured model that describes the biochemical and physicochemical processes of AD. The model is detailed by Batstone et al. (2002) and considers components, processes, stoichiometric coefficients, kinetic expressions, and relevant parameters, all incorporated into a Petersen matrix that quantitatively describes AD processes (MO et al., 2023).

6.5.1 ADM1

The existence of several models published in the literature indicates a need to consolidate and converge a set of studies into a framework with broad applicability. In response to this, the "IWA Task Group on Mathematical Modeling of Anaerobic Digestion Processes" developed the ADM1 as a unified basis for modeling the AD process. Among the models, ADM1 is characterized as a mechanistic or white-box model (BATSTONE et al., 2002). Lauwers et al. (2013) state that the term ADM1 is derived from Activated Sludge Models (ASM1, ASM2, and ASM3) (HENZE et al., 2015) and ADM1 is available for use for Matlab and Simulink (HAGOS et al., 2017; LÜBKEN et al., 2007), Aspen Plus (LOPES et al., 2018), and other water-related software such as Aquasim (CHEN et al., 2016; LAUWERS et al., 2013; LOHANI et al., 2016; ZHAO et al., 2019b).

After its publication, ADM1 was also used to simulate AD from a variety of substrates, including: grass silage (KOCH et al., 2010), maize silage (LÜBKEN et al., 2015b), dog food and flour (LEE et al., 2009), pretreated waste-activated sludge (RAMIREZ et al., 2009), sugarcane vinasse (ELAIUY et al., 2018), *Hydrilla verticillata* (CHEN et al., 2016),

swine manure (JURADO et al., 2016), domestic wastewater (LOHANI et al., 2016), food waste (CAPSON-TOJO; ASTALS; ROBLES, 2021; FRUNZO et al., 2019; LI et al., 2022), solid organic waste (food waste and green waste) (POGGIO et al., 2016), thermally pretreated waste activated sludge (RAMIREZ et al., 2009), OFMSW (PASTOR-POQUET et al., 2019b), and Food Industry Waste (FIW) (ALEXANDROPOULOU; ANTONOPOULOU; LYBERATOS, 2016).

Modifications were made to address other substrates and processes, including adjustments to the structure and kinetic parameters of the original model (CHEN et al., 2016; FEZZANI; BEN CHEIKH, 2008; HASSAM et al., 2015; LI et al., 2019; WEINRICH et al., 2021; XU; LI; WANG, 2015; ZHANG; PICCARD; ZHOU, 2015; ZHAO et al., 2019b; ZHOU et al., 2009). Despite the great model complexity, the reliability of the model is primarily influenced by the various parameters used that make the model reliable (FORTELA et al., 2019). The model has been applied in multiple areas, such as simulating cattle manure's energy production, which demanded a modification (LÜBKEN et al., 2007). ADM1 also describes the conversion of complex organic compounds to methane, simulating the main biochemical and physicochemical processes related to the liquid and gaseous phases (FRUNZO et al., 2019; ZHANG; PICCARD; ZHOU, 2015).

ADM1 can also be applied to digestion processes for hydrogen production (ALEXANDROPOULOU; ANTONOPOULOU; LYBERATOS, 2016; KOCH et al., 2010). Peiris et al. (2006) used it to simulate hydrogen production from various substrates, with modifications made to adapt the model to meet the process conditions. Penumathsa et al. (2009) proposed modifying ADM1 using a variable stoichiometric approach based on experimental data. Hierholtzer et al. (2012) used it to determine and simulate the sodium inhibition process, incorporating an additional function to account for the effect of sodium.

The ADM1 offers several advantages, as a mechanistic model that allows several applications and adaptations. However, some limitations persist, such as improved practicality, detailed substrate characterization, and the conversion and distribution of some elements (XIE et al., 2016). The model requires physicochemical data (biochemical composition, i.e., carbohydrates, proteins, and lipids) (ZHAO et al., 2019a). More detailed inflow characterization demand a large number of additional parameters, e.g., hemicellulose, cellulose, and lignin contents (LÜBKEN et al., 2015a; ZHAO et al., 2019b). Generally, these processes also have limiting steps that restrict their kinetics. Given the complexity of digestion, the

limiting step will sometimes differ depending on the substrate characteristics, the applied hydraulic load, temperature, pH, C/N ratio, and others.

The model also incorporates the integration of liquid-liquid and gas-liquid physicochemical processes. The default mass basis is kilograms of chemical oxygen demand (kg COD), the volume basis is in cubic meters (m^3), and the time basis is in days (d) (BATSTONE et al., 2002; FORTELA et al., 2019).

ADM1 is a model that utilizes a Petersen matrix comprising 24 components (12 particulate components, (Xi), and 12 soluble components (Si)), along with12 components for ion states and gases (CH_4, CO_2 and H_2), defined both the initial and final concentration of the process (BATSTONE et al., 2002; XIE et al., 2016). In the matrix, these components intersect with 19 biochemical processes, which are organized into four equations that capture the degradation of particulate matter (disintegration, hydrolysis of carbohydrates, proteins, and lipids), 8 equations that describe the degradation of soluble matter (absorption of sugars, amino acids, LCFA , valerate, butyrate, propionate, acetate and hydrogen) and 7 equations that represent the biomass concentration (Decay of X_{su}, X_{aa}, X_{fa}, X_{c4}, X_{pro}, X_{ac}, and X_{h2}). Biochemical processes are associated with 80 kinetic and mass transfer parameters (BATSTONE et al., 2002; BOUTOUTE et al., 2021). Additionally, the model also considers 6 acid/base balances related to pH calculation (NH_4^+/NH_3 [pKa = 9.25], CO_2/HCO_3 [pKa = 6.35] and VFA/VFA^- [pKa~4.8]); as well as 3 gas-liquid transfer processes (CH_4 – low solubility, CO_2 – medium solubility, H_2 – low solubility) and inhibitions.

Two steps are required to implement the model: (i) define the substrate composition based on the input state variables, and (ii) the calibration process (specific methodologies related to substrate and technology have been addressed in the literature (AHMED; RODRIGUEZ, 2018; COUTO et al., 2019; DAELS et al., 2009; NABATEREGA; NAZYAB; ESKICIOGLU, 2023)).

The COD in the model input consists of 13 components, 11 of which are biodegradable. They are: (i) composite substrate (X_c); (ii) polymers: carbohydrate (X_{ch}), protein (X_{pr}) and lipid (X_{li}); (iii) monomers: sugars (S_{su}), amino acids (S_{aa}) and long chain fatty acids (S_{fa}); (iv) VFAs: acetate (S_{ac}), propionate (S_{pro}), butyrate (S_{bu}) and valerate (S_{va}); (v) inert COD: soluble fraction (S_i) and particulate fraction (X_i).

Figure 6.2 illustrates how the components and their by-products, associated with the processes depicted in the Petersen matrix, are generated. The five phases of AD are shown, with the processes occurring between these phases organized to relate the production and

consumption of products. This organization allows for a clear visualization of how each stage benefits from the compounds produced in previous steps. It is important to note that methane production depends on the availability of acetate and hydrogen, which are influenced by earlier stages and specific compounds. Thus, the diagram facilitates an understanding of the interactions between the processes and how these relationships are represented within the model.

Figure 6.2 also presents the schematic of the biochemical reactions according to the model, which includes: (i) extracellular disintegration step and the conversion of the composite particulate material into carbohydrates, lipids, proteins, and inert compounds is converted, (ii) extracellular enzymatic hydrolysis step, the conversion of the degradation products into their chemical building blocks, such as, monosaccharides, LCFA and amino acids (AA), (iii) acidogenesis or fermentation of the building blocks to hydrogen, acetate and VFA, including propionate, butyrate, and valerate, (iv) acetogenesis of VFA to acetate, and (v) acetoclastic and hydrogenotrophic methanogenesis (BATSTONE et al., 2002; LAUWERS et al., 2013).

Figure 6.2 – Reaction Pathways Described in the ADM1 Model.

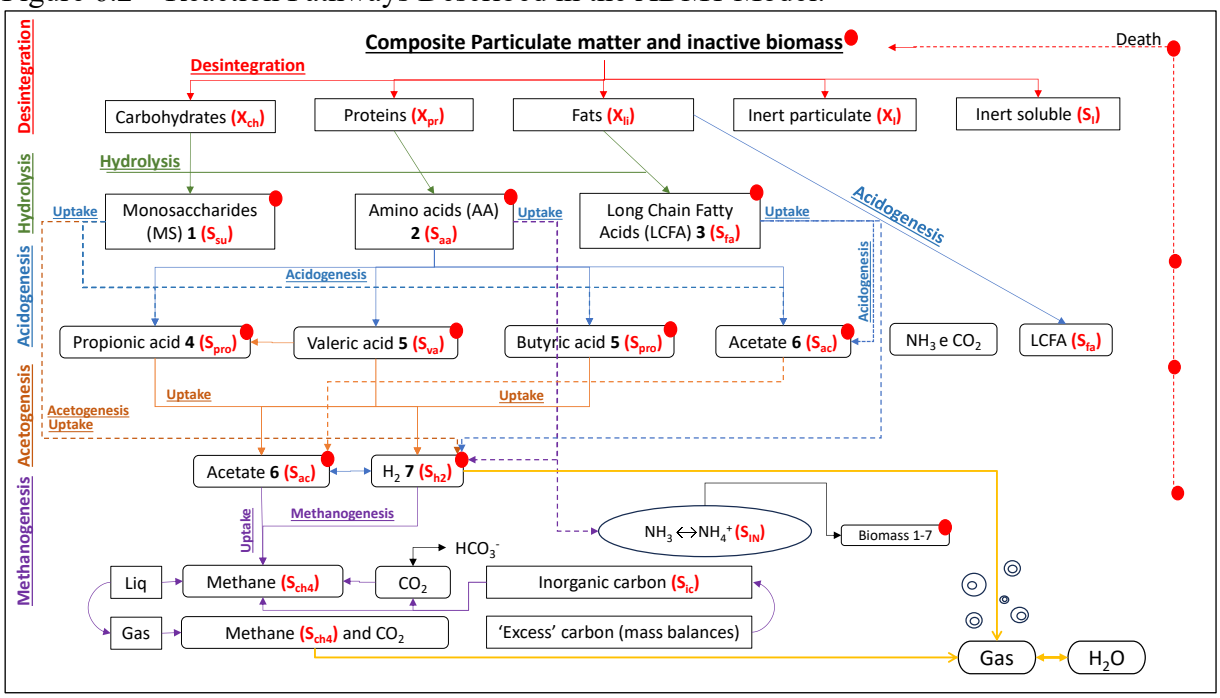

Data: Adapted from Batstone et al. (2002) and Lauwers et al. (2013).
Note: with the following microbial groups: (1) sugar degraders, (2) amino acid degraders, (3) LCFA degraders, (4) propionic acid degraders, (5) butyric and valeric acid degraders, (6) acetoclastic methanogens, and (7) hydrogenotrophic methanogen.

The kinetic study demonstrates the evolution of substrates, products, and microbial groups over time. The kinetics of a given process depict the growth rate of microorganisms, the rate of substrate utilization, and the rate of by-product formation. Several factors can influence the growth of microorganisms: type of substrate, nutrient concentration, medium composition, type of final electron acceptor, pH, temperature, and the presence of inhibitory substances.

The growth of microorganisms is divided into four phases: adaptation (lag), logarithmic growth, stationary, and endogenous (decay). The most critical phase for microorganisms is the logarithmic growth phase. The models are structured around three variables: substrate concentration, microorganism concentration, and elapsed time. Many researchers have developed kinetic expressions to characterize the rate of the metabolic reactions involved in the biological processes.

Myint et al. (2007) highlight out that in the early studies of anaerobic hydrolysis, first-order kinetics were assumed for acidogenic biomass (HILL; BARTH, 1977), after which second-order kinetics were assumed for acidogenic biomass concentration and VS concentration (NOYKOVA et al., 2002). In the Contois kinetic model, the hydrolysis rate decreases when biomass concentration is high. Munch et al. (1999) emphasize that this is due to the limited surface area, which reduces mass transfer. The hydrolysis rate was proposed considering the concentration of particles relative to the concentration of hydrolytic enzymes, called a surface-limited reaction, with a maximum hydrolysis rate. Based on this, the most common hydrolysis models are first-order, second-order, and surface-limiting reaction models.

According to Batstone et al. (2002) and Vavilin et al. (2008), hydrolysis can be represented by two models Vavilin et al. (2008): a) particles adsorb enzymes secreted by microorganisms or react with the soluble substrate; b) microorganisms adhere to the particle surface and produce enzymes, benefiting from the soluble products released. Michaelis-Menten kinetics can be applied for the hydrolysis of soluble substrates (Eq. [6.1]).

$$\frac{dS}{dt} = k.E\frac{S}{K_m + S} = V_m\frac{S}{K_m + S'} \qquad [6.1]$$

According to Vavilin et al. (2008), S and E represent the substrate and enzyme concentrations, respectively. $V_m = kE$ is the maximum hydrolysis rate, k is the maximum hydrolysis rate constant, and K_m is the half-saturation coefficient.

Extracellular biochemical steps follow first-order kinetics, intracellular biochemical reactions adhere to Monod-type kinetics for substrate uptake, accompanied by

biomass growth, and biomass death is first-order kinetics (dead biomass - composted particulate matter). The inhibition of biological activity due to pH (affecting all groups), hydrogen (acetogenesis), and free ammonia (acetoclastic methanogenesis) is also considered. Inorganic carbon and nitrogen, i.e., CO_2, HCO_3^-, NH_3, NH_4^+, act as source-drain terms and effectively close the mass balance for C and N (BATSTONE et al., 2002; LAUWERS et al., 2013).

ADM1 processes can be implemented as ordinary differential equations (ODEs) and/or algebraic differential equations (ADEs) (LAUWERS et al., 2013; ROSEN; JEPPSSON, 2006a), Equations 2 and 3 Adapted from Esposito et al. (2011a). Among them, 2 ODEs are intended for cations and anions, 3 ODEs for CH_4, H_2 and CO_2 in the vapor phase, 12 ODEs for CH_4, H_2, carbohydrates, lipids, amino acids, valeric acid, butyric acid, propionic acid, acetic acid, inorganic carbon and nitrogen and soluble inert components, 4 ODEs are dedicated to particulate matter and its lipids, proteins, carbohydrates and inert contents, 7 ODEs to the microbial groups: sugar degraders, amino acid degraders, fatty acid degraders, butyrate/valerate degraders, propionate degraders and acetoclastic and hydrogenotrophic methanogens. It also includes an algebraic equation (AE), which can also express the biogas hydrogen content (Eq.[6.2]).

$$\frac{dS}{dt} = \frac{q}{V_{liq}}(S_{in} - S) \sum\nolimits_{j=1\ldots n} \rho_j v_j \qquad [6.2]$$

Where: S is the substrate concentration [M L^{-3}]; q is the influent flowrate [L^3 T^{-1}]; V_{liq} is the liquid working volume of the anaerobic digester [L^3]; S_{in} is the substrate concentration in the digester influent [M L^{-3}]; ρ_j is the specific kinetic rate for process j involving the specific gas [L^{-3} T^{-1}]; v_j is the biochemical rate coefficient for process j involving the specific gas [M L^{-3} T^{-1}].

$$\frac{d[S]_{gas}}{dt} = \frac{V_{liq}}{V_{gas}} k_{La}([S]_l - [S^*]_l) - (Q_{out,g}/V_{gas})[S]_{g;} \qquad [6.3]$$

Where: $[S]_{(gas)}$ is the molar concentration of the specific gas in gaseous phase [L^{-3}]; $[S]_{(l)}$ is the molar concentration of the specific gas in aqueous phase [L^{-3}]; $[S^*]_{(l)}$ is the molar concentration of the specific gas in the aqueous bulk of the reactor at thermodynamic equilibrium [L^{-3}]; V_{gas} is the volume of the digester headspace [L^3]; k_{La} is the global transfer

coefficient of the specific gas [T^{-1}]; $Q_{out,g}$ is the total effluent gas flowrate from the digester [L^3 T^{-1}]; $[S]_g$ is the molar concentration of the specific gas in the gaseous phase [L^{-3}].

Initially, ADM1 was used to model methane production from sewage sludge fermentation (BUŁKOWSKA et al., 2018; CHEN et al., 2016; ZHAO et al., 2019b). The model considers a substrate with X_c particles in a CSTR; research shows that ADM1 accurately simulates the AD of sewage sludge (SIEGRIST et al., 2002; SOUZA et al., 2013).

Therefore, the model in its original structure is unsuitable for AD of some organic solid waste without adaptations and the process conditions. According to Zhao et al. (2019), ADM1 ignores the differences between the substrates and inoculum used in the AD of FVW, FW, and OFMSW; unlike sludge, the substrates mentioned are more granular and have a higher content of carbohydrates and fats (SOUZA et al., 2013; ZHAO et al., 2019b). The kinetic equations are also affected by the TS content, which is affected by the intermediate compounds throughout the process (LIOTTA et al., 2015).

In the case of D-AD, adaptations need to be made, as high-solid content substrates lead to a decreased first-order hydrolysis rate (JURADO et al., 2016) and gas and mass transfer (MO et al., 2023). At such conditions, the substrate has a lower fluidity, and the value of the liquid/gas mass transfer coefficient (k_L) must be reduced Abbassi-Guendouz et al. (2012) report that, in order to meet the substrate standards, the k_L value was reduced from 200 d^{-1} (standard for W-AD) to 0.5 d^{-1} (for D-AD). Given this, the process applied, and the substrate used in D-AD must be considered.

6.5.1.1 Modifications in ADM1

As previously described, ADM1's structure was already designed for further adjustments to meet certain characteristics of substrates and technologies. This demonstrates its versatility, which allowed for several model adaptations.

The main modifications to ADM1 pertain to the structuring of the substrate characteristics input, which generally varies according to its composition. Differences in composition affect the rate of disintegration and hydrolysis processes, which are adjusted by various authors (RAMIREZ et al., 2009). In addition to changes in the applied first-order equations suggested by some authors, these adjustments can be made based on the substrate's characteristics.

Li et al. (2021) applied ADM1 for vegetable crop residues (VCR), considering the fractionation of crystalline cellulose (CrC). Modifications were made to the model to meet the specifications proposed for the residue, considering the specificity of biodegradability and microstructures of the various substrates. Vegetable crop substrates contain a significant amount of lignocellulosic biomass in their composition, with a high proportion of CrC, which slows down the hydrolysis process. ADM1 is based on the degradation rate rather than the type of organic component, where the model accounts for the disintegration of components followed by hydrolysis. Therefore, it is necessary to segregate the parcels to account for lignocellulosic biomass.

The modifications proposed by Li et al. (2021) were based on the separation of the disintegration and hydrolysis processes into distinct stages, as well as on a revision of the bacterial growth kinetic equations. For a proper understanding, it is important to recognize that ADM1 encompasses 19 processes, with the initial ones including the disintegration and hydrolysis of carbohydrates, lipids, and proteins. The primary objective of the modifications made by Li et al. was to enhance the model's accuracy

On this basis, hydrolysis was divided into two portions: readily hydrolysis fraction (RHF) consisting of portions of carbohydrates (X_{ch}) and proteins (X_{pr}) due to their rapid degradation, while disregarding the reduced lipid content. They postulated cellulose to be a blend of CrC and amorphous cellulose (AmC). Consequently, the AmC and hemicellulose fractions were integrated into the slowly hydrolysis fraction (SHF), whereas lignin and CrC were categorized as inert fractions. Cellulose, a linear glucose polymer, and hemicellulose, composed of heteropolysaccharides, were assumed to undergo hydrolysis within the X_{ch}, leading to sugar formation, while enzymes acted upon inert solids (OGEDA; PETRI, 2010). Consequently, following these stages, the pathway remained consistent with the original model. Depending on the substrate characterization (FVW, OFSWM, or FW), one can discern the presence of components such as cellulose, hemicellulose, lignin, and others, emphasizing the substrate's specificity in process modeling, particularly using ADM1, which confines the initial stages of hydrolysis disintegration. Therefore, model generalizations should be avoided (VAVILIN et al., 2003). Li et al. (2021) also point out that it is necessary to fully characterize the residue to the amount of carbohydrates, lipids, proteins, hemicellulose, cellulose, and lignin, as well as the fraction's inert content and degradation rate.

In ADM1, the first-order kinetic model is applied, which is linked to substrate concentration. However, hydrolysis also depends on the concentration of hydrolytic bacteria,

particularly in the case of SHF, which has a complex structure. To address this, Li et al. (2021) adopted the Contois kinetic model for SHF hydrolysis, taking into account both the substrate and hydrolytic bacteria concentrations, while the hydrolysis of X_{ch} and X^{pr} remained described by the original first-order model. Table 6.6 outlines the modifications made to the Batstone et al. (2002) matrix, implemented in the AQUASIM 2.0 software.

Table 6.6 – Modification of the Petersen matrix in the original ADM1

	Process	Component							Rate (kgCOD $m^{-3}d^{-1}$)
		1	2	13	14	15	16	24	
		S_{su}	S_{aa}	X_c	X_{SHF}	X_{ch}	X_{pr}	X_i	
1	Disintegration of VCR			-1	$f_{SHF,C}$	$f_{Ch,C}$	$f_{Pr,C}$	$f_{i,C}$	$k_{dis} * X_c$
2	Hydrolysis of SHF				-1	$f_{Ch,SHF}$		$f_{i,SHF}$	$\frac{k_{hyd,SHF} * X_{SHF*} X_{Su}}{k_{a,SHP} + X_{SHF}}$
3	Hydrolysis of carbohydrates	1				-1			$k_{hyd,Ch} * X_{Ch}$
4	Hydrolysis of protein		1				-1		$k_{hyd,Pr} * X_{Pr}$

Data: adapted from Li et al. (2021).

The modification of ADM1 carried out by Li et al. (2021) resulted in a model that considers crystalline cellulose as the primary component, aiming to describe the anaerobic conversion of RCVs. The results demonstrated good agreement with experimental data following parameter optimization. Sensitivity analysis revealed a significant influence of the kinetic parameters associated with disintegration and hydrolysis. This new model enhanced the accuracy of simulations of anaerobic digestion of RCVs and provided a deeper understanding of the behavior of lignocellulosic waste. Additionally, the study validated the feasibility of the modification and identified key parameters by applying the model to batch anaerobic digestion, thereby establishing a foundation for simulations of more complex continuous digestion processes.

Other authors segregate the residue into fractions for the degradation process to apply in the model. Zhao et al. (2009) modified the ADM1 for aquatic plants by rumen cultures, with cattail residue as an example. Considering an approach similar to that of Li et al. (2021), but from a kinetic perspective, it is evident that the hydrolysis of lignocellulosic residues is not adequately described by the first-order kinetic equation as indicated in ADM1. Therefore, adopting a new model or adapting an existing one to describe the process more accurately becomes feasible. Zhao et al. (2009) conducted an analysis and identified, through substrate fractionation, that the SHF is the predominant step in substrate degradation. This illustrates that the different components constituting the substrate in the initial stage do not exhibit the same velocity or rate of degradation.

The main changes made by Zhao et al. (2009) involved simplifying the original matrix. The new matrix developed by the authors comprises 11 processes and 12 components. Initially, the substrate undergoes disintegration (process 1), resulting in three fractions: SHF, RHF, and inert fraction. Next, the SHF is subjected to hydrolysis (process 2), generating the RHF and inert solids. Subsequently, the RHF is hydrolyzed, producing soluble sugars (process 3). The soluble components (sugars, butyrate, acetate, and H_2) are then absorbed by the relevant microorganisms in processes 4 to 7, followed by the degradation of the microorganisms, which includes the breakdown of taboa, butyrate, acetate, and hydrogen in processes 8 to 11. The kinetic equations adopted for the hydrolysis processes of RHF and SHF were those of Contois, accounting for the concentrations of both the substrate and the microorganisms. The 12 components considered by the model include 8 soluble components, namely sugars, butyrate, propionate, acetate, H_2, CO_2, CH_4, and inerts, as well as 4 particulate components, which consist of composites, slowly fraction (SF), readily fraction (RF), and inerts.

The mathematical model developed by Zhao et al. (2009) based on the original ADM1, aimed to describe the anaerobic digestion of aquatic plants by rumen microbes and led to significant conclusions. Cattail can be fractionated into a slowly hydrolysable fraction, a readily hydrolysable fraction, and an inert fraction, allowing hydrolysis rates to be characterized as surface-limiting kinetics. The model is capable of simulating the anaerobic degradation of cattail, accounting for microbial growth and the formation of aqueous and gaseous products. Hydrolysis of SHF was identified as the rate-limiting step, with the hydrolysis constant ($k_{hyd,SF}$) being the most significant parameter. The sensitivity of the parameters to the production of VS, total volatile fatty acids (TVFA), and CH_4 followed the order: $K_{hyd,SF} > k_{hyd,RF} > K_{hyd,RF}$, providing valuable insights into the anaerobic degradation of aquatic plants (ZHAO et al., 2009).

Zhao et al. (2019) modified ADM1 to estimate methane production through AD of FW in semi-continuous and batch reactors, indicating that ADM1 demands modifications to simulate the AD of organic solid waste. D-AD is a system that involves a substrate (FW) and an inoculum, knowing that FW has a high content of carbohydrates and fats (CHATTERJEE; MAZUMDER, 2020; EDWIGES et al., 2018; MAGAMA; CHIYANZU; MULOPO, 2022; NGO et al., 2016). Zhao et al. (2019) suggested adopting the individual characteristics of FW and sludge, i.e., two separate influent substrates. It was considered that the disintegration process of sludge and FW are different, necessitating describing them separately. This

disintegration process follows surface kinetic expressions. For this, it is necessary to describe the particulate substrate microbial decomposition (ESPOSITO et al., 2011a) accurately.

Particle size must also be considered since the kinetic equations are based on surface area, and the enzymes responsible for substrate degradation are adsorbed on the particle surface. Thus, Zhao et al. (2019) determined the segregation of sludge disintegration and FW. The disintegration of the components was determined based on surface kinetic expressions, considering that particle size is an important factor in the FW disintegration process. For sludge, the original value of the disintegration rate equation described in ADM1 was adopted, while for FW, the rate was calculated according to Esposito et al. (2011a). For FW, the stoichiometric values of the particulate components X_{ch}, X_{pr}, X_{li}, and X_I, represented as f_{ch_Xc}, f_{pr_Xc}, f_{li_Xc}, and f_{Xi_Xc}, respectively, were determined. These values were calculated using four specific equations from Koch et al. (2010), applied to determine the ratios under the operating conditions analyzed by Zhao et al. (2019).

Zhao et al. (2019) modified the original ADM1 framework and calibrated the key kinetic parameters for AD of FW, focusing on the parameters k_{dec}, k_{dis}, $k_{hyd,ch}$, $k_{m,ac}$, and $k_{s,ac}$ due to their significant influence on methane production. The recommended calibration values for these parameters were 0.001, 0.16, 3, 1, and 0.23, respectively. The modified ADM1 model was shown to accurately predict methane production under different substrate characteristics and operational conditions, demonstrating its versatility.

These studies showed that the $k_{hyd,ch}$ values were the most sensitive for AD; however, Chen et al. (2016) found that it was $k_{hyd,pro}$ that had the greatest influence on AD. Despite this, the substrate disintegration process was the most sensitive, demonstrating the feasibility of segregating the substrate and sludge due to the different processing velocities.

Shi et al. (2014) modified the ADM1 for dairy manure (DM) and spent mushroom substrate (SMS) and segregated the residue into easily hydrolyzable, slowly hydrolyzable, and inert fractions. As can be inferred from research modeling organic waste containing cellulose, lignocellulose, and other constituents, the emphasis is consistently placed on adapting to the disintegration stage. This is attributed to the complexity of the components comprising various substrate parts, which degrade at different rates. Consequently, it is feasible to segment and apply different degradation velocities (or rates) based on the specific composition of the material.

In the co-digestion process described by Shi et al. (2014), disintegration was segregated for the two substrates: SMS and DM. The hydrolysis consisted of four components:

hydrolysis of the SHF, RHF, carbohydrates, and proteins, with the lipid content being disregarded due to its low concentration. With the inclusion of the disintegration and hydrolysis processes, the values of the fractions for each substrate were calculated to distinguish the characteristics of each material. The kinetics of carbohydrate and protein hydrolysis were modeled as first-order, while the Contois kinetic equations were adopted for the hydrolysis processes of SHF and RHF, relating the concentrations of the substrates to those of the microorganisms.

Pastor-Poquet et al. (2019b) implemented modifications to the original model to evaluate performance in the two-stage D-AD of OFMWS, focusing on substrates with high NH_3 levels. The main change was the addition of a reversible NH_3 competitive inhibition function, applied to the rate of uptake of soluble components such as valerate, butyrate, propionate, and hydrogen, in order to simulate the accumulation of VFA. In addition, the X_{ch} component was segregated into two fractions: one that is rapidly biodegradable ($X_{ch,fast}$) and one that is slowly biodegradable ($X_{ch,slow}$), the hydrolysis of which results in Ssu. Despite these modifications, the hydrolysis kinetics of X_{ch} remained first-order, as in the original model. However, the disintegration phase, normally included before the hydrolysis of the substrate, was not taken into account. As a result of the modifications, new values were assigned to the $k_{h,ch,slow}$ and $k_{h,ch,fast}$ parameters.

Pastor-Poquet et al. (2018) modified the ADM1 model to adapt it for two-stage OFMSW D-AD. In the implementation, the nitrogen and carbon balances were simulated based on four main assumptions: (1) the D-AD process was assumed to occur in a completely mixed (homogenized) reactor; (2) porosity and transport effects were considered negligible; (3) the specific weight of the solids and solvent was kept constant; and (4) the biochemical reactions were assumed to occur predominantly in water. In addition to these assumptions, other modifications were made, including adjustments to the mass balance to reflect the mass and volume of the reactor. However, the disintegration and hydrolysis processes remained unchanged from the original model, with the modifications focused on the aspects mentioned. Some of the changes made by Pastor-Poquet et al. (2018) were initially implemented by Blumensaat et al. (2005), who studied the application of ADM1 to simulate the two-stage AD of sewage sludge.

Liotta et al. (2015) proposed a model based on the modified version of ADM1 developed by Esposito et al. (2008, 2011a, 2011b) for D-AD of OFMSW, also studying the possibility of co-digestion and separation of the inflowing streams. Pastor-Poquet et al. (2018,

2019a) adjusted the ADM1 to include "non-ideality" corrections (needed to account for the ionic strength effect) and mass balances aimed at assessing the reactor mass and volume modifications (necessary to account for the removal of organic solids in D-AD). However, further research is needed to make ADM1 suitable for other types of waste considering additional technologies involved, such as DRANCO, Kompagas, Benkon, Valorga, and others.

Other research has attempted to modify the ADM1, based on waste characteristics. Abbassi-Guendouza et al. (2012) studied the impact of OFMSW TS content on D-AD by evaluating it through ADM1. The possibility of modifying ADM1 was analyzed, as it does not account for hydrolysis inhibition (VAVILIN et al., 2004). The first-order hydrolysis rate constant decreases with increasing TS, and the reaction rate decreases with TS content. It is also emphasized that TS levels between 30% and 35% significantly impact the cumulative methane production. The issues arising from mass transfer result in CO_2, dissolved methane, and dissolved hydrogen accumulations, which can inhibit methanogenesis. CO_2 is trapped in the digestate because the high TS content hinders metabolites permeation and diffusion, which potentially leading to local acidification. Likewise, dissolved hydrogen accumulation can inhibit the degradation of propionate, butyrate, and valerate, generating their accumulation. Abbassi-Guendouza et al. (2012) suggest that necessary adjustments should be made to the hydrolysis rate constants and the liquid/gas volumetric mass transfer coefficients to apply ADM1 in the D-AD, compared to W-AD.

A crucial point to observe and study is the disintegration and hydrolysis constants, which define and limit the subsequent stages of the process. Different materials have different constants, as they depend on the composition and characteristics of the substrate, as well as the presence of water, which facilitates the transfers occurring inside the reactor. Other important considerations include the division of the initial phases and the changes in the carbon and nitrogen balances that occur in the systems. D-AD is a process that warrants further exploration, given its specificities, not only operational but also related to degradation and potential inhibitions that may arise.

The modifications suggested by the authors considered the specificities of the substrate, allowing for adaptations to other types of substrates without the need to adopt the same values or adjustments. This approach enables the identification of key points that can enhance the model. In terms of efficiency, all the authors noted that the model has a high potential for application, demonstrating excellent adherence to the data.

6.5.1.2 Simplification in ADM1

The ADM1 model is criticized for its structural complexity and the abundance of parameters that are not easily determined experimentally. Some authors have suggested simplification to adapt it to specific approaches (ABUBACKAR et al., 2019).

Bollon et al. (2011) developed a model based on ADM1, specifically addressing the biochemical steps in the D-AD of OFMSW. The main modification involved consolidating the disintegration, hydrolysis, and acidogenesis stages, each represented by first-order kinetics—into a single disintegration stage, termed DHA. Due to the difficulty in determining the concentrations of acetate, hydrogen, and other degrading microorganisms, the maximum growth rates and biomass concentrations of each trophic group were consolidated into a specific parameter. In the case of Bollon et al. (2011), this parameter is termed k_mX_i, which represents the maximum rate of substrate consumption and reflects the activity of the microorganisms in component i.

This is due to OFMSW characteristics, in which the particulate material mainly comprises cellulose, limiting hydrolysis. Another modification considered the constant biomass in the digester due to the reduced growth rate in D-AD (BOLLON et al., 2011). Therefore, the maximum growth rate was associated with the biomass concentration in a single group (k_mX_i) maximum substrate growth rate. Bollon et al. (2011) also suggested adjusting the parameters related to acetate uptake. Also, they evaluated the variation of the kinetic parameters with the residue moisture content. The ADM1 parameter values do not fit the D-AD process, proposing adjusting the maximal acetate uptake rate (k_mX_{ac}) and the half-saturation constant ($k_{s,ac}$).

Hassam et al. (2015) developed a model with reduced dimensions. First, a hydrolysis step and the dynamics of ammonium were inserted into Anaerobic Model Nº. 2 (AM2) (BERNARD et al., 2001), producing a two-stage anaerobic digestion model (AM2HN) (HASSAM et al., 2015). Then, a generic and systematic state association was performed to find correspondence between ADM1 and AM2HN, calibrated with data generated by ADM1. Finally, it was possible to compare the models' responses. Thus, Hassam et al. (2015) contributed to the modification of AM2 to AM2HN and its association with ADM1 for the calibration of AM2HN, having a connection between the two models (ABBASSI-GUENDOUZ et al., 2012).

6.6 Possible future direction

Several publications have demonstrated the application of ADM1 since its release. The D-AD process has been the subject of recent research, with few studies addressing its modeling, particularly the application of ADM1. Thus, it is necessary to use ADM1 in D-AD, even in a simplified manner. When considering the D-AD of FW, FVW, or OFMSW, it is observed that further research is needed to consolidate the applicability of ADM1 in dry organic waste processes.

For instance, the effects of TS on the substrate disintegration rate and acetate and propionate uptake rates can be (LIOTTA et al., 2015), or the incorporation of the specific rate of substrate degradation ($k_{m,j}$) and the half-saturation coefficient ($k_{s,j}$) (LI et al., 2022). The modified ADM1 considered decoupling the absorption of butyrate and valerate by inserting a new bacterial group responsible for valerate absorption (X_{c5}). Considering this, X_{c4} was only responsible for butyrate absorption. In ADM1, X_{c4} consumes both butyrate and valerate (CAPSON-TOJO; ASTALS; ROBLES, 2021). Thus, other possible changes should be analyzed to adjust the ADM1 to the process type and residue.

Other problems must be considered in the D-AD modeling process. Boutoute et al. (2021) pointed out that the model includes the mass transfer of components from the liquid phase to the gas phase. However, there is a resistance to liquid-gas transfer, especially in the diffusion of CH_4, CO_2, and NH_3. This mass transfer is also related to biogas production. It is generally accompanied by the accumulation of VFAs and acidification of the reactor resulting from the significant impediment to hydrogen diffusion (H_2 and H^+) (ABBASSI-GUENDOUZ et al., 2012; OKORO-SHEKWAGA; ROSS; CAMARGO-VALERO, 2019; ZHU et al., 2020). Therefore, the gas balance must follow the outflow of biogas to be equal to the inflow of biogas, depending on the mass transfer equations.

According to Zhu et al. (2020), H_2 is responsible for transporting electrons produced by acidogens in digestion and is consumed by hydrogenotrophic methanogens that use H_2. Knowing that the oxidation of certain important intermediates such as NADH, $FADH_2$, and ferredoxin with H^+ is thermodynamically unfavorable, as $E_{NaD+/NaDH}$=-320 mV, $E_{FADH/FADH2}$ =-220 mV, $E_{Fd\text{-}ox/Fd\text{-}red}$=-398 mV, vs $E_{H+/H2}$=-414 mV, pH=7. The high TS content increases the residue viscosity and density, which slows down interspecies hydrogen transfer (IHT), thus representing a mass transfer. One of the alternatives to IHT is the direct interspecies electron transfer (DIET) (ZHU et al., 2020).

Simulations carried out by Abbassi-Guendouz et al. (2012) show that the limitation of mass transfer explains the low methane production at high TS, also reducing the hydrolysis rate. In high TS processes, the liquid/gas mass transfer coefficient (k_{La}) is reduced from 200 d^{-1} to 0.5 d^{-1} to compensate for the reduced gas transfer due to the pasty texture of the substrate-biomass mixture. They also report that the liquid/gas mass transfer coefficient has never been measured in D-AD processes. The reduction of the coefficient to 0.5 d^{-1} is due to: I) the solid-liquid-gas interface is low due to the reduced production of biogas bubbles and the non-mixing conditions, and II) the mass transfer coefficient is also affected by the low humidity. Other authors, such as Rosen and Jeppsson (2006b), suggest a reduction from 0.04 to 0.18 d^{-1}, depending on the TS content.

Abbassi-Guendouz et al. (2012) explain how low moisture content affects mass transfer. Equation [6.4] explains the difference between the diffusivity coefficients of the soluble components in the digestate D_i (digestate) and water D_i (water). The diffusivity coefficient decreases with the reduction in porosity (water content) and the increase in viscosity. The reduction from k_T = 0.5 d^{-1} to TS = 10% was considered for the tests carried out.

$$k_L(digestate) = k_L(water)\left(\frac{D_i(digestate)}{D_i(water)}\right)^{0.5} \quad [6.4]$$

At the end of the simulations, it was found that the reduction in cumulative methane production with TS between 15 and 35% cannot be attributed to mass transfer. However, TS between 30 and 35% clearly shows that the limitation is associated with the mass transfer that limited methane production (ABBASSI-GUENDOUZ et al., 2012).

There are still gaps that need to be filled, as the main papers on process modeling do not detail biogas trapping in the biomass/substrate or the loss of active biomass. The main papers that use ADM1 for D-AD use CSTR and UASB (YU et al., 2012) or only CSTR (LIOTTA et al., 2015; NOYKOVA et al., 2002; PASTOR-POQUET et al., 2018, 2019b), and others do not report on the reactor. It is necessary to study the main changes and/or adaptations for application in systems such as the Valorga system, Kompogas reactor, Bekon reactor (single-stage batch process), and other technologies that can be applied to D-AD to identify the main changes needed for efficient and realistic modeling.

6.7 Conclusions

This study conducted a bibliometric analysis of the prospects and trends for applying the ADM1 model to the AD of plant residues. The conventional model has been observed to face significant challenges under D-AD conditions, particularly due to mass transfer limitations, which are exacerbated in low-moisture environments. Furthermore, the rates of hydrolysis and disintegration, as reported in various studies, do not follow a uniform pattern and are often influenced by substrate characteristics such as particle size and structural composition. This adds another layer of complexity to the modeling process. While some researchers employ first-order equations to describe hydrolysis, others prefer the Contois model, which accounts for microbial concentration to adjust hydrolysis constants, especially for compounds like cellulose and hemicellulose. This variation in modeling approaches reflects the difficulty of accurately representing the complex interactions between substrates and microorganisms. Additionally, the requirement for detailed substrate characterization—encompassing the analysis of multiple parameters—escalates the need for extensive experimental data, complicating the simplified and efficient application of the ADM1 model across different scenarios.

In summary, this study has identified the need for adjustments to the ADM1 model to address the complexities associated with D-AD processes, particularly regarding the parameterization of disintegration and hydrolysis rates for various plant substrates, with a focus on components such as cellulose and lignin. Furthermore, model calibration based on experimental data is crucial for enhancing accuracy, especially in solid-state anaerobic digestion systems. A detailed analysis of the microbiomes involved also presents a promising avenue for improving the model's predictability, enabling better adaptation to the specific interactions between substrates and microorganisms.

7 FUTURE RESEARCH DIRECTIONS

Future research should aim to extend the modified ADM1 modeling framework to D-AD of FVW, representing a natural and relevant progression of the present work. While this thesis addressed dark fermentation and W-AD, experimental implementation under high-solids conditions remains to be performed. Dedicated experimental campaigns are needed to generate reliable datasets for model calibration and validation, systematically exploring variations in total solids content, organic loading rates, and reactor configurations. Such studies would allow refinement of disintegration and hydrolysis kinetics and explicit representation of mass transfer limitations and substrate accessibility constraints inherent to dry systems.

From a modeling perspective, D-AD operation requires further adaptation of the ADM1 structure to account for the altered physicochemical environment. Key aspects include effective hydrolysis rates, localized accumulation of volatile fatty acids, hydrogen partial pressure effects, pH gradients, and ammonia inhibition. Sensitivity and identifiability analyses of kinetic and inhibition parameters under high-solids conditions will ensure model robustness across a wide operational window.

To validate metabolic pathways and improve predictive accuracy, molecular biology studies should be incorporated, including analysis of microbial community dynamics and functional genes involved in acidogenesis, acetogenesis, and hydrogen production. Additional investigations on alternative metabolic routes and the formation of intermediate compounds, such as ethanol and lactate, are also necessary to capture the complexity of fermentation under dry conditions.

Further research should explore substrate variability, including lignocellulosic components and other complex organic fractions, to assess their impact on process kinetics and overall biogas yield. The effects of potential inhibitors, such as ammonia, and strategies for their mitigation should also be systematically studied.

Detailed compositional analyses of the carbohydrate fraction should also be conducted in future studies to improve the representation of hydrolysis processes in the modeling framework. Techniques capable of distinguishing structural and non-structural carbohydrates, such as the quantification of cellulose, hemicellulose, pectin, starch, and soluble sugars, would provide a more accurate description of substrate heterogeneity. Such characterization would enable the evaluation of multi-fraction approaches for the particulate carbohydrate pool (X_{ch}), allowing the differentiation between readily degradable and more

recalcitrant fractions with distinct hydrolysis kinetics. Incorporating this level of detail into the model could significantly improve the prediction of hydrolysis dynamics and overall process performance when treating fruit and vegetable waste.

Finally, the integration of advanced digital tools, including online sensors, machine learning, and digital twins, could significantly enhance process monitoring, real-time model calibration, and predictive optimization. Altogether, these efforts will strengthen the applicability of the modified ADM1 as a unified modeling platform for anaerobic biorefineries, enabling comprehensive assessment of both wet and D-AD routes and their contribution to sustainable energy recovery from organic residues.

8 GENERAL CONCLUSION

This doctoral research demonstrated that ADM1, although originally developed for conventional W-AD systems, can be successfully adapted, calibrated, and structurally extended to model the anaerobic conversion of FVW under different process configurations, reactor types, and metabolic conditions. In this context, the general and specific objectives proposed at the outset were fully achieved through an integrated experimental and computational approach, enabling a consistent evaluation of model performance across distinct anaerobic processes and operational scales.

More specifically, each specific objective was addressed through corresponding analytical and experimental stages. The bibliometric and systematic review not only identified the scientific evolution of ADM1 applications in AD of FVW, but also revealed clear research gaps regarding D-AD systems, high-solids substrates, and non-conventional anaerobic pathways. In addition, the critical evaluation of previous ADM1 applications demonstrated that many structural adaptations reported in the literature remain highly case-dependent, often lacking standardized calibration strategies and sufficient discussion of parameter identifiability, which limits model transferability across operational conditions.

In the wet anaerobic digestion stage, ADM1 calibration in UASB reactors confirmed that the model can satisfactorily predict methane production and intermediate compound dynamics when substrate-specific kinetic adjustments are introduced, particularly for hydrolysis-related parameters. In contrast, under dark fermentation conditions, the standard ADM1 exhibited systematic deviations in representing hydrogen production and acidogenic metabolite distribution, especially regarding lactate accumulation and competing fermentation pathways. These deviations justified the structural extension of the model through the incorporation of additional metabolic routes directly supported by experimental VFA profiles.

The modified ADM1 demonstrated robust predictive performance for hydrogen production, gas composition, and metabolite evolution, indicating that the proposed extensions improved the model's capacity to capture acidogenic pathway competition. Furthermore, sensitivity analysis identified hydrolysis constants, substrate uptake kinetics, and stoichiometric coefficients associated with acidogenic conversion as the most influential parameters governing hydrogen generation, confirming that parameter sensitivity is strongly concentrated in the early substrate conversion stages.

A central scientific contribution of this work lies in demonstrating that substrate-specific and process-specific modifications are essential to extend the applicability of ADM1 beyond its conventional domain. Rather than applying the model in its original form, the results showed that reliable prediction of FVW conversion requires targeted recalibration of hydrolysis, disintegration, and microbial kinetic parameters according to substrate characteristics and reactor operating conditions.

The research was structured around three complementary scientific stages, which together constitute an integrated modeling framework. First, the bibliometric analysis identified the current global scientific landscape of ADM1 applications, revealing a strong concentration of studies focused on conventional W-AD systems and a limited representation of high-solids and alternative anaerobic pathways. This analysis also highlighted that, despite the growing international adoption of ADM1, studies addressing tropical residues and process conditions relevant to emerging countries remain comparatively scarce, thereby reinforcing the importance of advancing mechanistic modeling under Brazilian waste management conditions.

Second, the model was calibrated and validated for the W-AD of the liquid fraction of FVW in UASB reactors, where high predictive accuracy was achieved for biogas production and intermediate dynamics. These results confirmed that even in conventional AD systems, substrate-specific adjustments are necessary to adequately represent hydrolysis-controlled behavior when processing highly biodegradable fruit and vegetable residues.

Third, in dark fermentation systems, the standard ADM1 structure proved insufficient to represent the metabolic pathways governing hydrogen production. The explicit incorporation of lactate formation and consumption pathways constituted an original contribution of this research, significantly improving model performance and enabling accurate prediction of hydrogen yield, gas composition, VFA profiles, and biogas production. This extension demonstrated that carbohydrate hydrolysis and sugar uptake are key controlling mechanisms in acidogenic metabolism and must be explicitly represented when ADM1 is applied to hydrogen-oriented systems.

Taken together, these three stages demonstrate that ADM1 can evolve from a conventional digestion model into a flexible mechanistic platform capable of supporting the virtual design of biorefineries for multiple anaerobic valorization routes of organic waste. This represents an original contribution, as it integrates bibliometric diagnosis, experimental validation, and structural model expansion within a single research framework applied to the same substrate under different energy recovery strategies.

From a broader perspective, the findings also contribute to strengthening Brazilian scientific participation in advanced anaerobic process modeling, particularly in the context of residues that are highly abundant in tropical food systems yet remain underrepresented in international mechanistic modeling studies.

From a scientific standpoint, the proposed calibration strategies and structural extensions enhance the predictive robustness of ADM1 and broaden its applicability to emerging anaerobic bioprocesses. From an applied perspective, the results provide a robust decision-support framework for process analysis, optimization, control strategy development, and the future implementation of integrated biorefineries for energy recovery from organic residues.

Overall, the findings confirm that mechanistic modeling, when experimentally grounded and properly adapted to substrate-specific conditions, constitutes a powerful tool for advancing anaerobic biotechnology and supporting the development of more efficient and sustainable waste-to-energy systems.

Future research should focus on extending the proposed modeling framework to fully integrated biorefinery configurations, including the coupling of hydrogen fermentation and methanogenic stages, the incorporation of additional metabolic intermediates, and the evaluation of dynamic operational disturbances under pilot- and full-scale conditions. Further advances may also include the integration of mechanistic modeling with techno-economic and life-cycle assessment tools, thereby strengthening the role of ADM1-based approaches in the design of circular and low-carbon waste management systems.

9 LIST OF REFERENCE

ABBASSI-GUENDOUZ, A. et al. Total solids content drives high solid anaerobic digestion via mass transfer limitation. **Bioresource Technology**, v. 111, p. 55–61, maio 2012.

ABUBACKAR, H. N. et al. Effects of size and autoclavation of fruit and vegetable wastes on biohydrogen production by dark dry anaerobic fermentation under mesophilic condition. **International Journal of Hydrogen Energy**, v. 44, n. 33, p. 17767–17780, jul. 2019.

AFONSO, M. H. F. et al. Como construir conhecimento sobre o tema de pesquisa? Aplicação do processo proknow-c na busca de literatura sobre avaliação do desenvolvimento sustentável. **Revista de Gestão Social e Ambiental**, v. 5, n. 2, p. 47–62, 27 fev. 2012.

AGBO, F. J. et al. Scientific production and thematic breakthroughs in smart learning environments: a bibliometric analysis. **Smart Learning Environments**, v. 8, n. 1, p. 1, 15 dez. 2021.

AHMED, W.; RODRIGUEZ, J. Modelling sulfate reduction in anaerobic digestion: Complexity evaluation and parameter calibration. **WATER RESEARCH**, v. 130, p. 255–262, mar. 2018.

AJAY, K. J. et al. Research advances in dry anaerobic digestion process of solid organic wastes. **African Journal of Biotechnology**, v. 10, n. 65, p. 14242–14253, 24 out. 2011.

ALEXANDROPOULOU, M.; ANTONOPOULOU, G.; LYBERATOS, G. Food Industry Waste's Exploitation via Anaerobic Digestion and Fermentative Hydrogen Production in an Up-Flow Column Reactor. **Waste and Biomass Valorization**, v. 7, n. 4, p. 711–723, 2 ago. 2016.

ALEXANDROPOULOU, M.; ANTONOPOULOU, G.; LYBERATOS, G. A novel approach of modeling continuous dark hydrogen fermentation. **Bioresource Technology**, v. 250, n. December 2017, p. 784–792, fev. 2018.

ALEXANDROPOULOU, M.; ANTONOPOULOU, G.; LYBERATOS, G. Modeling of continuous dark fermentative hydrogen production in an anaerobic up-flow column bioreactor. **Chemosphere**, v. 293, p. 133527, abr. 2022.

AMERICAN OIL CHEMISTS' SOCIETY (AOCS). Rapid Determination of Oil/Fat Utilizing High Temperature Solvent Extraction. **AOCS Approved Procedure Am 5-04 Approved**, p. 3–5, 2004.

ANGELIDAKI, I. et al. Defining the biomethane potential (BMP) of solid organic wastes and energy crops: a proposed protocol for batch assays. **Water Science and Technology**, v. 59, n. 5, p. 927–934, 1 mar. 2009.

ANGELIDAKI, I.; ELLEGAARD, L.; AHRING, B. K. A mathematical model for dynamic simulation of anaerobic digestion of complex substrates: Focusing on ammonia inhibition. **Biotechnology and Bioengineering**, v. 42, n. 2, p. 159–166, 1993.

ANGELIDAKI, I.; ELLEGAARD, L.; AHRING, B. K. A comprehensive model of anaerobic

bioconversion of complex substrates to biogas. **Biotechnology and Bioengineering**, v. 63, n. 3, p. 363–372, 1999.

ANGELIDAKI, I.; ELLEGAARD, L.; AHRING, B. K. Applications of the Anaerobic Digestion Process. In: **Biomethanation II**. Berlin: [s.n.]. p. 1–33.

ANGELIDAKI, I.; SANDERS, W. Assessment of the anaerobic biodegradability of macropollutants. **Reviews in Environmental Science and Bio/Technology**, v. 3, n. 2, p. 117–129, jun. 2004.

ANKOM. **Technology method 2:B91 rapid determination of oil/fat utilizing high temperature solvent extraction.** Macedon: [s.n.].

ANTONOPOULOU, G. et al. Modeling of fermentative hydrogen production from sweet sorghum extract based on modified ADM1. **International Journal of Hydrogen Energy**, v. 37, n. 1, p. 191–208, 2012a.

ANTONOPOULOU, G. et al. ADM1-based modeling of methane production from acidified sweet sorghum extract in a two stage process. **BIORESOURADM1-based modeling of methane production from acidified sweet sorghum extract in a two stage processCE TECHNOLOGY**, v. 106, p. 10–19, 2012b.

AOAC (ASSOCIATION OF OFFICIAL ANALYTICAL CHEMISTS). **Official methods of analysis.** 20. ed. USA: AOAC International, 2016.

APHA. **Standard Methods for the Examination of Water and Wastewater, American Public Health Association/American Water Works Association/Water Environment Federation**. 24. ed. Washington, DC: [s.n.].

ARELLI, V. et al. Dry anaerobic co-digestion of food waste and cattle manure: Impact of total solids, substrate ratio and thermal pre treatment on methane yield and quality of biomanure. **Bioresource Technology**, v. 253, n. January, p. 273–280, 2018.

ARIA, M.; CUCCURULLO, C. bibliometrix : An R-tool for comprehensive science mapping analysis. **Journal of Informetrics**, v. 11, n. 4, p. 959–975, nov. 2017.

ARIS, R. Mathematical Modelling Techniques. **SIAM Review**, v. 21, n. 4, p. 571–572, out. 1979.

ARNALDOS, M. et al. From the affinity constant to the half-saturation index: Understanding conventional modeling concepts in novel wastewater treatment processes. **Water Research**, v. 70, p. 458–470, 2015.

ASADI, M.; MCPHEDRAN, K. Biogas maximization using data-driven modelling with uncertainty analysis and genetic algorithm for municipal wastewater anaerobic digestion. **Journal of Environmental Management**, v. 293, n. May, p. 112875, set. 2021.

ASSIS, T. I.; GONÇALVES, R. F. Valorization of food waste by anaerobic digestion: A bibliometric and systematic review focusing on optimization. **Journal of Environmental Management**, v. 320, n. February, p. 115763, 2022.

ASTALS, S. et al. Anaerobic digestion of seven different sewage sludges: A biodegradability

and modelling study. **Water Research**, v. 47, n. 16, p. 6033–6043, out. 2013.

ATELGE, M. R. et al. Biogas Production from Organic Waste: Recent Progress and Perspectives. **Waste and Biomass Valorization**, v. 11, n. 3, p. 1019–1040, 19 mar. 2020.

AWADALLA, O. A. et al. Anaerobic digestion of lignocellulosic waste for enhanced methane production and biogas-digestate utilization. **Industrial Crops and Products**, v. 195, n. November 2022, p. 116420, maio 2023.

AXELSSON, L. et al. Perspective: Jatropha cultivation in southern India: Assessing farmers' experiences. **Biofuels, Bioproducts and Biorefining**, v. 6, n. 3, p. 246–256, 2012.

BASINAS, P.; RUSÍN, J.; CHAMRÁDOVÁ, K. Assessment of high-solid mesophilic and thermophilic anaerobic digestion of mechanically-separated municipal solid waste. **Environmental Research**, v. 192, n. June 2020, 2021a.

BASINAS, P.; RUSÍN, J.; CHAMRÁDOVÁ, K. Dry anaerobic digestion of the fine particle fraction of mechanically-sorted organic fraction of municipal solid waste in laboratory and pilot reactor. **Waste Management**, v. 136, n. July, p. 83–92, dez. 2021b.

BASSANEZI, R. C. **Ensino-aprendizagem com modelagem matemática:uma nova estratégia**. 4. ed. [s.l.] Contexto, 2002. v. 1

BASTIAN, M.; HEYMANN, S.; JACOMY, M. Gephi: An Open Source Software for Exploring and Manipulating Networks. **Proceedings of the International AAAI Conference on Web and Social Media**, v. 3, n. 1, p. 361–362, 19 mar. 2009.

BATSTONE, D. J. et al. Modelling anaerobic degradation of complex wastewater. I: model development. **Bioresource Technology**, v. 75, n. 1, p. 67–74, out. 2000.

BATSTONE, D. J. et al. The IWA Anaerobic Digestion Model No 1 (ADM1). **Water Science and Technology**, v. 45, n. 10, p. 65–73, 1 maio 2002.

BATSTONE, D. J. et al. Anaerobic Digestion Model No.1 (ADM1). **Water Intelligence Online**, v. 4, n. 13, p. 9781780403052–9781780403052, 30 dez. 2015.

BATSTONE, D. J.; KELLER, J. Industrial applications of the IWA anaerobic digestion model No. 1 (ADM1). **Water Science and Technology**, v. 47, n. 12, p. 199–206, 1 jun. 2003.

BATSTONE, D. J.; PIND, P. F.; ANGELIDAKI, I. Kinetics of thermophilic, anaerobic oxidation of straight and branched chain butyrate and valerate. **BIOTECHNOLOGY AND BIOENGINEERING**, v. 84, n. 2, p. 195–204, 2003.

BATSTONE, D. J.; TAIT, S.; STARRENBURG, D. Estimation of hydrolysis parameters in full-scale anerobic digesters. **Biotechnology and Bioengineering**, v. 102, n. 5, p. 1513–1520, 5 abr. 2009.

BEDOIĆ, R. et al. Green biomass to biogas – A study on anaerobic digestion of residue grass. **Journal of Cleaner Production**, v. 213, n. 2, p. 700–709, 23 mar. 2019.

BERNARD, O. et al. Dynamical model development and parameter identification for an anaerobic wastewater treatment process. Biotechnology and bioengineering 75.4 (2001) 424-

438..pdf. **Biotechnology and Bioengineering**, v. 75, n. 4, p. 424–438, 2001.

BLANCO, V. M. C.; OLIVEIRA, G. H. D.; ZAIAT, M. Dark fermentative biohydrogen production from synthetic cheese whey in an anaerobic structured-bed reactor: Performance evaluation and kinetic modeling. **Renewable Energy**, v. 139, p. 1310–1319, ago. 2019.

BLUMENSAAT, F.; KELLER, J. Modelling of two-stage anaerobic digestion using the IWA Anaerobic Digestion Model No. 1 (ADM1). **Water Research**, v. 39, n. 1, p. 171–183, jan. 2005.

BOCHER, B. T. et al. Anaerobic digestion of secondary residuals from an anaerobic bioreactor at a brewery to enhance bioenergy generation. **Journal of Industrial Microbiology & Biotechnology**, v. 35, n. 5, p. 321–329, 9 maio 2008.

BOGAERTS, P.; WOUWER, A. VANDE. Mathematical Modeling and Control of Bioprocesses. **Mathematical Methods in the Applied Sciences**, v. 47, n. 12, p. 10478–10489, 5 ago. 2023.

BOLLON, J. et al. Development of a kinetic model for anaerobic dry digestion processes: Focus on acetate degradation and moisture content. **Biochemical Engineering Journal**, v. 56, n. 3, p. 212–218, 24 out. 2011.

BONG, C. P. C. et al. The characterisation and treatment of food waste for improvement of biogas production during anaerobic digestion – A review. **Journal of Cleaner Production**, v. 172, p. 1545–1558, 2018.

BONK, F. et al. Determination of Microbial Maintenance in Acetogenesis and Methanogenesis by Experimental and Modeling Techniques. **FRONTIERS IN MICROBIOLOGY**, v. 10, 2019.

BOUALLAGUI, H. et al. Mesophilic biogas production from fruit and vegetable waste in a tubular digester. **Bioresource Technology**, v. 86, n. 1, p. 85–89, 2003.

BOUALLAGUI, H. et al. Effect of temperature on the performance of an anaerobic tubular reactor treating fruit and vegetable waste. **Process Biochemistry**, v. 39, n. 12, p. 2143–2148, 2004.

BOUALLAGUI, H. et al. Bioreactor performance in anaerobic digestion of fruit and vegetable wastes. **Process Biochemistry**, v. 40, n. 3–4, p. 989–995, 2005.

BOUALLAGUI, H. et al. Improvement of fruit and vegetable waste anaerobic digestion performance and stability with co-substrates addition. **Journal of Environmental Management**, v. 90, n. 5, p. 1844–1849, 2009.

BOUTOUTE, A. et al. Development of a Sensitivity Analysis method to highlight key parameters of a dry Anaerobic Digestion reactor model. **Biochemical Engineering Journal**, v. 173, n. 11, p. 108085, set. 2021.

BRASIL. **Boletim hortigranjeiro**. [s.l: s.n.]. v. 12

BRASIL. **Conab aponta queda de preços na maioria das frutas mais vendidas nas Ceasas**. Disponível em: <https://www.gov.br/conab/pt-br/assuntos/noticias/conab-aponta-queda-de-

precos-na-maioria-das-frutas-mais-vendidas-nas-ceasas>. Acesso em: 12 mar. 2026b.

BREIMAN, L. Random Forests. **Machine Learning**, v. 45, n. 1, p. 5–32, out. 2001.

BRITO-ESPINO, S. et al. Application of a mathematical model to predict simultaneous reactions in anaerobic plug-flow reactors as a primary treatment for constructed wetlands. **Science of The Total Environment**, v. 713, p. 136244, abr. 2020.

BRYERS, J. D. Structured modeling of the anaerobic digestion of biomass particulates. **Biotechnology and Bioengineering**, v. 27, n. 5, p. 638–649, maio 1985.

BUCHAUER, K.; INNSBRUCK, A.-. A comparison of two simple titration procedures to determine volatile fatty acids in influents to waste-water and sludge ... A comparison of two simple titration procedures to determine volatile fatty acids in influents to waste-water and sludge treatment. **Water Sa-Pretoria-**, v. 24, n. November, p. 49–56, 1998.

BUŁKOWSKA, K. et al. Kinetic parameters of volatile fatty acids uptake in the ADM1 as key factors for modeling co-digestion of silages with pig manure, thin stillage and glycerine phase. **Renewable Energy**, v. 126, p. 163–176, out. 2018.

BUSWELL, A. M. Important considerations in sludge digestion. Part II. Microbiology and theory of anaerobic digestion. **Sewage works journal**, v. 19, n. 1, p. 28–36, 1947.

BUSWELL, A. M.; SOLLO, F. W. The Mechanism of the Methane Fermentation. **Journal of the American Chemical Society**, v. 70, n. 5, p. 1778–1780, 1 maio 1948.

CAMPUZANO, R.; GONZÁLEZ-MARTÍNEZ, S. Characteristics of the organic fraction of municipal solid waste and methane production : A review. **Waste Management**, v. 54, p. 3–12, 2016.

CAPSON-TOJO, G.; ASTALS, S.; ROBLES, Á. Considering syntrophic acetate oxidation and ionic strength improves the performance of models for food waste anaerobic digestion. **Bioresource Technology**, v. 341, p. 125802, dez. 2021.

CARECCI, D. et al. A plant-wide modelling framework to describe microalgae growth on liquid digestate in agro-zootechnical biomethane plants. **Chemical Engineering Journal**, v. 485, n. February, p. 149981, 2024.

CAVALCANTE, W. A. et al. From start-up to maximum loading: An approach for methane production in upflow anaerobic sludge blanket reactor fed with the liquid fraction of fruit and vegetable waste. **Journal of Environmental Management**, v. 335, n. December 2022, 2023.

CHAKRABORTY, D.; PARTHIBA, O.; SELVAM, A. Bioresource Technology Two-phase anaerobic digestion of food waste : Effect of semi-continuous feeding on acidogenesis and methane production. **Bioresource Technology**, v. 346, n. November 2021, p. 126396, 2022.

CHANDRA, R. et al. **A biorefinery approach for dairy wastewater treatment and product recovery towards establishing a biorefinery complexity index**. **Journal of Cleaner Production**Elsevier Ltd, , maio 2018. Disponível em: <https://www.sciencedirect.com/science/article/pii/S0959652618304360?via%3Dihub>

CHATTERJEE, B.; MAZUMDER, D. New approach of characterizing fruit and vegetable

waste (FVW) to ascertain its biological stabilization via two-stage anaerobic digestion (AD). **Biomass and Bioenergy**, v. 139, n. June, 2020.

CHEN, C. CiteSpace II: Detecting and visualizing emerging trends and transient patterns in scientific literature. **Journal of the American Society for Information Science and Technology**, v. 57, n. 3, p. 359–377, 14 fev. 2006.

CHEN, X. et al. Application of ADM1 for modeling of biogas production from anaerobic digestion of Hydrilla verticillata. **Bioresource Technology**, v. 211, p. 101–107, jul. 2016.

CHEN, Y. et al. Mathematical modeling of upflow anaerobic sludge blanket (UASB) reactors: Simultaneous accounting for hydrodynamics and bio-dynamics. **CHEMICAL ENGINEERING SCIENCE**, v. 137, p. 677–684, 2015.

CHERNICHARO, C. A. DE L. **Biological Wastewater Treatment Vol.4: Anaerobic Reactors**. London: IWA Publishing, Alliance House, 12 Caxton Street, London SW1H 0QS, UK, 2007a. v. 04

CHERNICHARO, C. A. L. **Reatores Anaeróbios Princípios Do Tratamento Biológico Em águas Residuárias.** 2. ed. Belo Horizonte: [s.n.].

CHERNICHARO, C. A. L. et al. Anaerobic sewage treatment: state of the art, constraints and challenges. **Reviews in Environmental Science and Bio/Technology**, v. 14, n. 4, p. 649–679, 21 dez. 2015.

CHERNICHARO, C. A. L. Princípios do Tratamento Biológico de águas residuárias: Reatores Anaerobios. p. 379, 2017.

CHO, S. K. et al. Dry anaerobic digestion of food waste under mesophilic conditions: Performance and methanogenic community analysis. **Bioresource Technology**, v. 131, n. 2013, p. 210–217, 2013.

CHONG, S. et al. The performance enhancements of upflow anaerobic sludge blanket (UASB) reactors for domestic sludge treatment – A State-of-the-art review. **Water Research**, v. 46, n. 11, p. 3434–3470, jul. 2012.

CIANO, M. P. et al. How IJPR has addressed 'lean': a literature review using bibliometric tools. **International Journal of Production Research**, v. 57, n. 15–16, p. 5284–5317, 2019.

COBO, M. J. et al. Science mapping software tools: Review, analysis, and cooperative study among tools. **Journal of the American Society for Information Science and Technology**, v. 62, n. 7, p. 1382–1402, jul. 2011.

CONAB. **Comercialização Total de Frutas e Hortaliças**. [s.l: s.n.]. v. 7

CONTOIS, D. E. Kinetics of Bacterial Growth: Relationship between Population Density and Specific Growth Rate of Continuous Cultures. **Journal of General Microbiology**, v. 21, n. 1, p. 40–50, 1 ago. 1959.

CORTES, C.; VAPNIK, V. Support-vector networks. **Machine Learning**, v. 20, n. 3, p. 273–297, 9 set. 1995.

COSTELLO, D. J.; GREENFIELD, P. F.; LEE, P. L. Dynamic modelling of a single-stage high-rate anaerobic reactor—I. Model derivation. **Water Research**, v. 25, n. 7, p. 847–858, jul. 1991a.

COSTELLO, D. J.; GREENFIELD, P. F.; LEE, P. L. Dynamic modelling of a single-stage high-rate anaerobic reactor—II. Model verification. **Water Research**, v. 25, n. 7, p. 859–871, jul. 1991b.

COUTO, P. T. et al. Calibration of ADM1 using the Monte Carlo Markov Chain for modeling of anaerobic biodigestion of sugarcane vinasse in an AnSBBR. **Chemical Engineering Research and Design**, v. 141, p. 425–435, jan. 2019.

CREMONEZ, P. A. et al. Two-Stage anaerobic digestion in agroindustrial waste treatment: A review. **Journal of Environmental Management**, v. 281, n. August 2020, p. 111854, mar. 2021.

CURRY, N.; PILLAY, P. Biogas prediction and design of a food waste to energy system for the urban environment. **Renewable Energy**, v. 41, p. 200–209, maio 2012.

D. T. HILL. A Comprehensive Dynamic Model for Animal Waste Methanogenesis. **Transactions of the ASAE**, v. 25, n. 5, p. 1374–1380, 1982.

DA SILVA JÚNIOR, F. DAS C. G. et al. Anaerobic Digestion of the Liquid Fraction of Fruit and Vegetable Waste: Two-Stage versus Single-Stage Process. **ACS Omega**, v. 10, n. 22, p. 22847–22857, 29 maio 2025.

DAELS, T. et al. Calibration and statistical analysis of a simplified model for the anaerobic digestion of solid waste. **Environmental Technology**, v. 30, n. 14, p. 1575–1584, 14 dez. 2009.

DAIM, T. U. et al. Forecasting emerging technologies: Use of bibliometrics and patent analysis. **Technological Forecasting and Social Change**, v. 73, n. 8, p. 981–1012, 2006.

DANCKWERTS, P. V. Significance of Liquid-Film Coefficients in Gas Absorption. **Industrial & Engineering Chemistry**, v. 43, n. 6, p. 1460–1467, 1 jun. 1951.

DAREIOTI, M. A.; VAVOURAKI, A. I.; KORNAROS, M. Effect of pH on the anaerobic acidogenesis of agroindustrial wastewaters for maximization of bio-hydrogen production: A lab-scale evaluation using batch tests. **Bioresource Technology**, v. 162, p. 218–227, 2014.

DAVIS, P.; LIN, C. C.; SEGEL, L. A. **Mathematics Applied to Deterministic Problems in the Natural Sciences. The American Mathematical Monthly**, 1976.

DE BUCK, V.; POLANSKA, M.; VAN IMPE, J. Modeling Biowaste Biorefineries: A Review. **FRONTIERS IN SUSTAINABLE FOOD SYSTEMS**, v. 4, 2020.

DE MENEZES, C. A. et al. Two problems in one shot: Vinasse and glycerol co-digestion in a thermophilic high-rate reactor to improve process stability even at high sulfate concentrations. **Science of the Total Environment**, v. 862, n. December 2022, 2023.

DE MENEZES, C. A. et al. Innovative system to maximize methane production from fruit and vegetable waste. **Environmental Science and Pollution Research**, v. 31, n. 54, p. 62825–62839, 26 out. 2024.

DEENA, S. R. et al. **Enhanced biogas production from food waste and activated sludge using advanced techniques – A review**. **Bioresource Technology**Elsevier Ltd, , 2022. Disponível em: <https://doi.org/10.1016/j.biortech.2022.127234>

DEL NERY, V. et al. Hydraulic and organic rates applied to pilot scale UASB reactor for sugar cane vinasse degradation and biogas generation. **Biomass and Bioenergy**, v. 119, n. October, p. 411–417, dez. 2018.

DEMIREL, B.; SCHERER, P. The roles of acetotrophic and hydrogenotrophic methanogens during anaerobic conversion of biomass to methane: a review. **Reviews in Environmental Science and Bio/Technology**, v. 7, n. 2, p. 173–190, jun. 2008.

DEVI, M. K. et al. Bioresource Technology Recent advances in biogas production using Agro-Industrial Waste : A comprehensive review outlook of Techno-Economic analysis. **Bioresource Technology**, v. 363, n. June, p. 127871, 2022.

DIEKERT, G.; WOHLFARTH, G. Metabolism of homoacetogens. **Antonie van Leeuwenhoek**, v. 66, n. 1–3, p. 209–221, 1994.

DJAAFRI, M. et al. Anaerobic digestion of dry palms from five cultivars of Algerian date palm (Phoenix dactylifera L.) namely H'mira, Teggaza, Tinacer, Aghamou and Takarbouchet: A new comparative study. **Energy**, v. 269, n. January, p. 126774, abr. 2023.

DONOSO-BRAVO, A. et al. Model selection, identification and validation in anaerobic digestion: A review. **Water Research**, v. 45, n. 17, p. 5347–5364, 2011.

DUBOIS, M. et al. Colorimetric Method for Determination of Sugars and Related Substances. **Analytical Chemistry**, v. 28, n. 3, p. 350–356, 1 mar. 1956.

DUTTA, A.; DAVIES, C.; IKUMI, D. S. Performance of upflow anaerobic sludge blanket (UASB) reactor and other anaerobic reactor configurations for wastewater treatment: a comparative review and critical updates. **Journal of Water Supply: Research and Technology-Aqua**, v. 67, n. 8, p. 858–884, dez. 2018.

ECKENFELDER, W. W. **Industrial water pollution control.** 1st. ed. New York, NY: [s.n.].

ECONOMOU, C. N. et al. ADM1-Based Modeling of Biohydrogen Production through Anaerobic Co-Digestion of Agro-Industrial Wastes in a Continuous-Flow Stirred-Tank Reactor System. **Fermentation**, v. 10, n. 3, p. 138, 29 fev. 2024.

EDWIGES, T. et al. Influence of chemical composition on biochemical methane potential of fruit and vegetable waste. **Waste Management**, v. 71, p. 618–625, jan. 2018.

ELAIUY, M. L. C. et al. ADM1 modelling of large-scale covered in-ground anaerobic reactor treating sugarcane vinasse. **Water Science and Technology**, v. 77, n. 5, p. 1397–1409, 12 mar. 2018.

ELMITWALLI, T. et al. Anaerobic Biodegradability and Treatment of Egyptian Domestic Sewage. **Journal of Environmental Science and Health, Part A**, v. 38, n. 10, p. 2043–2055, out. 2003a.

ELMITWALLI, T. A. et al. Decentralised treatment of concentrated sewage at low temperature

in a two-step anaerobic system: two upflow-hybrid septic tanks. **Water Science and Technology**, v. 48, n. 6, p. 219–226, 1 set. 2003b.

ELSAMADONY, M.; TAWFIK, A.; SUZUKI, M. Surfactant-enhanced biohydrogen production from organic fraction of municipal solid waste (OFMSW) via dry anaerobic digestion. **Applied Energy**, v. 149, p. 272–282, 2015.

EMEBU, S.; PECHA, J.; JANACOVA, D. Review on anaerobic digestion models: Model classification \& elaboration of process phenomena. **RENEWABLE \& SUSTAINABLE ENERGY REVIEWS**, v. 160, 2022.

ESPOSITO, G. et al. Mathematical modelling of disintegration-limited co-digestion of OFMSW and sewage sludge. **Water Science and Technology**, v. 58, n. 7, p. 1513–1519, 2008.

ESPOSITO, G. et al. Modelling the effect of the OLR and OFMSW particle size on the performances of an anaerobic co-digestion reactor. **Process Biochemistry**, v. 46, n. 2, p. 557–565, fev. 2011a.

ESPOSITO, G. et al. Model calibration and validation for OFMSW and sewage sludge co-digestion reactors. **Waste Management**, v. 31, n. 12, p. 2527–2535, dez. 2011b.

FAGHRI, A.; ZHANG, Y. Generalized Governing Equations in Multiphase Systems: Local Instance Formulations. **Transport Phenomena in Multiphase Systems**, p. 177–237, 2006.

FAO. Marco estratégico de la FAO para 2022-2031. **Informe técnico**, p. 1–44, 2021.

FAO, (FOOD AND AGRICULTURE ORGANIZATION). **Global food waste by country: who's the biggest waster?** Disponível em: <www.fao.org/save-food/resources/infographic/en/>. Acesso em: 10 fev. 2024.

FDEZ-GÜELFO, L. A. et al. Dry-thermophilic anaerobic digestion of organic fraction of municipal solid waste: Methane production modeling. **Waste Management**, v. 32, n. 3, p. 382–388, mar. 2012.

FEDOROVICH, V.; LENS, P.; KALYUZHNYI, S. Extension of Anaerobic Digestion Model No. 1 with Processes of Sulfate Reduction. **Applied Biochemistry and Biotechnology**, v. 109, n. 1–3, p. 33–46, 2003.

FENG, Y. et al. Implementation of the IWA anaerobic digestion model No.1 (ADM1) for simulating digestion of blackwater from vacuum toilets. **Water Science and Technology**, v. 53, n. 9, p. 253–263, 1 maio 2006.

FERNÁNDEZ, J.; PÉREZ, M.; ROMERO, L. I. Effect of substrate concentration on dry mesophilic anaerobic digestion of organic fraction of municipal solid waste (OFMSW). **Bioresource Technology**, v. 99, n. 14, p. 6075–6080, 2008.

FERRER, P. et al. The use of agricultural substrates to improve methane yield in anaerobic co-digestion with pig slurry: Effect of substrate type and inclusion level. **Waste Management**, v. 34, n. 1, p. 196–203, jan. 2014.

FESTAG, S.; DENZLER, J.; SPRECKELSEN, C. Generative adversarial networks for biomedical time series forecasting and imputation. **Journal of Biomedical Informatics**, v. 129,

n. February, p. 104058, maio 2022.

FEZZANI, B.; BEN CHEIKH, R. Implementation of IWA anaerobic digestion model No. 1 (ADM1) for simulating the thermophilic anaerobic co-digestion of olive mill wastewater with olive mill solid waste in a semi-continuous tubular digester. **CHEMICAL ENGINEERING JOURNAL**, v. 141, n. 1–3, p. 75–88, jul. 2008.

FISGATIVA, H.; TREMIER, A.; DABERT, P. Characterizing the variability of food waste quality: A need for efficient valorisation through anaerobic digestion. **Waste Management**, v. 50, p. 264–274, 2016.

FORSTER-CARNEIRO, T. et al. Dry-thermophilic anaerobic digestion of organic fraction of the municipal solid waste: Focusing on the inoculum sources. **Bioresource Technology**, v. 98, n. 17, p. 3195–3203, dez. 2007.

FORTELA, D. L. B. et al. Computational evaluation for effects of feedstock variations on the sensitivities of biochemical mechanism parameters in anaerobic digestion kinetic models. **Biochemical Engineering Journal**, v. 143, p. 212–223, mar. 2019.

FRKOVA, Z. et al. Assessment of the production of biodiesel from urban wastewater-derived lipids. **Resources, Conservation and Recycling**, v. 162, n. July, p. 105044, 2020.

FRUNZO, L. et al. ADM1-based mechanistic model for the role of trace elements in anaerobic digestion processes. **Journal of Environmental Management**, v. 241, n. April, p. 587–602, jul. 2019.

FUESS, L. T.; ZAIAT, M.; DO NASCIMENTO, C. A. O. Novel insights on the versatility of biohydrogen production from sugarcane vinasse via thermophilic dark fermentation: Impacts of pH-driven operating strategies on acidogenesis metabolite profiles. **Bioresource Technology**, v. 286, p. 20–25, 2019.

GALI, A. et al. Modified version of ADM1 model for agro-waste application. **BIORESOURCE TECHNOLOGY**, v. 100, n. 11, p. 2783–2790, jun. 2009.

GARCIA-BERNET, D. et al. Rapid measurement of the yield stress of anaerobically-digested solid waste using slump tests. **Waste Management**, v. 31, n. 4, p. 631–635, abr. 2011.

GAVALA, H. N. et al. Anaerobic codigestion of agricultural industries' wastewaters. **Water Science and Technology**, v. 34, n. 11, p. 67–75, 1 dez. 1996.

GAVALA, H. N.; ANGELIDAKI, I.; AHRING, B. K. **Kinetics and modeling of anaerobic digestion process. Advances in biochemical engineering/biotechnology**, 2003.

GE, Y. et al. Modification of anaerobic digestion model No.1 with Machine learning models towards applicable and accurate simulation of biomass anaerobic digestion. **CHEMICAL ENGINEERING JOURNAL**, v. 454, n. 3, 2023.

GIRARDI NETO, J.; SILVA, J. D. DA; PINHEIRO, I. G. Balanço de massa no tratamento de resíduos sólidos orgânicos provenientes de restaurantes em biorreator. **Engenharia Sanitaria e Ambiental**, v. 22, n. 3, p. 491–499, maio 2017.

GLIVIN, G.; SEKHAR, S. J. Waste Potential, Barriers and Economic Benefits of Implementing

Different Models of Biogas Plants in a Few Indian Educational Institutions. **BioEnergy Research**, v. 13, n. 2, p. 668–682, 23 jun. 2020.

GOMEZ-ROMERO, J. et al. Selective adaptation of an anaerobic microbial community: Biohydrogen production by co-digestion of cheese whey and vegetables fruit waste. **International Journal of Hydrogen Energy**, v. 39, n. 24, p. 12541–12550, ago. 2014.

GOMPERTZ, B. XXIV. On the nature of the function expressive of the law of human mortality, and on a new mode of determining the value of life contingencies. In a letter to Francis Baily, Esq. F. R. S. &c. **Philosophical Transactions of the Royal Society of London**, v. 115, p. 513–583, 31 dez. 1825.

GONÇALVES NETO, J. et al. Modeling of biogas production from food, fruits and vegetables wastes using artificial neural network (ANN). **Fuel**, v. 285, n. June 2020, p. 119081, fev. 2021.

GRAEF, S. P.; ANDREWS, J. F. **AIChE symposium series**. New York, NY, 1973. Disponível em: <http://slubdd.de/katalog?TN_libero_mab2>

GUERRERO, L. et al. Fly ash as stimulant for anaerobic digestion: effect over hydrolytic stage and methane generation rate. **WATER SCIENCE AND TECHNOLOGY**, v. 80, n. 7, p. 1384–1391, 2019.

GUJER, W.; ZEHNDER, A. J. B. Conversion Processes in Anaerobic Digestion. **Water Science and Technology**, v. 15, n. 8–9, p. 127–167, 1 ago. 1983.

GULHANE, M. et al. Bioresource Technology Biomethanation of vegetable market waste in an anaerobic baffled reactor : Effect of effluent recirculation and carbon mass balance analysis. **Bioresource Technology**, v. 215, p. 100–109, 2016.

GUPTA, S. et al. Microbes and Parameters Influencing Dark Fermentation for Hydrogen Production. **Applied Sciences (Switzerland)**, v. 14, n. 23, p. 1–26, 2024.

HABIBA, L.; HASSIB, B.; MOKTAR, H. Improvement of activated sludge stabilisation and filterability during anaerobic digestion by fruit and vegetable waste addition. **Bioresource Technology**, v. 100, n. 4, p. 1555–1560, 2009.

HAGOS, K. et al. Anaerobic co-digestion process for biogas production: Progress, challenges and perspectives. **Renewable and Sustainable Energy Reviews**, v. 76, n. November 2016, p. 1485–1496, 2017.

HAI-LOU, X.; JING-YUAN, W.; JOO-HWA, T. A hybrid anaerobic solid-liquid bioreactor for food waste digestion. **Biotechnology Letters**, v. 24, p. 757–761, 2002.

HALLENBECK, P. C.; BENEMANN, J. R. Biological hydrogen production; Fundamentals and limiting processes. **International Journal of Hydrogen Energy**, v. 27, n. 11–12, p. 1185–1193, 2002.

HANGOS, K. M.; CAMERON, I. T. **Process Modelling and Model Analysis**. San Diego: Academic Press, 2001.

HASELI, Y. Fundamental concepts. In: **Entropy Analysis in Thermal Engineering Systems**. [s.l: s.n.]. p. 1–11.

HASSAM, S. et al. A generic and systematic procedure to derive a simplified model from the anaerobic digestion model No. 1 (ADM1). **Biochemical Engineering Journal**, v. 99, p. 193–203, 2015.

HATTA, A. H. et al. A short review on informetric analysis and recent progress on contribution of ceria in Ni-based catalysts for enhanced catalytic CO methanation. **Powder Technology**, v. 417, p. 118246, mar. 2023.

HE, Z. et al. High-solid co-digestion performance of lipids and food waste by mesophilic hollow fiber anaerobic membrane bioreactor. **Bioresource Technology**, v. 374, n. January, p. 128812, 2023.

HENZE, M. et al. **Activated sludge models ASM1, ASM2, ASM2d and ASM3**. [s.l.] IWA Publishing, Alliance House, 12 Caxton Street, London SW1H 0QS, UK, 2000.

HENZE, M. et al. Activated Sludge Models ASM1, ASM2, ASM2d and ASM3. **Water Intelligence Online**, v. 5, p. 9781780402369–9781780402369, 30 dez. 2015.

HIERHOLTZER, A.; AKUNNA, J. C. Modelling sodium inhibition on the anaerobic digestion process. **Water Science and Technology**, v. 66, n. 7, p. 1565–1573, 1 out. 2012.

HILKIAH IGONI, A. et al. Designs of anaerobic digesters for producing biogas from municipal solid-waste. **Applied Energy**, v. 85, n. 6, p. 430–438, 2008.

HILL, D. T.; BARTH, C. L. A dynamic model for simulation of animal waste digestion. **Journal of the Water Pollution Control Federation**, v. 49, n. 10, p. 2129–2143, 1977.

HOLM-NIELSEN, J. B.; AL SEADI, T.; OLESKOWICZ-POPIEL, P. The future of anaerobic digestion and biogas utilization. **Bioresource Technology**, v. 100, n. 22, p. 5478–5484, 2009.

HU, C. et al. Modeling the performance of anaerobic digestion reactor by the anaerobic digestion system model (ADSM). **Journal of Environmental Chemical Engineering**, v. 6, n. 2, p. 2095–2104, abr. 2018.

HUA, J.; WU, M.; KUMAR, K. Numerical simulation of the combustion of hydrogen–air mixture in micro-scaled chambers. Part I: Fundamental study. **Chemical Engineering Science**, v. 60, n. 13, p. 3497–3506, jul. 2005.

IBGE. **PIB da agropecuária cresce 11,7% e impulsiona resultado da economia em 2025**. Disponível em: <https://www.gov.br/agricultura/pt-br/assuntos/noticias/pib-da-agropecuaria-cresce-11-7-e-impulsiona-resultado-da-economia-em-2025>. Acesso em: 12 mar. 2026.

IPCC, I. P. O. C. C. Climate Change and Land An. **Encyclopedia of Biodiversity, Third Edition: Volume 1-7**, p. 906, 2019.

JENKINS, B. M. et al. Current Anaerobic Digestion Technologies Used for Treatment of Municipal Organic Solid Waste. n. March, 2008.

JEPPSSON, U. et al. Benchmark simulation model no 2: general protocol and exploratory case studies. **WATER SCIENCE AND TECHNOLOGY**, v. 56, n. 8, p. 67–78, 2007.

JEYASEELAN, S. A simple mathematical model for anaerobic digestion process. **Water**

Science & Technology, v. 35, p. 185–191, 1997.

JI, C. et al. A Review of the Anaerobic Digestion of Fruit and Vegetable Waste. **Applied Biochemistry and Biotechnology**, v. 183, n. 3, p. 906–922, 17 nov. 2017.

JIANG, Y.; HEAVEN, S.; BANKS, C. J. Strategies for stable anaerobic digestion of vegetable waste. **Renewable Energy**, v. 44, p. 206–214, ago. 2012.

JUNG, K. W. et al. Conversion of organic solid waste to hydrogen and methane by two-stage fermentation system with reuse of methane fermenter effluent as diluting water in hydrogen fermentation. **Bioresource Technology**, v. 139, p. 120–127, 2013.

JURADO, E. et al. Continuous anaerobic digestion of swine manure: ADM1-based modelling and effect of addition of swine manure fibers pretreated with aqueous ammonia soaking. **Applied Energy**, v. 172, p. 190–198, 2016.

KALFAS, H. et al. Application of ADM1 for the simulation of anaerobic digestion of olive pulp under mesophilic and thermophilic conditions. **Water Science and Technology**, v. 54, n. 4, p. 149–156, 1 ago. 2006.

KALYUZHNYI, S. V. Batch anaerobic digestion of glucose and its mathematical modeling. II. Description verification and application of model. **Bioresource Technology**, v. 59, n. 2–3, p. 249–258, 1997.

KAMADA, T.; KAWAI, S. An algorithm for drawing general undirected graphs. **Information Processing Letters**, v. 31, n. 1, p. 7–15, abr. 1989.

KAPDAN, I. K.; KARGI, F. Bio-hydrogen production from waste materials. **Enzyme and Microbial Technology**, v. 38, n. 5, p. 569–582, mar. 2006.

KARMEE, S. K. Liquid biofuels from food waste: Current trends, prospect and limitation. **Renewable and Sustainable Energy Reviews**, v. 53, p. 945–953, 2016.

KAYHANIAN, M. Ammonia inhibition in high-solids biogasification: An overview and practical solutions. **Environmental Technology (United Kingdom)**, v. 20, n. 4, p. 355–365, 1999.

KEGL, T. et al. Modeling and optimization of anaerobic digestion technology: Current status and future outlook. **Progress in Energy and Combustion Science**, v. 106, n. August 2024, p. 101199, jan. 2025.

KELLER, J. et al. Dynamic model simulation and verification of a two-stage high-rate anaerobic treatment process with recycle. **Water Science and Technology**, p. 197–207, 1993.

KHAN, M. et al. **Applications of artificial intelligence in anaerobic co-digestion: Recent advances and prospects**. **Bioresource Technology**Elsevier Ltd, , 2023. Disponível em: <https://doi.org/10.1016/j.biortech.2022.128501>

KIELY, G. et al. Physical and mathematical modelling of anaerobic digestion of organic wastes. **Water Research**, v. 31, n. 3, p. 534–540, mar. 1997.

KIM, M.; CUI, F. A simplified stoichiometric kinetic model for estimating the concentration

of reaction products in anaerobic digestion. **ENVIRONMENTAL TECHNOLOGY**, v. 38, n. 20, p. 2573–2580, 2017.

KLEINSTREUER, C.; POWEIGHA, T. Dynamic Simulator for Anaerobic Digestion Processes. v. XXIV, p. 1941–1951, 1982.

KOCH, K. et al. Biogas from grass silage - Measurements and modeling with ADM1. **Bioresource Technology**, v. 101, n. 21, p. 8158–8165, 2010.

KOCH, K. et al. Erratum to "Biogas from grass silage – Measurements and modeling with ADM1" [Bioresour. Technol. 101 (2010) 8158–8165]. **Bioresource Technology**, v. 102, n. 2, p. 2141, jan. 2011.

KOTHARI, R. et al. Different aspects of dry anaerobic digestion for bio-energy: An overview. **Renewable and Sustainable Energy Reviews**, v. 39, p. 174–195, 2014.

KRICH, K. K. et al. Stoichiometry of the Anaerobic Digestion Process. **Biomethane from Dairy Waste: A Sourcebook for the Production and Use of Renewable Natural Gas in California**, n. 3, p. A1–A6, 2005.

KUCHARSKA, K. et al. Key issues in modeling and optimization of lignocellulosic biomass fermentative conversion to gaseous biofuels. **RENEWABLE ENERGY**, v. 129, n. A, p. 384–408, 2018.

KUMAR, A.; SAMADDER, S. R. Performance evaluation of anaerobic digestion technology for energy recovery from organic fraction of municipal solid waste: A review. **Energy**, v. 197, p. 117253, abr. 2020.

LABATUT, R. A.; ANGENENT, L. T.; SCOTT, N. R. Biochemical methane potential and biodegradability of complex organic substrates. **Bioresource Technology**, v. 102, n. 3, p. 2255–2264, 2011.

LAUWERS, J. et al. Mathematical modelling of anaerobic digestion of biomass and waste: Power and limitations. **Progress in Energy and Combustion Science**, v. 39, n. 4, p. 383–402, ago. 2013.

LEE, M. Y. et al. Variation of ADM1 by using temperature-phased anaerobic digestion (TPAD) operation. **Bioresource Technology**, v. 100, n. 11, p. 2816–2822, jun. 2009.

LI, D. et al. Instability diagnosis and syntrophic acetate oxidation during thermophilic digestion of vegetable waste. **Water Research**, v. 139, p. 263–271, ago. 2018a.

LI, D. Model application to a lab-scale thermophilic hydrogenotrophic methanation system. **BIOCHEMICAL ENGINEERING JOURNAL**, v. 177, jan. 2022.

LI, D.; LEE, I.; KIM, H. Application of the linearized ADM1 (LADM) to lab-scale anaerobic digestion system. **Journal of Environmental Chemical Engineering**, v. 9, n. 3, p. 105193, jun. 2021.

LI, L. et al. Anaerobic digestion of food waste: Correlation of kinetic parameters with operational conditions and process performance. **BIOCHEMICAL ENGINEERING JOURNAL**, v. 130, p. 1–9, 2018b.

LI, L. et al. Insights into high-solids anaerobic digestion of food waste enhanced by activated carbon via promoting direct interspecies electron transfer. **Bioresource Technology**, v. 351, p. 127008, maio 2022.

LI, P. et al. Application of Anaerobic Digestion Model No. 1 for modeling anaerobic digestion of vegetable crop residues: Fractionation of crystalline cellulose. **Journal of Cleaner Production**, v. 285, p. 124865, fev. 2021.

LI, W. et al. A review of high-solid anaerobic digestion (HSAD): From transport phenomena to process design. **Renewable and Sustainable Energy Reviews**, v. 180, n. September 2022, p. 113305, 2023.

LI, X. et al. Modified anaerobic digestion model No.1 (<scp>ADM</scp> 1) for modeling anaerobic digestion process at different ammonium concentrations. **Water Environment Research**, v. 91, n. 8, p. 700–714, ago. 2019.

LI, Y. et al. Current Situation and Development of Kitchen Waste Treatment in China. **Procedia Environmental Sciences**, v. 31, p. 40–49, 2016.

LI, Y.; CHEN, Y.; WU, J. Enhancement of methane production in anaerobic digestion process: A review. **Applied Energy**, v. 240, n. January, p. 120–137, abr. 2019.

LI, Y.; PARK, S. Y.; ZHU, J. Solid-state anaerobic digestion for methane production from organic waste. **Renewable and Sustainable Energy Reviews**, v. 15, n. 1, p. 821–826, jan. 2011.

LI, Y. Y. et al. High-rate methane fermentation of lipid-rich food wastes by a high-solids co-digestion process. **Water Science and Technology**, v. 45, n. 12, p. 143–150, 2002.

LIMA, H. Q. DE; MARTINS, G. Anaerobic digestion (AD) of municipal solid waste in Santo André-SP: Review. **International Solid Waste Association World Congress**, n. January, p. 12, 2014.

LIN, C.-Y. et al. Optimization of Hydrolysis-Acidogenesis Phase of Swine Manure for Biogas Production Using Two-Stage Anaerobic Fermentation. **Processes**, v. 9, n. 8, p. 1324, 29 jul. 2021a.

LIN, C. Y. et al. Biogas production from beverage factory wastewater in a mobile bioenergy station. **Chemosphere**, v. 264, p. 128564, 2021b.

LINDMARK, J. et al. PROBLEMS AND POSSIBILITIES WITH THE IMPLEMENTATION OF SIMULATION AND MODELING AT A BIOGAS PLANT. n. 1, p. 1–8, 2012.

LIOTTA, F. et al. Modified Anaerobic Digestion Model No.1 for dry and semi-dry anaerobic digestion of solid organic waste. **Environmental Technology**, v. 36, n. 7, p. 870–880, 3 abr. 2015.

LIU, J. et al. Heat transfer analysis of cylindrical anaerobic reactors with different sizes: a heat transfer model. **Environmental Science and Pollution Research**, v. 24, n. 30, p. 23508–23517, 2017.

LIU, J.; XU, Y.; WEI, Y. A model-based approach for evaluating the effects of sludge rheology

on methane production during high solid anaerobic digestion: Focusing on mass transfer resistance. **Biochemical Engineering Journal**, v. 201, n. November 2023, p. 109147, jan. 2024.

LIU, X. et al. Pilot-scale anaerobic co-digestion of municipal biomass waste: Focusing on biogas production and GHG reduction. **Renewable Energy**, v. 44, p. 463–468, 2012.

LOHANI, S. P. et al. ADM1 modeling of UASB treating domestic wastewater in Nepal. **Renewable Energy**, v. 95, p. 263–268, 2016.

LOPES, A. DO C. P. et al. Biogas production from thermophilic anaerobic digestion of kraft pulp mill sludge. **Renewable Energy**, v. 124, p. 40–49, 2018.

LÓPEZ-ILLESCAS, C.; DE MOYA-ANEGÓN, F.; MOED, H. F. Coverage and citation impact of oncological journals in the Web of Science and Scopus. **Journal of Informetrics**, v. 2, n. 4, p. 304–316, out. 2008.

LÓPEZ-ILLESCAS, C.; DE MOYA ANEGÓN, F.; MOED, H. F. Comparing bibliometric country-by-country rankings derived from the Web of Science and Scopus: the effect of poorly cited journals in oncology. **Journal of Information Science**, v. 35, n. 2, p. 244–256, 21 abr. 2009.

LÜBKEN, M. et al. Modelling the energy balance of an anaerobic digester fed with cattle manure and renewable energy crops. **Water Research**, v. 41, n. 18, p. 4085–4096, out. 2007.

LÜBKEN, M. et al. Influent Fractionation for Modeling Continuous Anaerobic Digestion Processes. In: GUEBITZ, G. M. et al. (Eds.). **Biogas Science and Technology**. Advances in Biochemical Engineering/Biotechnology. Cham: Springer International Publishing, 2015a. v. 151p. 137–169.

LÜBKEN, M. et al. Parameter estimation and long-term process simulation of a biogas reactor operated under trace elements limitation. **Applied Energy**, v. 142, p. 352–360, mar. 2015b.

LUO, T. et al. The impact of immersed liquid circulation on anaerobic digestion of rice straw bale and methane generation improvement. **Bioresource Technology**, v. 337, n. April, p. 125368, 2021.

MAGAMA, P.; CHIYANZU, I.; MULOPO, J. Bioresource Technology Reports A systematic review of sustainable fruit and vegetable waste recycling alternatives and possibilities for anaerobic biorefinery. **Bioresource Technology Reports**, v. 18, n. February, p. 101031, 2022.

MANJUSHA, C.; BEEVI, S. B. **Mathematical Modeling and Simulation of Anaerobic Digestion of Solid Waste**. (C. Viswanathan, R. S. Kumar, Eds.)INTERNATIONAL CONFERENCE ON EMERGING TRENDS IN ENGINEERING, SCIENCE AND TECHNOLOGY (ICETEST - 2015). **Anais**...: Procedia Technology.SARA BURGERHARTSTRAAT 25, PO BOX 211, 1000 AE AMSTERDAM, NETHERLANDS: ELSEVIER SCIENCE BV, 2016.

MÄRKL, H. Modeling of Biogas Reactors. In: **Environmental Biotechnology**. [s.l.] Wiley, 2004. p. 40–202.

MARSILI-LIBELLI, S.; NARDINI, M. Stability and sensitivity analysis of anaerobic digestion models. **Environmental Technology Letters**, v. 6, n. 12, p. 602–609, 17 dez. 1985.

MASEBINU, S. O. et al. Experimental and feasibility assessment of biogas production by anaerobic digestion of fruit and vegetable waste from Joburg Market. **Waste Management**, v. 75, p. 236–250, maio 2018.

MATA-ALVAREZ, J. et al. Codigestion of solid wastes: A review of its uses and perspectives including modeling. **Critical Reviews in Biotechnology**, v. 31, n. 2, p. 99–111, 25 jun. 2011.

MATA-ALVAREZ, J.; MACÉ, S.; LLABRÉS, P. Anaerobic digestion of organic solid wastes. An overview of research achievements and perspectives. **Bioresource Technology**, v. 74, n. 1, p. 3–16, 2000.

MATHERI, A. N. et al. Optimising biogas production from anaerobic co-digestion of chicken manure and organic fraction of municipal solid waste. **Renewable and Sustainable Energy Reviews**, v. 80, n. February, p. 756–764, 2017.

MCCULLOCH, W. S.; PITTS, W. A logical calculus of the ideas immanent in nervous activity. **The Bulletin of Mathematical Biophysics**, v. 5, n. 4, p. 115–133, dez. 1943.

MEENA, R. A. A. et al. Biohythane production from food processing wastes – Challenges and perspectives. **Bioresource Technology**, v. 298, n. November 2019, p. 122449, fev. 2020.

MENEZES, C. A. DE et al. Using fruit and vegetable waste to generate hydrogen through dark fermentation. **Engenharia Sanitaria e Ambiental**, v. 29, p. 1–7, 2024.

MIHI, M. et al. Modeling and forecasting biogas production from anaerobic digestion process for sustainable resource energy recovery. **Heliyon**, v. 10, n. 19, p. e38472, 2024.

MO, R. et al. Modifications to the anaerobic digestion model no. 1 (ADM1) for enhanced understanding and application of the anaerobic treatment processes – A comprehensive review. **Water Research**, v. 244, n. May, p. 120504, out. 2023.

MOKHTARANI, B.; ZANGANEH, J.; MOGHTADERI, B. A Review on Biohydrogen Production Through Dark Fermentation, Process Parameters and Simulation. **Energies**, v. 18, n. 5, p. 1–24, 2025.

MOLETTA, R.; VERRIER, D.; ALBAGNAC, G. Dynamic modelling of anaerobic digestion. **Water Research**, v. 20, n. 4, p. 427–434, abr. 1986.

MOMAYEZ, F.; KARIMI, K.; TAHERZADEH, M. J. Energy recovery from industrial crop wastes by dry anaerobic digestion: A review. **Industrial Crops and Products**, v. 129, n. November 2018, p. 673–687, 2019.

MONOD, J. THE GROWTH OF BACTERIAL CULTURES. **Annual Review of Microbiology**, v. 3, n. 1, p. 371–394, out. 1949.

MORAN, M. J. et al. **Princípios De Termodinâmica Para Engenharia**. 7. ed. [s.l: s.n.].

MOSEY, F. E. Mathematical Modelling of the Anaerobic Digestion Process: Regulatory Mechanisms for the Formation of Short-Chain Volatile Acids from Glucose. **Water Science**

and Technology, v. 15, n. 8–9, p. 209–232, 1 ago. 1983.

MU, L. et al. Anaerobic co-digestion of sewage sludge, food waste and yard waste: Synergistic enhancement on process stability and biogas production. **Science of the Total Environment**, v. 704, p. 135429, 2020.

MUELLER, E. P. et al. **Shifts in ruminant fermentation during inhibition of methanogenesis are reflected in the isotope compositions of volatile fatty acids**. , 2025. Disponível em: <http://biorxiv.org/lookup/doi/10.1101/2025.10.16.682381>

MÛNCH, E. V. et al. Mathematical Modelling of Prefermenters-I . Model Development and Verification. **Water research**, v. 33, n. 12, p. 2844–2854, 1999.

MYINT, M.; NIRMALAKHANDAN, N.; SPEECE, R. E. Anaerobic fermentation of cattle manure: Modeling of hydrolysis and acidogenesis. **Water Research**, v. 41, n. 2, p. 323–332, jan. 2007.

NABATEREGA, R. et al. A review on two-stage anaerobic digestion options for optimizing municipal wastewater sludge treatment process. **Journal of Environmental Chemical Engineering**, v. 9, n. 4, p. 105502, ago. 2021.

NABATEREGA, R.; NAZYAB, B.; ESKICIOGLU, C. Modification and calibration of anaerobic digestion model 1 to simulate volatile fatty acids production during fermentation of municipal sludge. **Biochemical Engineering Journal**, v. 194, p. 108886, maio 2023.

NASH, J. E.; SUTCLIFFE, J. V. River flow forecasting through conceptual models part I — A discussion of principles. **Journal of Hydrology**, v. 10, n. 3, p. 282–290, abr. 1970.

NELDER, J. A.; MEAD, R. A Simplex Method for Function Minimization. **The Computer Journal**, v. 7, n. 4, p. 308–313, 1 jan. 1965.

NGO, A. VAN et al. A dynamic simulation of methane fermentation process receiving heterogeneous food wastes and modelling acidic failure. **JOURNAL OF MATERIAL CYCLES AND WASTE MANAGEMENT**, v. 18, n. 2, p. 239–247, 2016.

NGUYEN, H. H. Modelling of food waste digestion using ADM1 integrated with Aspen Plus. **Doctor thesis**, n. June, p. 273, 2014.

NI, J. Mechanistic Models of Ammonia Release from Liquid Manure: a Review. **Journal of Agricultural Engineering Research**, v. 72, n. 1, p. 1–17, jan. 1999.

NOYKOVA, N. et al. Quantitative analyses of anaerobic wastewater treatment processes: Identifiability and parameter estimation. **Biotechnology and Bioengineering**, v. 78, n. 1, p. 89–103, 2002.

OGEDA, T. L.; PETRI, D. F. S. Hidrólise Enzimática de Biomassa. **Química Nova**, v. 33, n. 7, p. 1549–1558, 2010.

OKORO-SHEKWAGA, C. K.; ROSS, A. B.; CAMARGO-VALERO, M. A. Improving the biomethane yield from food waste by boosting hydrogenotrophic methanogenesis. **Applied Energy**, v. 254, n. July, p. 113629, nov. 2019.

OLESZKIEWICZ, J. A.; POGGI-VARALDO, H. M. High-Solids Anaerobic Digestion of Mixed Municipal and Industrial Waste. **Journal of Environmental Engineering**, v. 123, n. 11, p. 1087–1092, nov. 1997.

PAGLIACCIA, P. et al. Variability of food waste chemical composition : Impact of thermal pre- treatment on lignocellulosic matrix and anaerobic biodegradability. **Journal of Environmental Management**, v. 236, n. February, p. 100–107, 2019.

PALANICHAMY, J.; PALANI, S. Simulation of anaerobic digestion processes using stochastic algorithm. **Journal of Environmental Health Science and Engineering**, v. 12, n. 1, p. 121, 4 dez. 2014a.

PALANICHAMY, J.; PALANI, S. Simulation of anaerobic digestion processes using stochastic algorithm. **Journal of Environmental Health Science and Engineering**, v. 12, n. 1, p. 121, 4 dez. 2014b.

PALATSI, J. et al. Long-chain fatty acids inhibition and adaptation process in anaerobic thermophilic digestion: Batch tests, microbial community structure and mathematical modelling. **Bioresource Technology**, v. 101, n. 7, p. 2243–2251, abr. 2010.

PARANHOS, A. G. DE O.; SILVA, E. L. Optimized 1,3-propanediol production from crude glycerol using mixed cultures in batch and continuous reactors. **Bioprocess and Biosystems Engineering**, v. 41, n. 12, p. 1807–1816, 30 dez. 2018.

PASSAS, I. Bibliometric Analysis: The Main Steps. **Encyclopedia**, v. 4, n. 2, p. 1014–1025, 20 jun. 2024.

PASTOR-POQUET, V. et al. High-solids anaerobic digestion model for homogenized reactors. **Water Research**, v. 142, n. 1, p. 501–511, 2018.

PASTOR-POQUET, V. et al. Modelling non-ideal bio-physical-chemical effects on high-solids anaerobic digestion of the organic fraction of municipal solid waste. **Journal of Environmental Management**, v. 238, n. March, p. 408–419, maio 2019a.

PASTOR-POQUET, V. et al. Assessing practical identifiability during calibration and cross-validation of a structured model for high-solids anaerobic digestion. **Water Research**, v. 164, n. 1, p. 114932, nov. 2019b.

PAUDEL, S. R. et al. Pretreatment of agricultural biomass for anaerobic digestion: Current state and challenges. **Bioresource Technology**, v. 245, n. July, p. 1194–1205, dez. 2017.

PAVLOSTATHIS, S. G.; GIRALDO-GOMEZ, E. Kinetics of anaerobic treatment: A critical review. **Critical Reviews in Environmental Control**, v. 21, n. 5–6, p. 411–490, jan. 1991.

PEIRIS, B. R. H. et al. ADM1 simulations of hydrogen production. **Water Science and Technology**, v. 53, n. 8, p. 129–137, 1 abr. 2006.

PENUMATHSA, B. K. V. et al. Erratum to “ADM1 can be applied to continuous bio-hydrogen production using a variable stoichiometry approach” [Water Res. 42 (2008) 16]. **Water Research**, v. 43, n. 2, p. 562, fev. 2009.

PENUMATHSA, B. K. V et al. ADM1 can be applied to continuous bio-hydrogen production

using a variable stoichiometry approach. **WATER RESEARCH**, v. 42, n. 16, p. 4379–4385, 2008.

POGGIO, D. et al. Modelling the anaerobic digestion of solid organic waste – Substrate characterisation method for ADM1 using a combined biochemical and kinetic parameter estimation approach. **Waste Management**, v. 53, p. 40–54, jul. 2016.

POKORNA-KRAYZELOVA, L. et al. Model-based optimization of microaeration for biogas desulfurization in UASB reactors. **Biochemical Engineering Journal**, v. 125, p. 171–179, set. 2017.

PONTES, R. F. F.; PINTO, J. M. Analysis of integrated kinetic and flow models for anaerobic digesters. **Chemical Engineering Journal**, v. 122, n. 1–2, p. 65–80, set. 2006.

QIAN, M. Y. et al. Industrial scale garage-type dry fermentation of municipal solid waste to biogas. **Bioresource Technology**, v. 217, p. 82–89, 2016.

RAJAGOPAL, R.; MASSÉ, D. I.; SINGH, G. A critical review on inhibition of anaerobic digestion process by excess ammonia. **Bioresource Technology**, v. 143, p. 632–641, 2013.

RALSTON, M. L.; JENNRICH, R. I. Dud, A Derivative-Free Algorithm for Nonlinear Least Squares. **Technometrics**, v. 20, n. 1, p. 7–14, fev. 1978.

RAMIREZ, I. et al. Modified ADM1 disintegration/hydrolysis structures for modeling batch thermophilic anaerobic digestion of thermally pretreated waste activated sludge. **Water Research**, v. 43, n. 14, p. 3479–3492, ago. 2009.

RAPPORT, J. L. et al. Anaerobic Digestion technologies for the treatment of Municipal Solid Waste. **International Journal of Environment and Waste Management**, v. 9, n. 1/2, p. 100, 2012.

RASMUSON, A. et al. **Mathematical modeling in chemical engineering**. [s.l: s.n.]. v. 9781107049

RAZAVIARANI, V.; BUCHANAN, I. D. Calibration of the Anaerobic Digestion Model No. 1 (ADM1) for steady-state anaerobic co-digestion of municipal wastewater sludge with restaurant grease trap waste. **Chemical Engineering Journal**, v. 266, p. 91–99, abr. 2015.

REGMI, P. et al. The future of WRRF modelling - Outlook and challenges. **Water Science and Technology**, v. 79, n. 1, p. 3–14, 2019.

REICHERT, P. **AQUASIM 2.0 — Computer program for the identification and simulation of aquatic systems**. Switzerland: [s.n.].

REN, N.; WANG, B.; HUANG, J.-C. Ethanol-type fermentation from carbohydrate in high rate acidogenic reactor. **Biotechnology and Bioengineering**, v. 54, n. 5, p. 428–433, 5 jun. 1997.

REN, T. et al. Hydrodynamics of upflow anaerobic sludge blanket reactors. **AIChE Journal**, v. 55, n. 2, p. 516–528, 23 fev. 2009.

RITTMANN, P.; MCCARTY, B. Environmental Biotechnology: Principles and Applications. 2001.

RITTMANN, S.; HOLUBAR, P. Rapid extraction of total RNA from an anaerobic sludge biocoenosis. **FOLIA MICROBIOLOGICA**, v. 59, n. 2, p. 127–132, mar. 2014.

RIYA, S. et al. The influence of the total solid content on the stability of dry-thermophilic anaerobic digestion of rice straw and pig manure. **Waste Management**, v. 76, p. 350–356, jun. 2018.

ROMERO-GÜIZA, M. S. et al. The role of additives on anaerobic digestion: A review. **Renewable and Sustainable Energy Reviews**, v. 58, p. 1486–1499, 2016.

ROMLI, M. et al. The Effect of Concentration and Hydraulic Shock Loads on the Performance of a Two-Stage High-Rate Anaerobic Wastewater Treatment System: Prediction and Validation. In: **Advances in Bioprocess Engineering**. Dordrecht: Springer Netherlands, 1994a. p. 379–384.

ROMLI, M. et al. The influence of pH on the performance of a two-stage anaerobic treatment system: model prediction and validation. **Water Science and Technology**, v. 30, n. 8, p. 35, 1994b.

ROSA, A. P. et al. Assessing the potential of renewable energy sources (biogas and sludge) in a full-scale UASB-based treatment plant. **Renewable Energy**, v. 124, p. 21–26, ago. 2018.

ROSEN, C.; JEPPSSON, U. Aspects on ADM1 implementation within the BSM2 framework 2 The IWA benchmark simulation models. **Adm1**, p. 1–34, 2006a.

ROSEN, C.; JEPPSSON, U. Aspects on ADM1 Implementation within the BSM2 Framework. **Technical report**, p. 1–37, 2006b.

RUGGERI, B.; TOMMASI, T.; SANFILIPPO, S. BioH2 & BioCH4 Through Anaerobic Digestion. **Green Energy and Technology**, Green Energy and Technology. p. 230, 2015.

RUZICKA, M. An extension of the Mosey model. **Water Research**, v. 30, n. 10, p. 2440–2446, out. 1996a.

RUZICKA, M. The effect of hydrogen on acidogenic glucose cleavage. **Water Research**, v. 30, n. 10, p. 2447–2451, out. 1996b.

RYUE, J. et al. Comparative effects of GAC addition on methane productivity and microbial community in mesophilic and thermophilic anaerobic digestion of food waste. **Biochemical Engineering Journal**, v. 146, n. November 2018, p. 79–87, jun. 2019.

SAADY, N. M. C. Homoacetogenesis during hydrogen production by mixed cultures dark fermentation: Unresolved challenge. **International Journal of Hydrogen Energy**, v. 38, n. 30, p. 13172–13191, out. 2013.

SAGAR, N. A. et al. Fruit and Vegetable Waste: Bioactive Compounds, Their Extraction, and Possible Utilization. **Comprehensive Reviews in Food Science and Food Safety**, v. 17, n. 3, p. 512–531, 25 maio 2018.

SAHA, S. et al. An integrated leachate bed reactor – anaerobic membrane bioreactor system (LBR-AnMBR) for food wACCCaste stabilization and biogas recovery. **Chemosphere**, v. 311, n. P2, p. 137054, jan. 2023.

SALAMAT, R. et al. Drying of biogas digestate: A review with a focus on available drying techniques, drying kinetics, and gaseous emission behavior. **Drying Technology**, v. 40, n. 1, p. 5–29, 2022.

SAMARSKII, A. A.; MIKHAILOV, A. P. **Principles of mathematical modeling: ideas, methods, examples**. 1. ed. Moscow, Russia: [s.n.]. v. 3

SANTOS, L. A. DOS et al. Methane generation potential through anaerobic digestion of fruit waste. **Journal of Cleaner Production**, v. 256, p. 120389, maio 2020.

SARKER, S. et al. A Review of the Role of Critical Parameters in the Design and Operation of Biogas Production Plants. **Applied Sciences**, v. 9, n. 9, p. 1915, 9 maio 2019.

SASIKALA, K. et al. Anoxygenic Phototrophic Bacteria: Physiology and Advances in Hydrogen Production Technology. In: [s.l: s.n.]. p. 211–295.

SCANO, E. A. et al. Biogas from anaerobic digestion of fruit and vegetable wastes: Experimental results on pilot-scale and preliminary performance evaluation of a full-scale power plant. **Energy Conversion and Management**, v. 77, p. 22–30, jan. 2014.

SEOL, E. et al. Metabolic engineering of Escherichia coli strains for co-production of hydrogen and ethanol from glucose. **International Journal of Hydrogen Energy**, v. 39, n. 33, p. 19323–19330, nov. 2014.

SEOL, E. et al. Co-production of hydrogen and ethanol from glucose by modification of glycolytic pathways in Escherichia coli – from Embden-Meyerhof-Parnas pathway to pentose phosphate pathway. **Biotechnology Journal**, v. 11, n. 2, p. 249–256, 14 fev. 2016.

SHAPOVALOV, Y. et al. Dry Anaerobic Digestion of Chicken Manure: A Review. **Applied Sciences**, v. 10, n. 21, p. 7825, 5 nov. 2020.

SHEFALI, V.; THEMELIS, N. J. **Anaerobic digestion of biodegradable organics in municipal solid waste**. [s.l.] Columbia University, 2002.

SHEN, F. et al. Performances of anaerobic co-digestion of fruit & vegetable waste (FVW) and food waste (FW): Single-phase vs. two-phase. **Bioresource Technology**, v. 144, p. 80–85, 2013.

SHI, X.-S. et al. Modeling of the methane production and pH value during the anaerobic co-digestion of dairy manure and spent mushroom substrate. **Chemical Engineering Journal**, v. 244, n. 1, p. 258–263, maio 2014.

SHI, X. et al. Effects of free ammonia on volatile fatty acid accumulation and process performance in the anaerobic digestion of two typical bio-wastes. **Journal of Environmental Sciences (China)**, v. 55, p. 49–57, 2017.

SHI, X. et al. A comparative study of thermophilic and mesophilic anaerobic co-digestion of food waste and wheat straw: Process stability and microbial community structure shifts. **Waste Management**, v. 75, p. 261–269, maio 2018.

SHOW, K. Y. et al. Biohydrogen production: Current perspectives and the way forward. **International Journal of Hydrogen Energy**, v. 37, n. 20, p. 15616–15631, 2012.

SHRESTHA, S. et al. Recent advances in co-digestion conjugates for anaerobic digestion of food waste. **Journal of Environmental Management**, v. 345, n. June, p. 118785, 2023.

SIEGRIST, H. et al. Mathematical Model for Meso- and Thermophilic Anaerobic Sewage Sludge Digestion. **Environmental Science & Technology**, v. 36, n. 5, p. 1113–1123, 1 mar. 2002.

SIEGRIST, H.; RENGGLI, D.; GUJER, W. Mathematical modelling of anaerobic mesophilic sewage sludge treatment. **Water Science and Technology**, v. 27, n. 2, p. 25–36, 1 jan. 1993.

SILVA-MARTÍNEZ, R. D. et al. Biological Hydrogen Production Through Dark Fermentation with High-Solids Content: An Alternative to Enhance Organic Residues Degradation in Co-Digestion with Sewage Sludge. **Fermentation**, v. 11, n. 7, p. 398, 11 jul. 2025.

SILVA JÚNIOR, F. DAS C. G. DA et al. Characterization of Fruits and Vegetables Waste Generated at a Central Horticultural Wholesaler: A Case Study for Energy Production Via Biogas. **Industrial Biotechnology**, v. 18, n. 4, p. 235–239, 1 ago. 2022.

SILVA, T. P. et al. Bioenergy recovery potential from upflow microaerobic sludge blanket reactor fed with swine wastewater. **Biochemical Engineering Journal**, v. 187, n. October, p. 108675, nov. 2022.

SILVA, T. P. et al. Monte Carlo-based model for estimating methane generation potential and electric energy recovery in swine wastewater treated in UASB systems. **Journal of Water Process Engineering**, v. 51, n. December 2022, p. 103399, fev. 2023.

SILVA, T. P. Potencial de recuperação de bioenergia da água residuária da suinocultura tratada em reatores UASB Potential recovery of bioenergy from swine wastewater treated in UASB reactors Potencial recuperación de bioenergía a partir de aguas residuales porcinas tr. **Revista Científica Foz,** p. 109–132, 2024.

SILVA, T. P. et al. Bibliometric analysis of Anaerobic Digestion Model No. 1 for dry anaerobic digestion of fruit and vegetable waste, food waste, and organic fraction of municipal solid waste. **Journal of Environmental Chemical Engineering**, v. 12, n. 6, p. 114664, dez. 2024.

SILVA, T. P. et al. Anaerobic Digestion Model No. 1 applied to bioenergy generation from fruit and vegetable waste in Upflow Anaerobic Sludge Blanket reactors. **Bioresource Technology**, v. 432, n. 1, p. 132644, set. 2025.

SILVA, T. P.; OLIVEIRA JÚNIOR, J. L. DE; CORDEIRO, R. DE M. Análise de viabilidade técnico-econômica da utilização do biogás / metano de reatores UASB , para geração de energia elétrica. **Revista Científica Foz,** v. 4, n. 1, p. 140–157, 2022.

SILVA, T. P.; OLIVEIRA JÚNIOR, J. L. DE; CORDEIRO, R. DE M. Evaluation of the technical and economic feasibility of generating bioenergy in UASB reactors treating domestic wastewater. **Revista DAE**, v. 72, n. 243, p. 30–43, 2023.

SINGLETON, A. M. T. et al. Experiments on Anaerobic Digestion of Wool Scouring Wastes. **Sew**, v. 21, n. 2, p. 286–293, 1949.

SKIADAS, I. V; GAVALA, H. N.; LYBERATOS, G. MODELLING OF THE PERIODIC

ANAEROBIC BAFFLED REACTOR (PABR) BASED ON THE RETAINING FACTOR CONCEPT. v. 34, n. 15, 2000.

SMITH, J. M. et al. **Introdução à Termodinâmica da Engenharia Química**. 8. ed. [s.l: s.n.].

SMITH, P. H. et al. Biological production of methane from biomass. **Methane from biomass: a systems approach**, p. 291–255, 1988.

SMOLDERS, G. J. F. et al. Stoichiometric model of the aerobic metabolism of the biological phosphorus removal process. **Biotechnology and Bioengineering**, v. 44, n. 7, p. 837–848, 1994.

SONG, S. et al. Ultrasonication-induced metabolic pathway shifts and reduced electron carrier washout with biomass enhanced hydrogen yield in a continuous stirred tank reactor. **Chemical Engineering Journal**, v. 493, n. May, p. 152594, ago. 2024.

SOUZA, T. S. O. et al. ADM1 calibration using BMP tests for modeling the effect of autohydrolysis pretreatment on the performance of continuous sludge digesters. **WATER RESEARCH**, v. 47, n. 9, p. 3244–3254, jun. 2013.

SPYRIDONIDIS, A. et al. Modeling of anaerobic digestion of slaughterhouse wastes after thermal treatment using ADM1. **Journal of Environmental Management**, v. 224, p. 49–57, out. 2018.

SUNDARA SEKAR, B.; SEOL, E.; PARK, S. Co-production of hydrogen and ethanol from glucose in Escherichia coli by activation of pentose-phosphate pathway through deletion of phosphoglucose isomerase (pgi) and overexpression of glucose-6-phosphate dehydrogenase (zwf) and 6-phosphogluconate dehyd. **Biotechnology for Biofuels**, v. 10, n. 1, p. 85, 29 dez. 2017.

TARTAKOVSKY, B. et al. Anaerobic digestion model No. 1-based distributed parameter model of an anaerobic reactor: II. Model validation. **Bioresource Technology**, v. 99, n. 9, p. 3676–3684, jun. 2008.

THAUER, R. K.; JUNGERMANN, K.; DECKER, K. Energy conservation in chemotrophic anaerobic bacteria. **Bacteriological Reviews**, v. 41, n. 1, p. 100–180, mar. 1977.

TIWARY, A. et al. Emerging perspectives on environmental burden minimisation initiatives from anaerobic digestion technologies for community scale biomass valorisation. **Renewable and Sustainable Energy Reviews**, v. 42, p. 883–901, 2015.

TUGTAS, A. E.; YESIL, H.; CALLI, B. Enhanced anaerobic digestion model no.1 for high solids fermentation: Integrating homoacetogenesis and chain elongation. **Bioresource Technology**, v. 417, n. 1, p. 131843, 2025.

TYAGI, V. K. et al. Anaerobic co-digestion of organic fraction of municipal solid waste (OFMSW): Progress and challenges. **Renewable and Sustainable Energy Reviews**, v. 93, n. May, p. 380–399, 2018.

ULLAH, R.; ASGHAR, I.; GRIFFITHS, M. G. An Integrated Methodology for Bibliometric Analysis: A Case Study of Internet of Things in Healthcare Applications. **Sensors**, v. 23, n. 1,

p. 67, 21 dez. 2022.

UMMAH, M. S. **Computational Methods for Fluid Dynamics**. 3. ed. [s.l: s.n.]. v. 11

UNEP. **Food Waste Index Report 2024**. Disponível em: <https://www.unep.org/resources/publication/food-waste-index-report-2024>.

URTNOWSKI-MORIN, C. et al. Upgrading waste material flow analysis with process models: The case of anaerobic digestion. **Journal of Cleaner Production**, v. 298, p. 126695, maio 2021.

VALENCIA, A.; ZHANG, W.; CHANG, N. BIN. Sustainability transitions of urban food-energy-water-waste infrastructure: A living laboratory approach for circular economy. **Resources, Conservation and Recycling**, v. 177, n. April 2021, p. 105991, 2022.

VAN ECK, N. J.; WALTMAN, L. Software survey: VOSviewer, a computer program for bibliometric mapping. **Scientometrics**, v. 84, n. 2, p. 523–538, 31 ago. 2010.

VAN ECK, N. J.; WALTMAN, L. Manual VOSviewer. **Univeristeit Leiden**, n. January, p. 54, 2022.

VAN LIER, J. B. et al. Celebrating 40 years anaerobic sludge bed reactors for industrial wastewater treatment. **Reviews in Environmental Science and Biotechnology**, v. 14, n. 4, p. 681–702, 2015.

VANDEVIVERE, P.; DE BAERE, L.; VERSTRAETE, W. Types of anaerobic digester for solid wastes. **Biomethanization of the organic fraction of municipal solid wastes**, n. June, p. 111–140, 2003.

VAVILIN, V. A. et al. Distributed Model of Solid Waste Anaerobic Digestion: Effects of Leachate Recirculation and pH Adjustment. **Biotechnology and Bioengineering**, v. 81, n. 1, p. 66–73, 2003.

VAVILIN, V. A. et al. Modeling solid waste decomposition. **Bioresource Technology**, v. 94, n. 1, p. 69–81, 2004.

VAVILIN, V. A. et al. Hydrolysis kinetics in anaerobic degradation of particulate organic material: An overview. **Waste Management**, v. 28, n. 6, p. 939–951, 2008.

VAVILIN, V. A.; RYTOV, S. V.; LOKSHINA, L. Y. A description of hydrolysis kinetics in anaerobic degradation of particulate organic matter. **Bioresource Technology**, v. 56, n. 2–3, p. 229–237, maio 1996.

VELP SCIENTIFICA. LAB SOLUTIONS NDA SERIES Dumas Nitrogen Analyzer Nitrogen / Protein Determination in a Flash NDA Series Nitrogen Analyzer Uses chemicals (VELP SCIENTIFICA (Rev F 11/20/2019)). p. 145, 2019.

VERSTEEG, H. K.; MALALASEKERA, W. **An Introduction to Computational Fluid Dynamics: The Finite Volume Method**. England: [s.n.]. v. M

VIEGAS, C. V. et al. Critical attributes of Sustainability in Higher Education: A categorisation from literature review. **Journal of Cleaner Production**, v. 126, p. 260–276, 2016.

VILMS PEDERSEN, S. et al. Management and design of biogas digesters: A non-calibrated heat transfer model. **Bioresource Technology**, v. 296, n. July 2019, p. 122264, jan. 2020.

VOGELS, M. et al. P. F. Verhulst's "notice sur la loi que la populations suit dans son accroissement" from correspondence mathematique et physique. Ghent, vol. X, 1838. **Journal of Biological Physics**, v. 3, n. 4, p. 183–192, dez. 1975.

VON SPERLING, M.; CHERNICHARO, C. A. . Biological Wastewater Treatment in Warm Climate Regions. **Iwa Publishing**, p. 856, 2005.

VYAS, S. et al. Opportunities and knowledge gaps in biochemical interventions for mining of resources from solid waste: A special focus on anaerobic digestion. **Fuel**, v. 311, n. August 2021, p. 122625, mar. 2022.

WALTMAN, L. A review of the literature on citation impact indicators. **Journal of Informetrics**, v. 10, n. 2, p. 365–391, 2016.

WAN, S. et al. Anaerobic digestion of municipal solid waste composed of food waste, wastepaper, and plastic in a single-stage system: Performance and microbial community structure characterization. **Bioresource Technology**, v. 146, p. 619–627, out. 2013.

WANG, S. et al. Mapping the research trends and hot topics of ventricular arrhythmia: A bibliometric analysis from 2001 to 2020. **Frontiers in Cardiovascular Medicine**, v. 9, n. October, 20 out. 2022a.

WANG, S.; ZHONG, J. Bioreactor Engineering. In: **Bioprocessing for Value-Added Products from Renewable Resources**. [s.l.] Elsevier, 2007. p. 131–161.

WANG, X. et al. From past to future: Bibliometric analysis of global research productivity on nomogram (2000–2021). **Frontiers in Public Health**, v. 10, 20 set. 2022b.

WANG, Z. et al. Impact of total solids content on anaerobic co-digestion of pig manure and food waste: Insights into shifting of the methanogenic pathway. **Waste Management**, v. 114, p. 96–106, 2020.

WANG, Z. et al. Research on nickel-based catalysts for carbon dioxide methanation combined with literature measurement. **Journal of CO2 Utilization**, v. 63, n. January, p. 102117, set. 2022c.

WANG, Z. et al. A critical review on dry anaerobic digestion of organic waste : Characteristics , operational conditions , and improvement strategies ☆. **Renewable and Sustainable Energy Reviews**, v. 176, n. January, p. 113208, 2023.

WARD, A. J. et al. Optimisation of the anaerobic digestion of agricultural resources. **Bioresource Technology**, v. 99, n. 17, p. 7928–7940, nov. 2008.

WASZKIELIS, K.; BIALOBRZEWSKI, I.; BULKOWSKAK, K. Application of anaerobic digestion model No. 1 for simulating fermentation of maize silage, pig manure, cattle manure and digestate in the full-scale biogas plant. **FUEL**, v. 317, jun. 2022.

WEINRICH, S. et al. Augmenting Biogas Process Modeling by Resolving Intracellular

Metabolic Activity. **FRONTIERS IN MICROBIOLOGY**, v. 10, 2019.

WEINRICH, S. et al. Systematic simplification of the Anaerobic Digestion Model No. 1 (ADM1) – Laboratory experiments and model application. **Bioresource Technology**, v. 333, p. 125104, ago. 2021.

WELLINGER, A.; MURPHY, J.; BAXTER, D. **The Biogas Handbook - science, prodution and applications**. [s.l.] Elsevier, 2013.

WONG, J. W. C. et al. Food waste treatment by anaerobic co-digestion with saline sludge and its implications for energy recovery in Hong Kong. **Bioresource Technology**, v. 268, n. June, p. 824–828, 2018.

XIA, A. et al. Production of hydrogen, ethanol and volatile fatty acids through co-fermentation of macro- and micro-algae. **Bioresource Technology**, v. 205, p. 118–125, abr. 2016.

XIAO, B. et al. Biogas production by two-stage thermophilic anaerobic co-digestion of food waste and paper waste: Effect of paper waste ratio. **Renewable Energy**, v. 132, p. 1301–1309, 2019.

XIE, S. et al. Anaerobic co-digestion: A critical review of mathematical modelling for performance optimization. **Bioresource Technology**, v. 222, p. 498–512, 2016.

XU, F. et al. A mass diffusion-based interpretation of the effect of total solids content on solid-state anaerobic digestion of cellulosic biomass. **Bioresource Technology**, v. 167, p. 178–185, set. 2014a.

XU, F. et al. Anaerobic digestion of food waste – Challenges and opportunities. **Bioresource Technology**, v. 247, n. July 2017, p. 1047–1058, 2018.

XU, F.; LI, Y.; WANG, Z.-W. Mathematical modeling of solid-state anaerobic digestion. **Progress in Energy and Combustion Science**, v. 51, p. 49–66, dez. 2015.

XU, S. et al. Responses of microbial community and acidogenic intermediates to different water regimes in a hybrid solid anaerobic digestion system treating food waste. **Bioresource Technology**, v. 168, p. 49–58, set. 2014b.

YAHAYA, E. et al. A review on process modeling and design of biohydrogen. **International Journal of Hydrogen Energy**, v. 47, n. 71, p. 30404–30427, ago. 2022.

YETILMEZSOY, K. et al. Black-, gray-, and white-box modeling of biogas production rate from a real-scale anaerobic sludge digestion system in a biological and advanced biological treatment plant. **Neural Computing and Applications**, v. 33, n. 17, p. 11043–11066, 2021.

YIN, Q.; GU, M.; WU, G. Inhibition mitigation of methanogenesis processes by conductive materials: A critical review. **Bioresource Technology**, v. 317, n. June, p. 123977, dez. 2020.

YU, L. et al. Experimental and modeling study of a two-stage pilot scale high solid anaerobic digester system. **Bioresource Technology**, v. 124, p. 8–17, nov. 2012.

YUAN, X.-Z. et al. Modeling anaerobic digestion of blue algae: Stoichiometric coefficients of amino acids acidogenesis and thermodynamics analysis. **Water Research**, v. 49, p. 113–123,

fev. 2014.

ZAHER, U. et al. A Procedure to Estimate Proximate Analysis of Mixed Organic Wastes. **Water Environment Research**, v. 81, n. 4, p. 407–415, abr. 2009.

ZAMRI, M. F. M. A. et al. A comprehensive review on anaerobic digestion of organic fraction of municipal solid waste. **Renewable and Sustainable Energy Reviews**, v. 137, n. December 2020, p. 110637, mar. 2021.

ZAYEN, A. et al. Potential valorization of fruits and vegetables waste from the wholesale market in Sfax (Tunisia) via anaerobic digestion: long-term characterization and stakeholders' attitude. **Biomass Conversion and Biorefinery**, n. 0123456789, 2025.

ZENG, R.; CHINI, A. A review of research on embodied energy of buildings using bibliometric analysis. **Energy and Buildings**, v. 155, p. 172–184, nov. 2017.

ZHANG, L.; LEE, Y. W.; JAHNG, D. Anaerobic co-digestion of food waste and piggery wastewater: Focusing on the role of trace elements. **Bioresource Technology**, v. 102, n. 8, p. 5048–5059, 2011.

ZHANG, Y.; BANKS, C. J.; HEAVEN, S. Co-digestion of source segregated domestic food waste to improve process stability. **Bioresource Technology**, v. 114, p. 168–178, 2012.

ZHANG, Y.; PICCARD, S.; ZHOU, W. Improved ADM1 model for anaerobic digestion process considering physico-chemical reactions. **Bioresource Technology**, v. 196, p. 279–289, nov. 2015.

ZHAO, B.-H. et al. Modeling anaerobic digestion of aquatic plants by rumen cultures: Cattail as an example. **Water Research**, v. 43, n. 7, p. 2047–2055, abr. 2009.

ZHAO, N. et al. A comprehensive simulation approach for pollutant bio-transformation in the gravity sewer. **FRONTIERS OF ENVIRONMENTAL SCIENCE \& ENGINEERING**, v. 13, n. 4, 2019a.

ZHAO, X. et al. Modified Anaerobic Digestion Model No. 1 for modeling methane production from food waste in batch and semi-continuous anaerobic digestions. **Bioresource Technology**, v. 271, n. 1, p. 109–117, jan. 2019b.

ZHOU, H.; LI, H.; WANG, F. Anaerobic digestion of different organic wastes for biogas production and its operational control performed by the modified ADM1. **Journal of Environmental Science and Health, Part A**, v. 47, n. 1, p. 84–92, jan. 2012.

ZHOU, M. et al. Enhanced volatile fatty acids production from anaerobic fermentation of food waste: A mini-review focusing on acidogenic metabolic pathways. **Bioresource Technology**, v. 248, p. 68–78, 2018.

ZHOU, X. et al. **Modeling An Anaerobic Reactor with An Outside Recycling Line for Municipal Wastewater Treatment by Modified Anaerobic Digestion Model No. 1 (ADM1)**. 2009 3RD INTERNATIONAL CONFERENCE ON BIOINFORMATICS AND BIOMEDICAL ENGINEERING, VOLS 1-11. **Anais**...345 E 47TH ST, NEW YORK, NY 10017 USA: IEEE, 2009.

ZHU, L. et al. Specific component comparison of extracellular polymeric substances (EPS) in flocs and granular sludge using EEM and SDS-PAGE. **Chemosphere**, v. 121, p. 26–32, 2015.

ZHU, Y. et al. Dual roles of zero-valent iron in dry anaerobic digestion: Enhancing interspecies hydrogen transfer and direct interspecies electron transfer. **Waste Management**, v. 118, p. 481–490, dez. 2020.

ZUPIC, I.; ČATER, T. Bibliometric Methods in Management and Organization. **Organizational Research Methods**, v. 18, n. 3, p. 429–472, 22 jul. 2015.

10 APPENDIX A: GENERAL INTRODUCTION AND STRUCTURE OF THE THESIS

Table 10.1 – Biochemical rate coefficients ($v_{i,j}$) and kinetic rate equations (ρ_j) for soluble components (i = 1–12; j = 1–19).

j	**Component → *i***	**1**	**2**	**3**	**4**	**5**	**6**	**7**	**8**	**9**	**10**	**11**	**12**	**Rate (ρj,kg COD($m^3 \cdot d)^{-1}$)**
	Process ↓	S_{su}	S_{aa}	S_{fa}	S_{va}	S_{bu}	S_{pro}	S_{ac}	S_{h2}	S_{ch4}	S_{IC}	S_{IN}	S_I	
1	Disintegration												$f_{SI,XC}$	$k_{dis} \cdot X_C$
2	Hydrolysis carbohydrates	*1*												$k_{hyd,ch} \cdot X_{ch}$
3	Hydrolysis of proteins		*1*											$k_{hyd,pr} \cdot X_{pr}$
4	Hydrolysis of lipids	$1\text{-}f_{fa,li}$		$1\text{-}f_{fa,li}$										$k_{hyd,li} \cdot X_{li}$
5	Uptake of Sugar	*-1*				$(1-Y_{su})\cdot f_{bu,su}$	$(1-Y_{su})\cdot f_{pro,su}$	$(1-Y_{su})\cdot f_{ac,su}$	$(1-Y_{su})\cdot f_{h2,su}$		$-\sum_{i=9,11-28} C_i v_{i,5}$	$-(Y_{su})\ N_{bac}$		$k_{m,su} \cdot \frac{S_{su}}{k_s + S_{su}} \cdot X_{su} \cdot I_1$
6	Uptake of amino acids		*-1*		$(1-Y_{aa})\cdot f_{va,aa}$	$(1-Y_{aa})\cdot f_{bu,aa}$	$(1-Y_{aa})\cdot f_{pro,aa}$	$(1-Y_{aa})\cdot f_{ac,aa}$	$(1-Y_{aa})\cdot f_{h2,aa}$		$-\sum_{i=9,11-28} C_i v_{i,6}$	$N_{aa}-(Y_{aa})\ N_{bac}$		$k_{m,aa} \cdot \frac{S_{aa}}{k_s + S_{aa}} \cdot X_{aa} \cdot I_2$
7	Uptake of LCFA			*-1*				$(1-Y_{fa})\cdot 0.7$	$(1-Y_{fa})\cdot 0.3$			$-(Y_{fa})\ N_{bac}$		$k_{m,fa} \cdot \frac{S_{fa}}{k_s + S_{fa}} \cdot X_{fa} \cdot I_2$
8	Uptake of valerate				*-1*		$(1-Y_{c4})\cdot 0.54$	$(1-Y_{c4})\cdot 0.31$	$(1-Y_{c4})\cdot 0.15$			$-(Y_{c4})\ N_{bac}$		$k_{m,c4} \cdot \frac{S_{va}}{k_s + S_{va}} \cdot X_{c4} \cdot \frac{1}{1 + S_{bu}/S_{va}} \cdot I_2$
9	Uptake of butyrate					*-1*		$(1-Y_{c4})\cdot 0.8$	$(1-Y_{c4})\cdot 0.2$			$-(Y_{c4})\ N_{bac}$		$k_{m,c4} \cdot \frac{S_{bu}}{k_s + S_{bu}} \cdot X_{c4} \cdot \frac{1}{1 + S_{va}/S_{su}} \cdot I_2$
10	Uptake of Propionate						*-1*	$(1-Y_{pro})\cdot 0.57$	$(1-Y_{pro})\cdot 0.43$		$-\sum_{i=9,11-28} C_i v_{i,10}$	$-(Y_{pro})\ N_{bac}$		$k_{m,pro} \cdot \frac{S_{pro}}{k_s + S_{pro}} \cdot X_{pro} \cdot I_2$
11	Uptake of Acetate							*-1*		$(1-Y_{ac})$	$-\sum_{i=9,11-28} C_i v_{i,11}$	$-(Y_{ac})\ N_{bac}$		$k_{m,ac} \cdot \frac{S_{ac}}{k_s + S_{ac}} \cdot X_{ac} \cdot I_3$
12	Uptake of Hydrogen								*-1*	$(1-Y_{h2})\cdot$	$-\sum_{i=9,11-28} C_i v_{i,12}$	$-(Y_{h2})\ N_{bac}$		$k_{m,h2} \cdot \frac{S_{h2}}{k_s + S_{h2}} \cdot X_{h2} \cdot I_1$
13	Decay of X_{su}													$k_{dec,Xsu} \cdot X_{su}$
14	Decay of X_{aa}													$k_{dec,Xaa} \cdot X_{aa}$
15	Decay of X_{fa}													$k_{dec,Xla} \cdot X_{fa}$
16	Decay of X_{c4}													$k_{dec,Xc4} \cdot X_{c4}$
17	Decay of X_{pro}													$k_{dec,Xpro} \cdot X_{pro}$
18	Decay of X_{ac}													$k_{dec,Xac} \cdot X_{ac}$
19	Decay of X_{h2}													$k_{dec,Xh2} \cdot X_{h2}$
		Monosaccharides (kg COD m^{-3})	Amino Acids (kg COD m^{-3})	Long chain fatty acid (kg COD m^{-3})	Total valerate (kg COD m^{-3})	Total Butyrate (kg COD m^{-3})	Total Propionate (kg COD m^{-3})	Total Acetate (kg COD m^{-3})	Hydrogen gas (kg COD m^{-3})	Methane gas (kg COD m^{-3})	Inorganic Carbon (kg mole C m^{-3})	Inorganic Nitrogen (kg mole N m^{-3})	Soluble Inerts (kg COD m^{-3})	Inhibition factors $I_1 = I_{pH} \cdot I_{IN,lim}$ $I_2 = I_{pH} \cdot I_{h2} \cdot I_{IN,lim}$ $I_3 = I_{pH} \cdot I_{NH3} \cdot I_{IN,lim}$

Data: (BATSTONE et al., 2002).

Table 10.2 – Biochemical rate coefficients ($v_{i,j}$) and kinetic rate equations (ρ_j) for soluble components (i = 13–24; j = 1–19)

j	Component → *i*	13	14	15	16	17	18	19	20	21	22	23	24	Rate (ρj,kg COD($m^3 \cdot d)^{-1}$)
	Process ↓	X_c	X_{ch}	X_{pr}	X_{li}	X_{su}	X_{aa}	X_{fa}	X_{c4}	X_{pro}	X_{ac}	X_{h2}	X_I	
1	Disintegration	*-1*	$f_{ch,XC}$	$f_{pr,XC}$	$f_{li,XC}$								$f_{SI,XC}$	$k_{dis} \cdot X_C$
2	Hydrolysis carbohydrates		*-1*											$k_{hyd,ch} \cdot X_{ch}$
3	Hydrolysis of proteins			*-1*										$k_{hyd,pr} \cdot X_{pr}$
4	Hydrolysis of lipids				*-1*									$k_{hyd,li} \cdot X_{li}$
5	Uptake of Sugar					Y_{su}								$k_{m,su} \cdot \frac{S_{su}}{k_s + S_{su}} \cdot X_{su} \cdot I_1$
6	Uptake of amino acids						Y_{aa}							$k_{m,aa} \cdot \frac{S_{aa}}{k_s + S_{aa}} \cdot X_{aa} \cdot I_2$
7	Uptake of LCFA							Y_{fa}						$k_{m,fa} \cdot \frac{S_{fa}}{k_s + S_{fa}} \cdot X_{fa} \cdot I_2$
8	Uptake of valerate								Y_{c4}					$k_{m,c4} \cdot \frac{S_{va}}{k_s + S_{va}} \cdot X_{c4} \cdot \frac{1}{1 + S_{bu}/S_{va}} \cdot I_2$
9	Uptake of butyrate								Y_{c4}					$k_{m,c4} \cdot \frac{S_{bu}}{k_s + S_{bu}} \cdot X_{c4} \cdot \frac{1}{1 + S_{va}/S_{su}} \cdot I_2$
10	Uptake of Propionate									Y_{pro}				$k_{m,pro} \cdot \frac{S_{pro}}{k_s + S_{pro}} \cdot X_{pro} \cdot I_2$
11	Uptake of Acetate										Y_{ac}			$k_{m,ac} \cdot \frac{S_{ac}}{k_s + S_{ac}} \cdot X_{ac} \cdot I_3$
12	Uptake of Hydrogen											Y_{h2}		$k_{m,h2} \cdot \frac{S_{h2}}{k_s + S_{h2}} \cdot X_{h2} \cdot I_1$
13	Decay of X_{su}	*1*				*-1*								$k_{dec,Xsu} \cdot X_{su}$
14	Decay of X_{aa}	*1*					*-1*							$k_{dec,Xaa} \cdot X_{aa}$
15	Decay of X_{fa}	*1*						*-1*						$k_{dec,Xla} \cdot X_{fa}$
16	Decay of X_{c4}	*1*							*-1*					$k_{dec,Xc4} \cdot X_{c4}$
17	Decay of X_{pro}	*1*								*-1*				$k_{dec,Xpro} \cdot X_{pro}$
18	Decay of X_{ac}	*1*									*-1*			$k_{dec,Xac} \cdot X_{ac}$
19	Decay of X_{h2}	*1*										*-1*		$k_{dec,Xh2} \cdot X_{h2}$
		Composites (kg COD m^{-3})	Carbohydrates (kg COD m^{-3})	Proteins (kg COD m^{-3})	Lipids (kg COD m^{-3})	Sugar degraders (kg COD m^{-3})	Amino acid degraders (kg COD m^{-3})	LCFA degraders (kg COD m^{-3})	Caproate, valerate and butyrate degraders (kg COD m^{-3})	Propionate degraders (kg COD m^{-3})	Acetate degraders (kg COD m^{-3})	Hydrogen degraders (kg COD m^{-3})	Particulate inerts (kg mole C m^{-3})	Inhibition factors $I_1 = I_{pH1} \cdot I_{IN,lim}$ $I_2 = I_{pH1} \cdot I_{h2} \cdot I_{IN,lim}$ $I_3 = I_{pH1} \cdot I_{NH3} \cdot I_{IN,lim}$

Data: (BATSTONE et al., 2002).

11 APPENDIX B: METHODS AND TOOLS

Figure 11.1 – Schematic representation of the proposed system highlighting the modeled components.

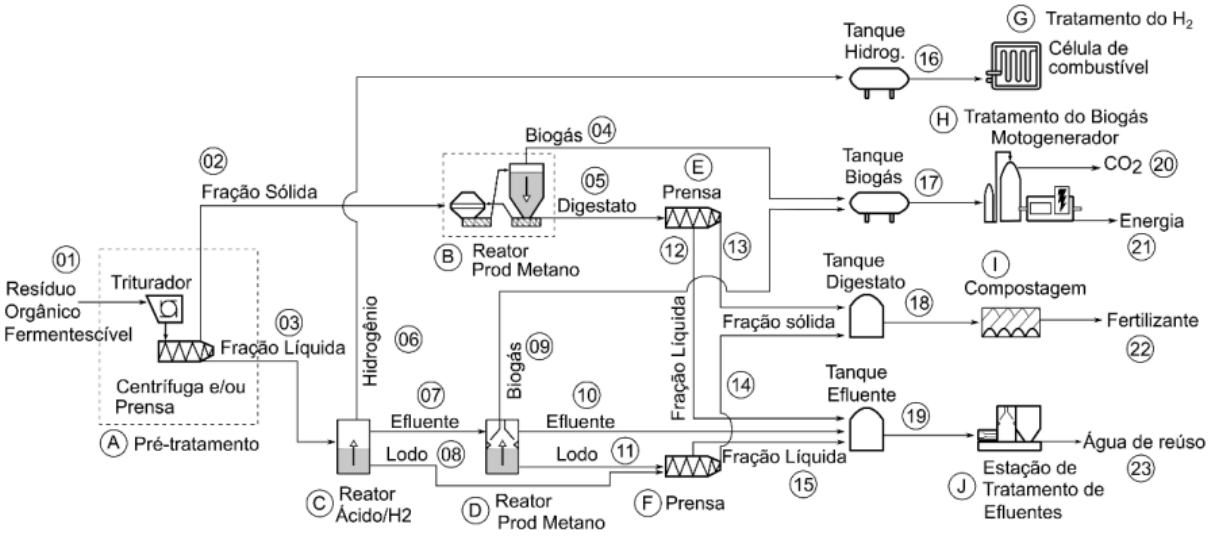

Note: Integrated Anaerobic Reactor System Unit[1]; By-Products and Flows[2]; By-Products and Flows (cont.)[3] Final effluent for treatment; Final Products[4].

[1] (A) Pre-treatment and separation of waste into solid and liquid fractions; (B) Dry-phase methanogenic reactor; (C) Dark fermentation reactor; (D) Methanogenic reactor; (E) and (F) Rotary screw presses; (G) Hydrogen treatment and utilization unit; (H) Biogas treatment and utilization unit; (I) Composting; (J) Wastewater treatment plant (WWTP).

[2] 1. Fermentable Organic Waste; 2. Solid fraction of waste (after pre-treatment); 3. Liquid fraction of waste (after pre-treatment); 4. Biogas; 5. Digestate from the dry phase methanization reactor; 6. (Not listed in the original image).

[3] 7. Effluent containing high content of organic acids; 8. Excess sludge from the dark fermentation reactor; 9. Biogas; 10. Effluent from the methanogenic reactor; 11. Excess sludge from the methanogenic reactor; 12. Liquid fraction from the digestate press; 13. Solid fraction from the digestate press; 14. Solid fraction from the excess sludge press; 15. Liquid fraction from the excess sludge press; 16. Hydrogen for treatment and use; 17. Biogas for treatment and use; 18. Digestate for composting; 19.

[4] 20. Biogenic carbon dioxide; 21. Renewable energy.

12 APPENDIX C: SUPPLEMENTARY MATERIAL – ARTICLE I

Figure 12.1 – Inhibition factors.

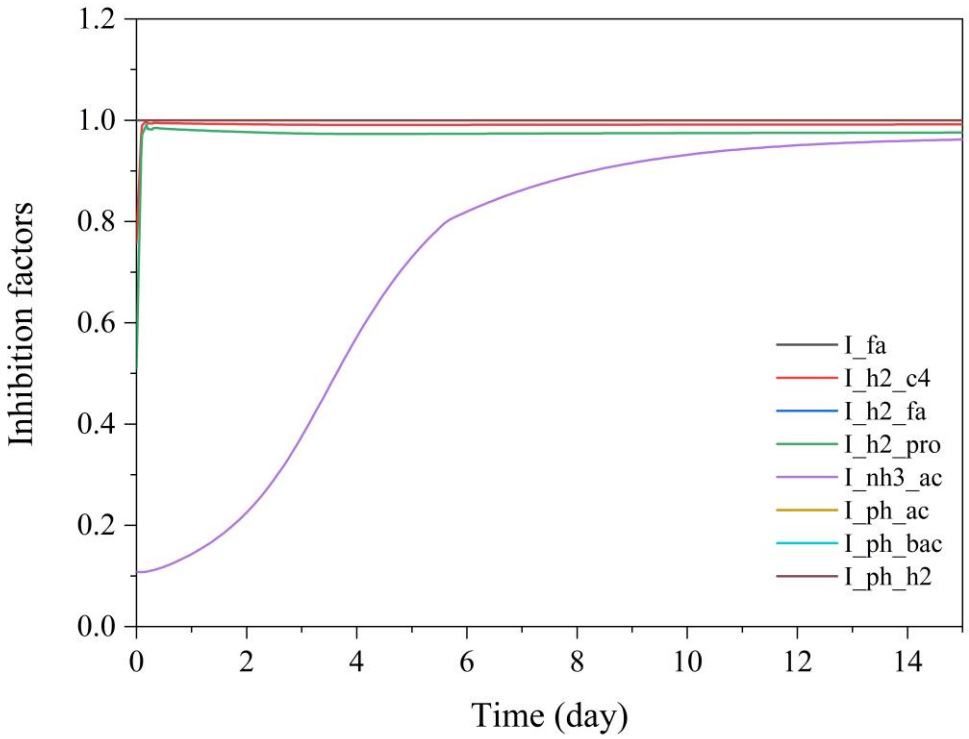

Table 12.1 – Stoichiometric parameters in ADM1

Fractions						
No	**Terms**	**Used**	**Unit**	**Expressions**	**i**	**J**
1	$f_{SI,Xc}$	0.10000	kg COD m^{-3}	fraction S_I from composites X_c	Soluble inert	Disintegration
2	$f_{xI,xc}$	0.20000	kg COD m^{-3}	fraction X_I from composites X_c	Particulate inert	Disintegration
3	$f_{ch,xc}$	0.20000	kg COD m^{-3}	fraction X_{ch} from composites X_c	Carbohydrates	Disintegration
4	$f_{pr,xc}$	0.20000	kg COD m^{-3}	fraction X_{pr} from composites X_c	Proteins	Disintegration
5	$f_{li,xc}$	0.30000	kg COD m^{-3}	fraction X_{li} from composites X_c	Lipids	Disintegration
6	$f_{fa,li}$	0.95000	kg COD m^{-3}	fraction solube S_{fa} from Li	VFA	Lipids
7	$f_{h2,su}$	0.19000	kg COD m^{-3}	fraction solube S_{h2} from sugar	H_2	Sugar
8	$f_{bu,su}$	0.13000	kg COD m^{-3}	fraction solube S_{bu} from sugar	Butyrate	Sugar
9	$f_{pro,su}$	0.27000	kg COD m^{-3}	fraction soluble S_{pro} from sugar	Propionato	Sugar
10	$f_{ac,su}$	0.41000	kg COD m^{-3}	fraction soluble S_{ac} from sugar	Acetato	Sugar
11	$f_{h2,aa}$	0.06000	kg COD m^{-3}	fraction S_{h2} from composites aa	H_2	Amino acids
12	$f_{va,aa}$	0.23000	kg COD m^{-3}	fraction S_{va} from composites aa	Valerate	Amino acids
13	$f_{bu,aa}$	0.26000	kg COD m^{-3}	fraction S_{bu} from composites aa	Butyrate	Amino acids
14	$f_{pro,aa}$	0.05000	kg COD m^{-3}	fraction S_{pro} from composites aa	Propionate	Amino acids
15	$f_{ac,aa}$	0.40000	kg COD m^{-3}	fraction S_{aa} from composites aa	Acetate	Amino acids

Carbon content in components				
No	**Terms**	**Used**	**Unit**	**Expressions**
1	C_{aa}	0.03	kmole C $kgCOD^{-1}$	Carbon content of amino acids
2	C_{ac}	0.0313	kmole C $kgCOD^{-1}$	Carbon content of acetate
3	C_{bac}	0.0313	kmole C $kgCOD^{-1}$	Carbon content of biomass
4	C_{bu}	0.025	kmole C $kgCOD^{-1}$	Carbon content of butyrate
5	C_{ch}	0.0313	kmole C $kgCOD^{-1}$	Carbon content of carbohyddrates
6	C_{ch4}	0.0156	kmole C $kgCOD^{-1}$	Carbon content of methane
7	C_{fa}	0.0217	kmole C $kgCOD^{-1}$	Carbon content of LCFA
8	C_{li}	0.022	kmole C $kgCOD^{-1}$	Carbon content of lipids
9	C_{pr}	0.03	kmole C $kgCOD^{-1}$	Carbon content of proteins
10	C_{pro}	0.0268	kmole C $kgCOD^{-1}$	Carbon content of propionate
11	C_{sI}	0.03	kmole C $kgCOD^{-1}$	Carbon content of soluble inerts
12	C_{su}	0.0313	kmole C $kgCOD^{-1}$	Carbon content of sugars
13	C_{va}	0.024	kmole C $kgCOD^{-1}$	Carbon content of valerate
14	C_{xc}	0.02786	kmole C $kgCOD^{-1}$	Carbon content of composites
15	C_{xI}	0.03	kmole C $kgCOD^{-1}$	Carbon content of particulate inerts

Nitrogen content incomponents				
No	**Terms**	**Used**	**Unit**	**Expressions**
1	N_{xc}	0.0026857	kmole N $kgCOD^{-1}$	Nitrogen content of composites
2	N_I	0.0042857	kmole N $kgCOD^{-1}$	Nitrogen content of inerts
3	N_{aa}	0.007	kmole N $kgCOD^{-1}$	Nitrogen content of amino acids and proteins
4	N_{bac}	0.0057143	kmole N $kgCOD^{-1}$	Nitrogen content of biomass

Table 12.2 – Physiochemical and biochemical kinetic parameters in ADM1

No	Terms	Original	Expressions	Units
			Yield uptake Components	
1	Y_{su}	0.1	Yield uptake sugars	$kgCOD_X\ kgCOD_S^{-1}$
2	Y_{aa}	0.08	Yield uptake amino cids	$kgCOD_X\ kgCOD_S^{-1}$
3	Y_{fa}	0.06	Yield uptake LCFA	$kgCOD_X\ kgCOD_S^{-1}$
4	Y_{c4}	0.06	Yield uptake buterate and valerate	$kgCOD_X\ kgCOD_S^{-1}$
5	Y_{pro}	0.04	Yield uptake propionate	$kgCOD_X\ kgCOD_S^{-1}$
6	Y_{ac}	0.05	Yield uptake acetate sugars	$kgCOD_X\ kgCOD_S^{-1}$
7	Y_{h2}	0.06	Yield uptake hydrogen	$kgCOD_X\ kgCOD_S^{-1}$
			Rates of disintegration, hydrolysis and coefficients	
No	**Terms**	**Original**	**Expressions**	**Units**
1	k_{dis}	0.5	Desintegration rate of composits	day^{-1}
2	$k_{hyd,ch}$	10	Hydrolysis rate of carbohydrates	day^{-1}
3	$k_{hyd,pro}$	10	Hydrolysis rate of proteins	day^{-1}
4	$k_{hyd,li}$	10	Hydrolysis rate of lipids	day^{-1}
5	$k_{m,su}$	30	Maximum uptake rate of sugar degraders	day^{-1}
6	$k_{m,aa}$	50	Maximum uptake rate amino acid degraders	day^{-1}
7	$k_{m,fa}$	6	Maximum uptake rate of LCFA degraders	day^{-1}
8	$k_{m,c4}$	20	Maximum uptake rate of valerate and butyrate degraders	day^{-1}
9	$k_{m,pro}$	13	Maximum uptake rate of propionate degraders	day^{-1}
10	$k_{m,ac}$	8	Maximum uptake rate of acetate degraders	day^{-1}
11	$k_{m,h2}$	35	Maximum uptake rate of hydrogen degraders	day^{-1}
12	$k_{dec,Xsu}$	0.02	Biomass decay of sugar degraders	day^{-1}
13	$k_{dec,Xaa}$	0.02	Biomass decay of amino acid degraders	day^{-1}
14	$k_{dec,Xfa}$	0.02	Biomass decay of LCFA degraders	day^{-1}
15	$k_{dec,Xc4}$	0.02	Biomass decay of valerate and butyrate degraders	day^{-1}
16	$k_{dec,Xpro}$	0.02	Biomass decay of propionate degraders	day^{-1}
17	$k_{dec,Xac}$	0.02	Biomass decay of acetate degraders	day^{-1}
18	$k_{dec,Xh2}$	0.02	Biomass decay of hydrogen deraders	day^{-1}
			Half saturation coefficients	
1	$k_{S,IN}$	0.0001	Half saturation coefficient of Soluble inerts	kg COD m^{-3}
2	$k_{S,su}$	0.5	Half saturation coefficient of Suger	kg COD m^{-3}
3	$k_{S,aa}$	0.3		kg COD m^{-3}
4	$k_{S,fa}$	0.4	Half saturation coefficient of LCFA degraders	kg COD m^{-3}
5	$k_{Ih2,fa}$	0.000005	50%inhibitory concentration of H2 to LCFA degraders	kg COD m^{-3}
6	$k_{S,pro}$	0.1	Half saturation concentrationof propionate uptake	kg COD m^{-3}
7	$k_{Ih2,pro}$	0.0000035	50 inhibitory concentration of H2 to propionate uptake	kg COD m^{-3}
8	$k_{S,ac}$	0.15	Half saturation coefficient of acetate degraders	kg COD m^{-3}
9	$k_{I,nh3}$	0.0018	50% inhibitory concentration of free NH3 to acetate uptake	kg COD m^{-3}
10	$k_{S,c4}$	0.2	Half saturation coefficient of valerate and butyrate degraders	kg COD m^{-3}
11	$k_{S,h2}$	0.000007	Half saturation coefficient of hydrogen uptake	kg COD m^{-3}
12	$k_{Ih2,c4}$	0.00001	50 inhibitory concentration of H2 to valerate and butyrate degraders	kg COD m^{-3}

Table 12.3 – Acid and gas parameters in ADM1

No	Terms	Original	Expressions	Units
1	k_La	200	Overall mass transfer coefficient kLtimes the specific transfer area	day^{-1}
2	$K_{H,h2o,base}$	0.0313	Henry law equillibrium constant of H_2O at 250C	M bar^{-1}
3	$K_{H,co2,base}$	0.035	Henry law equillibrium constante of CO_2 at 250C	M bar^{-1}
4	$K_{H,ch4,base}$	0.0014	Henry law equillibrium constante of CO_2 at 250C	kg Cod m^{-3} bar^{-1}
5	$K_{H,h2,base}$	0.00078	Henry law equillibrium constante of H_2 at 250C	kg Cod m^{-3} bar^{-1}
6	kp	10000	Pipe resistance coefficient	m^3 day^{-1} bar^{-1}
7	P_{atm}	1.013	External (atmospheric) pressure	bar
8	T_{base}	298.15		K
9	T_{op}	308.15	Operation temperature	K
10	R	0.083145	Universal gas constant	L bar $mole^{-1}$ K^{-1}
11	$pK_{w,base}$	NG	Water acid-base equillibrium constant at 250C	-
12	$pK_{a,va,base}$	NG	Valerate acid-base equillibrium constant at 250C	-
13	$PK_{a,bu,base}$	NG	Butyrate acid-base equillibrium constante at 250C	-
14	$pK_{a,pro,base}$	NG	Propionate acid-base equillibrium constante at 250C	-
15	$pK_{a,aCbase}$	NG	Acetate acid-base equillibrium constante at 250C	-
16	$pK_{a,co2,base}$	NG	CO2 acid-base equillibrium constante at 250C	-
17	$pK_{a,IN,base}$	NG	Inorganic Nitrogen acid-base equillibrium constant at 250C (assumed NH3/NH4+)	-
18	kA_Bva	1.00E+10	Valerate rate coefficient for acid-base	kmole day-1
19	kA_Bbu	1.00E+10	Butyrate rate coefficient for acid-base	kmole day-1
20	kA_Bpro	1.00E+10	Propionate rate coefficient for acid-base	kmole day-1
21	kA_Bac	1.00E+10	Acetate rate coefficient for acid -base	kmole day-1
22	kA_Bco2	1.00E+10	CO2 rate coefficient for acid-base	kmole day-1
23	kA_BIN	1.00E+10	Inorganic Nitrogen rate coefficient for acid-base	kmole day-1
24	pH_UL_h2	6	Upper pH limit for uptake hydrogen	-
25	pH_LL_h2	5	Lower pH limit for uptake hydrogen	-
26	pH_UL_aa	5.5	Upper pH limit for uptake amino acid	-
27	pH_LL_aa	4	Lower pH limit for uptake amino acid	-
28	pH_UL_ac	7	Upper pH limit for uptake acetate	-
29	pH_LL_ac	6	Lower pH limit for uptake acetate	-

13 APPENDIX D: SUPPLEMENTARY MATERIAL – ARTICLE II

Table 13.1 – Biochemical rate coefficients ($v_{i,j}$) and kinetic rate equations (ρ_j) for soluble components (i = 1–14; j = 1–23). Bold letters indicate additional processes or components added to the ADM1 in this work.

j	**Component → *i***	**1**	**2**	**3**	**4**	**5**	**6**	**7**	**8**	**9**	**10**	**11**	**12**	**13**	**14**	**Rate (ρj,kg COD($m^3 \cdot d)^{-1}$)**
	Process ↓	***S_{su}***	***S_{aa}***	***S_{fa}***	***S_{va}***	***S_{bu}***	***S_{pro}***	***S_{ac}***	***S_{h2}***	***S_{ch4}***	***S_{IC}***	***S_{IN}***	***S_{I}***	***S_{eth}***	***S_{lac}***	
1	Disintegration												$f_{SI,XC}$			$k_{dis} \cdot X_C$
2	Hydrolysis carbohydrates	*1*														$k_{hyd,ch} \cdot X_{ch}$
3	Hydrolysis of proteins		*1*													$k_{hyd,pr} \cdot X_{pr}$
4	Hydrolysis of lipids	$1\text{-}f_{fa,li}$		$1\text{-}f_{fa,li}$												$k_{hyd,li} \cdot X_{li}$
5.1	Uptake of Sugar	*-1*				$(1-Y_{su})\cdot f_{bu,su}$	$(1-Y_{su})\cdot f_{pro,su}$	$(1-Y_{su})\cdot f_{ac,su}$	$(1-Y_{su})\cdot f_{h2,su}$		$-\sum_{i=9,11-28} C_i v_{i,5}$	$-(Y_{su})\, N_{bac}$				$k_{m,su} \cdot \frac{S_{su}}{k_s + S_{su}} \cdot X_{su} \cdot I_1$
5.2	Uptake of Sugar	*-1*				$(1-Y_{su})\cdot f_{bu,su}$	$(1-Y_{su})\cdot f_{pro,su}$	$(1-Y_{su})\cdot f_{ac,su}$	$(1-Y_{su})\cdot f_{h2,su}$		$-\sum_{i=9,11-28} C_i v_{i,5}$	$-(Y_{su})\, N_{bac}$		$(1-Y_{su})\cdot f_{eth,su}$		$k_{m,su} \cdot \frac{S_{su}}{k_s + S_{su}} \cdot X_{su} \cdot I_1$
6	Uptake of amino acids		*-1*		$(1-Y_{aa})\cdot f_{va,aa}$	$(1-Y_{aa})\cdot f_{bu,aa}$	$(1-Y_{aa})\cdot f_{pro,aa}$	$(1-Y_{aa})\cdot f_{ac,aa}$	$(1-Y_{aa})\cdot f_{h2,aa}$		$-\sum_{i=9,11-28} C_i v_{i,6}$	$N_{aa}\text{-}(Y_{aa})\, N_{bac}$				$k_{m,aa} \cdot \frac{S_{aa}}{k_s + S_{aa}} \cdot X_{aa} \cdot I_2$
7	Uptake of LCFA			*-1*				$(1-Y_{fa})\cdot 0.7$	$(1-Y_{fa})\cdot 0.3$			$-(Y_{fa})\, N_{bac}$				$k_{m,fa} \cdot \frac{S_{fa}}{k_s + S_{fa}} \cdot X_{fa} \cdot I_2$
8	Uptake of valerate				*-1*		$(1-Y_{c4})\cdot 0.54$	$(1-Y_{c4})\cdot 0.31$	$(1-Y_{c4})\cdot 0.15$			$-(Y_{c4})\, N_{bac}$				$k_{m,c4} \cdot \frac{S_{va}}{k_s + S_{va}} \cdot X_{c4} \cdot \frac{1}{1 + S_{bu}/S_{va}} \cdot I_2$
9	Uptake of butyrate					*-1*		$(1-Y_{c4})\cdot 0.8$	$(1-Y_{c4})\cdot 0.2$			$-(Y_{c4})\, N_{bac}$				$k_{m,c4} \cdot \frac{S_{bu}}{k_s + S_{bu}} \cdot X_{c4} \cdot \frac{1}{1 + S_{va}/S_{su}} \cdot I_2$
10	Uptake of Propionate						*-1*	$(1-Y_{pro})\cdot 0.57$	$(1-Y_{pro})\cdot 0.43$		$-\sum_{i=9,11-28} C_i v_{i,10}$	$-(Y_{pro})\, N_{bac}$				$k_{m,pro} \cdot \frac{S_{pro}}{k_s + S_{pro}} \cdot X_{pro} \cdot I_2$
11	Uptake of Acetate							*-1*		$(1-Y_{ac})$	$-\sum_{i=9,11-28} C_i v_{i,11}$	$-(Y_{ac})\, N_{bac}$				$k_{m,ac} \cdot \frac{S_{ac}}{k_s + S_{ac}} \cdot X_{ac} \cdot I_3$
12	Uptake of Hydrogen								*-1*	$(1-Y_{h2})\cdot$	$-\sum_{i=9,11-28} C_i v_{i,12}$	$-(Y_{h2})\, N_{bac}$				$k_{m,h2} \cdot \frac{S_{h2}}{k_s + S_{h2}} \cdot X_{h2} \cdot I_1$
13	Decay of X_{su}															$k_{dec,Xsu} \cdot X_{su}$
14	Decay of X_{aa}															$k_{dec,Xaa} \cdot X_{aa}$
15	Decay of X_{fa}															$k_{dec,Xla} \cdot X_{fa}$
16	Decay of X_{c4}															$k_{dec,Xc4} \cdot X_{c4}$
17	Decay of X_{pro}															$k_{dec,Xpro} \cdot X_{pro}$
18	Decay of X_{ac}															$k_{dec,Xac} \cdot X_{ac}$
19	Decay of X_{h2}															$k_{dec,Xh2} \cdot X_{h2}$
20	Decay of X_{lac}															$k_{dec,Xla} \cdot X_{lac}$
21	Uptake of lactate					$(1-Y_{lac})\cdot f_{bu,lac}$	$(1-Y_{lac})\cdot f_{pro,lac}$	$(1-Y_{lac})\cdot f_{ac,lac}$	$(1-Y_{lac})\cdot f_{h2,lac}$						*-1*	$k_{m,lac} \cdot \frac{S_{lac}}{k_{s,lac} + S_{lac}} \cdot X_{lac} \cdot I_1$
22	Sugars uptake rate by Lactobacillus														$(1-Y_{su})\cdot f_{lac,su}$	$k_{m,lac,su} \cdot \frac{S_{su}}{k_{s,lac,su} + S_{su}} \cdot X_{lac,su} \cdot I_1$
23	Decay of Lactobacillus															$k_{dec,Xla,su} \cdot X_{lac,su}$
		Monosaccharides (kg COD m^{-3})	Amino Acids (kg COD m^{-3})	Long chain fatty acid (kg COD m^{-3})	Total valerate (kg COD m^{-3})	Total Butyrate (kg COD m^{-3})	Total Propionate (kg COD m^{-3})	Total Acetate (kg COD m^{-3})	Hydrogen gas (kg COD m^{-3})	Methane gas (kg COD m^{-3})	Inorganic Carbon (kg mole C m^{-3})	Inorganic Nitrogen (kg mole N m^{-3})	Soluble Inerts (kg COD m^{-3})	Total Ethanol (kg COD m^{-3})	Total Lactate (kg COD m^{-3})	Inhibition factors $I_1 = I_{pH}\, I_{IN,lim}$ $I_2 = I_{pH}\, I_{h2}\, I_{IN,lim}$ $I_3 = I_{pH}\, I_{NH3}\, I_{IN,lim}$

Data: Adapted from Alexandropoulou, Antonopoulou and Lyberatos (2018, 2022); Batstone et al. (2002 and Economou et al. (2024).

Table 13.2 – Biochemical rate coefficients ($v_{i,j}$) and kinetic rate equations (ρ_j) for soluble components (i = 15–28; j = 1–23). Bold letters indicate additional processes or components added to the ADM1 in this work.

j	Component → i	15	16	18	18	19	20	21	22	23	24	25	26	27	28	Rate (ρj,kg COD($m^3 \cdot d$)$^{-1}$)
	Process ↓	X_c	X_{ch}	X_{pr}	X_{li}	X_{su}	X_{aa}	X_{fa}	X_{c4}	X_{pro}	X_{ac}	X_{h2}	X_I	X_{lac}	$X_{lac,su}$	
1	Disintegration	-1	$f_{ch,XC}$	$f_{pr,XC}$	$f_{li,XC}$								$f_{SI,XC}$			$k_{dis} \cdot X_C$
2	Hydrolysis carbohydrates		-1													$k_{hyd,ch} \cdot X_{ch}$
3	Hydrolysis of proteins			-1												$k_{hyd,pr} \cdot X_{pr}$
4	Hydrolysis of lipids				-1											$k_{hyd,li} \cdot X_{li}$
5.1	Uptake of Sugar					Y_{su}										$k_{m,su} \cdot \frac{S_{su}}{k_s + S_{su}} \cdot X_{su} \cdot I_1$
5.2	Uptake of Sugar					Y_{su}										$k_{m,su} \cdot \frac{S_{su}}{k_s + S_{su}} \cdot X_{su} \cdot I_1$
6	Uptake of amino acids						Y_{aa}									$k_{m,aa} \cdot \frac{S_{aa}}{k_s + S_{aa}} \cdot X_{aa} \cdot I_2$
7	Uptake of LCFA							Y_{fa}								$k_{m,fa} \cdot \frac{S_{fa}}{k_s + S_{fa}} \cdot X_{fa} \cdot I_2$
8	Uptake of valerate								Y_{c4}							$k_{m,c4} \cdot \frac{S_{va}}{k_s + S_{va}} \cdot X_{c4} \cdot \frac{1}{1 + S_{bu}/S_{va}} \cdot I_2$
9	Uptake of butyrate								Y_{c4}							$k_{m,c4} \cdot \frac{S_{bu}}{k_s + S_{bu}} \cdot X_{c4} \cdot \frac{1}{1 + S_{va}/S_{su}} \cdot I_2$
10	Uptake of Propionate									Y_{pro}						$k_{m,pro} \cdot \frac{S_{pro}}{k_s + S_{pro}} \cdot X_{pro} \cdot I_2$
11	Uptake of Acetate										Y_{ac}					$k_{m,ac} \cdot \frac{S_{ac}}{k_s + S_{ac}} \cdot X_{ac} \cdot I_3$
12	Uptake of Hydrogen											Y_{h2}				$k_{m,h2} \cdot \frac{S_{h2}}{k_s + S_{h2}} \cdot X_{h2} \cdot I_1$
13	Decay of X_{su}	1				-1										$k_{dec,Xsu} \cdot X_{su}$
14	Decay of X_{aa}	1					-1									$k_{dec,Xaa} \cdot X_{aa}$
15	Decay of X_{fa}	1						-1								$k_{dec,Xla} \cdot X_{fa}$
16	Decay of X_{c4}	1							-1							$k_{dec,Xc4} \cdot X_{c4}$
17	Decay of X_{pro}	1								-1						$k_{dec,Xpro} \cdot X_{pro}$
18	Decay of X_{ac}	1									-1					$k_{dec,Xac} \cdot X_{ac}$
19	Decay of X_{h2}	1										-1				$k_{dec,Xh2} \cdot X_{h2}$
20	Decay of X_{lac}	1												-1		$k_{dec,Xla} \cdot X_{lac}$
21	Uptake of lactate	1												Y_{lac}		$k_{m,lac} \cdot \frac{S_{lac}}{k_{s,lac} + S_{lac}} \cdot X_{lac} \cdot I_1$
22	Sugars uptake rate by Lactobacillus														$Y_{lac,su}$	$k_{m,lac,su} \cdot \frac{S_{su}}{k_{s,lac,su} + S_{su}} \cdot X_{lac,su} \cdot I_1$
23	Decay of Lactobacillus	1													-1	$k_{dec,Xla,su} \cdot X_{lac,su}$
		Composites (kg COD m^{-3})	Carbohydrates (kg COD m^{-3})	Proteins (kg COD m^{-3})	Lipids (kg COD m^{-3})	Sugar degraders (kg COD m^{-3})	Amino acid degraders (kg COD m^{-3})	LCFA degraders (kg COD m^{-3})	Caproate, valerate and butyrate degraders (kg COD m^{-3})	Propionate degraders (kg COD m^{-3})	Acetate degraders (kg COD m^{-3})	Hydrogen degraders (kg COD m^{-3})	Particulate inerts (kg mole C m^{-3})	Lactate Degraders (kg COD m^{-3})	Lactobacillus (kg COD m^{-3})	Inhibition factors $I_1 = I_{pH} \cdot I_{IN,lim}$ $I_2 = I_{pH} \cdot I_{h2} \cdot I_{IN,lim}$ $I_3 = I_{pH} \cdot I_{NH3} \cdot I_{IN,lim}$

Data: Adapted from Alexandropoulou, Antonopoulou and Lyberatos (2018, 2022); Batstone et al. (2002 and Economou et al. (2024).

14 APPENDIX E: SUPPLEMENTARY MATERIAL – ARTICLE III

Figure 14.1 – Temporal evolution of the frequency of terms associated with anaerobic digestion, modeling, and organic residues in publications indexed in Web of Science..

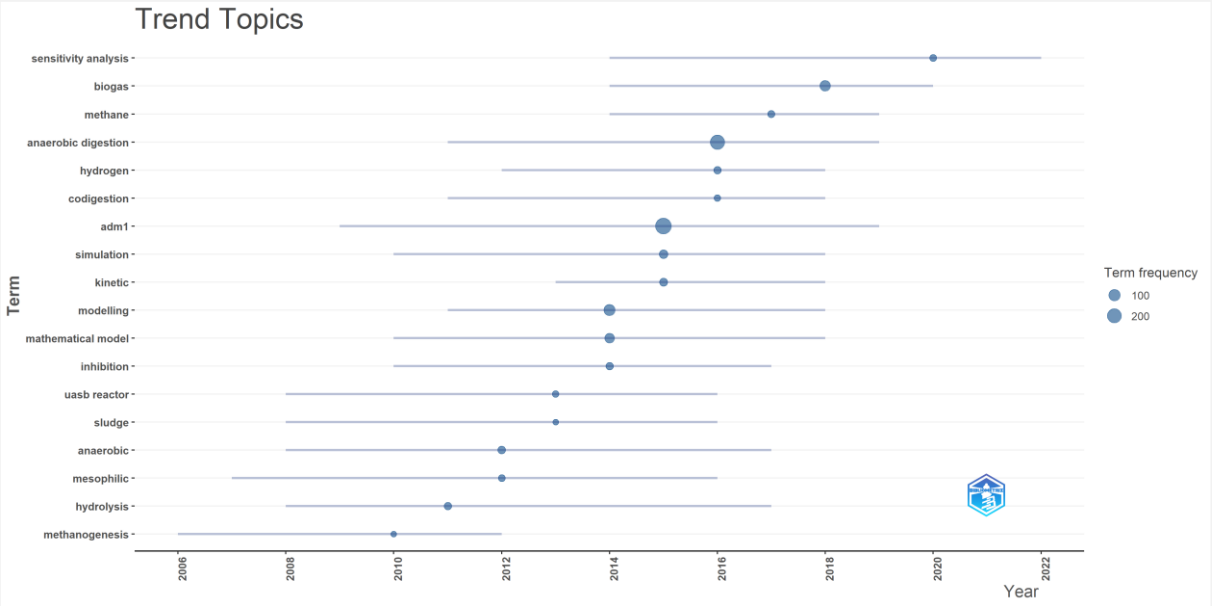

15 INDEX

A

Acetate, XIII, XVIII, 98, 106, 115, 117, 201, 202, 205, 207, 208, 209
Acetogenesis, 175
Acidogenesis, 186
ADM1, 1, 2, 4, IX, X, XI, XII, XIII, XIV, XV, XVI, XVII, XXIII, XXIV, 28, 29, 32, 33, 37, 38, 41, 42, 43, 44, 45, 46, 47, 48, 50, 52, 53, 55, 56, 57, 58, 59, 60, 62, 63, 65, 66, 68, 69, 70, 71, 74, 75, 77, 79, 81, 85, 87, 88, 90, 92, 94, 95, 96, 97, 98, 99, 101, 102, 105, 106, 107, 109, 110, 111, 112, 113, 115, 116, 117, 119, 120, 121, 122, 123, 124, 126, 128, 129, 130, 131, 132, 138, 139, 140, 141, 142, 143, 144, 145, 146, 147, 148, 150, 151, 152, 153, 155, 156, 157, 158, 159, 160, 161, 162, 163, 164, 165, 166, 167, 168, 169, 170, 171, 173, 174, 175, 176, 177, 178, 179, 180, 181, 183, 184, 185, 187, 188, 189, 190, 191, 192, 195, 198, 199, 205, 206, 207, 208, 209
Alkalinity, XVIII, 132
Ammonium, XX
Anaerobic Digestion, IX, XVII, XVIII, XIX, XXII, 28, 48, 55, 56, 60, 87, 88, 126, 128, 139, 150, 172, 173, 174, 175, 178, 180, 182, 183, 184, 185, 186, 187, 188, 190, 191, 192, 193, 194, 196, 198, 199
Anaerobic Reactors, 51, 177
AnSTBR, IX, XI, XV, XVII, 32, 87, 90, 93, 104
Aquasim, 150

B

Batch Reactor, XVII, 31
Biogas Production, 174, 186, 193
Biohydrogen, 179, 182, 188, 193
Biomethane, 185
Butyrate, XIII, 98, 115, 117, 201, 205, 207, 208

C

Carbohydrates, 70, 71, 91, 104, 114, 202, 205, 209
COD, XV, XVII, 42, 45, 52, 58, 59, 60, 62, 64, 66, 67, 68, 69, 70, 71, 91, 92, 93, 94, 95, 98, 99, 102, 104, 114, 115, 116, 118, 121, 128, 132, 152, 201, 202, 205, 206, 208, 209

D

Dark Fermentation, XIII, 117, 182, 188, 194
Disintegration, XX, 30, 102, 114, 158, 201, 202, 205, 208, 209

E

Ethanol, XXIV, 94, 95, 98, 115, 119, 191, 208

F

FAN, 144
Fruit and Vegetable Waste, XIII, XVII, XVIII, 48, 117, 178, 184, 192

G

Greenhouse Gas Emissions, XVIII

H

Hydraulic Retention Time, XVIII
Hydrogen Production, 172, 182, 193, 194
Hydrolysis, 102, 107, 114, 158, 159, 186, 196, 201, 202, 206, 208, 209

I

Inhibition, XIV, 55, 98, 105, 198, 201, 202, 204, 208, 209

K

Kinetics, XXII, 46, 174, 177, 181, 190
kLa, XX, 110, 155, 165, 207

L

Lactate, XIII, XXIV, 94, 95, 98, 115, 117, 208, 209
L-FVW, IX, XIII, XV, XVIII, 50, 70, 87, 89, 90, 91, 92, 93, 94, 104, 106, 107, 108, 109, 110, 112, 113, 114, 116, 117, 118, 119, 121, 122, 124
Lipids, 60, 70, 91, 92, 104, 114, 131, 202, 205, 209

M

Mass Balance, XIII, 42
Mathematical Modeling, 150, 175, 187
Methanogenesis, 30, 175, 178
Modified ADM1, 144, 191

O

ODEs, XVIII, 41, 42, 43, 155
OFMSW, XV, XVIII, 126, 129, 130, 131, 132, 133, 134, 138, 139, 140, 142, 144, 145, 149, 150, 151, 156, 161, 162, 163, 164, 180, 195
Organic Loading Rate, XVIII, 59

P

Particulate COD, 132
pH, XIII, 31, 35, 39, 43, 46, 52, 57, 59, 60, 62, 69, 72, 80, 81, 89, 92, 93, 94, 104, 105, 106, 108, 109, 121, 122, 123, 129, 130, 131, 135, 141, 144, 145, 149, 152, 154, 155, 164, 167, 178, 181, 192, 193, 196, 207
Process Modeling, 197
Propionate, XIII, 98, 115, 117, 201, 202, 205, 207, 208, 209
Proteins, 70, 114, 202, 205, 209

R

Renewable Energy, 175, 176, 178, 184, 187, 192, 198
RMSE, XVIII, 64, 75, 76, 77, 80, 100, 104, 116, 120, 121

S

Sensitivity Analysis, 175
S-FVW, IX, XVIII, 89

Simplex Method, 189
Stoichiometry, XXII, 44, 45, 185

T

Total Solids, XIX, 67, 91, 92, 104, 132

U

UASB, IX, XI, XIX, 31, 32, 48, 50, 58, 59, 62, 63, 67, 68, 75, 79, 134, 141, 165, 169, 170, 177, 179, 187, 191, 192, 194

V

VFA, IX, XIII, XIX, XX, XXI, 29, 31, 32, 43, 45, 50, 52, 60, 69, 80, 81, 92, 104, 110, 111, 114, 115, 116, 120, 124, 128, 129, 132, 135, 145, 149, 150, 152, 153, 161, 169, 170, 205
Volatile Solids, XIX, 67, 91, 92, 104, 132